

# **Lysosomal degradation of alpha-Synuclein:**

## ***Analysis in vivo and in vitro***

**Dissertation**

der Mathematisch-Naturwissenschaftlichen Fakultät

der Eberhard Karls Universität Tübingen

zur Erlangung des Grades eines

Doktors der Naturwissenschaften

(Dr. rer. nat.)

vorgelegt von

An Phu Tran Nguyen

aus

*Cantho, Vietnam*

Tübingen

2015

Tag der mündlichen Qualifikation: 23.03.2015

Dekan:

Prof. Dr. Wolfgang Rosenstiel

1. Berichterstatter:

Prof.Dr. Olaf Riess

2. Berichterstatter:

Prof. Dr. Boris Ferger



## Table of contents

<b>1</b>	<b>INTRODUCTION</b>	<b>16</b>
1.1	Generalities	16
1.2	Etiology of PD	17
1.2.1	Genetic factors	17
1.2.2	Environmental factors	20
1.3	Neuropathological features of PD	21
1.4	Neurobiology of $\alpha$ -Synuclein	23
1.4.1	$\alpha$ -Synuclein genetic and primary structure	23
1.4.2	Synuclein family	25
1.4.3	Localizations and physiological functions	26
1.4.4	Propensity of $\alpha$ -Synuclein for oligomerization and aggregation	27
1.4.4.1	Factors modulating $\alpha$ -Synuclein aggregation	27
1.4.4.2	Post-translational modifications (PTMs)	28
1.5	Current therapies in PD	30
1.6	Animal modeling for PD research	31
1.7	Reduction of $\alpha$ -Synuclein burden is a potential therapeutic strategy for PD	34
1.7.1	$\alpha$ -Synuclein has been proposed to be a substrate of both UPS and ALP	35
1.7.1.1	$\alpha$ -Synuclein was firstly described to be degraded by UPS	35
1.7.1.2	Degradation of $\alpha$ -Synuclein by UPS is conflicting	35
1.7.1.3	Increase of evidence for $\alpha$ -Synuclein degradation by ALP	36
1.7.1.4	CMA: a new player in $\alpha$ -Synuclein degradation	38
1.8	PhD thesis: Studying the role of $\alpha$ -Synuclein lysosomal degradation using <i>in vivo</i> and <i>in vitro</i> approaches	41
<b>2</b>	<b>RESULTS</b>	<b>42</b>
2.1	Kinetics of $\alpha$ -Synuclein degradation in HEK293 cells	42
2.2	Kinetic of $\alpha$ -Synuclein degradation in BE(2)-M17 cells	48
2.3	Generation of transgenic models overexpressing $\alpha$ -Synuclein	52
2.3.1	Pcp2 promoter drives $\alpha$ -Synuclein expression in cerebellar Purkinje cells (PCs)	52
2.3.2	Mutation of the CMA motif does not seem to affect the $\alpha$ -Synuclein steady-state level <i>in vivo</i>	58
2.4	Analysis of transgenic animals overexpressing $\alpha$ -Synuclein	59
2.4.1	Transgenic mice with overexpression of $\alpha$ -Synuclein in PCs show decline in locomotor performance compared to non-transgenic mice	60
2.4.2	Analysis of PC neurodegeneration	65
2.4.2.1	PC morphology	65
2.4.2.2	Synaptic density markers	68

2.4.2.3	GABA neurotransmitter release.....	70
2.4.2.4	Neuro-inflammation markers .....	72
2.4.2.5	Overexpressed $\alpha$ -Synuclein did not develop amyloid- like characters.....	74
<b>3</b>	<b>DISCUSSION.....</b>	<b>80</b>
<b>3.1</b>	<b><i>In vitro</i> studies: Establishing cellular paradigms to study protein degradation .....</b>	<b>80</b>
3.1.1	Mutation of CMA motif does not slow down $\alpha$ -Synuclein degradation.....	81
3.1.2	Absence of cellular toxicity mediated by overexpressing A53T mutant $\alpha$ -Synuclein.....	82
<b>3.2</b>	<b><i>In vivo</i> studies: Generating and analyzing conditional mouse model expressing human pathogenic <math>\alpha</math>-Synuclein.....</b>	<b>83</b>
3.2.1	Generation of animal models overexpressing $\alpha$ -Synuclein mutants in Purkinje cells.....	83
3.2.2	Overexpression of $\alpha$ -Synuclein in PCs causes mild motor behavioral changes.....	84
3.2.3	CMA motif mutation does not lead to differential $\alpha$ -Synuclein steady state levels <i>in vivo</i> .....	85
3.2.4	Overexpression of $\alpha$ -Synuclein in PCs did not lead to obvious neurohistopathology.....	86
3.2.5	No obvious LB-like pathology in transgenic mice up to 23 months .....	87
3.2.6	Absence of toxicity caused by overexpression of $\alpha$ -Synuclein.....	88
<b>3.3</b>	<b>Outlook .....</b>	<b>89</b>
3.3.1	<i>In vitro</i> studies .....	89
3.3.2	<i>In vivo</i> studies .....	90
<b>4</b>	<b>MATERIALS AND METHODS.....</b>	<b>92</b>
<b>4.1</b>	<b>Animal models.....</b>	<b>92</b>
4.1.1	Animals .....	92
4.1.1.1	TetO-SNCA animals .....	92
4.1.1.2	Driver Pcp2-tTA animals.....	92
4.1.1.3	Animal housing .....	92
4.1.2	Genotyping .....	93
4.1.2.1	DNA preparation.....	93
4.1.2.2	Tet-O-SNCA transgene PCR.....	93
4.1.2.3	Pcp2-tTA transgene PCR .....	94
4.1.3	Biochemical methods .....	95
4.1.3.1	Brain homogenization and protein extraction.....	95
4.1.3.2	Western-blot.....	95
4.1.4	Immunohistochemistry .....	95
4.1.4.1	Standard immunohistochemistry .....	95
4.1.4.2	Proteinase K (PK) digestion .....	98
4.1.5	Behavior analysis .....	99
4.1.5.1	Animal cohorts.....	99
4.1.5.2	Rotarod .....	99
4.1.5.3	Open-field test .....	99
4.1.5.4	Pole-climbing test .....	99
4.1.5.5	Beam-walk .....	100
<b>4.2</b>	<b>Cell models.....</b>	<b>100</b>
4.2.1	Generation of stable Tet inducible cell lines .....	100
4.2.1.1	Plasmid preparation.....	100

4.2.1.2	Cell transfection and selection.....	101
4.2.1.3	Comparison of $\alpha$ -Synuclein mRNA levels by qRT-PCR .....	103
4.2.2	Cell lysis/ Protein extraction.....	104
4.2.3	Western-blot .....	104
4.2.4	Immunocytochemistry.....	104
4.2.5	Kinetics of $\alpha$ -Synuclein degradation assay .....	105
<b>5</b>	<b>ANNEX FIGURES.....</b>	<b>108</b>

## Abbreviations

°C	Degre Celcius
6-OHDA	6-Hydroxydopamine
ABC	avidin-biotin-enzyme complexes
AD	Alzheimer's disease
AFM	Atomic force microcospy
ALP	Autophagy-lysosomal pathway
<i>Atg</i>	Autophagy-related gene
ATPase	Adenosine-triphosphatase
CB	Cerebellum
Cm	centimeter
CMA	Chaperone-mediated autophagy
COMT	Catechol-O-methyl transferase
Csp $\alpha$	Cysteine-string protein $\alpha$
DA	Dopamine
DAPI	4',6-diamidino-2-phenylindole
DBS	Deep brain stimulation
DCN	Deep cerebellar nuclei
DLB	Dementia with Lewy bodies
DMSO	Dimethyl sulfoxide
DNA	Deoxyribonucleic acid
dNTP	Deoxynucleotide
Dox	Doxicycline
EDTA	Ethylenediaminetetraacetic acid
EGTA	Ethylene glycol tetraacetic acid
ER	Endoplasmic reticulum
ES	Embryonic stem cell
EtBr	Ethidium bromide
FCS	Fetal calf serum
FL	Full-length
FRT	Flp Recombinase Target
GABA	Gamma-aminobutyric acid
GAPDH	Glyceraldehyde 3-phosphate dehydrogenase
<i>GBA</i>	Glucocerebrosidase gene
GCase	Glucocerebrosidase
GCL	Granular cell layer
GFAP	glial fibrillary acidic protein
H	hour
HEK-293	Human embryonic kidney-293
HRP	horseradish peroxidase
Hsp	Heat-shock protein
Iba-1	Ionized calcium-binding adapter molecule 1
ICC	Immunocytochemistry
IHC	Immunohistochemistry
KO	Knock-out
KRS	Kufor-Rakeb syndrome
<i>LacZ</i>	$\beta$ -galactosidase gene
LAMP2A	Lysosomal-associated membrane protein 2A
LB	Lewy body
LC3	Light-chain protein 3
L-DOPA	Levodopa

LRRK2	Leucine-rich repeat kinase 2
mA	milliampere
MAO	Monoamine oxidase
MB	Mid-brain
mGluR1	Metabotropic glutamate receptor 1
Min	minute
mL	milliliter
ML	Molecular layer
mM	millimolar
Mm	millimeter
MN	Meynert nucleus
MPTP	1-methyl-4-phenyl-1,2,3,6-tetrahydropyridine
mRNA	Messenger ribonucleic acid
Ms	millisecond
MSA	Multiple system atrophy
NAC	non-A $\beta$ - component amyloid
nAChR	Nicotinic Acetylcholine receptor
Ng	nanogram
Nm	nanometer
OB	Olfactory bulb
PAGE	Polyacrylamide gel electrophoresis
<i>PARK</i>	Parkinson-related gene
PBS	Phosphate buffer saline
PC	Purkinje cell
PC12	Pheochromocytoma-derived cells
PCL	Purkinje cell layer
Pcp2	Purkinje cell protein 2
PCR	Polymerase chain reaction
PD	Parkinson' s disease
PET	Paraffin-embedded tissue
Pff	Preformed fibril
PINK1	phosphatase and tensin [PTEN] homolog-induced putative kinase 1
PK	Proteinase K
PP2A	Protein phosphatase 2A
PTM	Post-translational modifications
PVDF	Polyvinylidene difluoride
qPCR	Quantitative PCR
RNAPol	RNA polymerase
RNase	Ribonuclease
ROCO	Ras-of-complex
Rpm	Round per minute
RT	Reverse transcription
S	Second
SEM	Standard error of the mean
SIAH	Seven in absentia homolog
SN	Substantia nigra
SNARE	Soluble N-ethylmaleimide-sensitive-factor attachment receptor
<i>SNCA</i>	$\alpha$ -Synuclein gene
SNpc	Substantia nigra parcs compacta
TBS	Tris buffer saline
Tet	Tetracycline
Tet-O	Tetracycline-binding operator

tTA	Transcription activator
UCHL-1	Ubiquitin carboxyl-terminal esterase L1
UPS	Ubiquitin-proteasome system
UV	Ultra-violet
v/v	Volume/volume
VGAT	Vesicular GABA transporter
w/v	Weight/ volume
WB	Western-blot
WT	Wild-type
$\Delta$ CT	C-terminal truncation
$\mu$ g	Microgram
$\mu$ l	Microliter
$\mu$ M	Micromolar

## **Publications**

Parts of this work have been published in:

Poster presentations

- 1) **Tran Nguyen AP. and Ciossek T., 2011: "Generating of Tet-regulation models *in vivo* and *in vitro* overexpressing C-terminal truncated alpha-Synuclein"**  
Poster presented at Satellite Meeting of the International Society for Neurochemistry: "From genes to pathogenesis: The evolving spectrum of synucleinopathies" *Naxos, September 2011*
- 2) **Tran Nguyen AP. and Ciossek T., 2013: "Lysosomal degradation of alpha-Synuclein: Analysis *in vivo* and *in vitro*"**  
Poster presented at NEURASYNC closing meeting, *Roma, September 2013*

Oral presentations

- 1) **NEURASYNC training week: "Effects of protein misfolding on neuronal cell homeostasis"**  
*April, 2010 (Athens, Greece)*
- 2) **NEURASYNC training week: "Animal models of Parkinson's and Huntington's disease"**  
*September, 2010 (Lund, Sweden)*
- 3) **NEURASYNC training week: "Introduction to Drug Discovery and Development; Drug Development in Synucleinopathies; Life Science and Entrepreneurship, From Founding to Funding"** *April, 2011 (Lisbon, Portugal)*
- 4) **NEURASYNC training week: "Structure of alpha-Synuclein oligomers"** *June, 2012 (Goettingen, Germany)*

Conference abstracts

- 1) **Tran Nguyen AP. and Ciossek T., 2013: "Generating of Tet-regulation models *in vivo* and *in vitro* overexpressing C-terminal truncated alpha-Synuclein"**  
Abstract submitted for EMBO's Meeting: "Autophagy in Health and Diseases" *November, 2011, Ma'ale Hachamisha, Israel*
- 2) **Tran Nguyen AP. and Ciossek T., 2013: "Lysosomal degradation of alpha-Synuclein: Analysis *in vivo* and *in vitro*"**  
Abstract submitted for NEURASYNC closing meeting, *Roma, September 2013*
- 3) **Tran Nguyen AP. and Ciossek T., 2015: "Lysosomal degradation of alpha-Synuclein: Analysis *in vivo* and *in vitro*"**  
Abstract submitted for ADPD meeting, *Nice, March 2015*



## Zusammenfassung

Die Parkinson-Krankheit ist die zweithäufigste neurodegenerative Erkrankung und betrifft 1-2% der Bevölkerung älter als 55 Jahre. Bis heute sind die Mechanismen der Neurodegeneration in dieser Erkrankung unklar. Vieles deutet auf eine Beteiligung von  $\alpha$ -Synuclein, ein präsynaptisch hochexprimiertes neuronales Protein. Fehlgefaltetes und aggregiertes  $\alpha$ -Synuclein stellt die Hauptkomponente von Lewy-Körpern, charakteristischen pathologischen Ablagerungen in Gehirnen von Parkinson Patienten, dar. Insofern stellt die Reduktion der Expression von  $\alpha$ -Synuclein durch eine erhöhte Degradation ein interessantes therapeutisches Ziel dar. Allerdings sind die genauen Mechanismen dieses intrazellulären Abbaus von  $\alpha$ -Synuclein unklar. In vitro wird monomeres  $\alpha$ -Synuclein sowohl proteasomal als auch lysosomal katabolisiert.  $\alpha$ -Synuclein ist als ein Substrat der Chaperon-vermittelten Autophagie (CMA) beschrieben, ein Prozess in dem zum Abbau vorgesehene Proteine direkt LAMP2A-vermittelt in das Lumen von Lysosomen translozieren. Eine Mutation des CMA-Erkennungsmotivs ( $\Delta$ CMA) von  $\alpha$ -Synuclein erhöht dessen Halbwertszeit; ebenso führt eine Reduktion der LAMP2A Expression in primären Neuronen zu erhöhter  $\alpha$ -Synuclein Expression. Pathogene Mutanten von  $\alpha$ -Synuclein (A30P, A53T) sind zudem als Inhibitoren des LAMP2A Rezeptors beschrieben und könnten daher den lysosomalen Abbau von  $\alpha$ -Synuclein hemmen. Das Ziel dieser Studie war es, die Auswirkungen einer CMA-Motiv-Mutation auf dessen Expression in in vitro- und in vivo-Modellen zu untersuchen:

(1) Für die in-vitro-Studien sind in induzierbaren Zelllinien (nicht-neuronalen und neuronalen) verschiedene C-terminal verkürzte ( $\Delta$ CT)  $\alpha$ -Synuclein Varianten (WT und A53T) mit dem normalen (Wildtyp) oder mutierten CMA-Motiv exprimiert worden ( $\Delta$ CMA). Durch den Vergleich der kinetischen Abbaukurven des  $\alpha$ -Synucleins in diesen Zelllinien fanden wir – unerwartet – dass die Mutation des CMA-Motivs nicht zu signifikanten Unterschieden in der Kinetik des Abbaus führt. Die zur Kontrolle analysierten Vollängenkonstrukte (Wildtyp und A53T-Mutante) zeigten – in Übereinstimmung mit früheren veröffentlichten Daten – eine verlangsamte Degradation bei der A53T-Mutante (im Vergleich zum Wildtyp Konstrukt).

(2) Für die in-vivo-Studien sind zwei transgene Mausmodelle mit Expression von C-terminal verkürzten  $\alpha$ -Synuclein in zerebellären Purkinje-Zellen (PZ) (Konstrukt 1: A53T- $\Delta$ CT, Konstrukt 2: A53T- $\Delta$ CMA) generiert wurden. Die Analyse dieser Tiere fand mit histologischen und biochemischen Methoden sowie in Verhaltensexperimenten statt.  $\alpha$ -Synuclein wurde stark in den präsynaptischen Bereichen der Purkinje-Zellen exprimiert, sowie im Perikaryon und den Neuriten der PZ. Es konnten jedoch keine  $\alpha$ -Synuclein Aggregate (resistent gegen Proteinase K) erkannt werden; ebenso konnte

kein signifikanter Verlust an Purkinje-Zellen nachgewiesen werden. Auch morphologischen Veränderungen der Purkinje-Zellen war nicht nachweisbar. Interessanterweise zeigten transgene Mäuse Beeinträchtigungen im Motorverhaltenstests (Pole Test und Open-Field). Die Korrelation dieser Verhaltensauffälligkeiten mit  $\alpha$ -Synuclein bleibt unklar. Die in unseren beiden transgenen Linien beobachteten ähnlichen Motorphänotypen und sowie fehlende Unterschiede in der  $\alpha$ -Synuclein Expression legen allerdings nahe, dass die Mutation des  $\alpha$ -Synuclein CMA Motiv keinen Einfluss auf die Abbaukinetik dieses Proteins in vivo hat. Folglich konnte keine wesentliche pathologische Rolle des CMA-System im in-vivo-Modell nachgewiesen werden.

Zusammen genommen zeigen die in vitro und in vivo Daten, dass das CMA-System in Zusammenhang mit der Überexpression eines C-terminal verkürzten  $\alpha$ -Synuclein keinen Einfluss auf die Abbaukinetik von  $\alpha$ -Synuclein hat. Das Fehlen einer offensichtlicher Pathologie in unserem Tiermodell begrenzt jedoch die Interpretation der in vivo Daten in Bezug auf eine eventuell unterschiedliche Bildungskinetik aggregierten  $\alpha$ -Synucleins.

## Summary

Parkinson's disease (PD) is the second most common neurodegenerative disease and affects 1-2% of the population older than 55 years. To date, the mechanisms of neurodegeneration in PD remain to be elucidated. Strong evidence suggests that aggregation of  $\alpha$ -Synuclein, a small membrane-bound protein abundantly present in presynaptic regions of neuronal cells, is highly involved in the process of neurodegeneration. Misfolded and aggregated structures of  $\alpha$ -Synuclein are the main components found in Lewy bodies and are characteristic pathological features in parkinsonian brains. Therefore, down-regulating of  $\alpha$ -Synuclein levels by enhancing its degradation represents an interesting therapeutic target. However, the exact mechanisms of intracellular  $\alpha$ -Synuclein clearance are unclear. *In vitro*, monomeric  $\alpha$ -Synuclein is degraded by both proteasomal and lysosomal systems, but  $\alpha$ -Synuclein oligomers are thought to block these degradation pathways. Recently,  $\alpha$ -Synuclein has also been demonstrated to be a substrate of the chaperone-mediated autophagy (CMA), a pathway in which proteins are directly translocated into the lysosome lumen via the lysosomal membrane receptor LAMP2A. Mutation of the CMA-motif ( $\Delta$ CMA) of  $\alpha$ -Synuclein increases its half-life and down-regulation of LAMP2A leads to increased  $\alpha$ -Synuclein levels in primary neurons. Pathogenic mutants of  $\alpha$ -Synuclein (A30P, A53T) have also been proposed to act as blockers of LAMP2A and therefore might inhibit the lysosomal degradation pathways in cellular models thereby increase cytotoxicity. The impact of these mutations *in vivo* remains to be explored.

The aim of this study was to determine the impact of CMA-motif mutation using *in vitro* and *in vivo* models:

(1) In *in vitro* studies, we generated inducible cell lines (non-neuronal and neuronal) expressing different C-terminal truncated ( $\Delta$ CT)  $\alpha$ -Synuclein (WT and A53T) containing wild-type or mutated CMA motif ( $\Delta$ CMA). By comparing kinetic degradation curves of  $\alpha$ -Synuclein in these cell lines using western-blot, we found that, unexpectedly, CMA mutation did not lead to significant differences in the kinetics of degradation. There was also no difference in  $\alpha$ -Synuclein clearance between cell lines expressing WT or A53T constructs. To further understand this, we generated two additional cell lines expressing full-length (FL)  $\alpha$ -Synuclein (WT and A53T). Interestingly, we found that A53T mutation slowed down the degradation of overexpressed  $\alpha$ -Synuclein compared to WT in agreement with previous published data.

(2) In *in vivo* studies, two transgenic mouse models expressing C-terminal truncated  $\alpha$ -Synuclein in cerebellar Purkinje cells (PCs) (construct 1: A53T- $\Delta$ CT, construct 2: A53T- $\Delta$ CMA) were generated. The analysis of these animals using histological, biochemical and behavioral approaches was conducted in parallel.  $\alpha$ -Synuclein was highly expressed in the presynaptic areas, and in the cell perikaryon and neurites of PCs. However, the presence of  $\alpha$ -Synuclein oligomers (resistant to proteinase K) was not

detected and there was no significant loss of PC numbers compared to control lines. Moreover, no morphological changes in neuritic layer of PCs were observed. Interestingly, transgenic mice showed impairments in motor behavioral tests (pole-climbing test and open-field). The correlation of these phenotypes with  $\alpha$ -Synuclein related pathology remains unclear. On the other hand, the similar motor behavior and  $\alpha$ -Synuclein protein levels observed in our two transgenic lines suggest that mutation of the  $\alpha$ -Synuclein CMA motif does not affect the clearance kinetics of this protein and consequently does not play a significant pathological role in the *in vivo* model.

Taken together, *in vitro* and *in vivo* data showed that overexpression of C-terminal truncated  $\alpha$ -Synuclein  $\Delta$ CMA does not affect the degradation kinetics of  $\alpha$ -Synuclein.  $\Delta$ CMA also does not result in a differentiation of pathological development in animal models. However, absence of obvious pathology in our animal models limits the interpretation from *in vitro* to *in vivo*.

# 1 Introduction

## 1.1 Generalities

The symptoms of Parkinson's disease (PD) have been described since ancient times. The disease was named in honor of James Parkinson, a London physician, who was the first one to describe the clinical features of this disorder in his monograph entitled "An Essay on the Shaking Palsy" appeared in 1817 (Figure 1.1). The term "Shaking Palsy" or "Paralysis Agitans" was defined in his manuscript as follows:

*"Involuntary tremulous motion, with lessened muscular power, in parts not in action and even when supported; with a propensity to bend the trunk forwards, and to pass from a walking to a running pace: the senses and intellects being uninjured..."*

PD is the second most common neurodegenerative disorder with an average onset age of about 60 years. Around 5 million people throughout the world get PD; the prevalence of PD in industrialized countries is estimated at 0.3% of the population and 1-2% of those older than 60 years. Reported standardized incidence rates of PD are 8-18 per 100 000 person-years. In addition to age, several prospective studies found evidence for a higher incidence of PD in men than in women. Interestingly, cross-cultural variations in the prevalence of PD suggest differences in environmental exposure or distribution of susceptibility genes. In the same manner, PD has been reported to be less common in African and Asian people than in the Caucasian population. The mortality rate is consistently reported to be about two-fold higher for PD patients than the general population (reviewed in Wirdefeldt et al., 2011). Socioeconomic impact of the disease is important, direct and indirect costs spent for PD are estimated at around \$23 billion in United States and €14 billion in Europe. These costs are predicted to increase in upcoming years due to an oncoming wave of world-wide aging population (reviewed in Mhyre et al., 2012; Olanow et al., 2009).

Parkinsonism is defined as a combination of four specific motor features: low-frequency resting tremor, rigidity of the skeletal muscles of the face and hands, slowness of movement (bradykinesia), gait dysfunction or postural instability. PD is the most common form of Parkinsonism representing about 75% of diagnosed movement disorder cases. Not all of these features need to be present but at least two of those are required to be diagnosed for Parkinsonism. Although mainly defined as a movement disorder, the disease can be associated with many non-motor symptoms such as autonomic dysfunction, pain and sensory disturbances, mood or sleep disorders and dementia (Mhyre et al., 2012; Olanow et al., 2009).



*Dr James Parkinson (1755-1824)*



*A Manual of Diseases of the Nervous System (William Richard Gowers, 1886)*

**Figure 1.1: Historical beginning of Parkinson's disease (PD) research.**

In 1817, James Parkinson described the clinical features of this disorder in his manuscript "An Essay on the Shaking Palsy". In 1886, Sir William Richard Gowers documented on PD in his book "A Manual of Diseases of the Nervous System".

## 1.2 Etiology of PD

### 1.2.1 Genetic factors

To date, 5 to 10% of patients with PD have a familial inheritance. At least 16 loci are associated with both autosomal dominant and autosomal recessive forms of monogenetic PD. These genes are designated as *PARK1* to *PARK16* (Table 1.1). The knowledge of monogenetic factors in PD is constantly evolving and the functions of all of these genes have not been fully elucidated. Functional studies of these genes have progressively revealed key converging molecular pathways involving mechanisms leading to neuronal cell death in PD. Impairments of lysosomal pathways and mitochondrial dysfunction are most prominent in PD pathogenesis (Figure 1.2).

Mutations of the two autosomal dominant PD genes *SNCA* (encoding  $\alpha$ -Synuclein) and *LRRK2* (encoding Leucine-rich repeat kinase 2) produce classical, late onset disease with  $\alpha$ -Synuclein-positive Lewy bodies. Accumulation of  $\alpha$ -Synuclein aggregates and other proteins in Lewy bodies is the main histopathology feature of PD. Interestingly,  $\alpha$ -Synuclein mutants are suggested to impair proteolytic systems such as ubiquitin proteasome system (UPS) (Stefanis, 2001) or autophagy-lysosomal pathways (ALP) (Cuervo et al., 2004) which subsequently prevent protein degradation (reviewed in Xilouri M, 2009) (Figure 1.3).

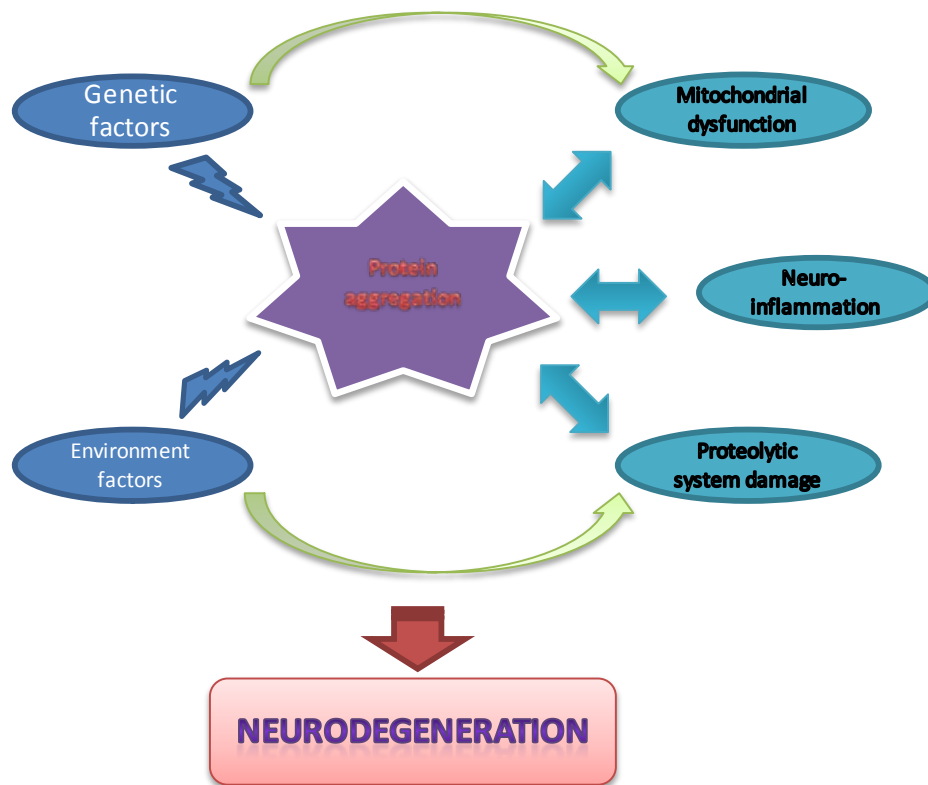


**Figure 1.2: Hypothesis of pathogenesis pathways in PD.**

Schema attempts to illustrate that many factors, and not a individual one, might contribute to events leading to neuronal cell death in PD (adapted from Olanow et al., 2007).

*LRRK2* encodes a large (280 kDa) kinase protein of the ROCO family which is widely expressed in diverse tissues and cell types. ROCO proteins contain a characteristic Ras-of-Complex (ROC) GTPase domain. Interestingly, all of *LRRK2* gene mutations are located in or near the “enzymatic core” of the protein. The native substrates and normal function of *LRRK2* remain however largely unknown. Interestingly, *LRRK2* had been identified *in vitro* to be implicated in diverse pathways including regulation of autophagy-lysosomal pathways (reviewed in Cookson, 2012;Manzoni, 2012).

Mutations of other *PARK* genes are also linked to ALP. Mutations of the *PARK9* gene *ATP 13A2* encoding a large trans-membrane lysosomal ATPase is associated with Kufor-Rakeb syndrome (KRS), a form of recessively inherited atypical Parkinsonism. Certain studies suggest that loss of functional *ATP 13A2* might lead to lysosomal dysfunction and impairs autophagic pathways (Usenovic et al., 2012a;Usenovic et al., 2012b). The most definitive evidence for lysosomal function in sporadic PD came from the discovery that *GBA* mutation carriers develop also Parkinsonism (Cullen et al., 2011). Mutations of *GBA* encoding glucocerebrosidase (GCase) cause Gaucher's disease, a lysosomal storage disorder while GCase enzymatic activity is crucial for lysosomal function (reviewed in Tofaris, 2012).

In contrast to autosomal dominant genes, mutations of autosomal recessive *PARK* genes like *PARKIN*, *PINK1* and *DJ1* tend to cause earlier onset Parkinsonism with or without  $\alpha$ -Synuclein positive Lewy pathology and generally with a more slowly evolving, more clinically manageable disease. Parkin and

PINK1 (PTEN-induced novel kinase -1) have been shown to regulate the process of mitochondria degradation by autophagy (mitophagy). PINK1 exists as a dimer present at mitochondrial membrane and might play a pivotal role in regulation of mitochondrial quality control. Parkin is a cytosolic E3 ubiquitin ligase capable of ubiquitination of mitofusins localized on mitochondrial surface and promotes mitochondrial fusion. Recruitment of Parkin requires the kinase activity of PINK1 under mitochondrial membrane depolarization (Rakovic et al., 2011; Shiba-Fukushima et al., 2012). DJ-1 is known as a chaperone protein which might function as a redox sensor helping to protect mitochondria against oxidative stress (Mullett et al., 2013; Ramsey et al., 2010). Similar pathology symptoms of mutation carriers of these genes and their close intracellular location suggest an interconnection between Parkin, PINK1 and DJ-1 playing a role in maintaining mitochondria integrity (reviewed in Cookson, 2012).

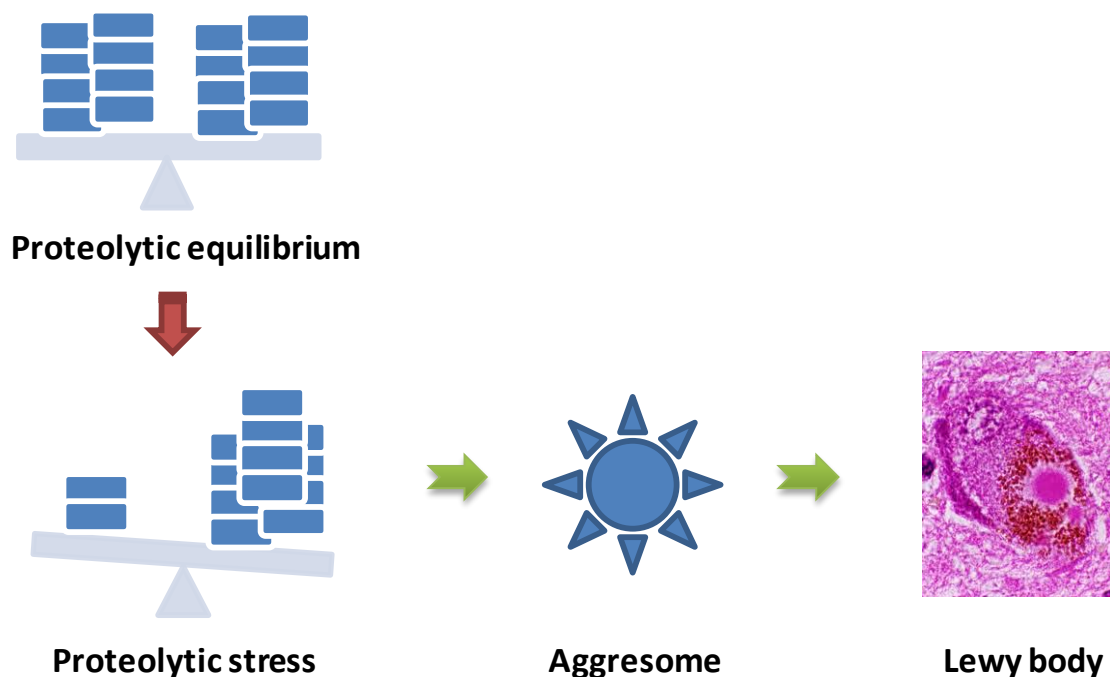


**Figure 1.3: A model for Lewy body (LB) formation.**

Under normal physiological conditions, there is a dynamic balance between the production of unwanted proteins and their degradation. In PD, proteolytic stress is induced as a result of impaired degradation or excess production of unwanted proteins (mutant, misfolded, denatured, and damaged proteins). These proteins begin to accumulate and aggregate and are actively transported along microtubules to the perinuclear centrosome. Sequestered components are encased by cytoskeletal elements such as neurofilaments to form an aggresome with a distinct core and a peripheral halo. If sequestered proteins are successfully degraded, proteolytic equilibrium is restored. However, if the proteolysis in aggresomes fails as a result of defects in the protein degradation machinery or the overwhelming production of abnormal proteins, the aggresome continues to expand and form an insoluble mass of proteins—a Lewy body (adapted from Olanow et al., 2004)

Gene/locus	Chromosomal location	Mode of inheritance	Distinctive clinical features	Reference
<i>SNCA</i> ( <i>PARK1</i> / <i>PARK4</i> )	4q21	Dominant	Relatively early onset, less tremor, rapid progression	Polymeropoulos, 1997 Singleton, 2003
<i>Parkin</i> ( <i>PARK2</i> )	6q25	Recessive	Early-juvenile onset, dyskinesia, dystonia, slow progression	Kitada, 1998
<i>PARK3</i>	2p13	Dominant	Dementia	Gasser, 1998
<i>UHCL-1</i> ( <i>PARK5</i> )	4p14	Dominant	None	Leroy, 1998
<i>PINK1</i> ( <i>PARK6</i> )	1p35-36	Recessive	Early onset, slow progression	Valente, 2004
<i>DJ-1</i> ( <i>PARK7</i> )	1p36	Recessive	Early onset, dystonia, psychiatric symptoms	Bonifati, 2003
<i>LRKK2</i> ( <i>PARK8</i> )	12q12	Dominant	None	Paisan-Ruiz, 2004 Zimprich, 2004
<i>ATP13A2</i> ( <i>PARK9</i> )	1p36	Recessive	Early onset, rapid progression, pyramidal signs, dementia	Ramirez, 2006
<i>PARK10</i>	1p32	-	None	Hicks, 2002
<i>GIGYF2</i> ( <i>PARK11</i> )	2q36-37	-	None	Pankratz, 2002 Lautier, 2008
<i>PARK12</i>	Xq21-25	-	None	Pankratz, 2003
<i>Omi/HtrA2</i> ( <i>PARK13</i> )	2p12	Dominant	None	Strauss, 2005
<i>PLA2G6</i> ( <i>PARK14</i> )	22q12-13	Recessive	Early onset, dystonia, pyramidal signs	Paisan-Ruiz, 2004
<i>FBXO7</i> ( <i>PARK15</i> )	22q12-13	Recessive	Early onset, pyramidal signs	Shojaee, 2008
<i>PARK16</i>	1q32	-	None	Satake, 2009

**Table 1.1: Parkinson's disease genes and loci** (adapted from Wirdefeldt et al., 2011)

### 1.2.2 Environmental factors

While genetic factors may explain disease risks for PD, the majority of PD cases are sporadic. This indicates that environmental factors or life styles represent potential risks for disease development. Interest in environmental factors has been raised over the past decades since the anecdotal report that intravenous injection of MPTP (1-methyl-4-phenyl-1,2,3,6-tetrahydropyridine) induced Parkinsonism in a 23-year-old man (Davis et al., 1979). MPTP is a neurotoxin precursor of MPP+ which is taken up by dopaminergic neurons via the dopamine transporter and provokes dopaminergic neuron loss in the substantia nigra in the brain (reviewed in Przedborski et al., 2004). MPTP has been largely used to generate various animal models for the disease studies (reviewed in

(Porras et al., 2012). Although the exposure risk to MPTP is rare for humans, MPTP structure is very similar to paraquat which is widely used as herbicide. Similarly, another compound frequently used as pesticide or insecticide, rotenone, was also identified to increase the risk of developing PD (reviewed in Tieu, 2011). Supporting this, epidemiological studies have correlated rural living, farming profession and well water use with higher risks of developing PD. However, a causal relationship between pesticides and PD has not been fully established.

Parallel to environmental "neurotoxic" factors, certain "neuroprotective" factors such as smoking, coffee or tea consuming, antioxidants or physical activities have been suggested. Both nicotine (Quik et al., 2012) and caffeine (Kalda et al., 2006) have been identified as neuroprotective factors. Interestingly, nicotine inhibits formation of  $\alpha$ -Synuclein fibrils *in vitro* (Ono et al., 2007). Mechanistically, nicotine may exert its effects by acting on nicotinic receptors (nAChRs) which are widely distributed throughout the brain by enhancing calcium signaling, that activates neuronal survival pathways and decrease apoptotic signals (reviewed in Wirdefeldt et al., 2011). Caffeine may act as an adenosine receptor antagonist. The enrichment of adenosine receptors in basal ganglia offers an interesting, unique non-dopaminergic target for the treatment of PD (reviewed in Wirdefeldt et al., 2011). The role of antioxidants has also been extensively studied based on the hypothesis that an increase in oxidative stress could be harmful to neurons. However, only few links are presently established nowadays between the intake of antioxidants and a lower risk of PD (vitamin E, B6, folic acid and others) and the beneficial effects of some antioxidants risk remain controversial (reviewed in Wirdefeldt et al., 2011).

### 1.3 Neuropathological features of PD

60-70% of dopaminergic neurons are lost in the substantia nigra pars compacta (SNpc or black substance) at the presence of motor symptoms (reviewed in Olanow et al., 2009). Histology studies from PD patients show that the disease is characterized by intracytoplasmic formation of inclusions, also known as Lewy bodies (LBs) or Lewy neurites (LNs) (Figure 1.4). The first descriptions of these inclusions were done by Heinrich Lewy in 1912. Later, the works from Russian neuropathologist Tretiakoff confirmed the presence of these inclusions which were termed as "corps de Lewy". Immunohistochemical staining showed that these inclusions are composed of a variety of proteins, with a majority of  $\alpha$ -Synuclein, ubiquitin (Ub) and neurofilaments (Lennox et al., 1989; Schmidt et al., 1991; Spillantini et al., 1997; Spillantini et al., 1998). They also contain components of the ubiquitin-proteasome system and heat-shock proteins Hsp70 and Hsp90 (Auluck et al., 2002; McNaught et al., 2002). Within LBs, proteins may be oxidized, nitrated, ubiquitinated or phosphorylated (Castellani et al., 2002; Fujiwara et al., 2002; Good et al., 1998). Proteomic studies have demonstrated 296 proteins in cortical LBs, whereas 90 proteins have been identified in brainstem LBs (Leverenz et al., 2007). Other than proteins, these inclusions are enriched in lipids, but carbohydrates and nucleic

acids have not been detected (Gai, 2000). The presence of LBs is, however, not related to cell toxicity, it remains to be elucidated their physiological role in neuron survival and whether their formation is neuroprotective or harmful.

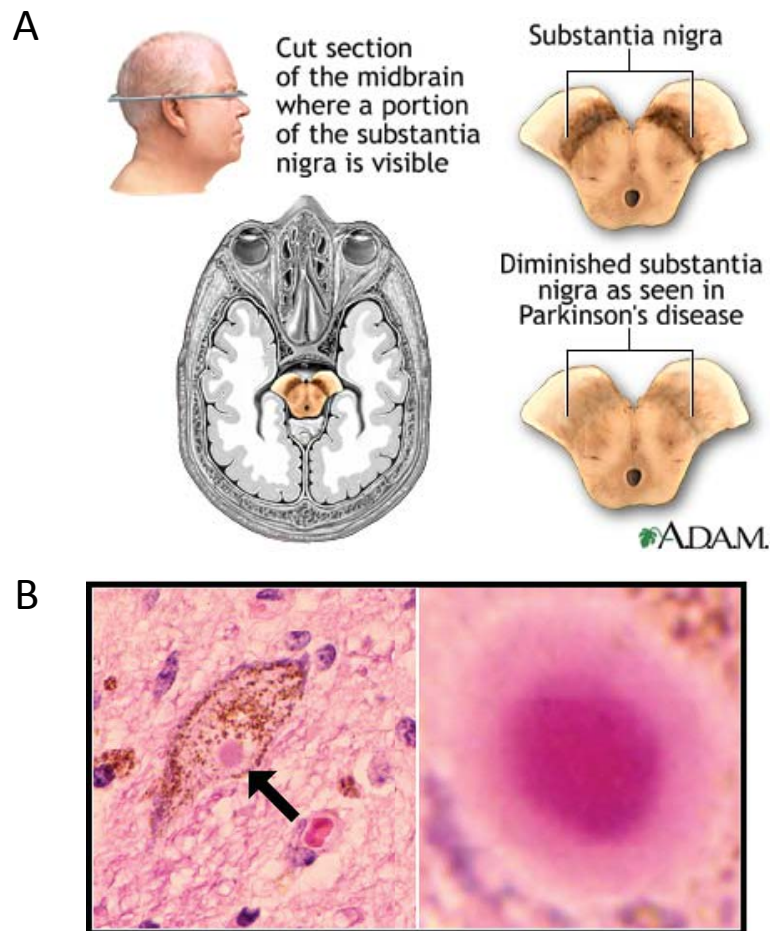


**Figure 1.4: Neuropathology features in PD.**

A: Schema representing loss of dopaminergic neurons in substantia nigra (SN) in PD compared to healthy brain.  
 B: Lewy body in SNc neurons stained with Hematoxylin and Eosin (Olanow and McKnaught, 2011). Structurally, classical LBs are spherical, 8-30  $\mu\text{m}$  in diameter and have pink color with hematoxylin and eosin staining. They are characterized by a central core intensely stained in contrast to peripheral halo which are slightly stained. Under electronic microscopy observation, their center contains dense granular material whereas the outer regions are composed of ordered arrangement of radiating filaments of 7-20 nm in diameter (Olanow et al., 2004)

Although LBs are found typically in dopaminergic neurons of the SNpc, they are also detected in other brain areas, spinal cord or peripheral nervous system. Other neurological disorders are also linked to the presence of LBs, such as dementia with Lewy bodies (DLB), Multiple System Atrophy (MSA) or Alzheimer's disease (AD). Braak's and collaborators have established six characteristic stages of the disease, the so-called "Braak's staging" (Braak, 2003). According to the authors,  $\alpha$ -Synuclein aggregate structures may appear and spread throughout the nervous systems in a "prion-like" manner, following a caudo-rostral progression (Figure 1.5). Recent evidence support this hypothesis: spreading and *in vivo* seeding of  $\alpha$ -Synuclein aggregation was first demonstrated by the

induction of Lewy bodies within normal neuronal stem cells transplanted into Parkinson's disease patients (Kordower et al., 2008; Li et al., 2008). This paradigm was subsequently replicated in mice (Desplats et al., 2009; Hansen et al., 2011; Luk et al., 2009). Moreover,  $\alpha$ -Synuclein exhibits a seeding behavior when introduced into cultured cells (Desplats et al., 2009; Hansen et al., 2011; Nonaka et al., 2010).

In addition to profound dopaminergic cell loss and presence of Lewy pathology, post-mortem analysis of PD brains show increased glial cell (astrocytes and microglia) number and activation state (McGeer et al., 1988). Activation of these cells responds inflammatory signals (Colton, 2009). The exact role of glial cell activation in PD pathogenesis is still debated, however evidence suggests that they might be both "initiators" and "progressors" of neurodegeneration (Halliday and Stevens, 2011).

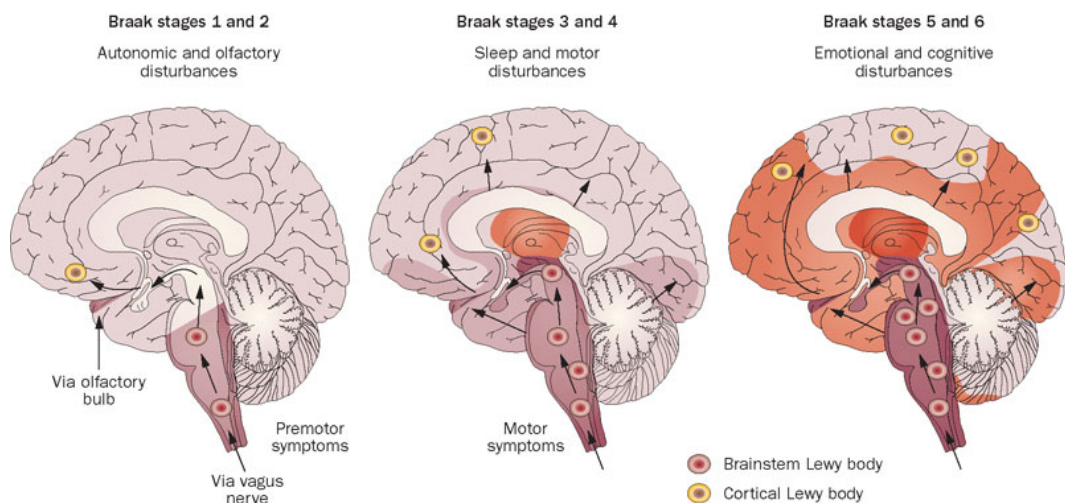


**Figure 1.5: The Braak's staging system of Parkinson's disease.**

Braak's stages showing the initiation sites in the olfactory bulb and the medulla oblongata, through to the later infiltration of Lewy pathology into cortical regions.

Two main subtypes of LBs may exist: classical brainstem LBs and cortical LBs. They are made of un-branched  $\alpha$ -Synuclein filaments at around 200-600 nm of length and 5-10 nm of width. Cortical LBs are eosinophilic, rounded, angular or reniform structures without a halo.

At stage 1, the first  $\alpha$ -Synuclein positive structures occur in the olfactory bulb and/or the dorsal motor nucleus of the glossopharyngeal and vagal nerves. During this stage the patients usually don't manifest motor impairment (pre-motor stage). At stage 2, Lewy pathology develops in the medulla oblongata and the pontine tegmentum. At stage 3, the pathology reaches the amygdala and the substantia nigra. During this stage 3, the motor symptoms of PD start to appear (in general bradykinesia with at least one of three cardinal features of PD such as rigidity, resting tremor or gait disturbance). At stage 4,  $\alpha$ -Synuclein inclusions reach the temporal cortex and the pathology worsens. The end stages 5 and 6 corresponding to the most severe ones,  $\alpha$ -Synuclein inclusions are present in neocortex relating to cognitive problems in most advanced PD patients.

Permission obtained from John Wiley and Sons©Halliday, G. et al. *Mov. Disord.* 26, 1015–1021 (2011)

## 1.4 Neurobiology of $\alpha$ -Synuclein

### 1.4.1 $\alpha$ -Synuclein genetic and primary structure

$\alpha$ -Synuclein aggregates are the principal components of Lewy bodies which are considered as the pathology hallmark of PD.  $\alpha$ -Synuclein is encoded by the *SNCA* or *PARK 1/4* gene located on

chromosome 4q21-q23. This is the first gene identified in familial inheritance of PD causing autosomal dominant PD (Figure 1.6).

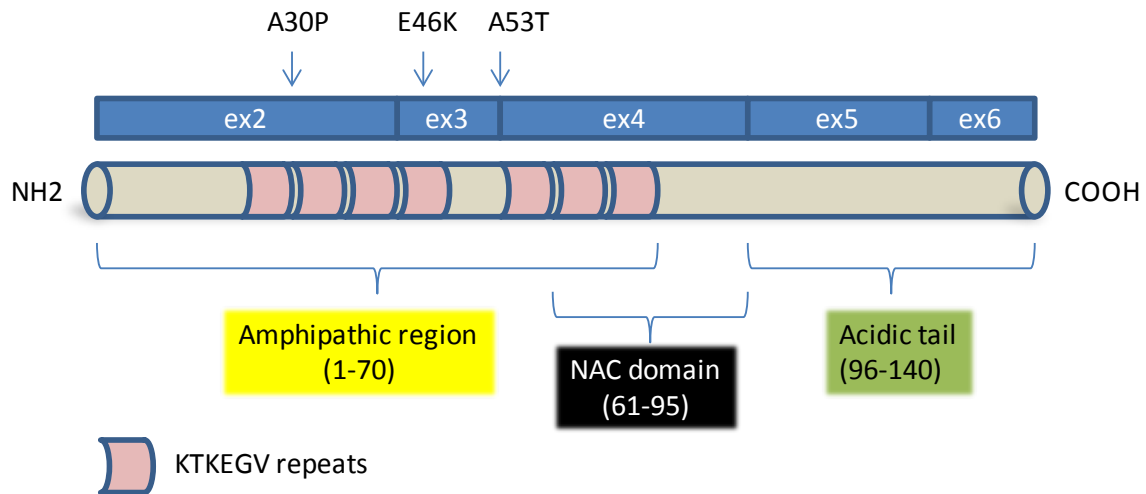


**Figure 1.6:  $\alpha$ -Synuclein gene and primary structure** (adapted from Weinreb et al., 1996 and Dickson et al., 2001)

Synuclein was first isolated from Pacific electric ray *Torpedo californica* and was cloned in 1988 (Maroteaux et al., 1988). The name Synuclein was proposed due to its localization in the nuclear envelope of neurons and in presynaptic nerve terminals. In 1993, Uéda et al. detected the non-A $\beta$ -component amyloid (NAC) fragment of Alzheimer's disease (AD) and interestingly, this fragment corresponds to the central part of  $\alpha$ -Synuclein (aa 61-95). From 1996 to 1998, successive work demonstrated that  $\alpha$ -Synuclein is a major component of the proteinaceous inclusions such as Lewy bodies or Lewy neurites in brains of patients with PD or DLB (Arima et al., 1998; Forno et al., 1996; Spillantini et al., 1997; Spillantini et al., 1998). The key years of  $\alpha$ -Synuclein discovery were marked by the findings of two familial mutations of PD in 1997 by Polymeropoulos et al. (substitution of Ala 53 by Thr or A53T) and 1998 by Kruger et al. (substitution of Ala 30 by Pro or A30P). Later, a third point mutation (substitution of Glu 46 Lys or E46K) was identified (Zarranz, 2004). Point mutations of *SNCA* gene remain extremely rare: A53T mutation has been found in only 15 Greek/Italian families who probably have a common ancestor and in two other Korean and Swedish PD families, but on different haplotype backgrounds. A30P and E46K were each found in one single family, German and Spanish respectively. Clinically, patients with A53T mutation represent relative young onset with rapid progression of the disease, whereas A30P mutation patients correspond to sporadic PD patients with mild phenotype. Patients with E46K mutations have the most severe Parkinsonism with early onset age and diffuse Lewy body dementia (reviewed in Corti et al., 2011). Furthermore, duplication and multiplication of the gene locus encoding  $\alpha$ -Synuclein have been associated with inherited forms of autosomal dominant PD (Chartier-Harlin et al., 2004; Ibanez et al., 2004; Singleton, 2003) leading to the hypothesis of a dose relationship between  $\alpha$ -Synuclein levels and severity of the

disease. The most common genetic predisposition of PD is due to Synuclein since it is found in around 15 families worldwide (reviewed in Corti et al., 2011).

Since its discovery,  $\alpha$ -Synuclein is widely accepted as being a monomeric, unfolded or disordered protein adopting a helical conformation when it binds to phospholipid membrane (Weinreb et al., 1996). However, this concept has been recently challenged by (Bartels et al., 2011; Wang et al., 2011b) who suggested that native forms of  $\alpha$ -Synuclein from human cell lines and red blood cells exist predominantly as structured (ordered) tetramers which may better resist aggregation. Structurally,  $\alpha$ -Synuclein is composed of three distinct domains: (1) The N-terminal (residues 1-70) is basic and highly conserved containing 7 imperfectly repeated hexamer (KTKEGV) motifs contributing essentially to its capacity to bind to lipid membranes, (2) The central part or NAC domain (residues 61-95) is variable and highly hydrophobic playing a determinant role in the oligomerization and fibrillization of  $\alpha$ -Synuclein. This NAC domain itself is able to form amyloid fibrils and its deletion or disruption can abolish the ability of  $\alpha$ -Synuclein to form fibrils as in the case for  $\beta$ -Synuclein, (3) The C-terminal (residues 96-140) is less well conserved, highly acidic and might function as a protein scaffold to recruit additional proteins (Davidson et al., 1998; George, 2002) (Figure 1.6).

#### 1.4.2 Synuclein family

The Synuclein family is a highly conserved family of small proteins. Members of synuclein family are only found in vertebrate and not in prokaryotic organisms. Thus, these proteins are widely accepted as having novel roles in eukaryotic cells without having ancestors from prokaryotic organisms. The apparition of these proteins probably corresponds to the requirement for novel sophisticated regulation of CNS processes such as synaptic transmission and plasticity, in vertebrate organisms during evolution.

The human  $\alpha$ -, $\beta$ -, $\gamma$ - Synuclein genes are mapped respectively to chromosomes 4q21.3-q22, 5q35 and 10q23.  $\alpha$ -Synuclein gene is organized in seven exons (five protein-coding exons),  $\beta$ -Synuclein has six exons (five protein-coding exons) and  $\gamma$ -Synuclein has five protein-coding exons. The translation start codon ATG is encoded by exon 2 and the stop codon TAA is encoded by exon 6. The NAC domain is encoded by exon 4. The predominant isoform of  $\alpha$ -Synuclein in humans is composed of 140 aa. The three other  $\alpha$ -Synuclein isoforms are composed of respectively 112, 126 and 98 aa (reviewed in Surguchov, 2008). The last one is overexpressed in the frontal cortices of LB disease and AD brains and is supposed to have very high amyloidogenic properties.  $\beta$ - and  $\gamma$ - Synuclein differ from  $\alpha$ -Synuclein by a lower propensity to form amyloid fibrils due to the absence of the NAC domain in  $\beta$ -Synuclein and the higher structural stability of  $\gamma$ -Synuclein (reviewed in Surguchov, 2008).

### 1.4.3 Localizations and physiological functions

$\alpha$ -Synuclein is abundantly expressed in nervous system and accounts for 1% of total soluble cytosolic protein (Iwai et al., 1995). For a long time,  $\alpha$ -Synuclein was considered mainly as an intracellular protein since it lacks the peptide signal for secretion. However, growing evidence shows the presence of extracellular  $\alpha$ -Synuclein supporting the hypothesis of cell-to-cell transfer of  $\alpha$ -Synuclein and the theory of prion-like spreading of  $\alpha$ -Synuclein in PD (Desplats et al., 2009; Luk et al., 2009; Volpicelli-Daley et al., 2011).  $\alpha$ -Synuclein is highly expressed in erythrocytes, platelets or lymphocytes. The mechanism of  $\alpha$ -Synuclein secretion has been reviewed and discussed by (Marques and Outeiro, 2012). In brain tissue, the protein is predominantly present at presynaptic terminals and less apparent in soma (Kahle, 2008). Due to structural similarities to fatty-acid binding proteins, especially the amphipathic feature of the N-terminal region,  $\alpha$ -Synuclein is prone to bind lipid vesicle membranes. Indeed, monomeric  $\alpha$ -Synuclein fluctuates both between free and membrane-bound state and the amount of membrane-bound  $\alpha$ -Synuclein was estimated to be around 15% in rat brain (Lee et al., 2002). The affinity of different  $\alpha$ -Synuclein mutants for lipidic membranes is variable: A30P is known for its low affinity whereas E46K is more tightly bound. A53T and WT  $\alpha$ -Synuclein however have similar affinities to membranes (Bussell and Eliezer, 2004; Choi et al., 2004).

Due to its abundant presence in the pre-synaptic regions and its lipid-binding properties, the main physiological function of  $\alpha$ -Synuclein is thought to be involved in the regulation of synaptic vesicle turnover and neurotransmitter release. Knock-down of  $\alpha$ -Synuclein in primary hippocampal neurons seems to reduce the reserve vesicle pool (Cabin et al., 2002; Murphy et al., 2000).  $\alpha$ -Synuclein-depleted mice are viable, fertile and do not show obvious pathological abnormalities (Abeliovich et al., 2000). However the absence of  $\alpha$ -Synuclein in mice results in reduced dopamine content in the striatum, but no loss of dopaminergic neurons (Al-Wandi et al., 2010). In the same manner,  $\alpha$ -, $\beta$ -, $\gamma$ -Synuclein triple knock-out mice show decrease in the synaptic size in the CA3 hippocampus of old mice (Al-Wandi et al., 2010), decrease levels of dopamine and its metabolites in the striatum and impaired motor behavior (Anwar et al., 2011). There is substantial proof that  $\alpha$ -Synuclein has an important role in the biology of SNARE proteins which are responsible for facilitating membrane fusion events. Knock-down of Cysteine-string protein  $\alpha$  (Csp $\alpha$ ), a co-chaperone promoting the SNARE complex assembly at synapses, leads to severe neurodegeneration, whereas overexpressing of  $\alpha$ -Synuclein in these mice rescues the motor impairment (Chandra et al., 2005). *In vitro*,  $\alpha$ -Synuclein binds to Synaptobrevin-2 and directly catalyzes SNARE complex assembly, whereas there is a decrease in SNARE markers during aging in Synuclein triple knock-out mice (Burré et al., 2010).

Other than the roles in regulation of synaptic vesicle dynamics, some other physiological functions of  $\alpha$ -Synuclein have been reported. Indeed,  $\alpha$ -Synuclein is implicated in the biosynthesis of dopamine

(DA) since it indirectly reduces the activity of tyrosine hydroxylase, the rate-limiting enzyme in DA synthesis (Perez et al., 2002) by activating protein phosphatase 2A (PP2A) (Peng et al., 2005).  $\alpha$ -Synuclein is also implicated in the regulation of endoplasmic reticulum (ER) or Golgi vesicle trafficking (Cooper et al., 2006). A chaperone-like activity of certain enzymes such as esterases and alcohol dehydrogenase has also been proposed for  $\alpha$ -Synuclein (Ahn et al., 2006; Rekas et al., 2012; Souza et al., 2000b).

#### 1.4.4 Propensity of $\alpha$ -Synuclein for oligomerization and aggregation

$\alpha$ -Synuclein can adopt different conformation states and aggregated morphologies including small aggregates, oligomers, protofibrils and fibrils. The aggregation process initially forms oligomeric species that are relatively soluble, these oligomers can then self-assemble to fibrillar structures which become more and more insoluble (Conway et al., 1998; Giasson et al., 1999). *In vitro*,  $\alpha$ -Synuclein fibrillization can be visualized by atomic force microscopy (AFM) (Khurana et al., 2003) (Figure 1.7) and these amyloid fibrils can be stained with fluorescent probes such as Thioflavin T or Congo Red (Naiki et al., 1989). In brain tissues,  $\alpha$ -Synuclein fibrils can be immunolabelled (Games et al., 2013; Spillantini et al., 1998) or visualized by electronic microscopy (Tofaris et al., 2006). Insoluble  $\alpha$ -Synuclein oligomers have been sequentially extracted from brain lysates by ultracentrifugation (Kahle et al., 2001). Insoluble  $\alpha$ -Synuclein fibrils are resistant to proteinase-K digestion and can be immunolabelled after digestion using specific antibodies (Neumann et al., 2002).

##### 1.4.4.1 Factors modulating $\alpha$ -Synuclein aggregation

###### 1.4.4.1.1 Physical properties

Physically, the  $\alpha$ -Synuclein monomer has a typical random coil conformation at neutral pH (Uversky et al., 2001b). *In vitro*, the unfolded structure of  $\alpha$ -Synuclein has relatively low hydrophobicity, but this structure is labile and flexible depending on pH and temperature of the environment: for example at pH 3.0 or at high temperature,  $\alpha$ -Synuclein gains some ordered secondary structure and becomes more compact or adopts a partially folded conformation (Uversky et al., 2001a).

###### 1.4.4.1.2 Genetic mutations

Familial mutant forms of  $\alpha$ -Synuclein accelerate its aggregation *in vitro* at different manners. Indeed, in dilute solution the A30P and A53T mutants have similar disordered structures like the WT but at higher concentrations both mutants rapidly aggregate, with the A53T mutant showing the highest acceleration compared to the WT. No fibrillizations but just oligomer formation was observed for A30P (Conway et al., 1998; Li et al., 2001). The third familial mutant E46K accelerates fibrillization (Greenbaum et al., 2005; Lewis et al., 2010). These observations might explain the pathogenicity of  $\alpha$ -Synuclein genetic mutations during PD pathogenesis (Figure 1.7).

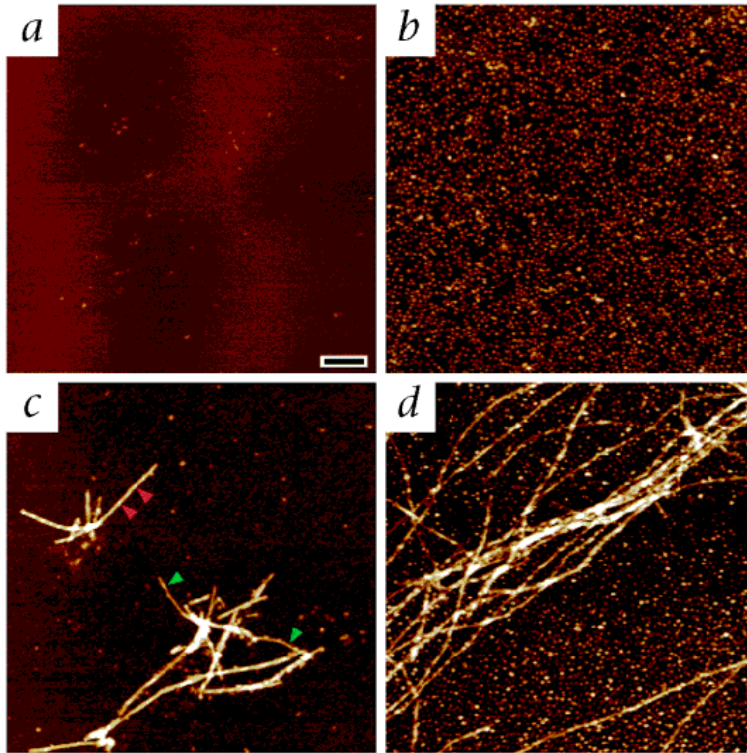


**Figure 1.7: Atomic force microscopy images.**

Solutions of  $\alpha$ -Synuclein were incubated for 3 weeks at a concentration of 300  $\mu$ M (a, WT; b, A30P; c, A53T) or 8 weeks at 50  $\mu$ M (d, A53T) (from Conway et al., 1998)

#### 1.4.4.2 *Post-translational modifications (PTMs)*

##### 1.4.4.2.1 Phosphorylation

Phosphorylation is one of the major PTMs of  $\alpha$ -Synuclein. In human brain, phosphorylated  $\alpha$ -Synuclein exists naturally and is concentrated in the regions of the nucleus basalis of Meynert (MN) and substantia nigra (SN) (Muntané et al., 2012). The level of phosphorylated  $\alpha$ -Synuclein is increased in pathological stages. In patient brains with PD, 90% of  $\alpha$ -Synuclein in LB or inclusions is phosphorylated at Ser129 (Anderson et al., 2006; Fujiwara et al., 2002). An additional phosphorylation site is mapped at Ser87 *in vitro* (Okochi et al., 2000). A recent report from Lashuel's lab showed that phosphorylation at position Ser87 is increased in brains of transgenic models of synucleopathies and patients with AD, DLB and MSA (Paleologou et al., 2010). Whether phosphorylation promotes or prevents aggregation is still a matter of debate. *In vitro* phosphorylation at Ser 129 (P-Ser129) inhibits fibrillization while mutants with substitution of Ser by Ala (S129A) form more fibrils (Paleologou et al., 2008). Mimicking phosphorylation of Ser87 by expressing mutant S87E also inhibits fibril formation in a rat model (Oueslati et al., 2012). Interestingly, in flies expressing the S129A mutant there are five times more insoluble, proteinase K resistant inclusions (Chen and Feany, 2005; Azeredo da Silveira et al., 2009). On the other hand, expression of S129A in SH SY5Y cells has been reported to dramatically decrease eosinophilic

cytoplasmic inclusions (Smith et al., 2005) or at least does not increase inclusions (Gorbatyuk et al., 2008;McFarland et al., 2009).

#### 1.4.4.2.2 Ubiquitination

Ubiquitination of  $\alpha$ -Synuclein is found in LBs (Gomez-Tortosa et al., 2000; Spillantini et al., 1998), (Sampathu et al., 2003; Tofaris et al., 2003). Purified protein from LBs confirmed that a fraction of  $\alpha$ -Synuclein is ubiquitinated (Anderson et al., 2006; Sampathu et al., 2003; Tofaris et al., 2003). Interestingly, the majority of  $\alpha$ -Synuclein found in LBs is mono-ubiquitinated. *In vivo* and *in vitro*  $\alpha$ -Synuclein is ubiquitinated by E3-ligases: Parkin, UCHL-1 and SIAH (Lee et al., 2008;Liani et al., 2004;Rott et al., 2008). The protein sequence of  $\alpha$ -Synuclein contains 15 lysine sites which can be potentially ubiquitinated (Nonaka et al., 2004; Rott et al., 2008). Another study using semi-synthetic monoubiquitin-modified  $\alpha$ -Synuclein showed that this ubiquitination site influences the aggregation rate (Meier et al., 2012).

#### 1.4.4.2.3 Truncation

Truncation of  $\alpha$ -Synuclein is a normal event in human brains and its concentration is directly proportional to the amount of full-length  $\alpha$ -Synuclein found in each brain region (Muntané et al., 2012). Several cleaved species of  $\alpha$ -Synuclein from LB including both N- and C-terminal truncations have been detected (Anderson et al., 2006; Chen and Feany, 2005). Importantly, *in vitro* truncation of C-terminus at different cleavage sites leads to faster fibrillization of  $\alpha$ -Synuclein (Liu et al., 2005b;Murray et al., 2003).

The C-terminal region (from residues 95 to 140) of  $\alpha$ -Synuclein is highly acidic and negatively charged. These negative charges are essential for the regulation of the kinetics of fibril formation: decreases in C-terminus charges shifts  $\alpha$ -Synuclein to wards fibrillar species (Hoyer et al., 2004;Levitan et al., 2011). Hong et al. (2011) proposed that C-terminal region forms bisulfide bonds with other regions inside of the  $\alpha$ -Synuclein monomer structure stabilizing it. Therefore in the absence of this C-terminus, aggregation is enhanced. In the same direction, Izawa et al. (2012) demonstrated that Tyr residues at the C-terminal region, especially Tyr136, are particularly implicated in the regulation the fibrillization kinetics and mutation of these residues dramatically decreases the time and rate of fibril formation.

*In vivo* data support these *in vitro* observations. Expression of  $\alpha$ -Synuclein ( $\Delta$ CT 1-110 and  $\Delta$ CT 1-120) in SH-SY5Y cell increases cell death (Liu et al., 2005b). Expression of C-terminal truncated  $\alpha$ -Synuclein ( $\Delta$ CT, 1-120) in *Drosophila* increases oligomer levels and reduces the number of dopaminergic neurons (Periquet et al., 2007). Pathological changes in the olfactory bulb and substantia nigra have been observed in mice expressing  $\alpha$ -Synuclein ( $\Delta$ CT, 1-120) driven by TH promoter (Tofaris et al., 2006). Remarkably, expression of  $\alpha$ -Synuclein ( $\Delta$ CT, 1-130) controlled by the same TH promoter

causes selective cell loss in the SNc and abnormal motor behavior. More interestingly, homozygote expression of  $\alpha$ -Synuclein ( $\Delta$ CT, 1-130) causes embryonic death (Wakamatsu et al., 2008). (Daher et al., 2009) have reported a reduction of striatal dopamine release without loss of dopaminergic neurons in mice expressing inducible  $\alpha$ -Synuclein ( $\Delta$ CT, 1-119) under the control of the ROSA26 promoter.

In addition to phosphorylation and ubiquitination, other PTMs of  $\alpha$ -Synuclein have also been explored, such as nitration (Souza et al., 2000a), sumoylation (Dorval and Fraser, 2006) and or methionine-oxidation (Glaser et al., 2005). Their potential influences on  $\alpha$ -Synuclein aggregation remain to be elucidated (reviewed in Surguchov, 2008 and Myhre et al., 2012).

## 1.5 Current therapies in PD

Pathologically, PD is characterized by profound loss of dopaminergic neurons in substantia nigra pars compacta (SNpc) which modulate motor circuits. Although there are therapies available to treat motor symptoms, an effective cure of PD does not exist. Dopamine replacement (L-DOPA and dopamine agonists) remains the most common therapy in PD treatment. The introduction of levodopa (L-DOPA) in the late 1960s was a major progress in improving life quality of PD patients (Carlson, 1959; Schwab et al., 1969). L-DOPA is a precursor of dopamine which is able to cross the blood-brain barrier. In the body, L-DOPA is converted to dopamine under action of DOPA decarboxylase (Figure 1.8). However, treatment with L-DOPA causes later complications such as motor-fluctuations or dyskinesia (Shannon et al., 1987). Alternatively, surgical techniques have been developed in an attempt to control motor symptoms using deep brain stimulation (DBS) for patients who do not respond well to medications (Benabid et al., 1987). Lack of knowledge in the neuronal circuitries to be targeted remains a major limit of this technique.

In the near future, based on current concepts of pathogenesis of cell death in PD, many putative neuroprotective agents are being proposed for clinical trials. However, most of the encouraging pre-clinical investigations have unfortunately so far not been translated successfully from animal models to PD. Absence of a well established biomarker and detailed knowledge of the pathogenesis pathways of PD remain principal limiting factors in PD research (reviewed in Olanow et al., 2009; Myhre et al., 2012).

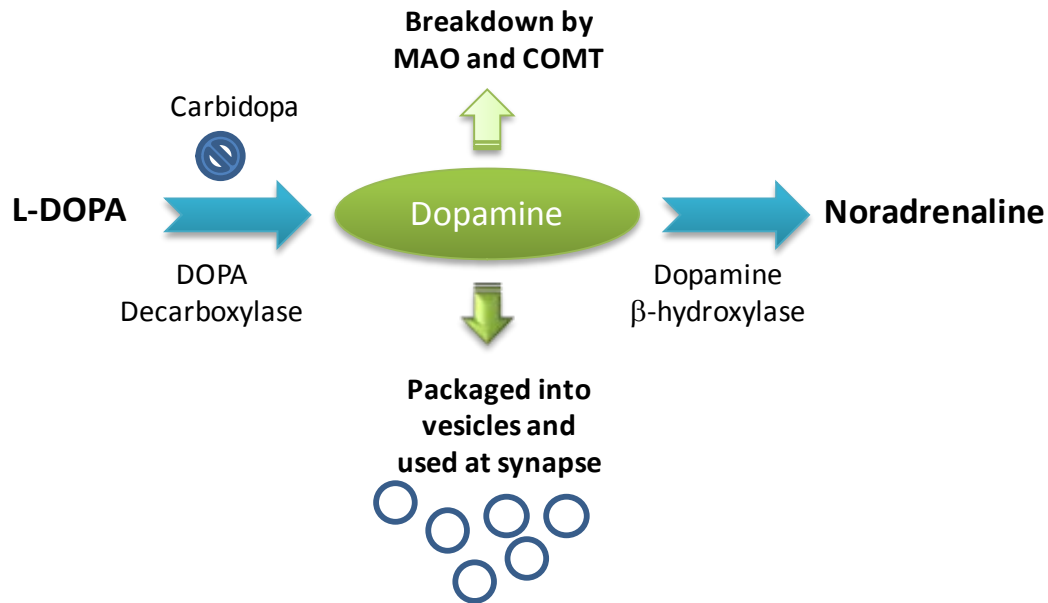


**Figure 1.8: Dopamine synthesis and activity in neurons.**

L-DOPA is converted to Dopamine catalyzed by DOPA decarboxylase enzymes (blocked by Carbidopa). Induced dopamine is either used in synaptic vesicles, degraded by MAO or COMT enzymes or transformed into noradrenaline (adapted from Olanow et al., 2009)

## 1.6 Animal modeling for PD research

Lack of good animal models mimicking the pathogenesis the disease is problematic in PD research. An ideal model should reproduce the main pathological and clinical features of PD consisting of cell loss in the dopaminergic and non-dopaminergic systems with motor or non-motor symptoms. Moreover, the age-dependent onset and progressive apparition of the symptoms are appreciable criteria. Unfortunately, at this stage of advancement, none of current animal models display all these key PD features (reviewed in Chesselet and Richter, 2011; Magen and Chesselet, 2010)).

Current animal models of PD can be divided into two categories: neurotoxic and genetic models. Each group of models has strengths and weaknesses. Neurotoxic animal models are produced by lesioning dopaminergic systems using specific targeting drugs (neurotoxin models). These models have advantages as they induce rapid and robust nigrostriatal cell loss accompanied by severe motor-symptoms. The disadvantages are that they do not mimic either the progressive nature of the disease or the late age-onset or non-motor symptoms (reviewed in Bové and Perier, 2012;Tieu, 2011). The most common neurotoxins used to generate nigrostriatal lesions in PD animals models are 6-Hydroxydopamine (6-OHDA) (Senoh et al., 1959), MPTP (Davis et al., 1979), paraquat (Snyder and D'Amato, 1986) and rotenone (Heikkila et al., 1985) (Table 1.2).

Models	Nigro-striatal damage	Behavioral alterations	Lewy-bodies/ $\alpha$ -Synuclein inclusions	Reference
6-OHDA (unilateral injection into rodent MFB)	<ul style="list-style-type: none"> <li>• 90% loss of dopaminergic neurons</li> <li>• Dose-dependent loss of striatal dopamine innervation</li> </ul>	<ul style="list-style-type: none"> <li>• Quantifiable turning behavior after systemic administration of a dopaminergic agonist</li> <li>• Bradykinesia and impaired paw use on contralateral side</li> </ul>	No intracellular inclusions	Przedborski, 1995
6-OHDA (unilateral injection into rodent striatum)	<ul style="list-style-type: none"> <li>• 30-75% loss of dopaminergic neurons</li> <li>• Circumscribed loss of striatal dopamine innervation at injection site</li> </ul>	<ul style="list-style-type: none"> <li>• Quantifiable turning behavior after systemic administration of a dopaminergic agonist</li> <li>• Bradykinesia and impaired paw use on contralateral side after multiple injections</li> </ul>	No intracellular inclusions	Kirik, 1998
MPTP (acute mouse model)	<ul style="list-style-type: none"> <li>• 70% loss of dopaminergic neurons</li> <li>• Reduced dopamine levels in the striatum</li> </ul>	Motor and coordination impairments in challenging situations	No intracellular inclusions	Jackson-Lewis, 1995
MPTP (chronic mouse model)	<ul style="list-style-type: none"> <li>• 30-50% loss of dopaminergic neurons</li> <li>• Reduced dopamine innervation in the striatum</li> </ul>	Motor and coordination impairments in aged mice	<ul style="list-style-type: none"> <li>• Increase <math>\alpha</math>-Syn immunoreactivity in the SN</li> <li>• No intracellular inclusions</li> </ul>	Perier, 2007
MPTP (non human primate model)	<ul style="list-style-type: none"> <li>• 60-90% loss of dopaminergic neurons</li> <li>• Reduced dopamine innervation in the striatum</li> </ul>	<ul style="list-style-type: none"> <li>• Motor impairments resembling PD symptoms</li> <li>• Cognitive impairments</li> </ul>	Inclusions resembling LBs in locus coeruleus of old monkeys	Langston, 1984
Rotenone (in rodents)	<ul style="list-style-type: none"> <li>• 20-75% loss of dopaminergic neurons</li> <li>• Reduced dopamine innervation in the striatum (rat)</li> <li>• Reduced TH levels in the striatum (mouse)</li> </ul>	<ul style="list-style-type: none"> <li>• Reduced motor activity (rats) and endurance time in rotarod (mouse)</li> </ul>	$\alpha$ -Syn aggregation in dopaminergic and other neuron populations	Betarbet, 2000
Paraquat (in mice)	<ul style="list-style-type: none"> <li>• &lt;20% loss of dopaminergic neurons</li> <li>• Little changes in dopamine innervation in the striatum</li> </ul>	• No clear motor impairments	<ul style="list-style-type: none"> <li>• Increase <math>\alpha</math>-Syn immunoreactivity in the SN</li> <li>• No intracellular inclusions</li> </ul>	Thiffault, 2000

**Table 1.2 : Representative neurotoxic animal models** (adapted from Bove and Perier, 2012)

Alternatively, progress in genetic studies has linked some key genetic mutations to the pathogenesis of PD which have permitted lead to the production of an increasing number of transgenic models. Several transgenic animal models have been generated; the most common overexpress WT or mutant human  $\alpha$ -Synuclein in mice ("humanized models") using different exogenous promoters. The use of exogenous promoters is often helpful as they drive high transgene expression. However, distribution and expression of human  $\alpha$ -Synuclein differs from endogenous level. Mouse and human

promoters differ too, leading to differences in expression in mouse model compared to the situation in humans. Additionally, different genetic backgrounds between animal models potentially result in different histopathologies or phenotypes. At this stage, no mouse model is known to develop true LBs, although  $\alpha$ -Synuclein oligomeric structures can be detected. Behavior impairments are also variable between models and do not always mimic the progression of motor decline seen in patients (reviewed in Chesselet et al., 2010 and 2011). To overcome obstacles due to the use of exogenous promoters, bacterial artificial chromosomes (BAC) that allow expression of  $\alpha$ -Synuclein under its normal promoter are being used to generate transgenic mice, and these models will hopefully shed light on the physiological functions and pathological pathways of  $\alpha$ -Synuclein (reviewed in Lu, 2009) (Table 1.3).

Transgene	Promoter	Histology	Biochemistry	Neurochemistry	Behavior	Reference
WT SNCA	PDGF $\beta$	<ul style="list-style-type: none"> <li>Marked somal and neuritic accumulation of transgenic <math>\alpha</math>-Syn</li> <li>Amorphous inclusions</li> </ul>	Detergent-insoluble transgenic $\alpha$ -Syn	Non progressive reduction of TH+ neurons and terminals	Mild reduction of locomotor activity	Masliah, 2000
WT SNCA	CaM-tTA	<ul style="list-style-type: none"> <li>Somatodendritic accumulation of transgenic <math>\alpha</math>-Syn</li> <li>Highest expression in the forebrain</li> </ul>		Trend of reduction of TH+ neurons in SN	<ul style="list-style-type: none"> <li>Young onset</li> <li>Progressive reduction of locomotor activity</li> </ul>	Nuber, 2008
A53T SNCA	CaM-tTA	<ul style="list-style-type: none"> <li>Somatodendritic accumulation of transgenic <math>\alpha</math>-Syn</li> <li>Gliosis</li> </ul>	Phosphorylated, ubiquitinated transgenic $\alpha$ -Syn	-	Memory impairment	Lim, 2011
WT SNCA	mThy-1	Somatodendritic accumulation of transgenic $\alpha$ -Syn	-	-	Very young onset sensorimotor impairments	Fleming, 2006
A53T SNCA	mThy-1	<ul style="list-style-type: none"> <li>Marked somal and neuritic accumulation of transgenic <math>\alpha</math>-Syn</li> <li>Amorphous inclusions</li> </ul>	-	-	Fulminant progressive neuromuscular junction loss	Van der Putten, 2000
A30P SNCA	mThy-1	<ul style="list-style-type: none"> <li>Somatodendritic accumulation of transgenic <math>\alpha</math>-Syn</li> <li>Argyrophilic, thioflavin S-positive fibrillar inclusions</li> </ul>	<ul style="list-style-type: none"> <li>Detergent-insoluble transgenic <math>\alpha</math>-Syn aggregates</li> <li>Progressive proteinase K resistant</li> </ul>	Normal	Progressive cognitive and locomotor decline	Kahle, 2000

Transgene	Promoter	Histology	Biochemistry	Neurochemistry	Behavior	Reference
A53T SNCA	mPrion	<ul style="list-style-type: none"> <li>• Somatodendritic accumulation of transgenic <math>\alpha</math>-Syn</li> <li>• Argyrophilic, thioflavin S-positive fibrillar inclusions</li> <li>• Gliosis</li> <li>• Neurodegeneration</li> </ul>	Detergent-insoluble transgenic $\alpha$ -Syn aggregates	Normal	Progressive locomotor decline	Giasson, 2002
A30P SNCA	hamPrion	<ul style="list-style-type: none"> <li>• Somatodendritic accumulation of transgenic <math>\alpha</math>-Syn</li> <li>• Gliosis</li> </ul>	$\alpha$ -Syn aggregates	Normal	Progressive locomotor decline	Gomez-Isla, 2003
WT SNCA	ratTH	<ul style="list-style-type: none"> <li>• Somatodendritic accumulation of transgenic <math>\alpha</math>-Syn</li> <li>• No fibrillar inclusion</li> </ul>	-	Normal	Normal	Richfield, 2002
A30P SNCA	ratTH	<ul style="list-style-type: none"> <li>• Somatodendritic accumulation of transgenic <math>\alpha</math>-Syn</li> </ul>	Normal	Normal	-	Rathke-Hartlieb, 2001
A53T SNCA	ratTH	<ul style="list-style-type: none"> <li>• Somatodendritic accumulation of transgenic <math>\alpha</math>-Syn</li> </ul>	-	-	-	Richfield, 2002
A30P +A53T SNCA	ratTH	<ul style="list-style-type: none"> <li>• Somatodendritic accumulation of transgenic <math>\alpha</math>-Syn</li> <li>• No fibrillar inclusion</li> </ul>	-	Reduction of TH+ neurons and DA levels upon aging	Mild reduction of locomotor activity upon aging	Matsuoka, 2001
Truncated 1-120 WT SNCA	ratTH	<ul style="list-style-type: none"> <li>• Somatodendritic accumulation of transgenic <math>\alpha</math>-Syn</li> <li>• Thioflavin S-positive fibrillar inclusions</li> </ul>	Detergent-insoluble transgenic $\alpha$ -Syn	Very young onset, non progressive DA reduction	Progressive locomotor decline	Tofaris, 2006
Truncated 1-130 A53T SNCA	ratTH	Somatodendritic accumulation of transgenic $\alpha$ -Syn	-	Embryonal, non progressive DA reduction	Reduction locomotion	Wakamatsu, 2008
A53T SNCA	$\alpha$ -Syn (BAC)	$\alpha$ -Syn expression in brain and in colon	Proteinase K-resistant aggregates in enteric neurons	-	<ul style="list-style-type: none"> <li>• Reduction of colonic motility</li> <li>• Progressive reduction of locomotion</li> </ul>	Kuo, 2010

**Table 1.3: Representative  $\alpha$ -Synuclein transgenic animal models** (adapted from Kahle, 2008 and Chesselet et al., 2011)

## 1.7 Reduction of $\alpha$ -Synuclein burden is a potential therapeutic strategy for PD

Although pathophysiology mediated by  $\alpha$ -Synuclein misfolding and aggregation is not fully understood, reduction of  $\alpha$ -Synuclein burden by preventing formation of  $\alpha$ -Synuclein oligomers and fibrils appears to be a convincing strategy. Unfortunately, there are no validated inhibitors of  $\alpha$ -Synuclein oligomerization in clinical trials. In this context, maintaining  $\alpha$ -Synuclein homeostasis might

be an attractive approach. However the mechanisms by which  $\alpha$ -Synuclein is degraded under normal and pathological conditions remains largely unknown. Theoretically, ubiquitin-proteasome system (UPS) and autophagy-lysosomal pathways (ALP) are the major degradation systems of intracellular proteins and their implication in neurodegenerative diseases have been investigated extensively (reviewed by Ciechanover, 2013; Ihara et al., 2012).

### 1.7.1 $\alpha$ -Synuclein has been proposed to be a substrate of both UPS and ALP

#### 1.7.1.1 $\alpha$ -Synuclein was firstly described to be degraded by UPS

Due to its crucial role in regulating the intracellular protein burden, the UPS is being extensively researched in human disease therapies including neurodegenerative diseases (Ciechanover, 2013). The first link between  $\alpha$ -Synuclein and UPS in cell culture was established by (Bennett et al., 1999) who showed that inhibition of UPS in SH-SY5Y cells by  $\beta$ -lactone increased the amount of non-degraded  $\alpha$ -Synuclein. Interestingly, the authors also noticed that the pathogenic mutant A53T has a longer half-life than the WT  $\alpha$ -Synuclein.  $\alpha$ -Synuclein can be digested by proteasome 20S *in vitro* producing different C-terminal truncated forms (Liu et al., 2005a) and this can be inhibited by adding a proteasome inhibitor (MG132).

Overexpression of  $\alpha$ -Synuclein mutants also enhances cytotoxicity by compromising the function of UPS (Stefanis, 2001; Tanaka et al., 2001; Tofaris et al., 2001). In parallel, (McNaught and Jenner, 2001) reported that proteasomal enzyme activities (chymotryptic, tryptic and postacidic) are decreased in SN of idiopathic PD brains. In the same manner, inhibition of the proteasome leads to increased  $\alpha$ -Synuclein inclusion formation and neurotoxicity *in vivo* (McNaught et al., 2002; Rideout et al., 2001; Sawada et al., 2004). The impairment of UPS function might come from aggregated  $\alpha$ -Synuclein itself (Chen et al., 2006; Emmanouilidou et al., 2010; Snyder et al., 2003; Zhang et al., 2008). Interestingly, overexpression of Parkin reduces toxicity in an  $\alpha$ -Synuclein toxicity-induced model (Haywood and Staveley, 2006; Oluwatosin-Chigbu et al., 2003) suggesting that activating UPS pathways might be protective. Taken together, these observations seem to indicate that UPS is implicated in the regulation of  $\alpha$ -Synuclein homeostasis.

#### 1.7.1.2 Degradation of $\alpha$ -Synuclein by UPS is conflicting

Evidence for  $\alpha$ -Synuclein degradation by UPS has been challenged by other studies. Indeed,  $\alpha$ -Synuclein is not ubiquitinated in stably transfected TSM1 neurons and inhibition of the proteasome does not change the  $\alpha$ -Synuclein level in HEK293 cells (Ancolio et al., 2000). Although inhibition of the proteasome leads to inclusion formation, (Rideout et al., 2001) did not see an upregulation of  $\alpha$ -Synuclein levels.  $\alpha$ -Synuclein found in LBs indeed can be ubiquitinated and its ubiquitination is a hallmark of  $\alpha$ -Synuclein aggregation. However, the ubiquitinated states of  $\alpha$ -Synuclein from LB do not necessarily determine its targeting to the proteasome system since non-ubiquitinated  $\alpha$ -

Synuclein can be degraded by the proteasome and  $\alpha$ -Synuclein in LBs are essentially mono-ubiquitinated, not poly-ubiquitinated (Anderson et al., 2006; Tofaris et al., 2003). Moreover ubiquitination of  $\alpha$ -Synuclein by SIAH, an  $\alpha$ -Synuclein E3 ligase, does not lead to its degradation by the proteasome, but rather increases aggregation and cell death (Lee et al., 2008; Liani et al., 2004; Rott et al., 2008). The presence of SIAH together with mono-ubiquitinated  $\alpha$ -Synuclein in LBs reinforces the thesis that mono-ubiquitinated  $\alpha$ -Synuclein is not degraded by proteasome (Liani et al., 2004).

### 1.7.1.3 Increasing evidence for $\alpha$ -Synuclein degradation by ALP

Autophagy plays a key role in maintenance of cell homeostasis, and in neuronal cells, disruption of autophagy leads to devastating consequences (Figure 1.9). Actually, *in vivo* depletion of the *Atg5* gene provokes neuronal cell loss, progressive motor deficits and accumulation of ubiquitin-positive inclusions (Hara et al., 2006). In the same manner, depletion of the *Atg7* gene causes severe cell loss in the cerebral and cerebellar cortices, motor impairments and inclusion formation. These mice also show axonal swelling and die at around 28 weeks (Komatsu et al., 2006; Komatsu et al., 2007). In many neurodegenerative disorders such as AD, HD or PD, the role of autophagy is crucial to degrade abnormal inclusions (reviewed by Wong and Cuervo, 2010).

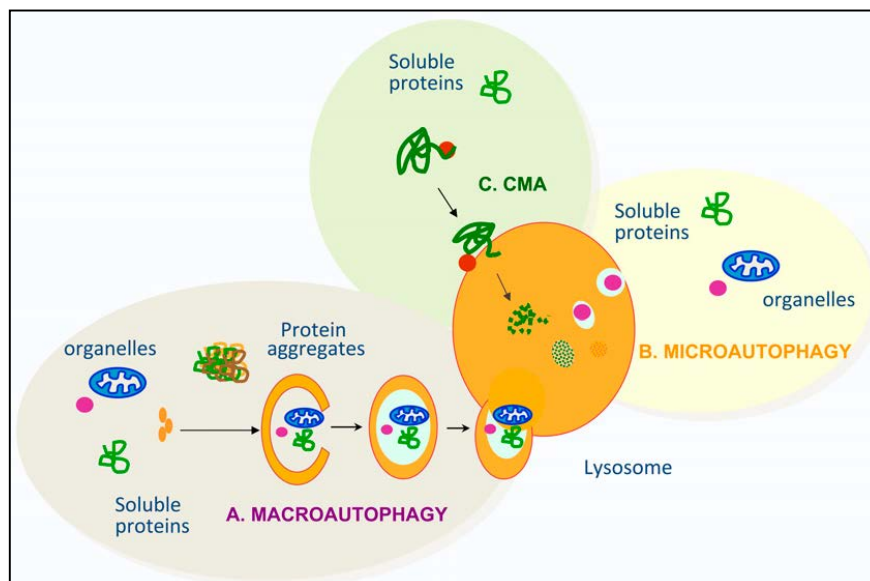


**Figure 1.9: Three main routes to entering lysosomal lumen.**

A. *Macroautophagy* represents the formation of autophagosome and fusion with lysosome for protein degradation. Autophagosome formation is a highly conserved process including several steps. The first step consists of isolation of the unique membrane (called “phagophore”) which sequesters a portion of cytoplasm, organelles or other substrates. The second step consists of complete elongation and fusion of phagophore extremities forming “autophagosome” which is typically a double-membrane organelle. During its maturation, autophagosome can fuse with other endosomes and no degradation occurs. Autophagosomes are docking and fusing in the last step with lysosome forming “autolysosome”, its content is then delivered to lysosome lumen and is degraded by lysosomal hydrolases. (Mizushima, 2007; Tanida, 2011).

B. *Microautophagy* consists of a non specific uptake of substrates or organelles into the lysosome vacuole directly by invagination of the lysosome membrane.

C. *Chaperone-mediated autophagy*, in difference to micro- and macro-autophagy, is a selective process which doesn't require the formation of autophagosome.

The first link between autophagy and PD was established by (Anglade et al., 1997) who observed apoptosis and autophagic vacuole accumulation in nigral neurons of patients with PD. This was supported by (Crews et al., 2010) who observed increasing levels of mTOR and decreasing levels of Atg7 in patient brains with DLB. Interestingly, autophagic cell death is accompanied by increasing  $\alpha$ -Synuclein levels in human neuroblastoma SH-SY5Y cells (Gómez-Santos et al., 2003). In the same year, (Webb, 2003) reported that  $\alpha$ -Synuclein can be degraded by both autophagy (activated by rapamycin and inhibited by bafilomycin) and the proteasome (inhibited by exopomicin or lactone) using PC12 cells that inducible expressed  $\alpha$ -Synuclein. Inhibition of lysosomes with ammonium chloride slows down the degradation of  $\alpha$ -Synuclein even more than inhibiting the proteasome with exopomicin in cultured midbrain neurons (Cuervo, 2004).

In animal models, disrupting autophagy by abolishing *Atg7* gene in mouse dopaminergic neurons promotes presynaptic accumulation of  $\alpha$ -Synuclein (Friedman et al., 2012). In view of the conflicting results concerning the role of proteasome in  $\alpha$ -Synuclein degradation these observations suggest that the lysosomal autophagic pathway may be an alternative mechanism of  $\alpha$ -Synuclein degradation.

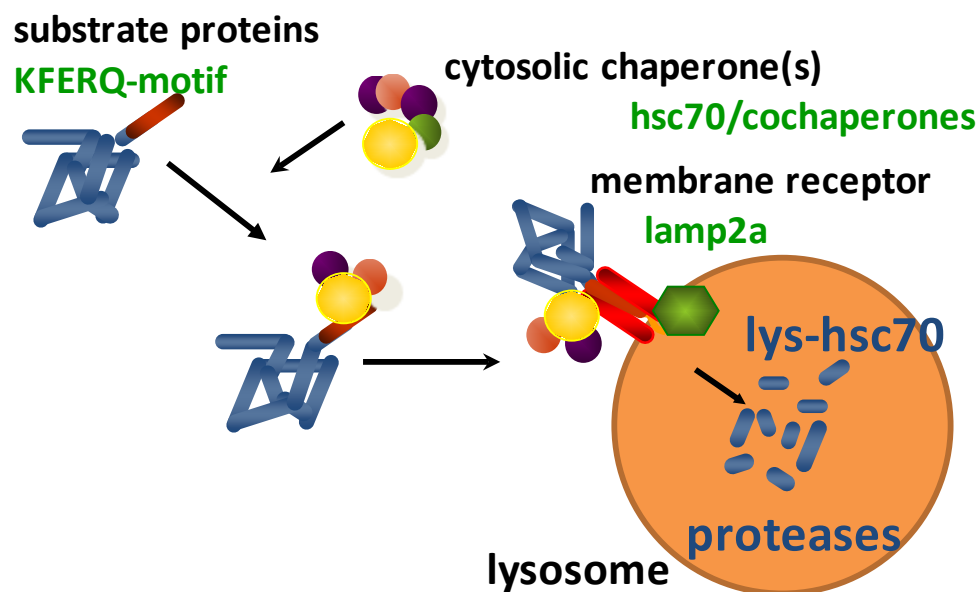


**Figure 1.10: Mechanism of CMA degradation pathway.**

*Step 1:* CMA substrates possess in their sequence the pentapeptide “KFERQ” which is specifically recognized by chaperones Hsp70 and co-chaperones.

*Step 2:* Complex substrate-chaperone is transferred to the lysosome surface and binds to the lysosome-associated membrane protein type 2A (LAMP-2A).

*Step 3:* CMA substrate is translocated one-by-one through the LAMP-2A complex to the lysosomal lumen to be degraded (Kaushik and Cuervo, 2012).

#### 1.7.1.4 CMA: a new player in $\alpha$ -Synuclein degradation

Chaperone-mediated autophagy, in contrast to micro- and macro-autophagy, is a selective process which does not require the formation of autophagosome (Figure 1.10). The protein sequences of CMA substrates contain the pentapeptide “KFERQ” (~30% of cytosolic proteins) which is specifically recognized by chaperones Hsp70 and co-chaperones. The substrate-chaperone complex is transferred to the lysosome surface and binds to the lysosome-associated membrane protein type 2A (LAMP-2A). The substrate is then translocated one-by-one through the LAMP-2A complex to the lysosomal lumen for degradation. LAMP-2A is the rate limiting-step of CMA and is organized as a dynamic structure which rapidly switches from a monomeric form (~100 kDa) at a basal level to a high molecular weight complex of about 700 kDa when bound to a substrate. Once the substrate is released into the lumen, the LAMP-2A complex disassembles into monomers. The stability of LAMP-2A is crucial for an effective translocation of the substrate. Several factors may regulate this stability. Interestingly, declining of lipid binding profile of the lysosomal membrane is correlated with physiological aging that associates CMA with aging diseases (Kaushik and Cuervo, 2012).

Recently, (Cuervo, 2004) noticed that  $\alpha$ -Synuclein carries in the sequence a pentapeptide sequence <sup>95</sup>VKKDQ<sup>99</sup> corresponding to the CMA motif. Recognition of this motif by chaperones such as Hsp70 might target  $\alpha$ -Synuclein directly to the lysosomal lumen via binding to LAMP-2A. Experiments of binding with purified lysosomes confirmed the prediction that  $\alpha$ -Synuclein is a substrate of CMA. Interestingly, mutation of the CMA motif by replacing <sup>98</sup>DQ<sup>99</sup> by AA ( $\Delta$ DQ or  $\Delta$ CMA mutant) showed impairment of translocation of this mutant into the lysosomal lumen and therefore led to a slower degradation (Figure 1.11A). Wild-type  $\alpha$ -Synuclein is able to bind LAMP-2A whereas the  $\Delta$ CMA mutant cannot. Supporting this, inducible overexpression of wild-type and  $\Delta$ CMA mutant in SHSY-5Y and PC12 cells revealed a slower turn-over of  $\alpha$ -Synuclein. Importantly, down-regulation of LAMP-2A in PC12 leads to slower degradation of  $\alpha$ -Synuclein and  $\alpha$ -Synuclein interacts physically with LAMP-2A rat cortical and midbrain neurons (Vogiatzi et al., 2008). Moreover, *in vivo*  $\alpha$ -Synuclein-induced mice with paraquat treatment increased expression of CMA-markers such as LAMP-2A or Hsp70 in nigral neurons suggesting that  $\alpha$ -Synuclein is degraded *in vivo* via CMA (Mak et al., 2010).

In brains of PD or DLB patients CMA markers LAMP-2A and Hsp70 levels are reduced suggesting that defects in CMA lead to  $\alpha$ -Synuclein accumulation (Alvarez-Erviti et al., 2010; Alvarez-Erviti et al., 2013). In the same manner, CMA activity is reduced in brain regions that are most vulnerable to  $\alpha$ -Synuclein inclusions (for example in brain stem and spinal cord of transgenic mice overexpressing A53T  $\alpha$ -Synuclein under the control of the PrP promoter (Giasson, 2002; Malkus and Ischiropoulos, 2012). Recently, overexpression of LAMP-2A enhances CMA activity and boosts the degradation of  $\alpha$ -Synuclein in cell culture. Interestingly in the same study, overexpression of LAMP-2A also rescues the toxicity induced by  $\alpha$ -Synuclein in a rat model (Xilouri et al., 2013a) (Figure 1.11C). Taken together,

these data indicate that CMA participates, at least in part, in the degradation of intracellular  $\alpha$ -Synuclein.

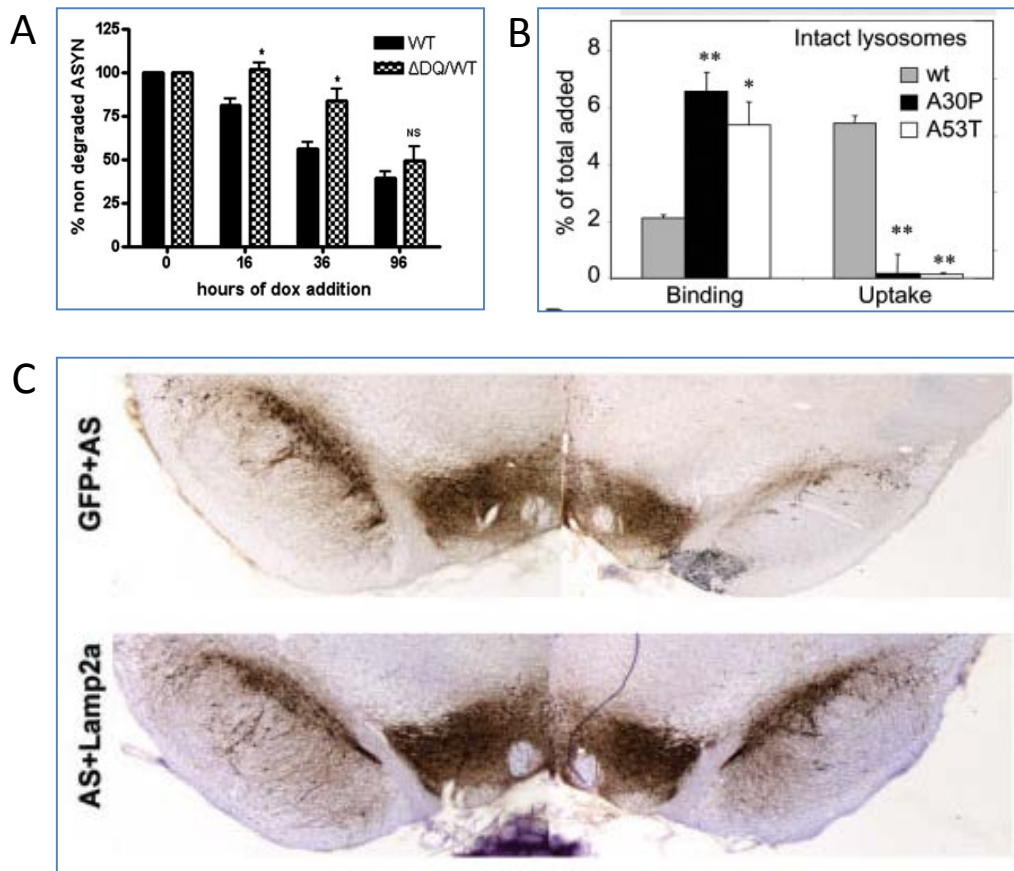


**Figure 1.11: Evidence for  $\alpha$ -Synuclein degradation by CMA *in vitro* and *in vivo***

A. Mutation of CMA targeting motif leads to slower turn-over in SHSY-5Y cells overexpressing  $\alpha$ -Synuclein (Vogiatzi et al., 2008)

B. Familial mutants of  $\alpha$ -Synuclein block their internalization into lysosomal lumen (Cuervo et al., 2004)

C. Enhancing CMA pathways by overexpression of LAMP-2A rescue  $\alpha$ -Synuclein-induced neurotoxicity in animal model (Xilouri et al., 2012).

Interestingly CMA does not appear to degrade all  $\alpha$ -Synuclein monomeric forms. Pathogenic forms of  $\alpha$ -Synuclein including genetical mutants or post-translational modified variants may affect the efficiency of CMA degradation. Compared to the WT  $\alpha$ -Synuclein, the two familial mutants A30P and A53T bind more strongly to LAMP-2A and are less efficiently translocated into the lysosome lumen. This tight binding prevents the proteolysis of other CMA substrates (such as GAPDH) *in vitro* and significantly slows down their own degradation kinetics in PC12 cells (Cuervo, 2004). Thus, these mutants are supposed to act as uptake blockers at the “entry gate” to the lysosome and binding to LAMP-2A is a limiting step of CMA pathway (Figure 1.11B). These observations were confirmed by (Xilouri et al., 2009) who observed that an inhibition of lysosomal degradation in cells expressing A53T mutant has little effect on long-lived protein degradation, whereas in cells expressing double mutant A53T- $\Delta$ CMA, inhibiting lysosome leads to increase of non-degraded protein. This result

suggests that A53T may block the degradation of long-lived proteins by blocking their translocation to lysosomes. Various post-translational modified variants can not undergo CMA. (Martinez-Vicente et al., 2008) reported that phosphorylation and nitration alter the degradation of  $\alpha$ -Synuclein by CMA reducing its binding and uptake into lysosomes. Interestingly, dopamine-modified  $\alpha$ -Synuclein, as A53T and A30P, binds more strongly to lysosomes and blocks CMA suggesting an explanation for the vulnerability of dopaminergic neurons in synucleopathies. Remarkably in the same paper, Martinez-Vincente showed that only  $\alpha$ -Synuclein monomers and dimers, but not oligomers, are efficiently taken up by lysosomes although oligomers do not themselves inhibit CMA. This result is inconsistent with previous observation that oligomeric  $\alpha$ -Synuclein overlaps with LAMP-2A in cell culture models (Lee et al., 2004), but predicts however, that oligomers may still undergo lysosomal degradation, probably through autophagosomes, since  $\alpha$ -Synuclein aggregates are seen in lysosome lumen and inhibiting lysosomal degradation with bafilomycin or 3MA stabilizes the oligomer level of  $\alpha$ -Synuclein (Lee et al., 2004; Webb, 2003). These primary observations suggest that macroautophagy and CMA may function in a synergistic manner to maintain the balance of intracellular  $\alpha$ -Synuclein. On the other hand, the capacity of macroautophagy to degrade pathogenic species of  $\alpha$ -Synuclein is still under debate. Overexpression of A53T impairs macroautophagy in a cellular model (Winslow, 2010). Recently, Tanik et al. (2013) showed that transfection of preformed fibrils (Pffs) in HEK293 cells impairs macroautophagy and clearance of  $\alpha$ -Synuclein aggregates. This observation however contradicts similar experiments from (Watanabe et al., 2012) who reported that the incorporation of  $\alpha$ -Synuclein aggregates into autophagosomes depends on the presence of p62. Nevertheless, induction of macroautophagy remains an efficient strategy to reduce the accumulation of  $\alpha$ -Synuclein species (Gonzalez-Polo et al., 2007; Hebron et al., 2013; Klucken et al., 2012; Steele et al., 2012; Wang et al., 2011a).

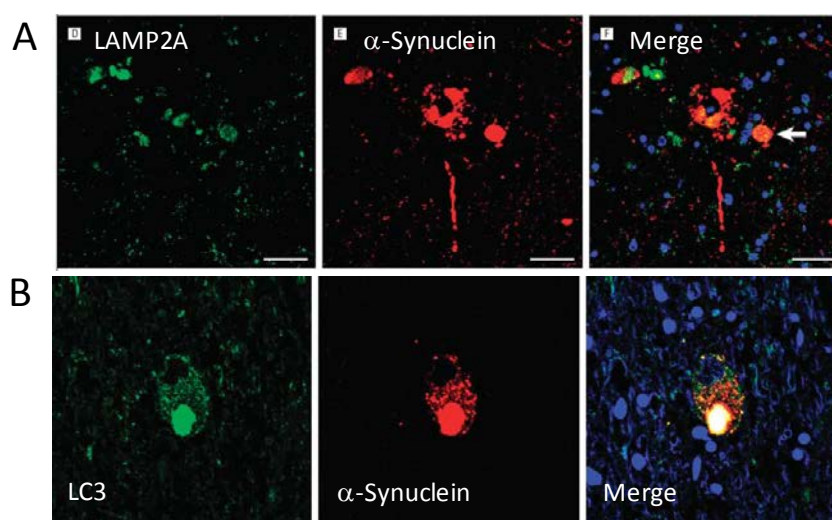


**Figure 1.12: Evidence for  $\alpha$ -Synuclein degradation by ALP in PD and DLB patients**  
A.  $\alpha$ -Synuclein is colocalized with CMA marker (LAMP-2A) in some abnormal inclusions but not in LBs in PD and DLB patients (Alvarez-Erviti et al., 2010)  
B. Most of  $\alpha$ -Synuclein colocalized with an general marker of lysosome (LC3) in inclusions including LBs in PD and DLB patients (Alvarez-Erviti et al., 2010)

## 1.8 PhD thesis: Studying the role of $\alpha$ -Synuclein lysosomal degradation using *in vivo* and *in vitro* approaches

The overall aim of my thesis was to determine the role/contribution of lysosomal degradation, in particular CMA autophagy in the regulation of  $\alpha$ -Synuclein homeostasis using both *in vitro* and *in vivo* approaches.

### ***In vitro* studies:**

Mutation of the CMA motif ( $\Delta$ CMA) by replacing <sup>98</sup>DQ<sup>99</sup> with AA has been shown to prevent translocation of  $\alpha$ -Synuclein into lysosomes *in vitro* (Cuervo, 2004), and results in increases of  $\alpha$ -Synuclein protein levels in cell culture models (Vogiatzi et al., 2008). In these studies, to validate our *in vivo* concepts, inducible cell lines (non-neuronal and neuronal) using the Tet-inducible system were generated following approaches applied in the development of previous cell culture models (Vogiatzi et al., 2008; Xilouri M, 2009). These cell lines express four different C-terminal truncated ( $\Delta$ CT)  $\alpha$ -Synuclein constructs (construct 1: WT- $\Delta$ CT, construct 2: WT- $\Delta$ CMA, construct 3: A53T-  $\Delta$ CT, construct 4: A53T-  $\Delta$ CMA). By comparison of kinetic degradation curves of  $\alpha$ -Synuclein in these cell lines established by quantitative western-blot, we wanted to answer the following questions:

- (1) Does mutation of CMA motif affect the kinetics of  $\alpha$ -Synuclein degradation?
- (2) Do kinetics of degradation differ in cell lines expressing WT and A53T  $\alpha$ -Synuclein constructs?
- (3) Does overexpression of our  $\alpha$ -Synuclein constructs enhance cell toxicity?

These data from cell culture served as base element for the discussion of our *in vivo* studies that were conducted in parallel.

### ***In vivo* studies:**

The effects of  $\alpha$ -Synuclein CMA motif mutation have not yet been verified *in vivo*. For these studies, two conditional transgenic mouse lines overexpressing truncated (1-130) A53T  $\alpha$ -Synuclein: line 1 overexpressing  $\alpha$ -Synuclein containing "normal" CMA motif (A53T- $\Delta$ CT line), line 2 overexpressing  $\alpha$ -Synuclein containing "mutated" CMA motif (A53T- $\Delta$ CMA line) were generated. Expression of  $\alpha$ -Synuclein transgene is targeted specifically to cerebellar Purkinje cells (PCs) under the control of Pcp2 promoter. The level of mRNA transcription is comparable in these two transgenic lines since  $\alpha$ -Synuclein transgene is targeted to a defined locus (*ROSA26*). The animal pathologies were analyzed using standard methods including histology, biochemistry and behavior. The objectives are to response to following questions:

- (1) Does mutation of the CMA motif affect the kinetics of  $\alpha$ -Synuclein degradation *in vivo*?
- (2) Does mutation of the CMA motif change the disease onset in animal models?
- (3) Does overexpression of  $\alpha$ -Synuclein lead to pathological development (aggregation, neuroinflammation or neurotoxicity) in the cerebellum?

## 2 Results

### 2.1 Kinetics of $\alpha$ -Synuclein degradation in HEK293 cells

To investigate if CMA is the major route for  $\alpha$ -Synuclein degradation, we examined whether mutating the CMA motif (replacing <sup>98</sup>DQ<sup>99</sup> by AA) in the  $\alpha$ -Synuclein primary structure induces changes in the kinetics of  $\alpha$ -Synuclein clearance. To do this *in vitro*, we applied a cellular approach using stable Doxycycline (Dox) inducible cell lines as previously described (Vogiatzi et al., 2008). We generated four cell lines expressing C-terminal truncated WT and A53T  $\alpha$ -Synuclein with or without CMA motif mutation (line 1: WT-  $\Delta$ CT; line 2: WT-  $\Delta$ CMA; line 3: A53T-  $\Delta$ CT and line 4: A53T-  $\Delta$ CMA). A caveat when studying the kinetics of soluble protein degradation in stable cell lines is how to obtain comparable expression of the protein of interest. In addition to influencing the expression level, the insertion locus may alter the physiology of the cells. To test this possibility,  $\alpha$ -Synuclein was expressed in HEK293 (derived from Human Embryonic Kidney) with the Flp-In™ host system (Life technologies). The host cells contain a single, stably integrated FRT (Flp Recombinase Target) site at a transcriptionally active genomic locus. Targeted integration of the Flp-In™ expression vector ensures high-level expression of the gene of interest. The Flp-In™ T-REx™-293 cell line contains pFRT/lacZeo and pcDNA™6/TR (from the T-REx™ System) stably integrated (Tet-on). Co-transfection of the Flp-In™ cell lines with Flp-In™ expression vector and the Flp recombinase vector, pOG44, results in targeted integration of the expression vector to the same locus in every cell, ensuring homogeneous levels of gene expression (Annex 1). To verify expression levels, RT-qPCR was performed to compare mRNA transcription in cells fully induced to express  $\alpha$ -Synuclein (cells were cultured in presence of 1 $\mu$ g/mL Dox during 7 consecutive days with media changes every 2-3 days). The comparison of relative mRNA amounts estimated by  $\Delta\Delta$ Ct method showed highly comparable mRNA expression between cell lines (Figure 2.1A). Equal  $\alpha$ -Synuclein expression was further confirmed by western-blot using 15G7 antibody (specific for human  $\alpha$ -Synuclein). Interestingly, a weak band was observed at the same molecular weight in non-induced cells (in the absence of Dox in the culture medium). This residual expression of  $\alpha$ -Synuclein suggests a "leaky" expression which is commonly observed in Tet inducible systems (Figure 2.1C). Importantly, these cell lines showed a high expression level of  $\alpha$ -Synuclein at a concentration of 1 $\mu$ g/mL Dox, and this expression was not efficiently decreased when Dox was removed from the medium by two washes with PBS (data not shown). This observation suggested that the system might well be activated by lower Dox concentrations. After testing lower Dox concentrations, it was found that efficient induction to express highest protein expression level could be attained from 10ng/mL Dox (Figure 2.1B).

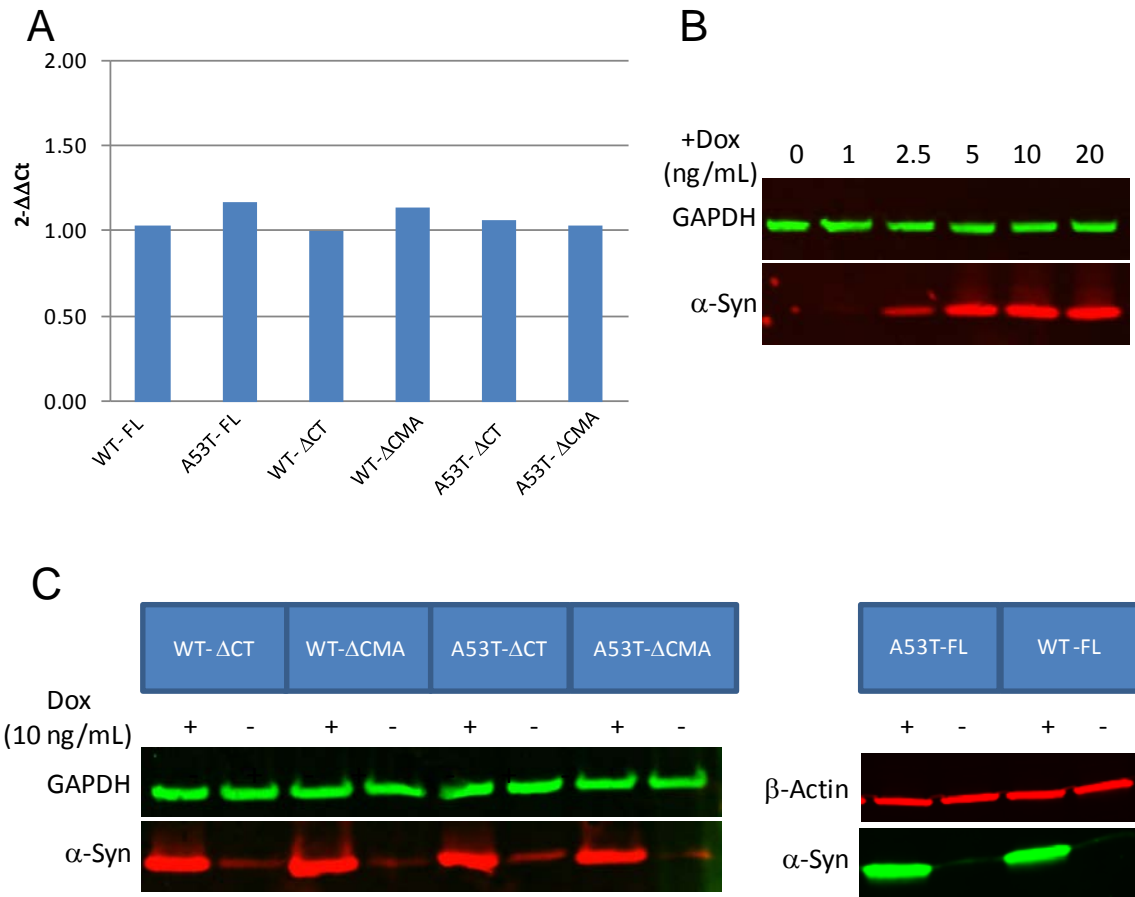


**Figure 2.1: Generation of Tet-on HEK293 Trex Flip-In inducible cell lines overexpressing  $\alpha$ -Synuclein.**  
 A: RT-qPCR comparing relative  $\alpha$ -Synuclein mRNA level using  $\Delta\Delta Ct$  method, expression of GAPDH is used as internal control.  
 B: Optimization of Dox concentration inducing highest  $\alpha$ -Synuclein protein level. Western-blot showing  $\alpha$ -Synuclein protein level after 5 days of induction at different concentrations of Dox, antibody 15G7 anti-  $\alpha$ -Synuclein, GAPDH is used as loading control.  
 C: Control of inducibility of cell clones chosen for further studies. Cells were cultured with or without Dox (10ng/mL) in enriched culture media (containing 10% of FCS) during 5 days and total protein was solubilized in Triton lysis buffer. Western-blot showing  $\alpha$ -Synuclein level using antibody 15G7 anti-  $\alpha$ -Synuclein.

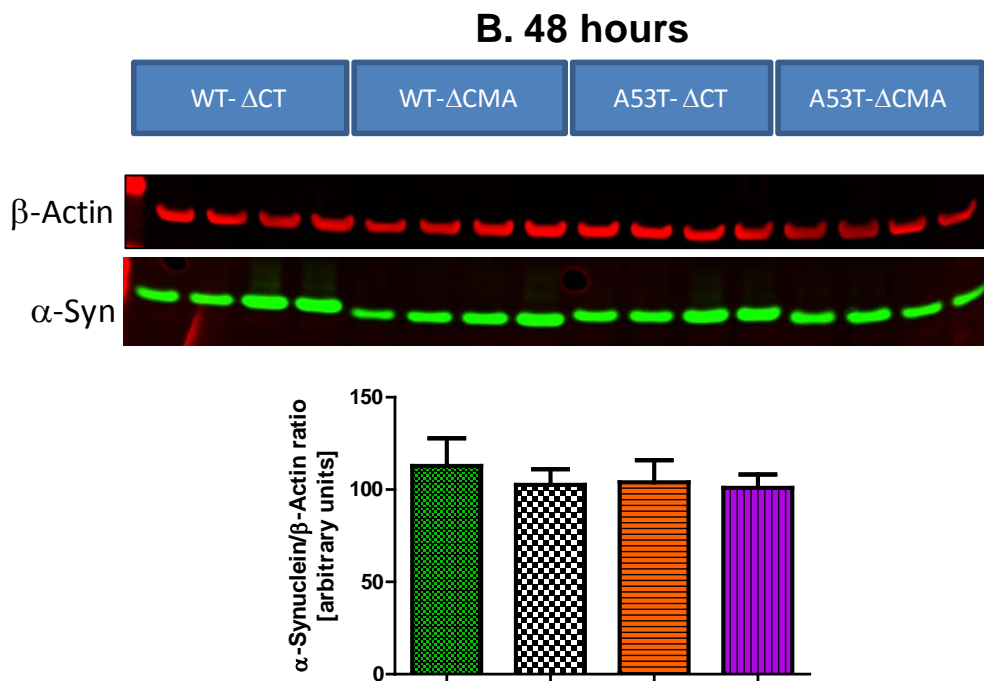
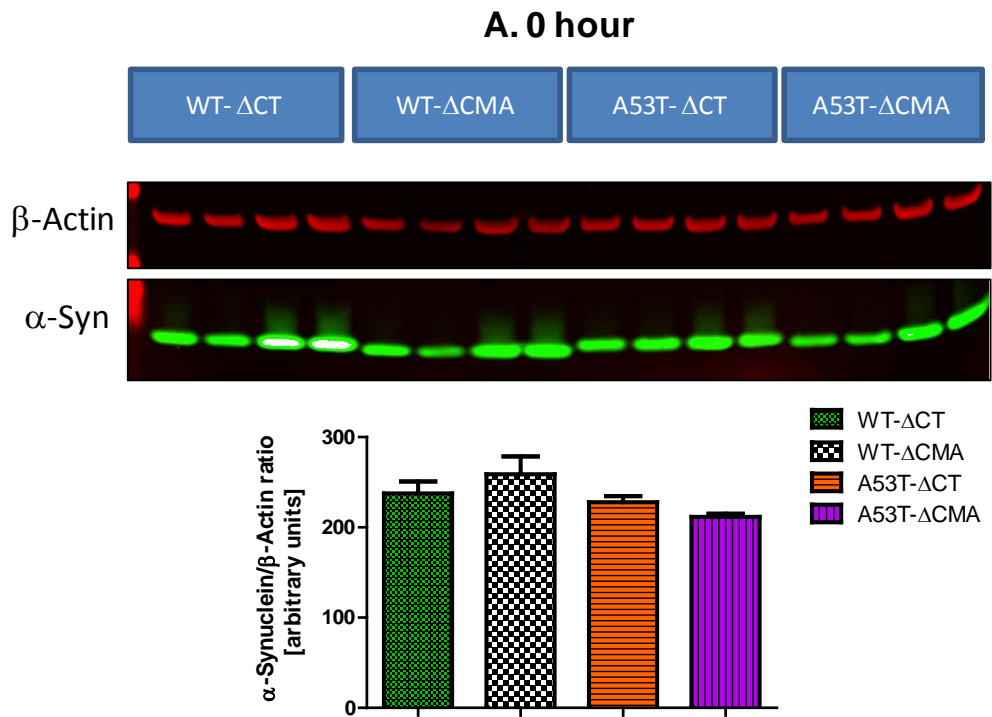


**Figure 2.2: α-Synuclein steady-state levels at 0h and 48h after removing Dox in Tet-on HEK293 cells.** Cells are cultured in enriched culture media (10% of FCS) containing Dox (10ng/mL) during 5 days. Cells are washed twice in PBS and immediately processed for total protein extraction in Triton lysis buffer for time point 0h (in A) or transferred into new culture dishes for 48h in absence of Dox (in B). Above: Western-blot showing α-Synuclein level using 15G7 antibody, β-Actin is used as loading control. Below: Quantification of α-Synuclein level, data is presented as the mean ±SEM of ratio α-Synuclein/β-Actin (signal obtained from Odyssey software) from n=4 independent experiments.

To determine  $\alpha$ -Synuclein degradation kinetics using the inducible cell lines, western-blots were used to measure the amount of remaining  $\alpha$ -Synuclein in each cell line after terminating  $\alpha$ -Synuclein mRNA transcription. Firstly, maximum expression of  $\alpha$ -Synuclein was obtained by culturing in enriched medium containing 10% of FCS and then transcription was stopped by removing Dox from culture media. Cells continued to be cultured in serum-enriched medium and total protein extracts were prepared at different time points; time point "0" was defined as time when Dox was removed. Protein levels for each time point were calculated by normalizing the signal of the  $\alpha$ -Synuclein band to the signal of the  $\beta$ -Actin band [ $\alpha$ -Syn/  $\beta$ -Actin] of the same well (Odyssey quantification method). Firstly, to assess the steady state protein levels in the different cell lines, their protein levels were compared at time point 0 in fully induced cells. All four cell lines showed similar  $\alpha$ -Synuclein protein levels at this time point (Figure 2.2A), confirming homogenous steady state expression (Figure 2.1). On the other hand, this result also indicates that there is no apparent difference in  $\alpha$ -Synuclein turnover between the lines because a difference in protein degradation would be expected to alter steady state levels, given that the protein synthesis was comparable between the lines. In the same manner, no significant changes in protein levels were observed at 48 hours after stopping expression of  $\alpha$ -Synuclein (Figure 2.2B). In contrast with an early report (Vogiatzi et al., 2008), mutating the CMA motif does not affect the turnover of  $\alpha$ -Synuclein. To confirm this, kinetic curves of  $\alpha$ -Synuclein degradation were determined for each cell line by quantifying the amount of  $\alpha$ -Synuclein protein at various time points (0, 24, 48 and 72 and 96 h) in three independent experiments (a triplicate per cell line was made per experiment).  $\alpha$ -Synuclein protein level per time point in each experiment was calculated as the mean of [ $\alpha$ -Syn/  $\beta$ -Actin]. To determine the degradation rate at each time point, we normalized all time points to time point 0 (100%). These data served to estimate the corresponding  $\alpha$ -Synuclein protein half-life in each cell line. No significant difference in protein degradation rates either between WT-  $\Delta$ CT and WT-  $\Delta$ CMA or between A53T-  $\Delta$ CT and A53T-  $\Delta$ CMA (Figure 2.3A,B). This result confirmed the precedent observation in Figure 2.2. Surprisingly, the rate of protein degradation in the WT-  $\Delta$ CT line seemed even to be higher, although not significantly, than in WT-  $\Delta$ CMA. Although in contradiction with published data suggesting that mutating CMA motif slows degradation rate of WT  $\alpha$ -Synuclein (Vogiatzi et al., 2008). The present results indicate that mutating CMA in either the WT or A53T mutant has no effect on the  $\alpha$ -Synuclein degradation rate.

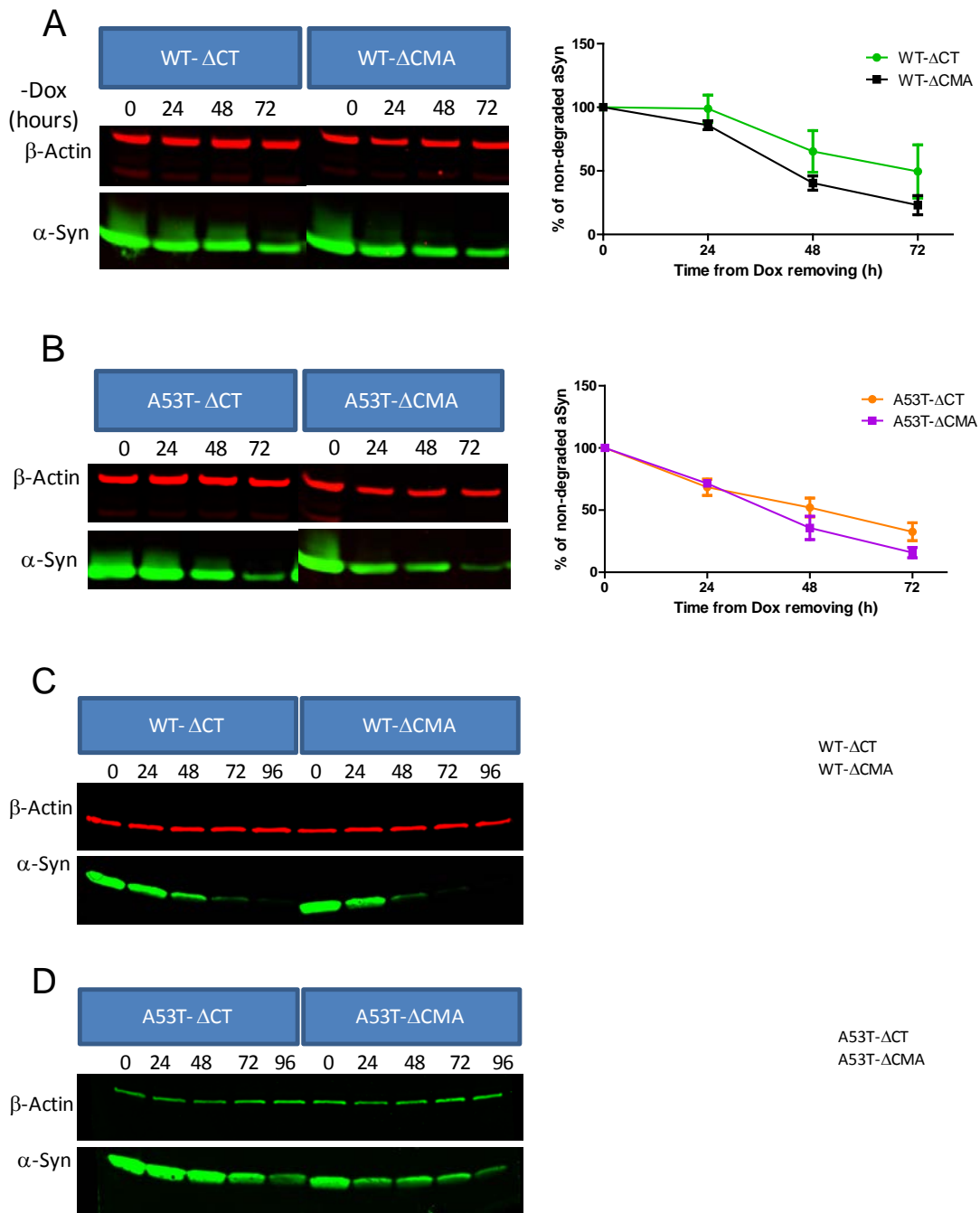


**Figure 2.3: Kinetics of  $\alpha$ -Synuclein degradation in Tet-on HEK293 cells.**

A and B: Degradation under enriched culture media of wild-type (A) and A53T mutant (B)  $\alpha$ -Synuclein. Cells were cultured in medium (10% of FCS) containing Dox (10ng/mL) during 5 days. Cells were washed twice in PBS and immediately processed for total protein extraction in Triton lysis buffer for time point 0h or transferred into new culture dishes in absence of Dox and repeating the process for different time points (24, 48 and 72h). Culture medium is refreshed every 24 hours. For each image (A or B): Left: Western-blot showing  $\alpha$ -Synuclein level using 15G7 antibody,  $\beta$ -Actin is used as loading control. Right: Quantification of  $\alpha$ -Synuclein level. A triplicate per experiments is done. Data are presented as the mean of ratio  $\alpha$ -Synuclein/ $\beta$ -Actin of time points (24, 48 or 72h) compared to ratio  $\alpha$ -Synuclein/ $\beta$ -Actin of time point 0, calculated in % (signal obtained from Odyssey software) from n=3 independent experiments.

C and D: Degradation under starvation condition of wild-type (C) and A53T mutant (D)  $\alpha$ -Synuclein. Cells were cultured in medium (10% of FCS) containing Dox (10ng/mL) during 5 days. Cells were washed twice in PBS and immediately processed for total protein extraction in Triton lysis buffer for time point 0h or transferred into new culture dishes containing serum-reduce medium (0.5% FCS) in absence of Dox and repeating the process for different time points (24, 48 and 72h). Data are collected and presented as in A and B.

$\alpha$ -Synuclein has been reported to have a relatively long half-life varying from 16.8-24h and depends on multiple factors including genetic background and culture conditions (number of passages, cell confluence, frequency of media change...) (Cuervo, 2004; Vogiatzi et al., 2008; Rott et al., 2011). CMA is also more active when cells are cultured in serum-free medium, thereby accelerating degradation rates (Cuervo, 2004). Since our observations did not confirm with the initial hypothesis that CMA motif mutation leads to slower degradation kinetics, the experiment was repeated with reduced serum (0.5% instead of 10% of FCS) in the culture medium.

Since four of the  $\alpha$ -Synuclein constructs lack the C-terminus which has been suggested to play a role in the physiology of  $\alpha$ -Synuclein (Choi et al., 2012), two control cell lines expressing WT and A53T full-length (Control 1: WT- FL, Control 2: A53T- FL) were generated to establish base-line controls for  $\alpha$ -Synuclein degradation rates. The degradation kinetics were calculated using the previous experimental design except that after removing Dox from medium, cells were cultured in medium containing 0.5% FCS (instead of 10 % FCS). Media were refreshed every 24 hours. In this reduced-serum culture condition, the degradation rates of WT- FL and A53T- FL were first compared and found that interestingly, A53T- FL showed constantly higher % of non-degraded protein than WT- FL up to 96h and the difference between these cell lines is significant (Figure 2.4A). Quantification of steady state levels of WT-FL and A53T-FL  $\alpha$ -Synuclein also demonstrated that A53T-FL  $\alpha$ -Synuclein exhibited higher protein levels than WT-FL at 0h and 48h (Figure 2.4B). This observation correlated with previous published data (Cuervo, 2004) suggesting that, A53T  $\alpha$ -Synuclein itself might prevent its entry into the lysosome lumen. However, no significant in difference of degradation rates was observed either between WT-  $\Delta$ CT and WT-  $\Delta$ CMA or between A53T-  $\Delta$ CT and A53T-  $\Delta$ CMA (Figure 2.3C,D) confirming our observation in cells cultured with serum-enriched medium (Figure 2.3A,B). Based on their kinetic curves, the half-life of A53T-FL  $\alpha$ -Synuclein is estimated to be about 16 h greater than WT-FL  $\alpha$ -Synuclein whereas half-life of all four  $\Delta$ CT  $\alpha$ -Synuclein is very similar (Table 2.1).

In conclusion, these results with non-neuronal HEK293 cell lines showed that mutating of CMA motif did not slow down the kinetics of  $\Delta$ CT  $\alpha$ -Synuclein in two culture conditions (enriched serum and reduced serum). This observation raised the questions about the part of CMA in regulation of  $\alpha$ -Synuclein turn-over under normal physiological condition. The significant difference in half-life between FL  $\alpha$ -Synuclein also suggests that  $\alpha$ -Synuclein C-terminus might be crucial in regulating the CMA pathway.

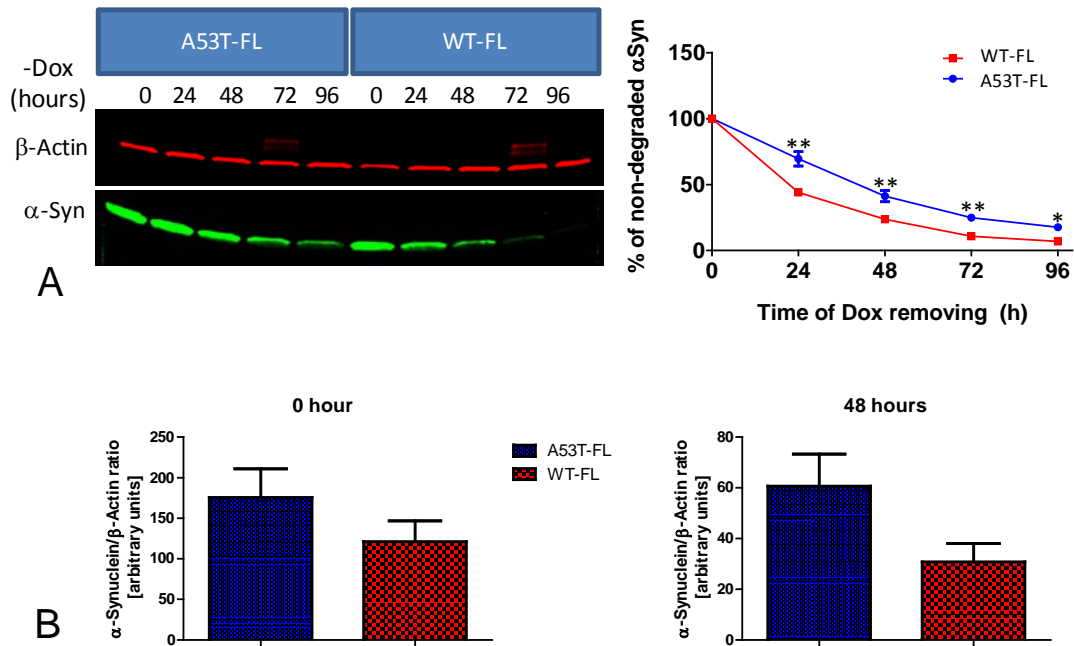


**Figure 2.4: Exploring the impact of C-terminus and the presence of CMA-motif mutation on the regulation of  $\alpha$ -Synuclein half-life.**

- A. Kinetics of full-length  $\alpha$ -Synuclein degradation under starvation condition (culture media containing 0.5% of FCS) in Tet-on HEK293 cells. Cells were cultured in medium containing Dox (10ng/mL) during 5 days. Cells were washed twice in PBS and immediately proceed for total protein extraction in Triton lysis buffer for time point 0 or transferred into new culture dishes in absence of Dox and repeating the process for different time points (24, 48, 72 and 96h). Left: Western-blot showing  $\alpha$ -Synuclein level using 15G7 antibody,  $\beta$ -Actin is used as loading control. Right: Quantification of  $\alpha$ -Synuclein level. A triplicate per experiment is done. Data are presented as the mean of ratio  $\alpha$ -Synuclein / $\beta$ -Actin of time points (24, 48, 72 or 96h) compared to ratio  $\alpha$ -Synuclein / $\beta$ -Actin of time point 0, calculated in % (signal obtained from Odyssey software) from n=3 independent experiments (\*\* P < 0.01 \*P < 0.05, Student's t test).
- B.  $\alpha$ -Synuclein steady-state level at 0h and 48h after removing Dox in Tet-on HEK293 cells. Diagram showing the mean of protein level from experiments in A at 0h and 48h. Data are presented as the mean  $\pm$ SEM of ratio  $\alpha$ -Synuclein / $\beta$ -Actin of time points 0h and 48h from n=3 independent experiments.

## 2.2 Kinetics of $\alpha$ -Synuclein degradation in BE(2)-M17 cells

The use of HEK293 cells has the advantage of maintaining the homogenous transcription levels, but these cells do not reflect neuronal cell properties. Therefore, in parallel with these experiments, four stable, inducible Tet-off BE(2)-M17 cells (derived from a neuroblastoma) were generated. They were designed to express C-terminal truncated WT and A53T  $\alpha$ -Synuclein mutants with or without CMA motif mutation (line 1: WT-  $\Delta$ CT; line 2: WT-  $\Delta$ CMA; line 3: A53T-  $\Delta$ CT and line 4: A53T-  $\Delta$ CMA). For these cell lines, the traditional method for stable cell line generation based on random integration into the cellular genome was used. To ensure comparable expression levels, clones which showed similar mRNA levels were chosen after full induction during 7 days (in absence of Dox in culture medium). Unfortunately, the four cell lines did not have the same expression level. For subsequent studies, clones with comparable mRNA levels between line 1 and line 2 (WT-  $\Delta$ CT vs WT-  $\Delta$ CMA) and between line 3 and line 4 (A53T-  $\Delta$ CT vs A53T-  $\Delta$ CMA) were selected. The mRNA levels in cells expressing A53T  $\alpha$ -Synuclein were 3-4 fold higher than in cells expressing WT  $\alpha$ -Synuclein (Figure

2.5A). However, protein levels observed by western-blot in cells expressing A53T  $\alpha$ -Synuclein were constantly 2-fold higher than in cells expressing WT  $\alpha$ -Synuclein. This might be interpreted in part as "leaky" expression that was also observed in non-induced cells when cells re cultured in medium containing 1 $\mu$ g/mL Dox (Figure 2.5B).

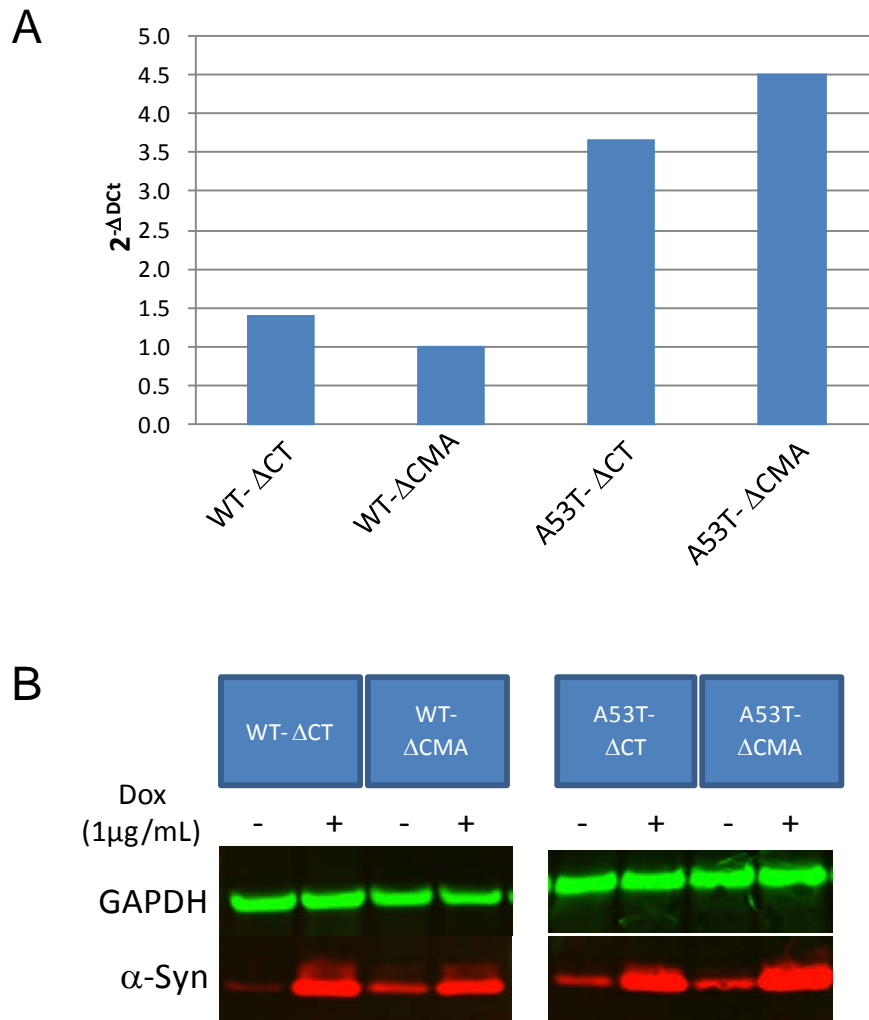


**Figure 2.5: Generation of Tet-off BE(2)-M17 inducible cell lines expressing  $\alpha$ -Synuclein .**

A: RT-qPCR comparing relative  $\alpha$ -Synuclein mRNA level using  $\Delta\Delta$ Ct method, expression of GAPDH is used internal control.

B: Control of inducibility of cell clones chosen for further studies, cells are cultured with or without Dox (1 $\mu$ g/mL) in enriched culture media (containing 10% of FCS) during 5 days and total protein are solubilized in Triton lysis buffer. Western-blot showing  $\alpha$ -Synuclein level using antibody 15G7 anti- $\alpha$ -synuclein.

As previously done with HEK293 cell lines, steady state protein levels were examined in the four cell lines. At time points 0 and 48h after adding Dox, protein levels in cells expressing WT-  $\Delta$ CT and A53T-  $\Delta$ CT were significantly higher than ones express WT-  $\Delta$ CMA and A53T-  $\Delta$ CMA respectively (Figure 2.6). The kinetics of degradation curves of  $\alpha$ -Synuclein were established in these cell lines and their estimated half-lives are presented in Table 2.1. No significant differences in degradation kinetics were observed between WT- $\Delta$ CT and WT- $\Delta$ CMA or between A53T- $\Delta$ CT and A53T- $\Delta$ CMA up

to 96h in culture conditions with serum-reduced medium (0.5%FCS) (Figure 2.7). Interestingly, in BE(2)-M17 cell lines, the estimated half-lives of  $\Delta$ CT  $\alpha$ -Synuclein are about 1 day longer than the ones in HEK-293 cells (Table 2.1). Once again, in neuronal BE(2)-M17  $\alpha$ -Synuclein with mutated CMA motif did not exhibit a slower turnover than  $\alpha$ -Synuclein- $\Delta$ CT with a normal CMA motif.

HEK293 cells		BE(2)-M17 cells	
Construct	Half-life (h) $\pm$ SEM	Construct	Half-life (h) $\pm$ SEM
WT-FL	20.20 $\pm$ 2.41	WT- $\Delta$ CT	50.66 $\pm$ 8.41
WT- $\Delta$ CT	29.17 $\pm$ 4.88	WT- $\Delta$ CMA	57.84 $\pm$ 16.43
WT- $\Delta$ CMA	25.21 $\pm$ 4.80	A53T- $\Delta$ CT	43.60 $\pm$ 14.17
A53T-FL	36.25 $\pm$ 7.06	A53T- $\Delta$ CMA	60.44 $\pm$ 3.523
A53T- $\Delta$ CT	26.89 $\pm$ 3.84		
A53T- $\Delta$ CMA	25.10 $\pm$ 3.84		

**Table 2.1: Recapitulation of  $\alpha$ -Synuclein half-life in different cell lines.**

Half-lives are represented as the mean $\pm$ SEM of half-life values calculated from each independent experiment (n=3) after correction of the degradation curves using “Nonlinear regression (curve fit), one phase decay” (GraphPrism, version 5).

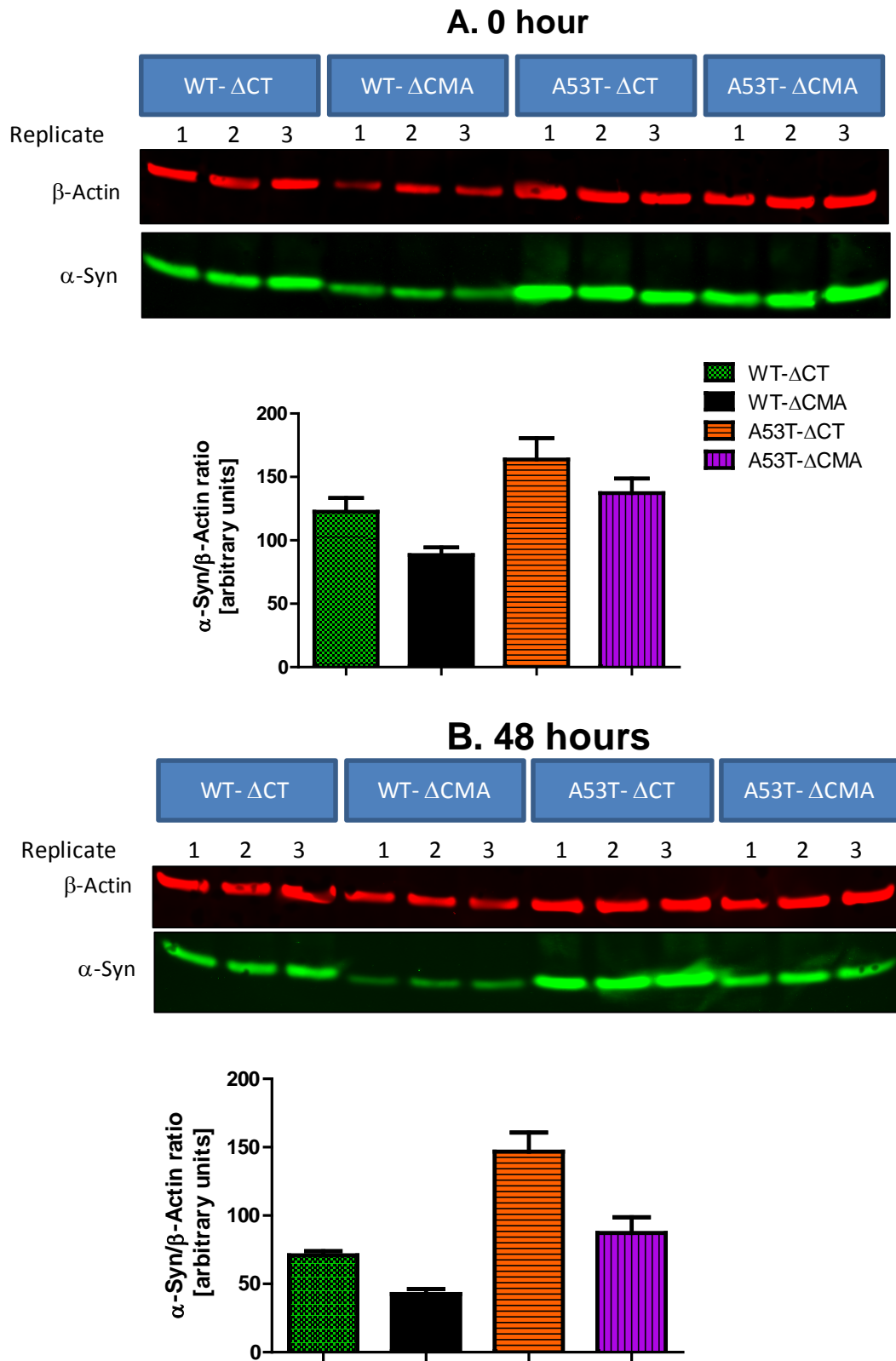


**Figure 2.6: α-Synuclein steady-state level at 0 and 48h after adding Dox in Tet-off BE(2)-M17 cells.**

Cells were cultured in enriched culture media (10% of FCS) in absence of Dox (10ng/mL) during 5 days. 1μg/mL of Dox was added to culture medium and total protein is immediately extracted in Triton lysis buffer for time point 0 (in A) or cells were cultured under starvation condition (medium containing 0.5% FCS) during 48 h in presence of Dox (in B). For each image (A or B): Above: Western-blot showing α-Synuclein level using 15G7 antibody, β-Actin is used as loading control. Below: Quantification of α-Synuclein level, data are presented as the mean of ratio α-Synuclein/β-Actin (signal obtained from Odyssey software) from n=3 independent experiments.

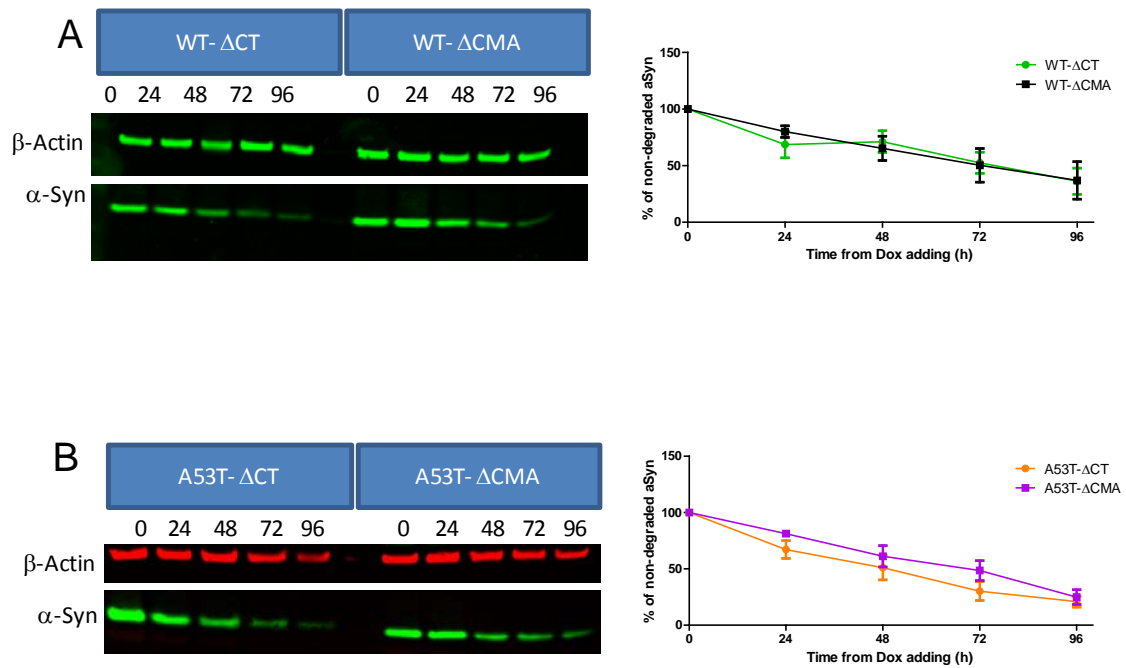


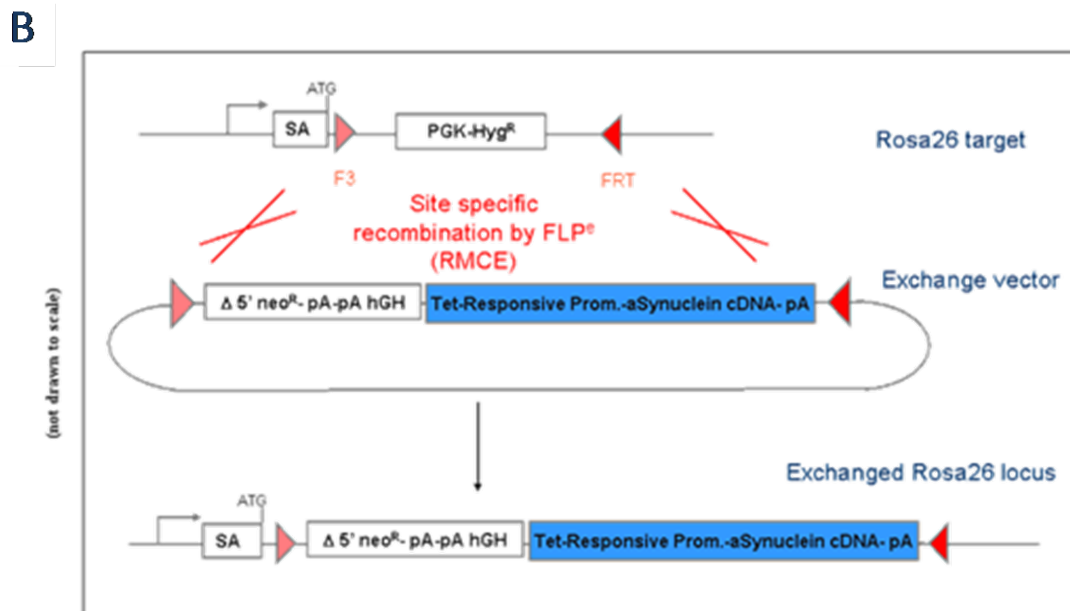
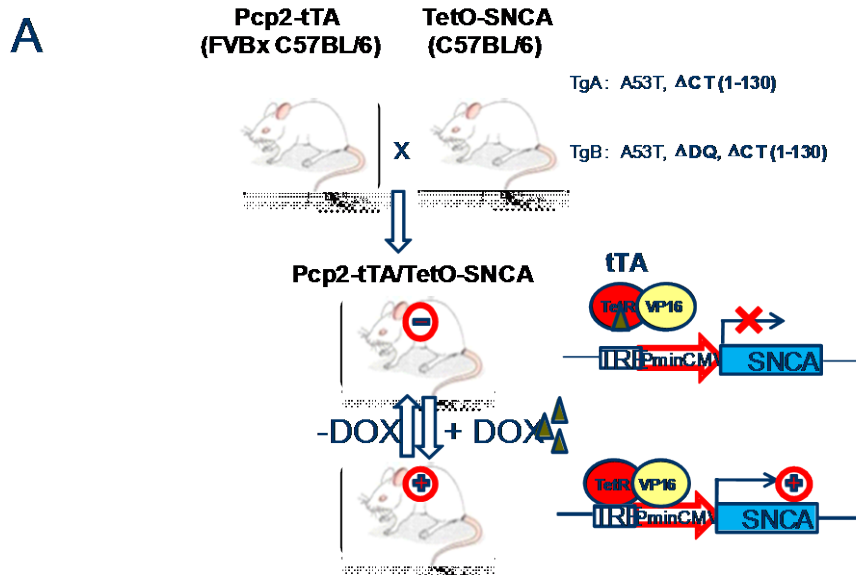
**Figure 2.7: Kinetics of  $\alpha$ -Synuclein degradation in Tet-off BE(2)-M17 cells under starvation condition in presence or absence of CMA-motif mutation for wild-type (A) and A53T mutant (B)  $\alpha$ -Synuclein .** Cells were cultured in medium (10%FCS) without Dox during 5 days. 1 $\mu$ g/mL of Dox is added to culture medium (0.5% FCS) and total protein is immediately extracted in Triton lysis buffer for time point 0h (in A) or cells were kept in culture under starvation condition (medium containing 0.5% FCS) for additional time periods (24, 48, 72 or 96h). Medium culture is refreshed every 24 hours. For each image (A or B): Left: Western-blot showing  $\alpha$ -Synuclein level using 15G7 antibody,  $\beta$ -Actin is used as loading control. Right: Quantification of  $\alpha$ -Synuclein level. A triplicate per experiments is done. Data are presented as the mean of ratio  $\alpha$ -Synuclein/ $\beta$ -Actin of time points (24, 48, 72 or 96h) compared to ratio  $\alpha$ -Synuclein/ $\beta$ -Actin of time point 0h, calculated in % (signal obtained from Odyssey software) from n=3 independent experiments.

## 2.3 Generation of transgenic models overexpressing $\alpha$ -Synuclein

### 2.3.1 Pcp2 promoter drives $\alpha$ -Synuclein expression in cerebellar Purkinje cells (PCs)

To study the long-term effect of the CMA motif mutation in animal models, two transgenic mouse lines expressing respectively A53T- $\Delta$ CT (1-130) and A53T- $\Delta$ CMA (1-130) were generated (Figure 2.8A). Two large cohorts (30-40 animals per line) were obtained by crossing the driver line Pcp2-tTA (at the 6th backcross with wild-type C57BL/6 mice) with *TetO-SNCA* animals. These animal cohorts served for pilot studies using standard techniques such immunohistochemistry and western-blot. These preliminary studies aimed to: (1) confirm the efficiency and validate strategies of  $\alpha$ -Synuclein overexpression, (2) optimize and standardize technical approaches which would be used for subsequent studies, (3) detect eventual age-dependent pathological changes in transgenic animals. The distribution of transgene expression under the control of Pcp2 promoter which expresses tTA (transactivator) specifically in cerebellar Purkinje cells was assessed. Expression of tTA, in the absence of Dox, activates expression of the transgene which is preceded by the *TetO* sequence. The inducibility of transgene expression by Pcp2-tTA driver line was previously checked by crossing it with *Tet-O-LacZ* mice. *LacZ* gene encodes for  $\beta$ -galactosidase which can be detected by its enzymatic

activity revealed by the presence of X-gal. Expression of  $\beta$ -galactosidase was found to appear specifically in Purkinje cell perikaryon in transgenic mice from around post-natal (P25) day 25. No leaky expression was observed in other brain regions. This transgene expression could be completely abolished by feeding adult mice (at 2 months) Dox (chow) for 18 days (Cawthorne et al., 2007) (Annex 2). These results indicated that overexpression of transgene under direction of the Pcp2-tTA line satisfied criteria for specifically localizing and inducing transgene expression.



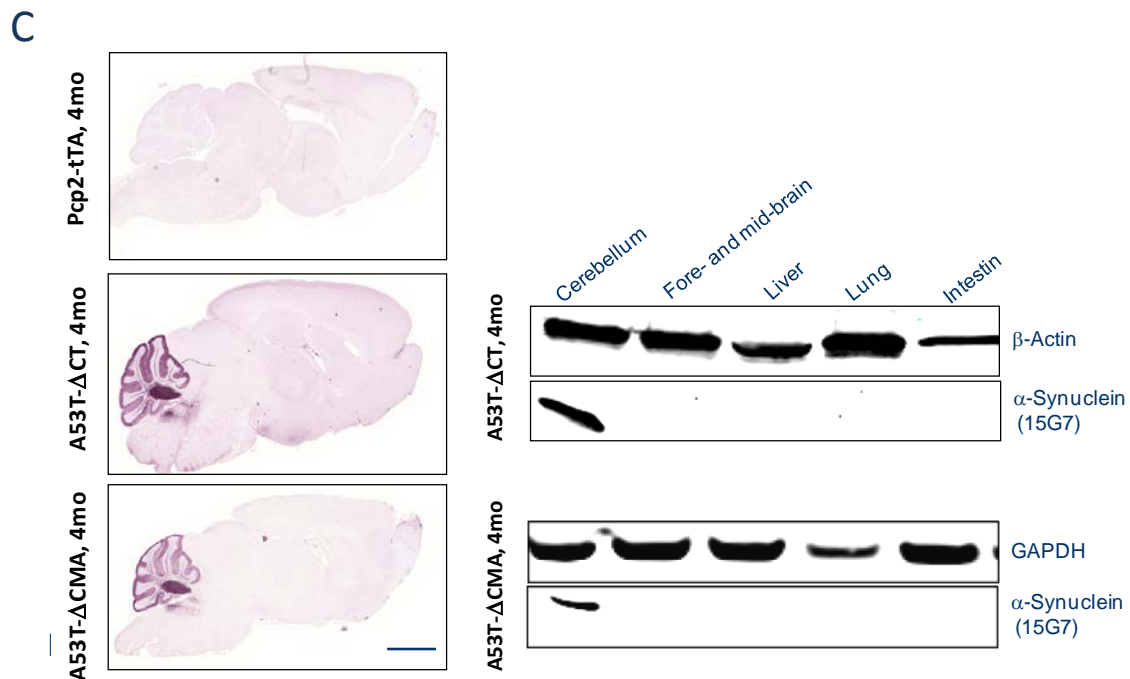


**Figure 2.8: Overexpression of human C-terminal truncated  $\alpha$ -Synuclein driven by mouse Pcp2 promoter.**

A: Diagram representing the crossing procedure (Pcp2: Purkinje cell protein-2, tTA: tetracycline-controlled transactivator). Two transgenic lines expressing  $\alpha$ -Synuclein were generated (A53T- $\Delta$ CT, A53T- $\Delta$ CMA). Pcp2-tTA mice are used as non-transgenic control.

B: Diagram showing strategy of generating *TetO-SNCA* mice: *TetO-SNCA* sequences are targeted specifically at ROSA26 locus ensuring isogenic insertion

C: Expression of  $\alpha$ -Synuclein is specifically targeted to cerebellum: immunostaining of 7- $\mu$ m thick sagittal cerebellar sections and western-blot of brain and peripheric tissue homogenates from 4-month-old mice, antibody 15G7 anti- $\alpha$ -Synuclein, (Red), DAPI (Blue).

To further confirm these results in  $\alpha$ -Synuclein transgenic lines, sagittal brain sections from young adult animals at 2-3 months of age were immunostained for  $\alpha$ -Synuclein. As brain tissues were embedded in paraffin blocks, a step of antigen retrieval after tissue deparaffinization was necessary to enhance the quality of the labeling signal. Pre-treatment by prolonged heating (around 20min) of tissue sections at 90°C in citrate buffer (pH 7.6) produced optimal  $\alpha$ -Synuclein staining using 15G7 and LB509 antibodies (specific for human  $\alpha$ -Synuclein) or Syn-1 antibody (specific for mouse and human  $\alpha$ -Synuclein). Additional pretreatment with formic acid 88% during 5 min at room temperature increased the specific signal of  $\alpha$ -Synuclein. Immunostaining using 15G7 antibody indicated specific  $\alpha$ -Synuclein expression in cerebellum of transgenic mice compared to control non-transgenic mice for human  $\alpha$ -Synuclein (Pcp2-tTA mice, Figure 2.8C). This expression was particularly concentrated in the Purkinje cell layer (PCL), and the molecular layer (ML) which is the projection area of PC dendrites and the deep cerebellar nuclei (DCN) which contains axonal extensions of PCs

(Figure 2.8C). Some weak leaky expression of  $\alpha$ -Synuclein was found in olfactory bulb (OB), but not observed in any other brain regions, in sagittal or coronal sections (Figure 2.8C, coronal sections not shown). This result was further confirmed by western-blot using the same 15G7 antibody: we could detect a distinct band of  $\alpha$ -Synuclein at around 16kD was evident in cerebellum homogenate, but no signal was detected in other brain regions or in non-brain tissue homogenates (Figure 2.8B). These results validated the strategy of  $\alpha$ -Synuclein overexpression directed by Pcp2 promoter in cerebellum without significantly inducing leaky expression in other brain regions.

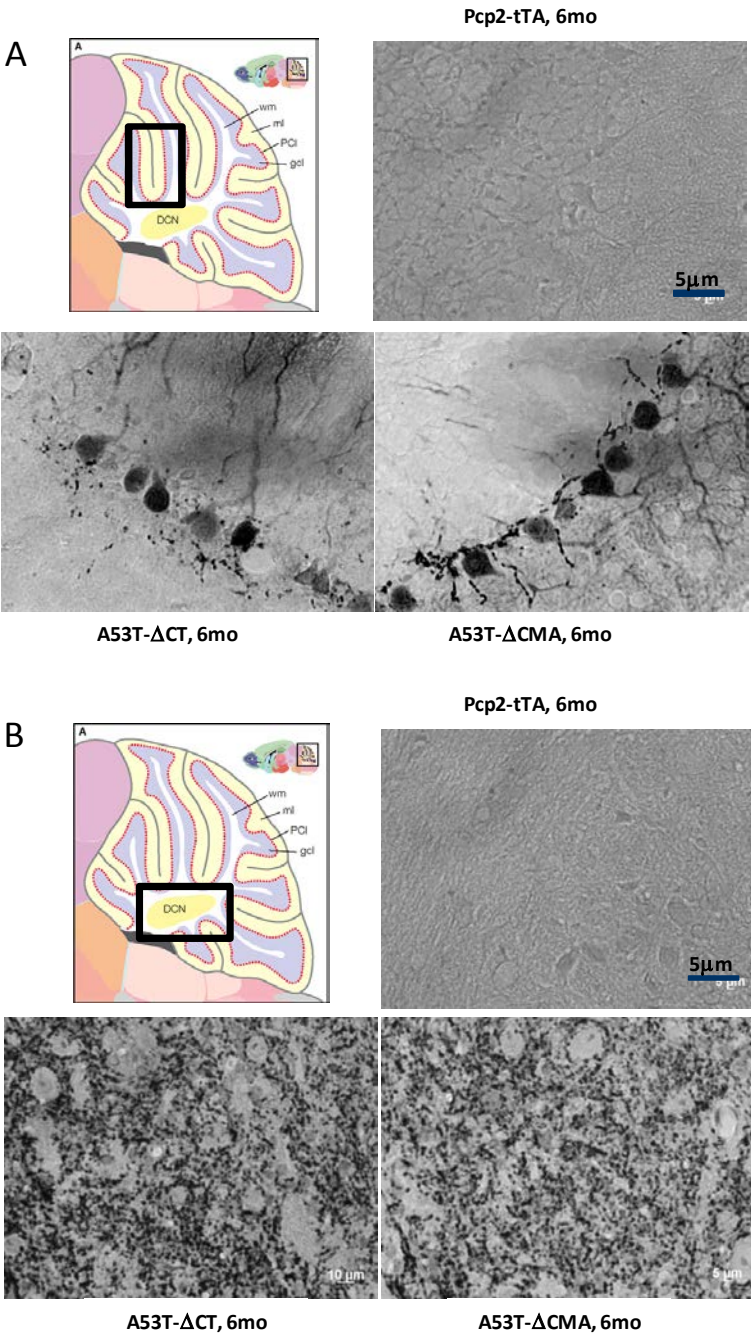


**Figure 2.9: Localization of overexpressed human  $\alpha$ -Synuclein driven by mouse Pcp2 promoter by immunostaining of 7- $\mu$ m thick sagittal cerebellar sections from 6-month-old mice (6mo), antibody 15G7 anti- $\alpha$ -Synuclein.**

A: Overexpressed human  $\alpha$ -Synuclein is located in neurites and Purkinje cell perikaryon (enlargement of Purkinje cell layer area).  
 B: Overexpressed human  $\alpha$ -Synuclein is located axon terminals of Purkinje cells (enlar in Deep cerebella nuclei area).  
 Abbreviations: PCL: Purkinje cell layer, DCN: Deep cerebella nuclei, ML: molecular layer, WM: white matter, GCL: granular cell layer).

Next we further characterized the distribution pattern of overexpressed  $\alpha$ -Synuclein to determine its cellular localization, by focusing on the two main regions of abundant  $\alpha$ -Synuclein expression (at

higher magnification). In the PCL, we observed that overexpressed  $\alpha$ -Synuclein was principally in Purkinje cell bodies. Surprisingly, the protein level of overexpressed  $\alpha$ -Synuclein was not homogenous, but varied in a mosaic-like manner between the cells. Unexpectedly, strong  $\alpha$ -Synuclein signal was observed in the PC dendrite arborescence in the ML. Anatomically, PC dendrites form synapses and receive excitatory input directly from nuclei via climbing fibers or indirectly via granule cells located in the granule cell layer (GCL) which project their bifurcated parallel fibers in ML region. We found numerous punctuate of overexpressed  $\alpha$ -Synuclein around Purkinje cell bodies although its precise intracellular location remained unclear (Figure 2.9A). In DCN, abundant "dots" corresponding to  $\alpha$ -Synuclein signal were observed. These  $\alpha$ -Synuclein dots were widely distributed in the DCN and some of them are clustered around cell bodies of DCN neurons. DCN are known as output areas where PCs make inhibitory synapses with relay neurons which are inter-connected with motor-cortex neurons in the thalamus. As  $\alpha$ -Synuclein is known to be abundant in pre-synaptic regions, these  $\alpha$ -Synuclein dots might well correspond to PC pre-synaptic regions (Figure 2.9B).

To confirm the cellular type overexpressing  $\alpha$ -Synuclein, sections were double immunostained for  $\alpha$ -Synuclein and specific marker for PCs, Calbindin-D28K. Calbindin-D28K is a calcium buffer protein which is highly expressed in all PCs and only at low levels in other cerebellar cell types such as in parallel fibers of granule cells. Immunostaining of Calbindin confirmed that PCs can be clearly distinguished from other cell types in the cerebellum. In sagittal sections, Calbindin signal concentrated in PC perikaryons (PCL), dendritic arborescences (ML) and deep cerebellar nuclei (DCN). The Calbindin signal in the ML is particularly intensive, clearly separating the cerebellar cortex (PCL + ML) from the cerebellar white matter (Figure 2.10A). However, within the cerebellar white matter Calbindin labelled axonal fibers of PCs which depart from the PCL and project to the DCN. The human  $\alpha$ -Synuclein and Calbindin signals perfectly overlap in PCs in ML, PCL and DCN, confirming overexpressed  $\alpha$ -Synuclein is localized in PCs. In PCL and ML, the overlapping signals were particularly strong in Purkinje cell perikaryon and cytoplasm, but also in dendrites confirming the presence of overexpressed  $\alpha$ -Synuclein in post-synaptic regions. Numerous punctuate staining of  $\alpha$ -Synuclein around Purkinje cell bodies are overlapped with Calbindin signals at the region of axonal departure or dendritic connection even though the latter are not as intensively stained for Calbindin. This observation suggested that  $\alpha$ -Synuclein "dots" around PC are rather intracellular than secreted (Figure 2.10B). Interestingly, not all PCs with strong Calbindin staining showed strong signal of  $\alpha$ -Synuclein confirming our observation that overexpression of  $\alpha$ -Synuclein was not homogenous between the cells and followed a random mosaic distribution. In DCN, the Calbindin staining was homogenous and diffusely distributed, whereas  $\alpha$ -Synuclein presented a rough, coarse pattern of wasdistribution.  $\alpha$ -Synuclein and Calbindin are perfectly overlapped in this region with comparable

signal intensities, a portion of Calbindin signal however did not co-stain with  $\alpha$ -Synuclein confirming the mosaic pattern of  $\alpha$ -Synuclein expression. Localization of  $\alpha$ -Synuclein with Calbindin in DCN demonstrated that overexpressed  $\alpha$ -Synuclein was abundant in pre-synaptic regions of PCs.

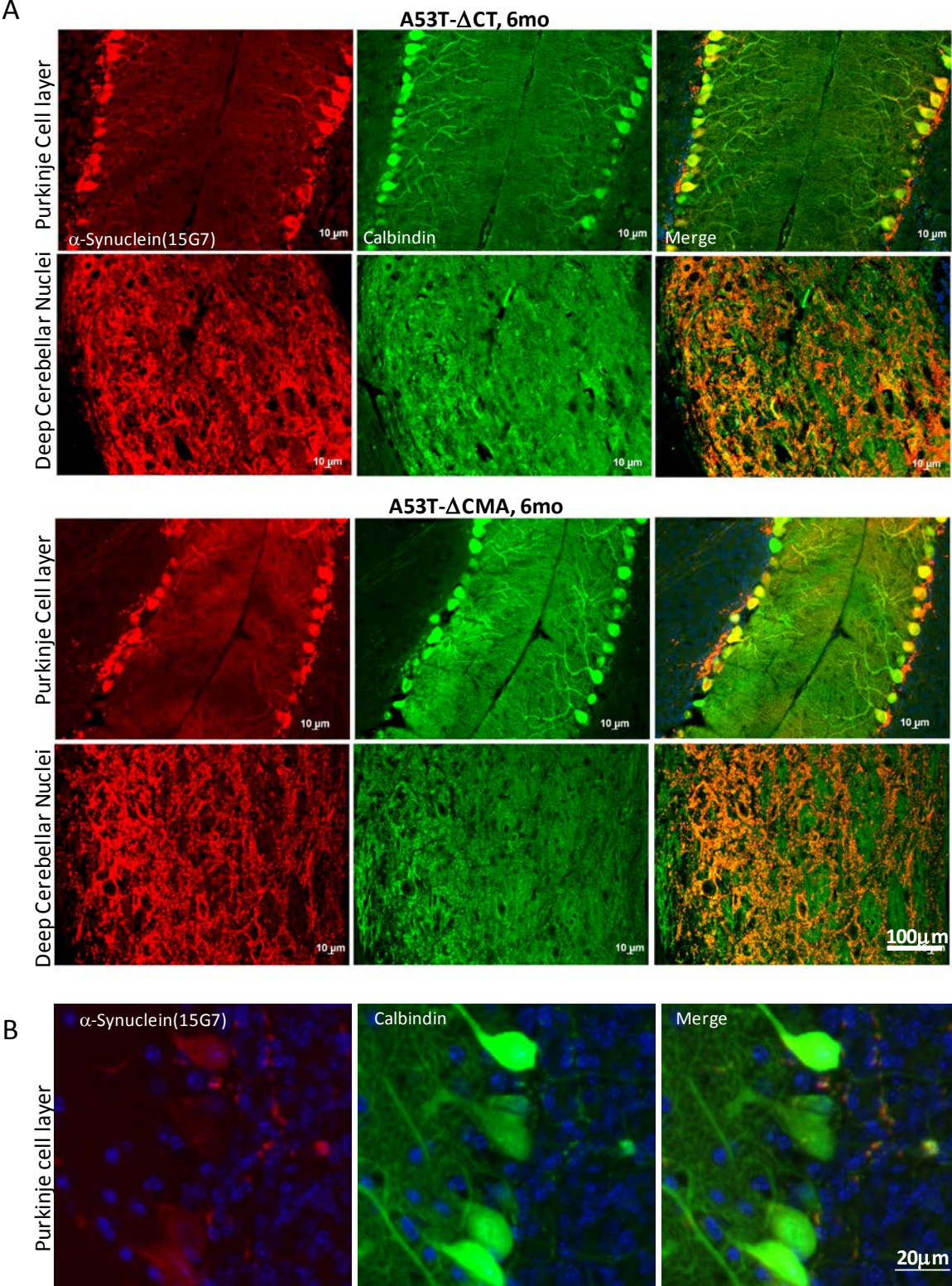


**Figure 2.10: Co-localization of  $\alpha$ -Synuclein and specific marker of PCs, Calbindin D28-K. Immunofluorescent staining of 7 $\mu$ m-thick sagittal cerebellar sections from 6-month old transgenic mice.**

A:  $\alpha$ -Synuclein and Calbindin D28-K are co-localized in molecular layer (ML), Purkinje cell layer (PCL) and Deep cerebellar nuclei (DCN) in A53T- $\Delta$ CT and A53T- $\Delta$ CMA lines. Antibody anti-human  $\alpha$ -Synuclein (15G7, Red), antibody anti-mouse Calbindin D28-K (Green).

B: Co-localization of  $\alpha$ -Synuclein and Calbindin D28-K in PCL at high magnification view. Antibody anti-human  $\alpha$ -Synuclein (15G7, Red), antibody anti-mouse Calbindin D28-K (Green).

### 2.3.2 Mutation of the CMA motif does not affect the steady-state level of $\alpha$ -Synuclein *in vivo*

The effect of CMA-motif mutation on the  $\alpha$ -Synuclein turnover *in vivo* had not been previously elucidated. *In vitro*, the A53T mutant has been shown to act as a blocker at the entrance gate of the lysosomes and to prevent its translocation to the lysosomal lumen (Cuervo, 2004). Expression of A53T  $\alpha$ -Synuclein has been reported to partially inhibit total protein degradation in the lysosome while expression of A53T- $\Delta$ CMA had no effect in proliferating SHSY-5Y cells. In contrast, overexpression of both mutants blocked lysosomal degradation in differentiated SHSY-5Y cells in the same study (Xilouri et al., 2009). In current animal models, similar staining intensities and intracellular distributions were observed for both mutants by immunohistochemistry intensity (Figure 2.11C). To further explore this, the mRNA levels of  $\alpha$ -Synuclein of each transgenic line were measured by RT-qPCR and these results confirmed that expression levels were similar (data not shown). This indicated that the isogenic insertion strategy by knocking-in *TetO-SNCA* transgene at the *ROSA26* locus created transgenic animals with identical genetic backgrounds (Figure 2.8B). In these transgenic lines at 4-months of age, western-blot analyses revealed no differences in protein expression levels (Annex 4). As well,  $\alpha$ -Synuclein migrated as a single band as in non-transgenic controls (data not shown). The means of ratios [ $\alpha$ -Synuclein/GAPDH] were compared. No significant difference in  $\alpha$ -Synuclein protein levels was found in both lines (Figure 2.11A,B). This suggests that the deletion of the CMA-motif had no effect on  $\alpha$ -Synuclein turnover *in vivo*. Therefore, we should expect from this result no great difference in disease onset or behavior in our two transgenic mouse lines.

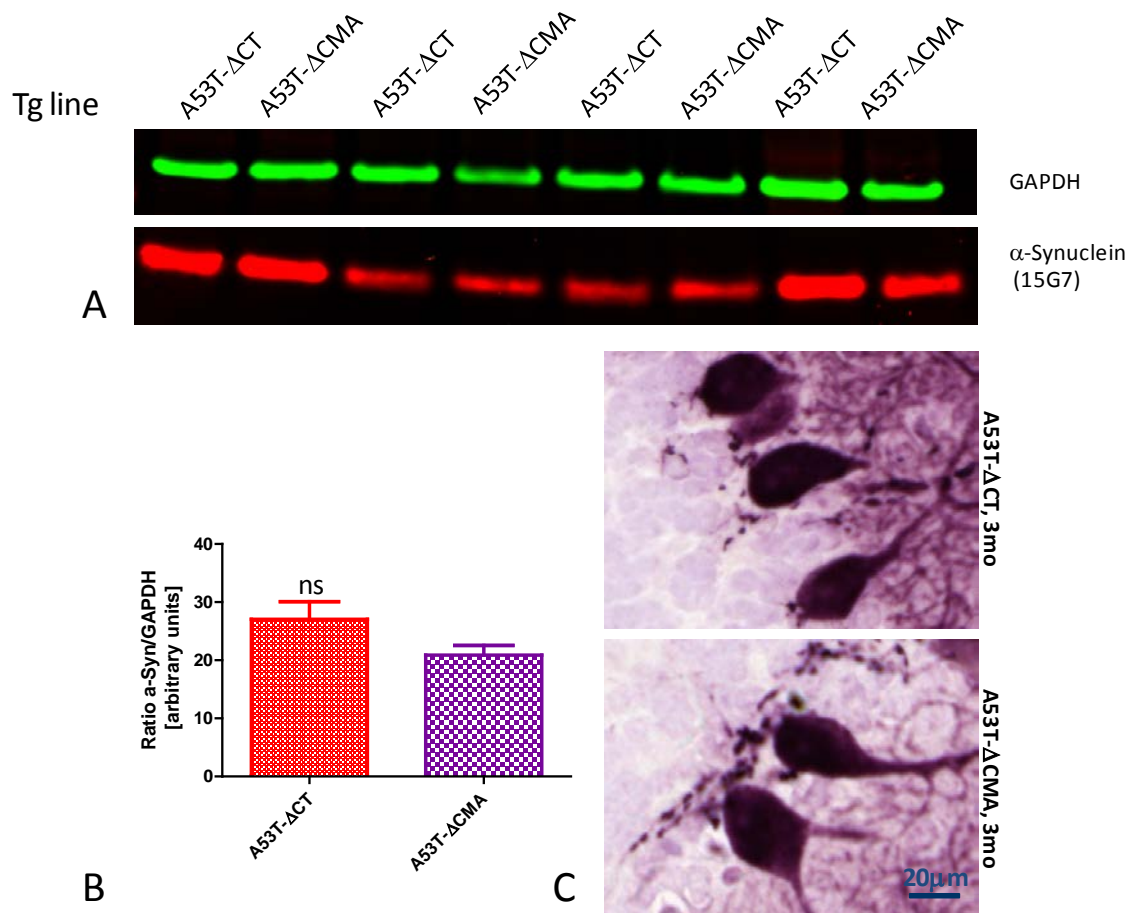


**Figure 2.11: Similar  $\alpha$ -Synuclein protein levels in both transgenic lines despite mutation of the Chaperone-mediated autophagy motif in A53T- $\Delta$ CMA line.**

A: Western-blot showing in  $\alpha$ -synuclein level in cerebellum tissue homogenates from 4-month old transgenic mice, antibody 15G7 anti- $\alpha$ -Synuclein, GAPDH is used as loading control.

B: Quantification of  $\alpha$ -Synuclein protein level from A. Diagram representing the mean of signal ratio  $\alpha$ -Synuclein/GAPDH of transgenic lines (signal obtained from Odyssey software, no-background quantification method), data are expressed as the mean  $\pm$  SEM; n= 8.

C: Immunostaining of 7- $\mu$ m thick sagittal cerebellar sections from 3- month-old mice (3mo), antibody 15G7 anti- $\alpha$ -Synuclein followed by chromogenic revelation method.

## 2.4 Analysis of transgenic animals overexpressing $\alpha$ -Synuclein

Overexpression of  $\alpha$ -Synuclein in rodents has been reported to cause pathological conditions, but the severity probably varies between models depending on different factors: the promoters used for driving transgene expression, the  $\alpha$ -Synuclein transgene construct, the level of overexpression, the genetic background of the host animal, the location of the transgene insertion, the absence or presence of  $\alpha$ -Synuclein aggregates. These variable factors contribute to the diversity in the age of disease-onset observed in different animal models (Table 1.3 and reviewed in Chesselet et al., 2011). In general, overexpression of  $\alpha$ -Synuclein causes progressive behavior changes with onset starting between 8 and 12 months. These behavioral dysfunctions may be preceded or followed by histopathological features. The difficulty in determining the onset of the disease constitutes major

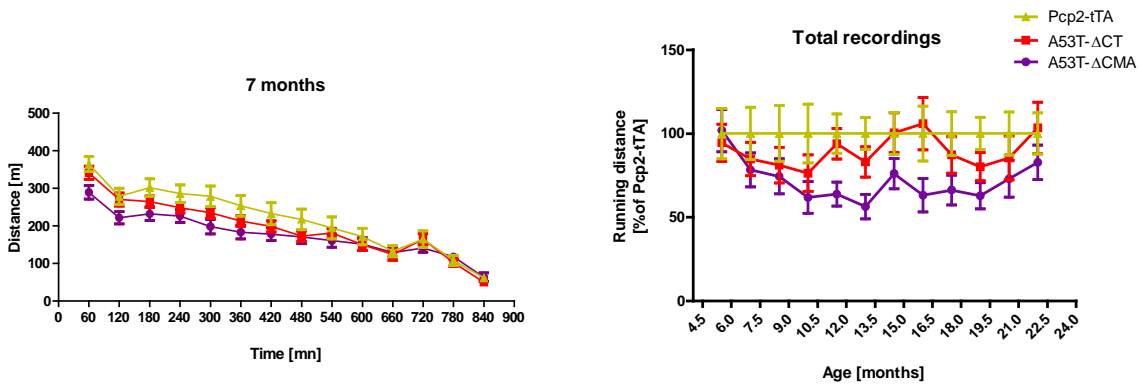
challenge when analyzing new  $\alpha$ -Synuclein transgenic models. For this reason, two lines of investigation were carried out in parallel: one surveying behavior changes and the second examining the histopathology of the cerebellum at different ages.

#### 2.4.1 Transgenic mice overexpressing of $\alpha$ -Synuclein in PCs show decline in locomotor performance compared to non-transgenic mice

Transgenic mice overexpressing  $\alpha$ -Synuclein did not show any particular phenotype up to 5 months of age. To further investigate animal behavior, we generated new cohorts of animals by crossing Pcp2-tTA mice (from 7th backcrossing to C57BL/6) with *TetO-SNCA* mice. Two age-matched cohorts of control non-transgenic animals were used: control 1: WT= purchased C57BL/6 mice, control 2: Pcp2-tTA at 8th generation of backcrossing. Any behavioral deficits, once identified, are predicted to depend on the degree of neurodegeneration. Concretely, pronounced PC degeneration should affect motor coordination or motor balance in our transgenic animals (Donald et al., 2008;Komatsu et al., 2007). Therefore, a broad range of motor coordination behavior was evaluated using standard tests: rotarod, pole test and beam-walk. In addition, basal locomotor activities (ambulatory and rearing) were recorded using open-field test (automatic home-cage).

In *open-field*, locomotor activities of animals were recorded every 6 weeks using Actimot system (TSE). Two main parameters which featured locomotor activities, ambulatory activity (reflected by traveling distance) and rearing frequency were extracted from the raw data. The mean of each parameter in each group at each time point is plotted in a graph to establish the cumulative activity curves (total recordings) (Figure 2.12 A, B). To facilitate the analysis, data from transgenic groups were normalized to the control group Pcp2-tTA (100% correspond to ~ 3000-3500 meters of traveling distance and ~ 1500-2000 rearing times) (Annex 6). Both parameters, traveling distance and rearing, from all animal groups were relatively stable over time indicating that locomotion does not decline in an age-dependent manner up to 16.5 months. Interestingly, the A53T- $\Delta$ CMA line showed significantly lower traveling distances and rearing activities compared to the control Pcp2-tTA. Although the A53T- $\Delta$ CT line showed a lower trend towards rearing activities compared to the control Pcp2-tTA, this was not statistically significant. No difference in the ambulatory activities of the A53T- $\Delta$ CT and control Pcp2-tTA lines were detected. Interestingly, WT (C57BL/6) mice exhibited significantly higher rearing activities compared to all other lines (Pcp2-tTA, A53T- $\Delta$ CT and A53T- $\Delta$ CMA) (Annex 6).

## A. Traveling distance



## B. Rearing activities

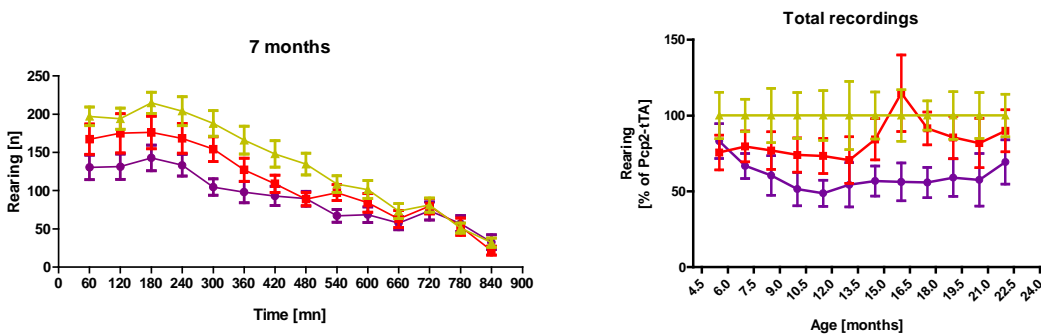


**Figure 2.12: Locomotor activities of animals recorded by Open-field test during active phase.** (Pcp2-tTA: n=22, A53T-ΔCT: n=16, A53T-ΔCMA: n=18)

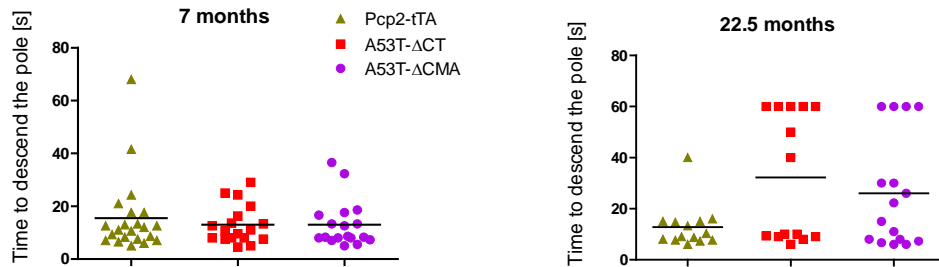
A: *Left*: Typical curve of ambulatory movement. Data represented the mean  $\pm$ SEM of traveling distance (in meters) recorded every 60min. *Right*: Total traveling distance from ages of 6 to 22.5 months. Data mean traveling distance normalized to Pcp2-tTA group.

B: *Left*: Typical curve of vertical movement. Data represented the mean  $\pm$ SEM of rearing times recorded every 60min. *Right*: Total rearing activities from ages of 6 to 22.5 months. Data mean rearing activities normalized to Pcp2-tTA group.

In *pole climbing test*, the time necessary for animals to turn downward (t-turn) and total time to descend the pole (t-total) were measured. The pole test has been used to detect bradykinesia and motor coordination in PD mouse models (Fleming et al., 2006; Glajch et al., 2012; Price et al., 2010). Behavioral deficits in the pole test have been ameliorated by dopamine agonist treatment in MPTP mice and in a Parkinsonian genetic mouse model (Luchtman et al., 2012; Ono et al., 2009; Park et al., 2013). Experiments were done with animals at young and mid-advanced ages of 5, 7, 10 months. Starting from 14 months, animal performance was regularly assessed every 6 weeks. Data per animal in each experiment was represented as the mean (t-turn and t-total) of five trials. Since the t-turn is proportional to t-total, only data here representing t-total are shown. In young animals, there was no significant difference in total time to descend the pole. Curiously, occasionally some transgenic animals could not turn downward or slide-off the pole (t-total was counted as 60s). Starting from 14 months of age, there was an increase in the number of animals in the transgenic groups that slide-off

the pole (7 animals from A53T- $\Delta$ CT line and 7 animals from A53T- $\Delta$ CMA line). These animals were called "symptomatic" animals. However, there was no progressive increase between 14 and 22.5 months. Other transgenic animals continued to perform the test well and did not show an increase in the total time to descend the pole (7 animals from A53T- $\Delta$ CT line and 9 animals from A53T- $\Delta$ CMA line) (Figure 2.13A). These were called "non-symptomatic" animals. Performance of the non-transgenic group Pcp2-tTA was stable over time and was similar to "non-symptomatic" transgenic animals. There was no significant difference in the time to descend the pole in aged animals compared to young animals in the control group. Interestingly, re-analyzing the open-field data revealed that "symptomatic" animals clearly exhibited a decreased trend for rearing activities starting from around 15 months. Compared to control Pcp2-tTA mice, the rearing activities of "symptomatic" A53T- $\Delta$ CMA and A53T- $\Delta$ CT are 29.98 % 7.73 and 51.11% 11.13, respectively. The same activity in "non-symptomatic" animals remained stable (Figure 2.13B). However, there was no substantial decrease in traveling distance between "symptomatic" groups and "non-symptomatic" groups (Annex 7).

## A. Pole test



## B. Rearing activities

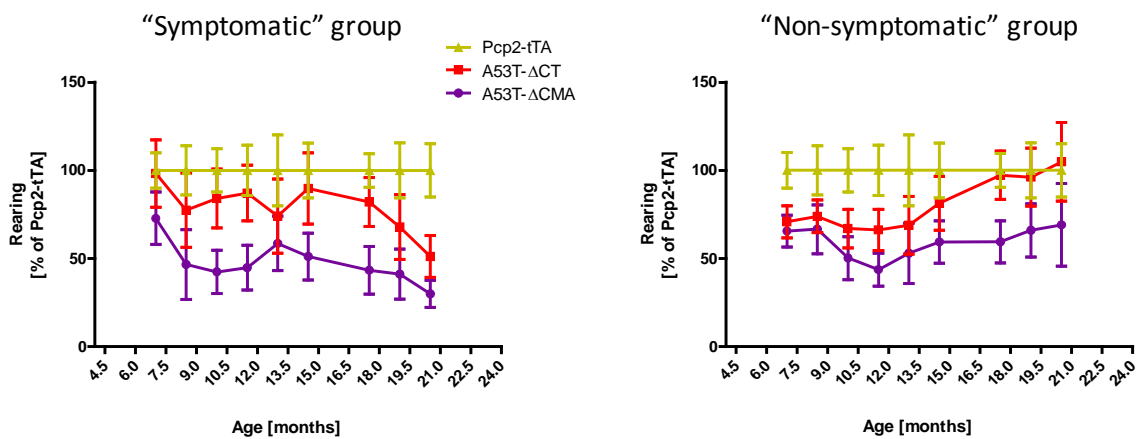


**Figure 2.13: Motor coordination and motor balance phenotyping.**

A: Latency of animals on pole . Data represented the mean of total time to descend the pole (in s) in five trials of individual animals (Pcp2-tTA: n=22, A53T-ΔCT: n=16, A53T-ΔCMA: n=18).

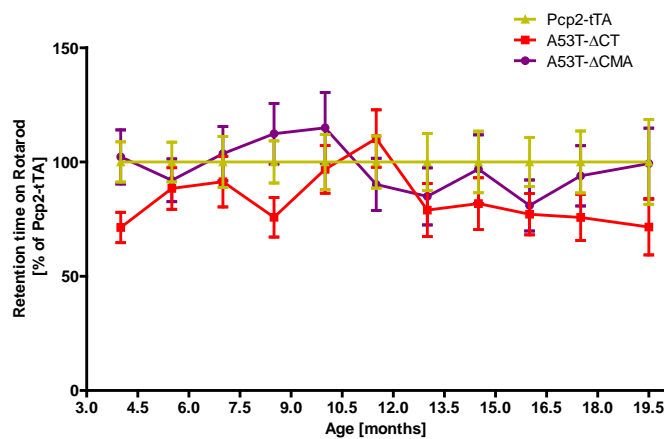
B: Post-analysis of vertical movement activities for “symptomatic” (left) and “non-symptomatic” (right) groups . Data represents the mean  $\pm$ SEM of total rearing times ages of 6 to 21 months normalized to Pcp2-tTA group (Pcp2-tTA: n=22, A53T-ΔCT: n=7, A53T-ΔCMA: n=7).

In *rotarod*, motor coordination capacity was measured by the duration in which animals were still able to run on an accelerating rotarod (latency to fall). The mean of latency to fall of each group at each time point is plotted in a graph to establish cumulative curves. To avoid variation between experiments, the scores of transgenic groups were normalized to the ones of Pcp2-tTA group (100 % corresponding to ~80-120 s of latency on rod). A mild, progressive, age-dependent diminishing motor performance was observed in all animal groups (Annex 8A). However, no significant difference in the latency to fall could be detected up to 19.5 months of age between transgenic lines and Pcp2-tTA control group (Figure 2.14A). The retention time on rotarod of the two sub-groups “symptomatic” and “non-symptomatic” defined as precedent from pole climbing test was also re-analyzed. Interestingly, transgenic “symptomatic” animals again showed a difference of 20 s of retention time

on rotarod at 13, 15 and 16.5 months of age compared to Pcp2-tTA control line. No clear difference was observed in "non-symptomatic" groups (Annex 8B).

In *beam-walk*, the total time that animals needed to cross the challenge beam in a single walk was measured, a maximal allowed duration of crossing was fixed at 60s. Experiments were conducted at three time points: 15, 17 and 19 months. On the day of test, five trials per animal were done and the mean of five scores was considered as the crossing time. Animals that failed in 3 or more of the 5 times to cross the beam ("fallen-out") were counted as 60s. Interestingly, transgenic groups at 15 months took significantly longer time to cross the beam than non-transgenic control group. However, no significant difference was observed at later time points (17 and 19 months) suggesting a certain adaptation of transgenic animals to the task (Figure 2.14B).

### A. Rotarod



### B. Beam-walk

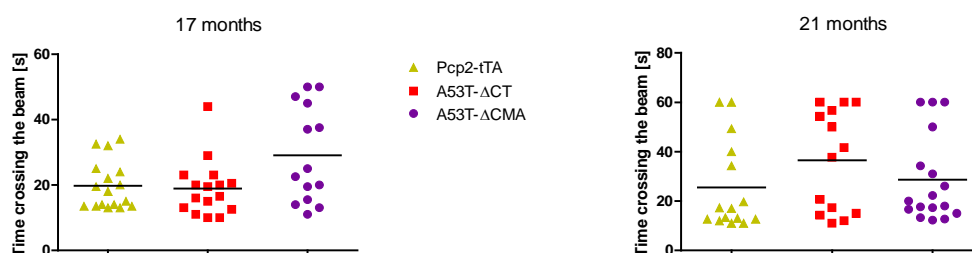


**Figure 2.14: Motor coordination and motor balance phenotyping.**

A: Latency of animals on rotarod. Data represent the mean of total time to stay on accelerating rod (in s) normalized to Pcp2-tTA group (Pcp2-tTA: n=22, A53T-ΔCT: n=16, A53T-ΔCMA: n=18).

B: Ability to cross the beam. Data represented the mean of total time to cross the beam in four trials.

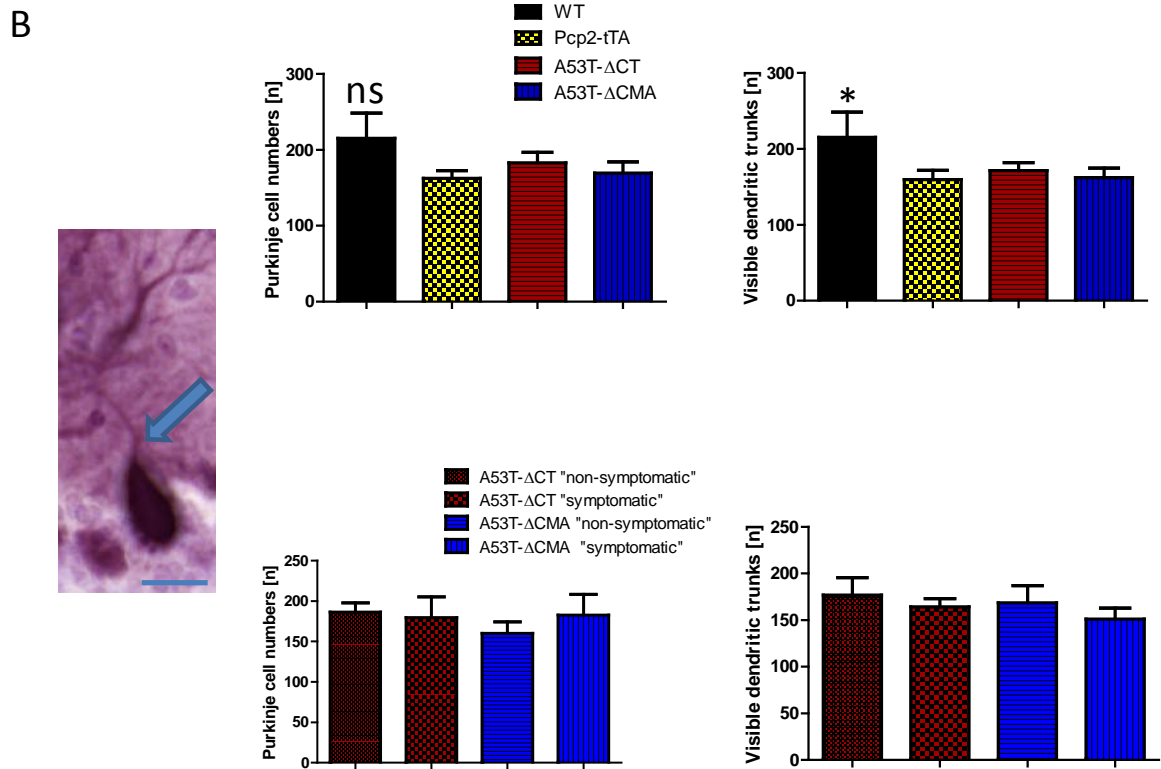
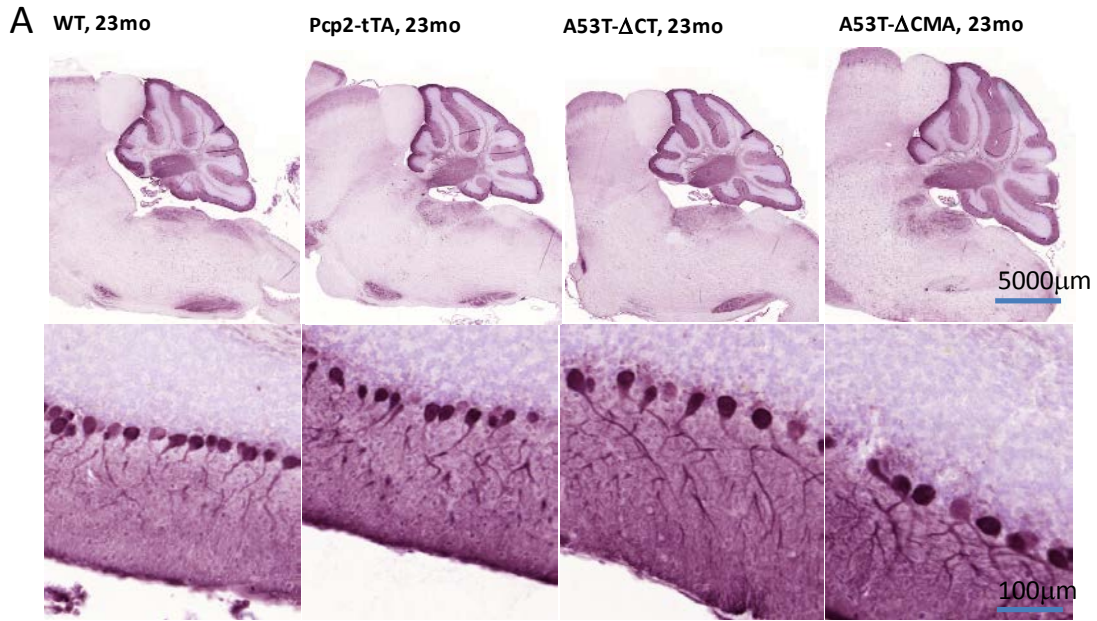
Taken together, this behavioral data suggested a certain tendency of locomotor and motor coordination deficits in transgenic animals. In terms of specificity, vertical movement (rearing, pole climbing) seems to be more affected than horizontal movement (traveling distance, latency on rotarod, beam crossing). These deficits however did not clearly decline in an age-dependent manner. In addition it should be noted that not all animal in transgenic groups were affected to the same degree and only some animals in each transgenic group were sensible to the behavioral tests.

#### 2.4.2 Analysis of PC neurodegeneration

Our primary immunohistochemistry results obtained from analyses of pilot groups did not show prominent neurodegeneration in the cerebellum (data not shown). To clarify pathological changes in transgenic animals and to identify a link between phenotype and molecular pathologies, detailed histological and biochemical studies were performed on the animal groups which had been used for behavioral tests. All animals were sacrificed and transcardially perfused with PBS at 23 months of age, the right hemisphere of cerebellum was used for immunohistochemical staining and the left hemisphere was used for western-blot. Transgenic lines- A53T- $\Delta$ CT and A53T- $\Delta$ CMA were compared with non-transgenic lines- WT and Pcp2-tTA.

##### 2.4.2.1 PC morphology

To determine whether overexpression of  $\alpha$ -Synuclein lead to neurodegeneration of PCs, number of Purkinje cells was counted in cerebellum sections stained with antibody anti-Calbindin-D28K. Sections were cut at 12 $\mu$ m of thickness and staining was revealed by chromogenic method to reduce the risk of autofluorescence detection due to accumulation of lipofuscin in old brain tissues (Figure 2.15A). Triplicate staining was made for each animal and only cells with well-shaped cell body (as shown in Figure 2.15B) were taken in account. The mean of triplicate is defined as the PC number of corresponding animal. No significant difference in PC number was found between Pcp2-tTA and the two transgenic lines A53T- $\Delta$ CT and A53T- $\Delta$ CMA. Interestingly, PC number in WT line ( $205.3 \pm 31.77$ , n=11) showed a non-significant trend for more PCs than the Pcp2-tTA ( $154.7 \pm 11.79$ , n=12), A53T- $\Delta$ CT ( $180.4 \pm 14.24$ , n=14) and A53T- $\Delta$ CMA ( $169.3 \pm 15.02$ , n=14) (Figure 2.15B). The A53T- $\Delta$ CT line also tended to have more PCs than the A53T- $\Delta$ CMA line. In two sub-groups "symptomatic" vs. "non-symptomatic" within the same transgenic line, no significant difference in PC numbers in these sub-groups was observed (Figure 2.15B).



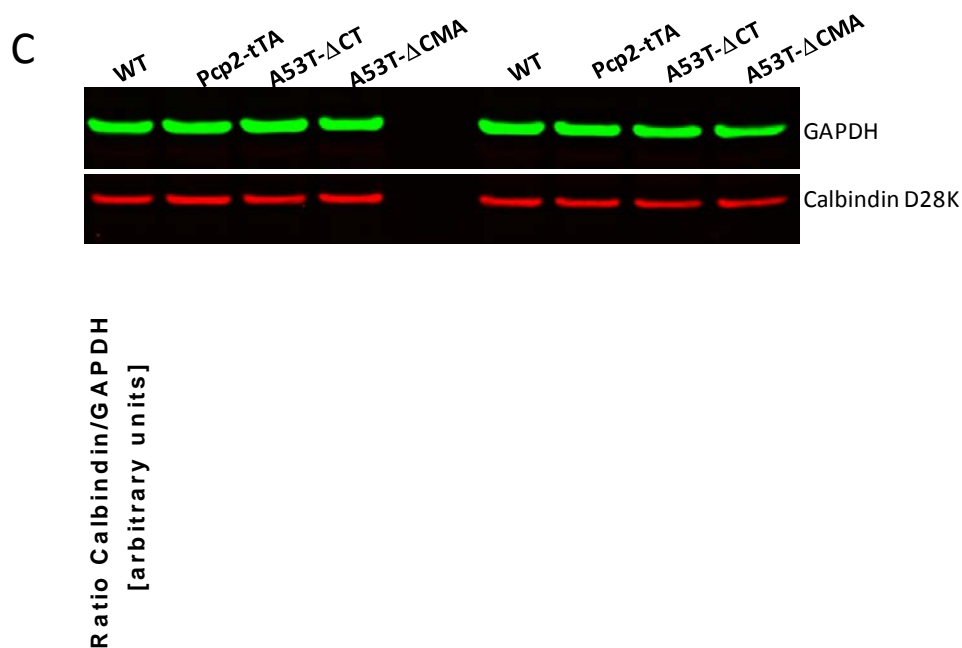


**Figure 2.15: Change in number of Purkinje cells is independent of  $\alpha$ -Synuclein overexpression in 23-month old animals .**

A: Immunostaining of Purkinje cells in 12- $\mu$ m thick sagittal cerebellar sections from 23-month-old mice (23mo), antibody anti-Calbindin D-28K (chromogenic stain)

B: Counting of PCs with sharpened cell bodies and visible main trunk of neuritic arborization (arrowed). Data are expressed as the mean of PCs  $\pm$  SEM; n= 7 per animal group, 3 slices per animal.

C: Western-blot showing Calbindin protein level in cerebellum tissue homogenates from the same animals (antibody anti-Calbindin D-28K, GAPDH is used as loading control) and diagram comparing relative protein level of Calbindin, data expressed as the mean of ratio Calbindin/GAPDH  $\pm$  SEM; n= 7 per animal group .

Changes in Purkinje cell dendrite morphology has been reported to induce deficits in motor coordination (Donald et al., 2008). Using the same sections, the number of visible main trunks of dendrites was counted. Only trunks directly connected to cell bodies were taken in account, the ones which were not linked to cell bodies were considered as unordered structures. There was a significant difference in the number of visible main trunks in WT line ( $215.1 \pm 33.42$ , n=10) and the transgenic animal lines but not between Pcp2-tTA ( $159.6 \pm 12.04$ , n=10), A53T- $\Delta$ CT ( $171.3 \pm 10.67$ , n=11) and A53T- $\Delta$ CMA ( $162.1 \pm 12.57$ , n=11) lines. Again, there was a higher but non-significant trunk number in A53T- $\Delta$ CT line compared to A53T- $\Delta$ CMA line. Within the same transgenic line, the trunk number in "symptomatic" and "non-symptomatic" within the same transgenic line (Figure 2.15B) in agreement with the analysis of Purkinje cell number.

Since  $\alpha$ -Synuclein overexpression has been reported to induce abnormalities in axon terminals (Komatsu et al. 2007). No remarkable morphological changes or abnormal redistributions of Calbindin was observed in cerebellar nuclei in any of the animal groups. This suggests that the

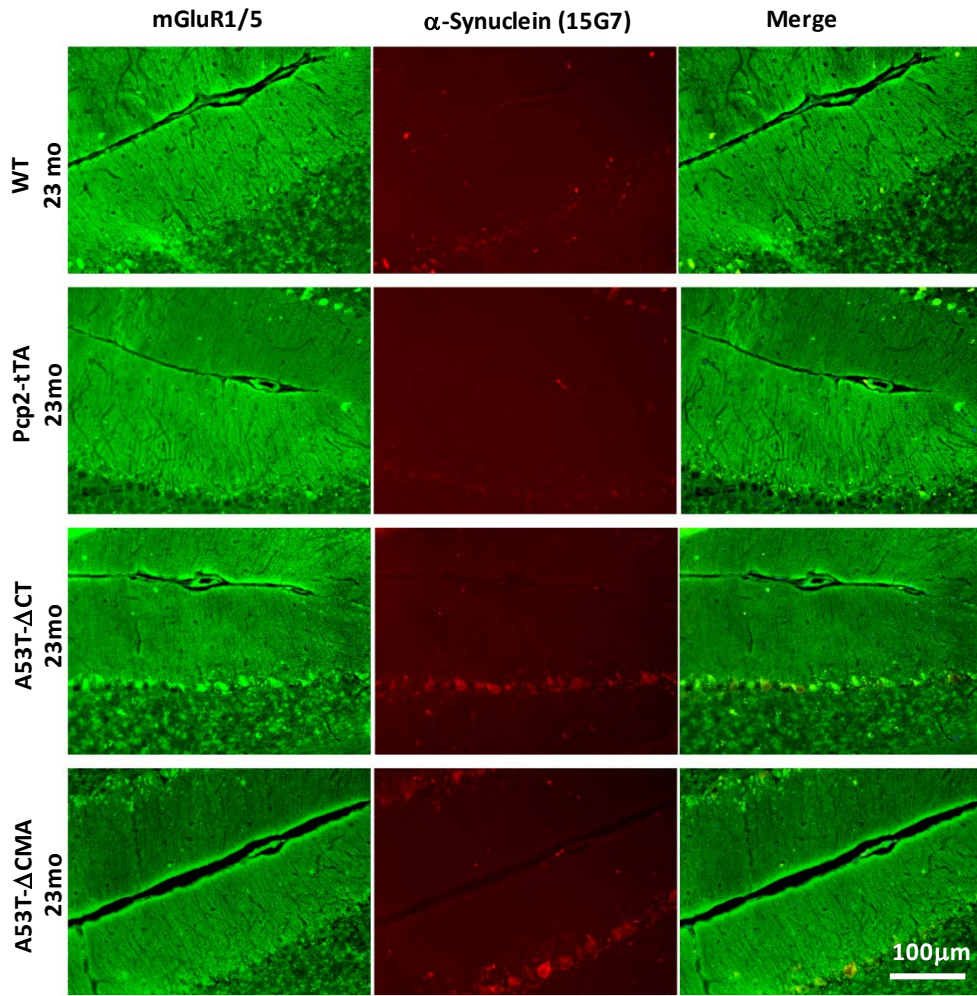
elevated expression of  $\alpha$ -Synuclein in pre-synaptic regions, does not provoke massive axonal degeneration of PC before 23 months of age (Figure 2.15A).

To validate these histological studies, western-blot analysis was also performed. We compared protein level of Calbindin in cerebellum homogenates from the same animals which were used for immunohistostaining. Calbindin was detected by the same antibody anti-Calbindin-D28K used in histological studies. As shown in Figure 2.15C, the Calbindin protein levels between were similar in cerebellum homogenates from the four lines. Taken together, the absence of significant differences in PC numbers and Calbindin levels between transgenic lines and Pcp2-tTA control line indicates that there is no massive PC loss. In addition, the quantification of visible main trunks did not reveal any disorganization of dendritic trees of PCs in transgenic mice compared to non-transgenic control animals. Furthermore, the presence of excess  $\alpha$ -Synuclein in axonal terminals did not dramatically alter either axonal morphology or pre-synaptic density in cerebellar nuclei. However, the fact that WT line showed consistently higher PC numbers and more homogeneously organized dendritic structures imply that overexpression of tTA itself is unexpectedly toxic for PCs.

#### 2.4.2.2 *Synaptic density markers*

PC dendrites form synapses with parallel fibers in the molecular layer and PC degeneration may be linked to loss of synaptic connections in this region. Overexpressed  $\alpha$ -Synuclein was also found in dendritic trees suggesting that PC degeneration, when it occurs, might also happen in dendritic spines. To further explore this possibility, synaptic density in the molecular layer (ML) reflected by synaptic marker expression level was examined using a synaptic marker, the glutamate receptor mGluR1 which is concentrated in PC dendritic spines innervated by parallel fibers. Glutamate receptor mGluR1 is localized at high level in PC dendritic spines where PCs are innervated by parallel fibers. mGluR1 has been previously used to characterize PC degeneration (Zu et al., 2004; Komatsu et al., 2007). Immunohistochemistry revealed a high concentration of mGluR1 widely distributed in the ML, clearly distinguishing the cerebellar cortex from the rest of the cerebellum. The staining intensity and distribution of mGluR1 was comparable in transgenic mice and control mice suggesting that no dramatic change in dendritic spine density occurs in the ML (Figure 2.16A). However, this method was not quantitative since dendritic spine could not be visualized with high precision under microscope at low magnification. In addition, the localization of another synaptic marker, Syntaxin which is a component of the SNARE complex was examined. Immunolocalization of Syntaxin revealed a similar distribution to mGluR1 in the ML (data not shown). To quantify synaptic densities, Syntaxin levels in cerebellar homogenates from the transgenic animal lines were compared by western-blot. Equivalent levels of syntaxin were found in all lines (Figure 2.16B), again indicating that overexpression of  $\alpha$ -Synuclein does not affect synaptic density in the ML (Figure 2.16A).

A



B

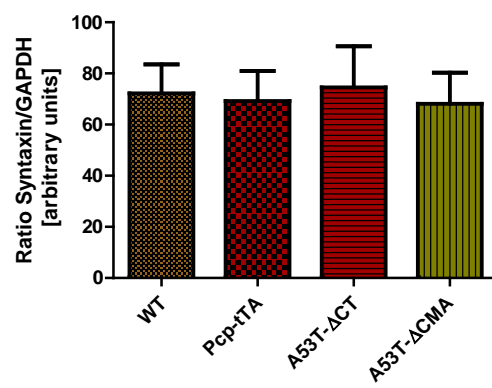
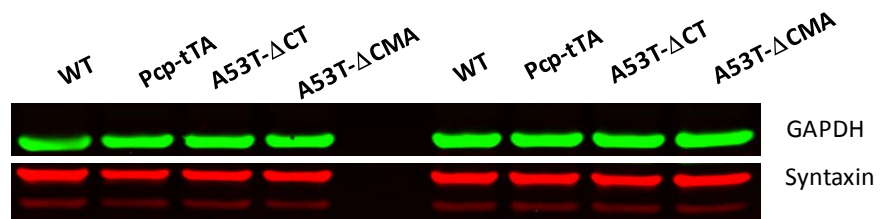


**Figure 2.16: Overexpression of  $\alpha$ -Synuclein doesn't lead to changes in synaptic density up to 23 months of age.**

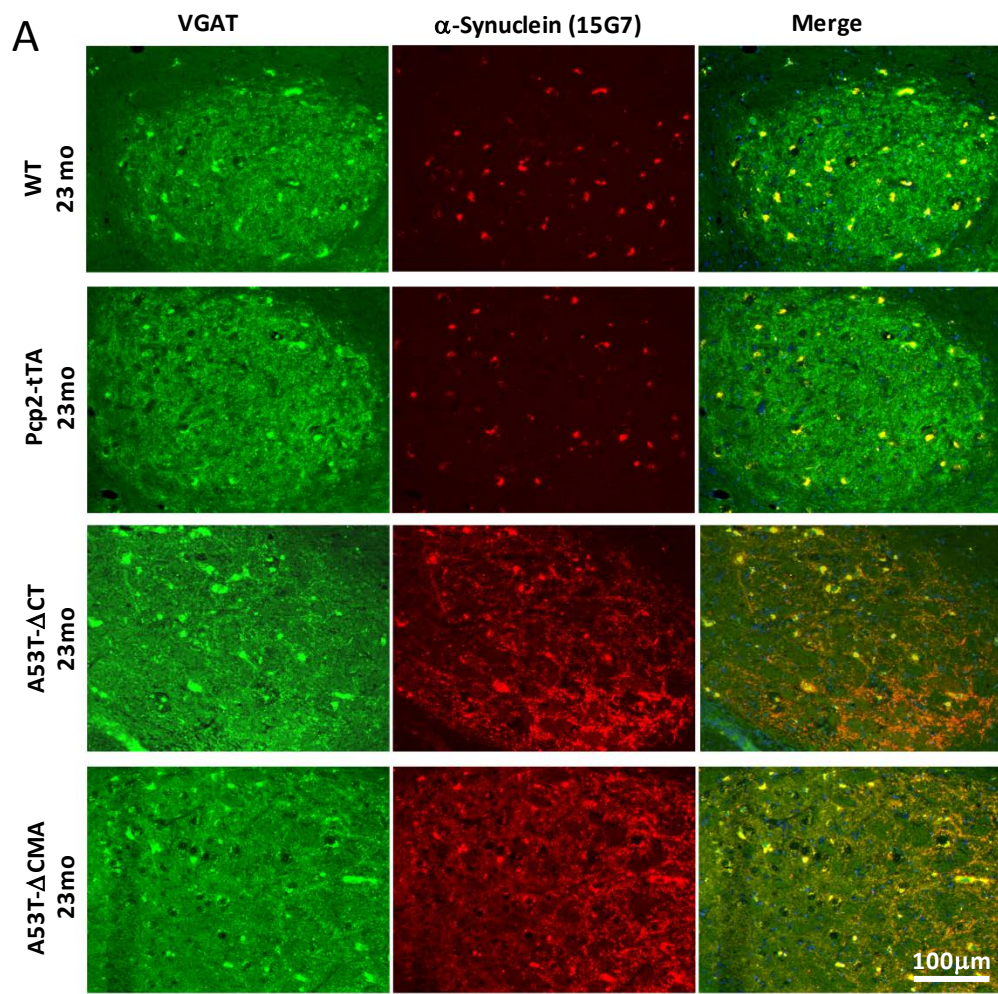
A. Immunofluorescent co-labeling of glutamate receptor (mGluR1/5) and  $\alpha$ -Synuclein in the molecular layer from 7 $\mu$ m- thick sagittal cerebellar sections. Antibody anti-mouse mGluR1/5 (Green) and antibody anti-human  $\alpha$ -Synuclein (15G7, Red).

B. Western-blot showing protein level of synaptic marker protein Syntaxin in cerebellar tissue homogenates from the same animals (antibody anti-Syntaxin, GAPDH is used as loading control) and diagram comparing relative protein levels of Syntaxin, data expressed as the mean of ratio Syntaxin/GAPDH  $\pm$ SEM; n= 4 per animal group

### 2.4.2.3 GABA neurotransmitter release

The involvement of  $\alpha$ -Synuclein in regulating neurotransmitter release remains controversial. Some findings suggest that overexpression of  $\alpha$ -Synuclein in old mice elevates dopamine levels at the pre-synaptic region of nigrostriatal dopaminergic cells and induces abnormal accumulation of dopamine vesicles reserve pool prior to neurodegeneration (Kurz et al., 2010). PCs are known as GABAergic inhibitory neurons which make synapses with relay neurons in deep cerebellar nuclei (DCN). To evaluate the effect of  $\alpha$ -Synuclein overexpression on GABA transmission, GABA releasing terminals were immunostained for the vesicular GABA transporter (VGAT) (Mandolesi et al., 2012), in particular the DCN where PC axon terminals are concentrated. The signals for VGAT and  $\alpha$ -Synuclein observed in this region highly overlapped in transgenic mice confirming that the majority of axon terminals were from PCs (Figure 2.17A). Nevertheless, the densities of VGAT signals were highly comparable in transgenic mice and non-transgenic control animals. Using this approach, no notable accumulation or redistribution of VGAT dots in transgenic animals was found in contrast to previous studies (Halliday et al., 2011). This observation suggests that despite the presence of overexpressed  $\alpha$ -Synuclein and GABA vesicle, GABA vesicle homeostasis is maintained in PC axon terminals (Figure 2.17A).

GABAergic synaptic inputs in cerebellum do not exclusively come from PCs, but also from Golgi cells which synapse on mossy fibers in the granule cell layer and from other inter-neurons which synapse on soma or dendrites of PCs in the ML (Mandolesi et al., 2012). Thus immunostaining of VGAT also reveals afferent PC inputs. VGAT was widely distributed in punctate, but was less dense than mGluR1 revealed a widely punctuate distribution of this marker in ML but with lower density as observed with mGluR1 staining (Figure 2.17B). As predicted, punctuate VGAT staining was also present on PC soma as expected. Similarly to mGluR1, no obvious change in VGAT density either in ML or on PC soma in transgenic mice compared to control animals. Once again this supports the view that there is no clear-cut reduction in the direct innervation of PCs by other cells in the ML and PCL on PC (Figure 2.17B).



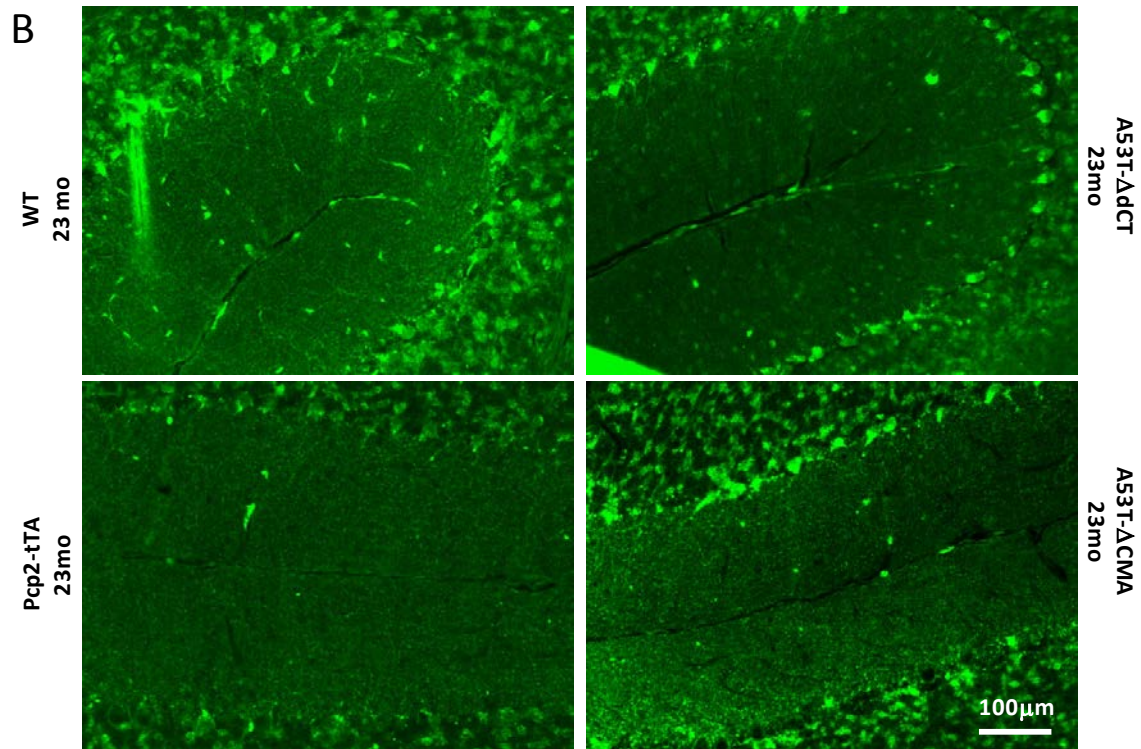


**Figure 2.17: Overexpression of  $\alpha$ -Synuclein doesn't lead to change of pre-synaptic vesicle density up to 23 months of age.**

A: Immunofluorescent co-labelling vesicular GABA transporter (VGAT) and  $\alpha$ -Synuclein in deep cerebellar nuclei of 7 $\mu$ m- thick sagittal cerebellar sections. Antibody anti-mouse VGAT (Green) and antibody anti-human  $\alpha$ -Synuclein (15G7, Red).

B: Staining of VGAT in Purkinje cell layer and molecular layer of 7 $\mu$ m- thick sagittal cerebellar sections.

#### 2.4.2.4 Neuroinflammation markers

Activation of glial cells is widely recognized as a feature of neurodegeneration although molecular mechanisms underlining this activation are not fully understood. Glial activation accompanying with PC degeneration has been reported in previous studies (Mandolesi et al., 2012;Zhao et al., 2011). Overexpression of  $\alpha$ -Synuclein in transgenic animal model commonly showed an increase in glial cell activation (Lim et al., 2011;Nuber et al., 2008). In order to check whether overexpression of  $\alpha$ -Synuclein in our animal models increased inflammation, immunohistochemistry of glial fibrillary acidic protein (GFAP) and Iba-1 to characterize astrocyte activation (astrogliosis) and microglia activation (microgliosis) respectively was performed.

Immunostaining of GFAP revealed a ubiquitous distribution of astrocytes throughout the cerebellum with a high concentration of cells in cerebellar white matter along PC axonal beams. Astrocytes were also seen at a lower density in cerebellar nuclei. These cells were present in high quantity in all animals and expression was comparable between the lines (non-transgenic and transgenic)

suggesting that overexpression of  $\alpha$ -Synuclein in transgenic lines does not significantly enhance astrogliosis (Figure 2.18).

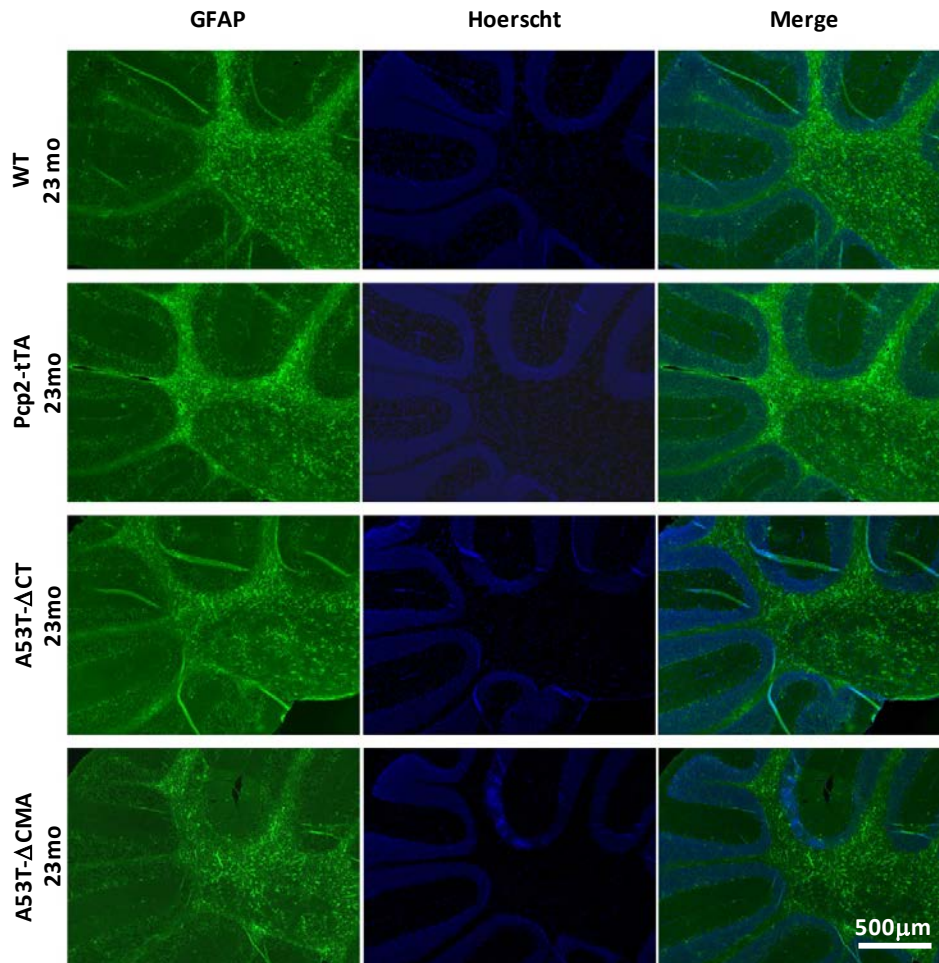


**Figure 2.18: Astroglial staining in cerebellum at 23 months of age.**

Immunofluorescent labelling glial fibrillary acidic protein (GFAP) from 7 $\mu$ m- thick sagittal cerebellar sections. Antibody anti-mouse GFAP (Green) and Hoerscht staining (Blue).

Immunolabeling of Iba-1 showed a uniform distribution of microglia in cerebellum. Microglial cells were more concentrated in the cerebellar nuclei. The cells exhibited both resting state (small cell bodies with long ramifications) and activated state (round, dense cell body with small extensions). From our general observation, there were more resting cells than activated cells in all animal groups. Similarly to GFAP, Iba-1 expression was comparable between animal lines indicating that overexpression of  $\alpha$ -Synuclein was probably not the cause for microglia activation (Figure 2.19).

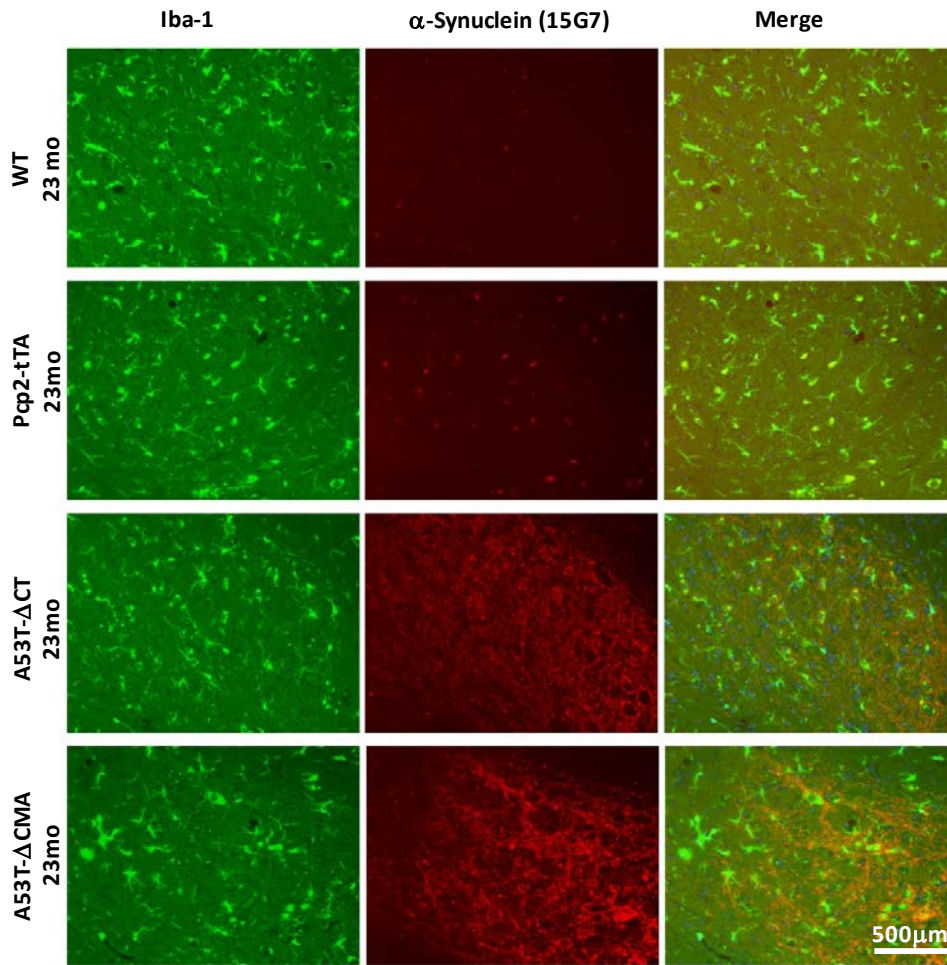


**Figure 2.19: Microgliosis in cerebellum at 23 months of age.**

Immunofluorescent co-labelling microglial cells and  $\alpha$ -Synuclein in deep cerebellar nuclei from 7 $\mu$ m- thick sagittal cerebellar sections. Antibody anti-Iba1 (Green) and antibody anti-human  $\alpha$ -Synuclein (15G7, Red).

Taken together, overexpression of  $\alpha$ -Synuclein in our transgenic models up to 23 months of age did not show enhanced astrogliosis or microgliosis indicating that neuroinflammation is not induced, in agreement with the absence of neurodegeneration in these models.

#### 2.4.2.5 Absence of amyloid-like feature of overexpressed $\alpha$ -Synuclein

Amyloid-like (Lewy body-like) deposits of  $\alpha$ -Synuclein resulting from the oligomerization and aggregate formation process are "hallmarks" of  $\alpha$ -Synuclein pathologies.  $\alpha$ -Synuclein oligomers are characterized by multiple features: abnormal accumulation, insolubility, resistance to enzymatic digestion (for example with proteinase K) and reactivity to Thioflavin S. They have also been shown to be phosphorylated or ubiquitinated (Neumann et al., 2002; Rieker et al., 2011). Based on these criteria, the development of pathological species of  $\alpha$ -Synuclein (with amyloid features) in the transgenic models was examined by immunohistochemistry and western-blot.

Oligomeric forms of  $\alpha$ -Synuclein could be detected in Triton soluble fractions by western-blot. Using 15G7 antibody, the presence of high-molecular-weight bands in brain homogenates were regularly checked from animal at different ages. The presence of relevant high-molecular-weight bands specific for  $\alpha$ -Synuclein oligomers in brain homogenates of transgenic animals up to 23 months of age was not detected. High-molecular-weight bands could be inconsistently observed in immunoblots using 15G7 antibody as well as in absence of primary antibody showing non-specificity of secondary binding (Annex 4).

In immunohistochemistry, it was observed that overexpressed  $\alpha$ -Synuclein in our transgenic models showed similar sub-cellular distribution pattern and there was not remarkable variation of this distribution at 3, 12 or 21 months (Figure 2.20). As previously mentioned,  $\alpha$ -Synuclein labeling using 15G7 antibody showed punctuate, dot-like immunoreactivity that could lead to think about abnormal accumulation of the protein (Figure 2.9). Nevertheless, these dots were already detected at early age (1 month, data not shown) and there was not a broad spreading of dots over time. Together with the observation in co-labeling with Calbindin-D28K, we supposed that dot-like  $\alpha$ -Synuclein corresponds rather to the normal localization of overexpressed  $\alpha$ -Synuclein than an abnormal accumulation (Figure 2.10).

Further,  $\alpha$ -Synuclein resistance to PK digestion in cerebellum of our transgenic animals was assessed. For this, PK digestion of paraffin sections from mouse brains at 18 months after transferring sections on PVDF membrane (PET-Blots) was performed according to Neumann et al. (2002) protocol. As positive control, brain sections from mice overexpressing A30P  $\alpha$ -Synuclein under the control of Thy-1 promoter (Thy-1 A30P mice) which showed strong phenotype (15-17 months) were used (Kahle et al., 2001). After paraffin de-waxing, tissues were digested in 50 $\mu$ g/mL of PK solution at 37°C during 15 hours.  $\alpha$ -Synuclein detection was done with 15G7 antibody. Numerous remaining spherical or longitudinal structures of  $\alpha$ -Synuclein in brain sections from Thy-1 A30P mice were observed whereas no background staining was seen (data not shown). This observation proved that  $\alpha$ -Synuclein structures in Thy-1 A30P mice could resist robust digestion by PK. However, none of remaining  $\alpha$ -Synuclein structure in our transgenic models was seen. In order to check how resistant overexpressed  $\alpha$ -Synuclein in our transgenic models was, milder digestion conditions were applied (in 50 $\mu$ g/mL of PK solution at 37°C during 1 h) to treat brain sections from animals at 3, 12 and 21 months. This time, the staining on glass slides without transferring the brain tissues onto PVDF membrane was performed (adapted from Wagner et al., 2013). By this approach, there was still remaining homogenous background signal after 1 hour of digestion but no clear deposits  $\alpha$ -Synuclein was seen (Figure 2.20). This observation suggested that  $\alpha$ -Synuclein overexpression did not develop prominent aggregates in our transgenic models.

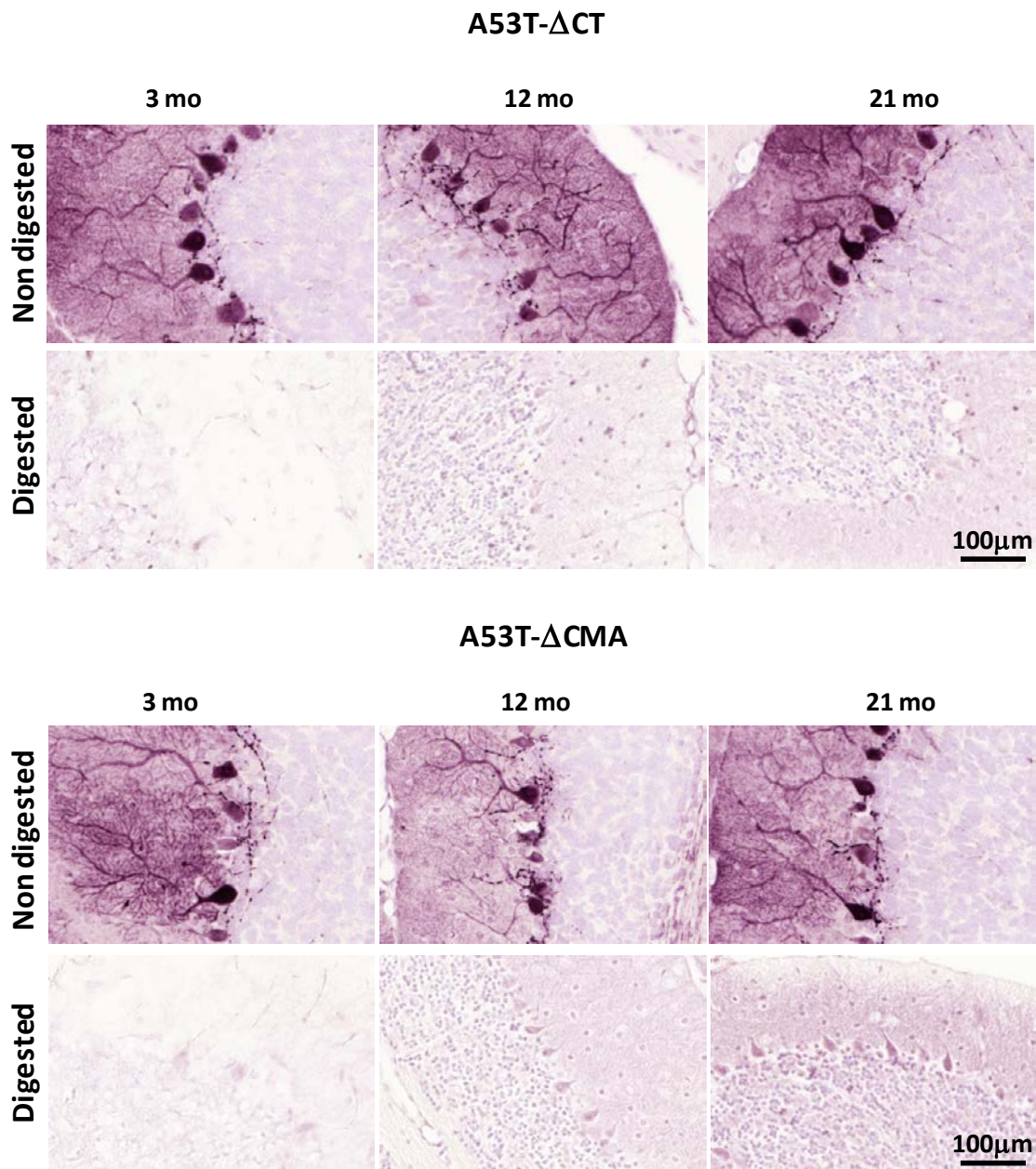
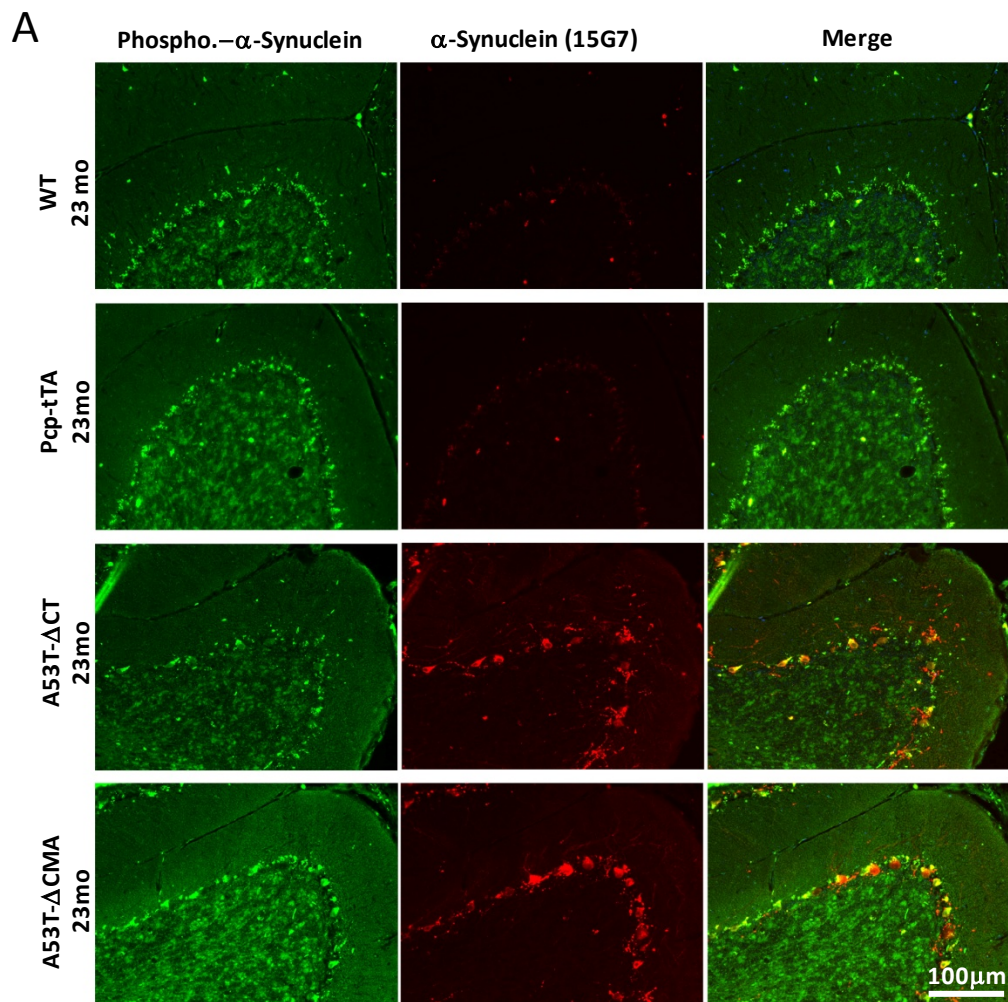


**Figure 2.20:  $\alpha$ -Synuclein at 3, 12 and 21 months of age doesn't resist to proteinase K digestion.**

Cerebellar sections on glass slides are incubated in 50 $\mu$ g/mL of proteinase K at 37°C during 10 min. Immunostaining of  $\alpha$ -Synuclein in PC and molecular layers from 3 $\mu$ m- thick sagittal cerebellar sections, Antibody anti-human  $\alpha$ -Synuclein (15G7) (chromogenic stain).

We asked whether overexpression of  $\alpha$ -Synuclein enhanced disease-associated post-translational modifications such as phosphorylation or ubiquitination. Phosphorylation at Ser129 residue of  $\alpha$ -Synuclein is widely accepted as one of pathological modifications found in  $\alpha$ -Synuclein inclusions in human cases but also in animal models (Kahle et al., 2002; Chen and Feany, 2005). Additional immunostaining in brain sections of animals from behavior groups as precedent were performed. Monoclonal antibody recognizing specifically phosphorylated  $\alpha$ -Synuclein at Ser129 residue was used

(Table 4.1). This antibody was first tested in brain sections from Thy-1 A30P mice which exhibited strong motor phenotype (15-17 months). Abundant fibrillar and spherical structures of  $\alpha$ -Synuclein showing that we were able to detect phosphorylated  $\alpha$ -Synuclein using this approach could be detected (data not shown). To localize overexpressed  $\alpha$ -Synuclein, co-labeling on the same sections  $\alpha$ -Synuclein using 15G7 antibody was performed. Staining of phosphorylated  $\alpha$ -Synuclein at Ser129 showed diffuse cytoplasmic signal, except for unspecific autofluorescence signal emitted by accumulation of lipofuscin usually seen in old brain tissues. No up-regulation or abnormal accumulation of phosphorylated  $\alpha$ -Synuclein signal was observed either in Purkinje cell bodies or cerebellar nuclei in transgenic animals compared to non-transgenic control animal (WT and Pcp2-tTA). Overlapped images confirmed that there was no relevant co-localization of overexpressed  $\alpha$ -Synuclein and phosphorylated  $\alpha$ -Synuclein, we supposed that yellow signals were resulted from the overlapping lipofuscin autofluorescence (Figure 2.21A,B).



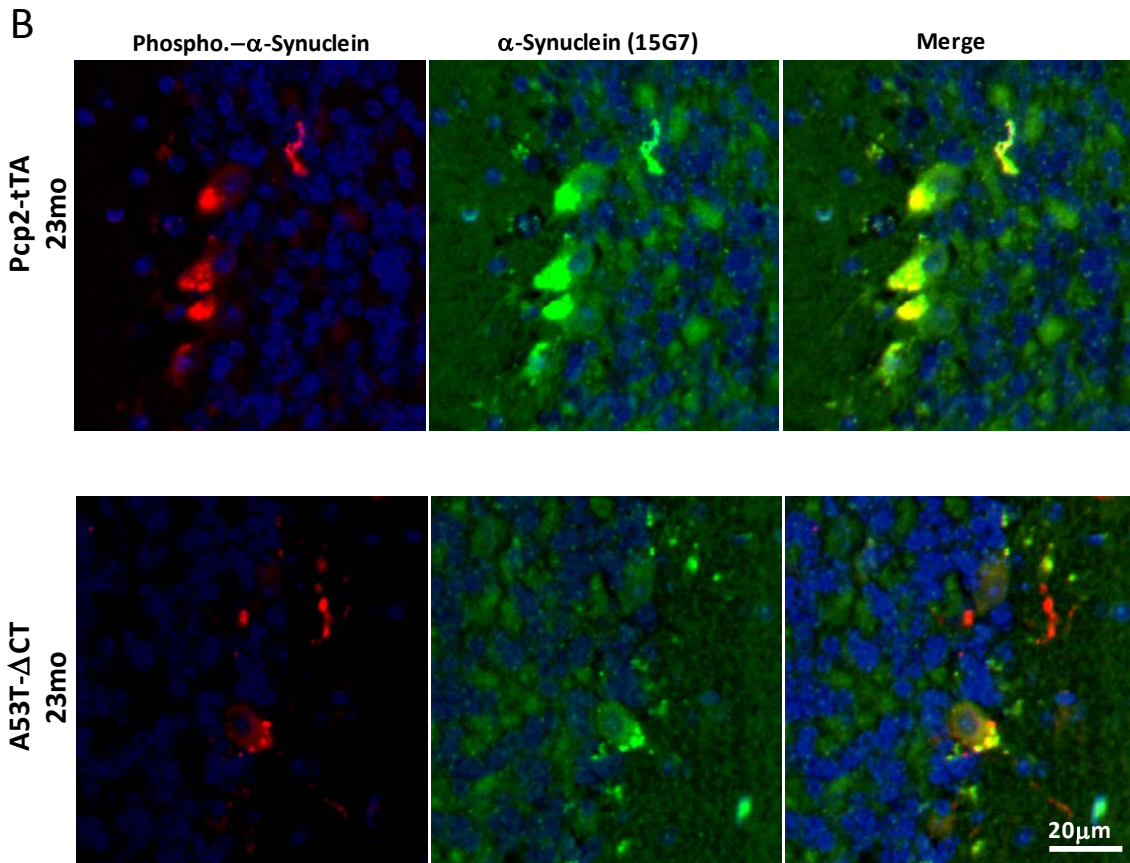


**Figure 2.21: No clear evidence of increased phosphorylated  $\alpha$ -Synuclein level at 23 months of age .**

A: Immunofluorescent co-labelling phosphorylated  $\alpha$ -Synuclein at Ser-129 and  $\alpha$ -Synuclein in PC and molecular layers from 7 $\mu$ m- thick sagittal cerebellar sections, scale bar 100 $\mu$ m. Antibody anti-phosphoSynuclein (Green) and antibody anti-human  $\alpha$ -Synuclein (15G7, Red)

B: High-magnification pictures comparing phosphorylated  $\alpha$ -Synuclein staining in PCL between non-transgenic mouse and transgenic mouse, scale bar 20 $\mu$ m. Antibody anti-phospho  $\alpha$ -Synuclein (Green) and antibody anti-human  $\alpha$ -Synuclein (15G7, Red), Hoerscht (Blue).

In a parallel study, the question whether overexpressed  $\alpha$ -Synuclein in our transgenic models was conjugated to ubiquitin was asked. Ubiquitination of  $\alpha$ -Synuclein is also one of the pathological modifications of  $\alpha$ -Synuclein which is accumulated in Lewy bodies (LBs) (Gomez-Tortosa et al., 2000; Sampathu et al., 2003). As previously for detection of phosphorylated  $\alpha$ -Synuclein, co-staining of ubiquitin and human  $\alpha$ -Synuclein using 15G7 antibody was performed on brain sections of animals from the same precedent cohorts. Similarly, the efficiency of the antibody was tested on brain sections from Thy-1 A30P mice and could also detect positive signal, although with less abundance, showing existence ubiquitinated  $\alpha$ -Synuclein structures in this line. Using the same approach, it was observed that there was homogenous, diffuse signal in cell bodies but no remarkable accumulation of ubiquitin signal was detected in our transgenic animals. In the same manner than in immunostaining of phosphorylated  $\alpha$ -Synuclein, there was no observation of up-regulation of

ubiquitin signal in transgenic animals compared to non-transgenic control animals neither in PCL nor in DCN where overexpressed  $\alpha$ -Synuclein was abundantly found. Background signal caused by accumulation of autofluorescence from lipofuscin was also detectable (Figure 2.22). Overlapped image demonstrated that there was no significant co-localization between overexpressed  $\alpha$ -Synuclein and ubiquitin, yellow signals might come from overlapping of lipofuscin autofluorescence. Our result of western-blot validated this observation: using the same antibody anti-ubiquitin, there was not detection of obvious change of ubiquitin protein level in both brain homogenate fractions (triton soluble and non-soluble) comparing transgenic and non-transgenic mice (data not shown).

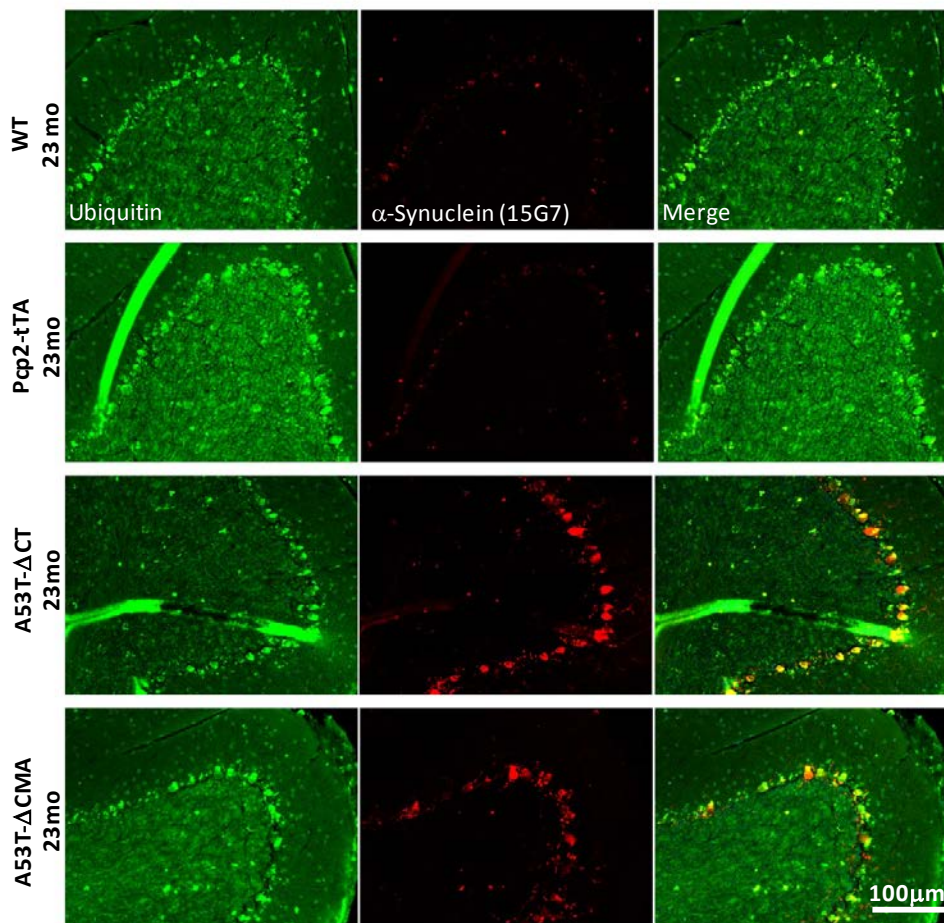


**Figure 2.22: No clear up-regulation of ubiquitination in transgenic animals at 23 months of age .**

Immunofluorescent co-labelling ubiquitin and  $\alpha$ -Synuclein in PC and molecular layers from 7 $\mu$ m- thick sagittal cerebellar sections. Antibody anti-Ubiquitin (Green) and antibody anti-human  $\alpha$ -Synuclein (15G7, Red).

Taken together, our results of immunohistochemistry and PK-PET blots indicate that overexpression of  $\alpha$ - Synuclein in transgenic animal models did not lead to the build-up of insoluble, oligomeric structures which could resist PK digestion. This result was also supported by absence of other pathological posttranslational modifications as described for  $\alpha$ -Synuclein inclusions such as phosphorylation at Ser129 or ubiquitination.

## 3 Discussion

### 3.1 *In vitro* studies: Establishing cellular paradigms to study protein degradation

$\alpha$ -Synuclein is central in PD since it is accumulated in LBs which constitute the main histopathological feature of the disease. Enhanced clearance of  $\alpha$ -Synuclein is a potential therapeutic strategy (reviewed in Verkrellis and Stefanis, 2012). Although efforts have been made to determine the main degradation pathways of  $\alpha$ -Synuclein a consensus on how  $\alpha$ -Synuclein is degraded has not yet been achieved (Bennett et al., 1999; Ancolico et al., 2000; Rideout et al., 2002). The lack of consistency from previous studies including our own is due to various factors including the choice of cell type used for the studies (neuronal vs non neuronal cells) or culture conditions (proliferation vs. differentiation, starvation vs. non-starvation, duration of treatment with inhibitors...) (Figure 2.3). Discovery of CMA degradation of  $\alpha$ -Synuclein has opened new interesting perspectives, since enhancing CMA activity rescued toxicity induced by  $\alpha$ -Synuclein in animal model a recent study (Xilouri et al., 2013).

The main foundation of our study is based on previous findings showing that CMA is one major route of degradation for numerous intracellular proteins including  $\alpha$ -Synuclein. Indeed, this protein is also described as a substrate of this process since it contains the consensus KFERQ motif in its sequence (Cuervo, 2004). This conserved motif is recognized by chaperones Hsp70 and protein substrates are delivered directly to lysosomal vacuole. Inducible cell culture models examining the impact of CMA motif mutation on kinetics of  $\alpha$ -Synuclein turnover have been previously established and analyzed (Vogiatzi et al., 2008; Xilouri M, 2009). Modifying the composition of CMA motif such as substitution of  $_{98}DQ_{99}$  by AA ( $\Delta DQ$ ) in  $\alpha$ -Synuclein sequence was sufficient to slow the turn-over of this protein in different cell culture models (Vogiatzi et al., 2008). However, in these studies  $\alpha$ -Synuclein full-length constructs were expressed, in contrast to our animal models which overexpress C-terminal truncated  $\alpha$ -Synuclein (1-130). Recent report has suggested that post-translational modifications in  $\alpha$ -Synuclein C-terminus might influence its own degradation pathways (Choi et al., 2012).

In this *in vitro* study, we have generated cell lines using Tet-inducible system as in our animal models and previous cell culture models (Vogiatzi et al., 2008; Xilouri M, 2009). We have compared the kinetics of  $\alpha$ -Synuclein degradation in cell lines expressing WT and A53T (full-length and C-terminal truncation). To study the impact of CMA on  $\alpha$ -Synuclein degradation in our cell lines, we mutated CMA motif in  $\Delta CT$   $\alpha$ -Synuclein constructs by replacing  $_{98}DQ_{99}$  by AA. These data from cell culture gave us a side-by-side control for our animal models to determine whether mutation of CMA motif really affects the kinetics of degradation of  $\alpha$ -Synuclein.

### 3.1.1 Mutation of CMA motif doesn't slow down $\alpha$ -Synuclein degradation

Surprisingly, we found that the absence of the CMA recognition motif did not result in significant difference in degradation rate of  $\alpha$ -Synuclein for both WT and A53T constructs compared to expression of  $\alpha$ -Synuclein with normal CMA motif. These observations were consistent in two different culture conditions in enriched (Figure 2.3A,B) or serum-reduced medium (Figure 2.4B,C). We also confirmed that there was no significant difference in  $\alpha$ -Synuclein protein steady state levels in independent experiments (Figure 2.2A) between these cell lines. Similar to HEK293 cells, we could also not detect a significant difference in the degree of non-degraded  $\alpha$ -Synuclein in Tet-off BE(2)-M17 cell lines at various time points even though steady-state level of  $\alpha$ -Synuclein in these cells differed significantly. Together, our data of HEK293 and BE(2)-M17 cells for kinetics of  $\alpha$ -Synuclein degradation suggest that in our cellular models, CMA might not play a determining role in regulation of intracellular  $\alpha$ -Synuclein protein level.

Difficulties one could meet when studying the kinetics of protein degradation in tissue culture is how to maintain comparable culture conditions between experiments. Variation or lack of consistency in determination of protein half-life in former studies might be due to degree of transgene overexpression, frequency of media change, exposure time to pharmacological treatment, method of revelation or quantification. A key difference between our studies and the work by Vogiatzi et al. (2008) is that we chose to overexpress  $\alpha$ -Synuclein transgene in HEK293 Flip-In system allowing a unique, isogenic insertion of transgene promoted by Flp recombinase. Vogiatzi et al. chose to overexpress  $\alpha$ -Synuclein in PC12 and SHSY-5Y cells using random integration method. Using isogenic insertion method, we could generate stable Tet-on cell lines with comparable levels of transcription and protein translation (Figure 2.1A,C). Moreover, these cell lines have identical genetic background. Nevertheless, as HEK293 cells might not exhibit all properties of neuronal cells, we generated additionally neuroblastome-derived Tet-off cells, BE(2)-M17, overexpressing the same  $\Delta$ CT  $\alpha$ -Synuclein constructs. In contrast to HEK293 cells, these cell lines have disadvantage that they were generated by random transgene insertion (similar to Vogiatzi et al.) which could not guaranteeing comparable genetic background and expression levels between the lines (Figure 2.5A,B).

The fate of  $\alpha$ -Synuclein seems to depend on different degradation pathways (Rott et al.,2011; Vogiatzi et al.,2008; Webb et al., 2003). Although substantial evidence has shown that CMA participate in  $\alpha$ -Synuclein degradation process (Cuervo et al., 2004; Vogiatzi et al.,2008), the degree of CMA in this process in physiological conditions might have been overestimated in prior studies. Our observations suggest that  $\alpha$ -Synuclein could be regularly degraded by other proteolytic pathways different than CMA. Blocking degradation by CMA due to mutation of CMA therefore did not seem to dramatically affect the efficiency of  $\alpha$ -Synuclein clearance in our experiments.

"Traditionally", two main proteolytic systems contribute to regulate expression of cytosolic proteins: ubiquitin-proteasome system (UPS) and autophagy- lysosomal pathways (ALP). The evidence for degradation of  $\alpha$ -Synuclein by UPS remains conflicting since its inhibition failed to show the expected increase in cytosolic  $\alpha$ -Synuclein levels in certain studies (Ancolico et al., 2000; Rideout et al., 2001). Another argument is that accumulated  $\alpha$ -Synuclein found in LBs is mostly mono-ubiquitinated while proteasome preferentially degrades poly-ubiquitinated proteins. Recent findings have shown that mono-ubiquitinated  $\alpha$ -Synuclein could also "exceptionnally" be targeted to proteasome (Rott et al., 2011) but as long-lived protein,  $\alpha$ -Synuclein is thought to be rather degraded by ALP than UPS (Cuervo, 2004). Among ALP, macroautophagy is known to be play a major role in removal of cytosolic proteins. Inhibition of macroautophagy by 3-MA led to accumulation of  $\alpha$ -Synuclein in primary neurons as well as in cells overexpressing  $\alpha$ -Synuclein (Vogiatzi et al.,2008). The role of another autophagic pathway, microautophagy, in transporting  $\alpha$ -Synuclein to lysosome is still poorly understood. Further studies using pharmacological inhibitors would be interesting to determine which pathway is dominant in regulation of  $\alpha$ -Synuclein burden in our models. Recently, an elegant study using live imaging on cranial window proposed a distinct regulation: UPS might degrade  $\alpha$ -Synuclein under normal conditions whereas ALP is implicated to  $\alpha$ -Synuclein degradation when protein burden is increased ("pathological" conditions) (Ebrahimi-Fakhari et al., 2011).

The constructs of  $\alpha$ -Synuclein chosen for this study might not be the appropriate structures for studying degradation by CMA in living systems. Mutation by substitution of  $_{98}DQ_{99}$  by AA might not be enough pertinent to affect the normal binding of Hsp70 chaperones in cellular systems although it was shown to reduce affinity of  $\alpha$ -Synuclein to LAMP2-A in purified lysosomes (Cuervo, 2004). Additional PTMs might modulate the affinity of binding to Hsp70. Interestingly, in their recent findings, Choi et al. (2012) have identified that phosphorylation at different tyrosine residues in the region of C-terminus, especially Y136, was important to ensure the correct binding to Hsp70. Mutation of Y136A significantly reduced Hsp70 binding detected by immunoprecipitation. This Y136 residue was absent in our constructs since we overexpressing C-terminal truncated  $\alpha$ -Synuclein (1-130). A53T-FL  $\alpha$ -Synuclein in HEK-293 cell lines has shown a delay of  $\sim 10$ h compared to  $\Delta$ CT $\alpha$ -Synuclein and  $\sim 16$ h compared to WT-FL  $\alpha$ -Synuclein (Figure 2.4 and Table 2.1). These data support the hypothesis that  $\alpha$ -Synuclein might require the complete C-terminus to be properly translocated into the lysosome via CMA pathway.

### 3.1.2 Absence of cellular toxicity mediated by overexpressing A53T mutant $\alpha$ -Synuclein

Mutant  $\alpha$ -Synuclein, especially A53T, exhibited a stronger affinity to LAMP2-A at membrane of purified lysosomes compared to WT  $\alpha$ -Synuclein. A53T mutant was also found to be poorly internalized in lysosomal lumen as it might act as uptake blocker compromising the internalization of

other CMA substrates (Cuervo, 2004). Overexpression of A53T  $\alpha$ -Synuclein was also reported to disrupt the normal functioning of CMA pathways and to induce cellular toxicity (Xilouri et al., 2009). Toxicity effects were variable as a function of culture conditions (A53T- $\Delta$ CMA mutant rescued the toxicity effect in propagating culture but not in differentiation conditions in SHSY-5Y cells). In our cellular models, we found that A53T full-length but not A53T C-terminal truncated mutants showed a delay in degradation compared to WT full-length (Figures 2.3 and 2.4). This observation confirmed the earlier finding that A53T mutant half-life was longer than WT (Cuervo, 2004). No obvious change in degradation rate was observed between WT and A53T C-terminal truncated constructs in both HEK293 and BE(2)-M17 cells. In this regard, we also have not seen any toxic effect due to overexpression of  $\alpha$ -Synuclein in proliferating (HEK293 and BE(2)-M17) as well as in differentiating conditions (BE(2)-M17, data not shown). Together, our results contradict previous findings that overexpression of A53T mutant could induce cellular toxicity. A part of explanation might come from different genetic background between our cell lines. Furthermore, we have detected the presence of mycoplasma in the SHSY-5Y lines used in the studies by Xilouri et al. (2009). We are not certain that contamination by mycoplasma is the origin of our different observation but it might also be considered as an element of interpretation. Indeed, microarray analysis on contaminated cultured human cells revealed that mycoplasma may alter the expression profile of hundreds of genes including genes encoding for transcription regulators, transporters or signal transducers (Miller et al., 2003). We speculate that these alterations might interfere with protein degradation pathways. A deeper investigation would be helpful to clarify the reasons of variability between these different cell models.

## **3.2 *In vivo* studies: Generating and analyzing conditional mouse model expressing human pathogenic $\alpha$ -Synuclein**

### **3.2.1 Generation of animal models overexpressing $\alpha$ -Synuclein mutants in Purkinje cells**

In this part of the study we generated a novel conditional model specifically expressing human pathogenic mutant  $\alpha$ -Synuclein in cerebellar PCs driven by the *Pcp2* promoter. This model was expected to have several advantages compared to previous  $\alpha$ -Synuclein transgenic models: (1)  $\alpha$ -Synuclein overexpression is cell-type specific; (2) it is a model to study the relationship between  $\alpha$ -Synuclein and neuropathology in cerebellum; (3) the expression of  $\alpha$ -Synuclein is tightly controlled by Doxycycline; (4) it is the first *in vivo* model expressing  $\alpha$ -Synuclein with CMA motif mutation (mutation by substitution of  $_{98}DQ_{99}$  by AA) providing a new tool to study the role of CMA in  $\alpha$ -Synuclein degradation.

Most of  $\alpha$ -Synuclein transgenic mouse models express  $\alpha$ -Synuclein in more than one brain region. Expression of  $\alpha$ -Synuclein driven by *Thy-1* promoter is found throughout telencephalon, brain stem

and spinal cord (van der Putten et al., 2000). Inclusions of  $\alpha$ -Synuclein have been found in deep neocortex layers, hippocampal CA3, olfactory bulb and occasionally in SN (PDGF mice, (Masliah et al., 2000)) and in brain stem, spinal cord and deep cerebellar nuclei (Prion mice, Giasson et al., 2002). So far, generated animal models have not fully reproduced all PD features but just mimicked certain aspects of the diseases: they have not show the expected high expression in SN cells or PD-related phenotypes (reviewed in Chesselet et al., 2012). On the other hand, using TH promoter (Wakamatsu et al., 2008), the authors could drive  $\alpha$ -Synuclein expression selectively in SN cells but expression of  $\alpha$ -Synuclein was also seen in OB in another study using this promoter (Tofaris et al., 2006).

Although cerebellum is not typically affected in PD, some studies revealed the existence of LBs in DLB patient cerebella (Mori et al., 2003). In this context, specifically targeting PCs using Pcp2 promoter in our model was hoped to give clear transgene expression in a specific neuron-type that would make the quantification of the overexpression and its related effects easier. Moreover, Pcp2-tTA mice are available for *for-profit* research structures like Boehringer Ingelheim Pharma GmbH & Co KG.

Several models have been reported with expression of  $\alpha$ -Synuclein in cerebellum and PCs (Giasson et al., 2002; Kahle et al., 2001; Lin et al., 2012) but no effect of  $\alpha$ -Synuclein overexpression was specifically documented.  $\alpha$ -Synuclein is endogenously expressed in PCs, its physiological role is however poorly understood although a role in interfering the DA transport and release have been suggested (Al-Wandi et al., 2010; Anwar et al., 2011). PCs are not DAergic neurons but GABAergic neurons. However, similar roles could also be expected in PCs. Having a clear transgene expression in PCs, we furnish an interesting model to further study the role of  $\alpha$ -Synuclein in PCs. Our model abundantly express  $\alpha$ -Synuclein in DCN, which is the main projection area of PC axons, and therefore is interesting for assessing  $\alpha$ -Synuclein presynaptic functions.

### **3.2.2 Overexpression of $\alpha$ -Synuclein in PCs causes mild motor behavioral changes**

Our transgenic animals did not develop profound motor disabilities up to 23 months of age: no signs of paralysis, no obvious change in hind-limb clasp frequency or clear disproportional gait width (data not shown). However, they exhibited lower locomotion activities compared to non-transgenic animals in open-field and in pole test (Figures 2.12 and 2.13). Indeed, in open-field recordings, we observed lower locomotor activities, in particular rearing activities, in A53T- $\Delta$ CMA line than non-transgenic line Pcp2-tTA. This difference is less pronounced in A53T- $\Delta$ CT line compared to non-transgenic line (Figure 2.12). Interestingly, transgenic animals also showed lower motor coordination starting from 14 months of age in pole test reflected by increase of total time to descend the pole compared to the non-transgenic group Pcp2-tTA (Figure 2.13B). This result supports the impairment of vertical movement observed in open-field. A reserve one could make is that this impairment did not affect all animals in transgenic groups. Total locomotor activities (ambulatory and rearing) were

also stable over time indicating that there was no age-dependent decline (Figure 2.12). This feature does not mimic the progressive motor disabilities in PD patients. In pole test, the affected animals ("symptomatic" group) did not show clear worsening between 14 and 23 months even though they exhibited a clear trend for decreased locomotor activity (rearing) (Figure 2.13B). Another reserve could be that motor coordination impairments of transgenic animals were not clearly reproduced in other tests (rotarod and beam-walk) (Figure 2.14).

Our behavioral observations suggest that overexpression of  $\alpha$ -Synuclein might lead to functional deficits of PCs due to increased intracellular levels of this protein (reviewed in (Eisbach and Outeiro, 2013)) rather than being due to massive neurodegeneration. Due to specific location of transgene expression and the role of PCs as principal inhibitory neurons in cerebellum, we suppose that PC dysfunction might in consequence affect the integrity of cerebellar circuitries. Pathologies linked to PC dysfunction might differently affect the two transgenic lines as A53T- $\Delta$ CMA showed constantly lower scores than A53T- $\Delta$ CT line in open-field. Mutation of CMA motif reduces affinity of  $\alpha$ -Synuclein to LAMP-2A and reduce the capacity of the cells to degrade  $\alpha$ -Synuclein by this pathway (Cuervo, 2004). Overexpression of A53T- $\Delta$ CMA mutant might preserve the lysosomal system (since it does not block uptake by LAMP-2A). However, extensive accumulation of non-degraded  $\alpha$ -Synuclein by CMA in cytosol might interfere with other biological pathways resulting in lower locomotor activities of A53T- $\Delta$ CMA line in open-field recordings.

We also emphasize that locomotor performance of Pcp2-tTA line was seen constantly lower than performance of other non-transgenic line (WT) (Annex 6) suggesting that genetic background might be involved in causing difference of locomotor behavior. It has been shown that overexpression of tTA might induce non desired toxicity effect as reported in previous studies (Gallia and Khalili, 1998;Kuhnel et al., 2004).

### 3.2.3 CMA motif mutation does not lead to differential $\alpha$ -Synuclein steady state levels *in vivo*

We wanted to examine the part of autophagy-lysosomal pathways (ALP), especially the implication of the emerging concept that CMA might be the major route for intracellular  $\alpha$ -Synuclein degradation and that failure of this pathway might cause potential deleterious consequences on living organisms (Cuervo, 2004; Xilouri et al, 2009). From our general observations, we have not found a determinant role of CMA pathway in regulation of excess  $\alpha$ -Synuclein protein burden in both cellular and animal models as the presence of CMA motif mutation of  $\alpha$ -Synuclein sequence did not lead to increased steady state levels or changes in the clearance dynamics in cell culture (Figures 2.3, 2.4 and 2.7). Our transgenic animals also did not show a clear difference in disease-onset up to 23 months of age although significant differences in locomotor activities and motor coordination were observed (Figures 2.12 and 2.13).

One possible molecular explanation for that is the choice of the primary constructs of  $\alpha$ -Synuclein. C-terminal truncated  $\alpha$ -Synuclein are known to promote aggregation in animal models leading (Tofaris et al., 2006; Wakamatsu et al., 2008). However, lacking residue components of C-terminus might lead to modify primary structure of  $\alpha$ -Synuclein leading to missing PTMs required for degradation pathways (Choi et al., 2012). Our results on state protein level *in vivo* do not allow us, unfortunately, to explain the difference of behavioral scores. We agree that this statement is certainly limited by the absence of obvious pathologies. The different reasons of absence of toxicity will be discussed in more details in 3.2.6.

### 3.2.4 Overexpression of $\alpha$ -Synuclein in PCs did not lead to obvious neurohistopathology

Despite interesting behavioral changes, we have not detected evident pathological changes in our transgenic animals up to the age of 23 months by immunohistochemical or biochemical approaches. PC staining using Calbindin-D28K marker showed no significant difference of PC number between transgenic and non-transgenic (Pcp2-tTA) lines indicating that overexpression did not lead to significant PC loss. This result of PC counting was further confirmed by western-blot showing comparable expression levels of Calbindin between lines (Figure 2.15). Comparing cell numbers and expression of specific markers are not the sole criteria to analyze neurodegeneration. Multiple reports showed that beside diminution of cell numbers, PC degeneration might be manifested by a change of morphological characters including disorganization of dendritic trees in molecular layer (Donald et al., 2008; Unno et al., 2012), diminished synaptic density at dendritic spines (Giza et al., 2010; Zu et al., 2004) or axon terminal atrophy (Komatsu et al., 2007). Interestingly, counting of visible main trunks of dendrites showed greater homogeneity in non-transgenic WT compared to non-transgenic Pcp2-tTA line and  $\alpha$ -Synuclein transgenic lines (Figure 2.15B). Examination of DCN staining showed homogenous axonal density and no particular morphological change (Figure 2.17A). These observations suggest that the difference in genetic background between the animal lines, for example overexpression of tTA (Gallia et al, 1998; Kuhnel et al, 2004), might cause unexpected changes in mouse cerebellum architecture independent of the overexpression of  $\alpha$ -Synuclein. These results of immunohistochemistry and western-blot support our observation in behavioral studies showing that WT line exhibited highest locomotor performance compared to the three other lines (Annex 6).

Parallel to morphological aspects, PC physiological function seemed to be well preserved until the oldest age analyzed in these studies (23 months). Indeed, we did not observe clear-cut reductions of synaptic marker expression or change in distribution patterns (Figure 2.16). Synaptic marker staining was unchanged in regions of PCL, ML and DCN where the main communication activities between PCs and other cells in cerebellum are concentrated. According to these observations, the role of PC in regulation of cerebellar circuitries is not compromised even in case of overexpression of  $\alpha$ -Synuclein.

However, we are aware that such interpretation should be made with care due to limits of methodological approaches used in these studies. Immunohistochemistry is not quantitative therefore observation on immunostained brain tissues might not reflect well the real activities of PCs. Synaptic markers are present at high density in communicating areas such as ML or DCN and therefore it might be difficult to detect minor changes of their density based on intensity of staining, although efforts have been made to analyze a large set of brain samples.

We reported the absence of glial cell activation which was usually shown to be a feature of brain regions affected by neurodegeneration. The relationship between glial cell activation and neurodegeneration is not fully understood but both processes may act reciprocally in a vicious circle fashion (reviewed by Halliday and Stevens, 2011). Microglia typically exist in a resting state characterized by a ramified morphology. They are activated in response to pro-inflammatory stimuli such as neuronal damage signals of degenerating cells (Block and Hong, 2007; Marin-Teva et al., 2004). Activation of microglia provides beneficial effects to eliminate pathogens and cells dying by apoptosis (Marin-Teva et al., 2004). However, microglia might be overactivated and activates in turn astrocytes under certain circumstances by producing excess of TNF- $\alpha$  and IL- $\beta$  which initiates a perpetual cycle of neuron death (Zhang et al., 2010). Both immunostaining of astrocytes (GFAP marker) and microglia (Iba-1) in our animal models revealed similar density of these cells in cerebellum indicating that they were not recruited to this brain area to a significant degree. Examination of their morphology also did not show increases in activation state in transgenic animals compared to non-transgenic lines (WT and Pcp2-tTA) (Figure 2.19).

### 3.2.5 No obvious LB-like pathology in transgenic mice up to 23 months

Our transgenic animals did not show accumulation of LB-like  $\alpha$ -Synuclein aggregates as commonly characterized by resistance to PK digestion (Neumann et al., 2002) or phosphorylation at Ser129 (Emmer et al., 2011; Neumann et al., 2002) or conjugation to ubiquitin (Masliah et al., 2000; Lim et al., 2011) (Figures 2.21 and 2.22). The choice of labeling phosphorylated  $\alpha$ -Synuclein at Ser129 might be compromised by the truncation of  $\alpha$ -Synuclein at 130 amino acids while the antibody recognizes specifically phospho-Ser129 epitope which is located close to our truncation site. Western-blotting confirmed absence of high-molecular-weight or ubiquitinated- $\alpha$ -Synuclein or both in triton soluble and insoluble fractions (data not shown). These observations indicate that overexpression of these two mutants in PCs did not result in  $\alpha$ -Synuclein oligomerization. The absence of aggregation is concomitant with the absence of cellular toxicity induced by overexpression as observed in immunohistochemistry analysis.

### 3.2.6 Absence of toxicity caused by overexpression of $\alpha$ -Synuclein

Several factors might explain the absence of toxicity in our models compared to previous observations in other studies, the most important of them would be the method used for the generation of our models. We would like to emphasize here that in order to minimize as much as possible differences in transgene transcription, we have chosen a specific, well-defined locus (FlpIn HEK293 cells and *ROSA26* locus in animal models). Of course, consequences of suppression of these loci should not be neglected as their contribution to physiological functioning is poorly elucidated. However, by using this approach, we assure that our models are generated by isogenic insertion resulting in highly comparable expression (Figure 2.1). This condition is crucial, from our expectations, in order to compare protein steady-state levels for studies on the dynamics of protein degradation. Since any change of behavior or pathology cannot be due to deviation in mRNA transcription or translation, we also expect comparable physiological functioning in our systems as they should have homogenous genetic background.

The level of protein overexpression compared to endogenous mouse  $\alpha$ -Synuclein in our transgenic lines is the next critical point to explain absence of neurotoxicity. Indeed, using isogenic insertion method into *ROSA26*, we obtained a single integration of our *SNCA* transgene. We could state from our experience in immunohistochemistry and western-blot using 157G antibody specific for human that our overexpression level is rather weak (Figures 2.10 and 2.11). Western-blotting using Syn-1 specific for mouse and human  $\alpha$ -Synuclein revealed very a low level of human  $\alpha$ -Synuclein compared to endogenous mouse  $\alpha$ -Synuclein (Annex 4). Furthermore, as the protein overexpression is variable between PCs (mosaic-like) the effects of overexpression might not be comparable between cells (Figure 2.9). Protein overexpression burden is a crucial condition in transgenic models of synucleopathies. Level of protein expression is determined by the combination of vector design, copy numbers of transgene integration or targeted cell areas (reviewed in Chesselet et al., 2010). So far, relevant transgenic models overexpressing  $\alpha$ -Synuclein showing pathologies or strong phenotype have been found correlated with high expression level: two-fold higher than endogenous  $\alpha$ -Synuclein in Thy-1 A30P mice (Kahle et al., 2000), 2.5-30 fold higher than endogenous  $\alpha$ -Synuclein in mPrion (WT or A53T) mice (Giasson et al., 2002). However, too strong protein overexpression inducing robust and rapid phenotype (Giasson et al., 2002) might still not mimic the progressive development of PD symptoms. Recent animal models using CaM-tTA promoter have shown mild expression levels linking to interesting progressive phenotypes (Marxreiter et al., 2009; Nuber et al., 2008).

Absence of  $\alpha$ -Synuclein aggregation as discussed in 3.2.5 might also explain, in part, the lack of neurotoxicity in our models. Although the principal toxic species of  $\alpha$ -Synuclein are still need to be identified, the presence of  $\alpha$ -Synuclein is largely assumed to be linked to neurodegeneration (reviewed in (Oueslati et al., 2010)). Animal models exhibiting clear-cut phenotype also show

appreciable abundance of  $\alpha$ -Synuclein oligomeric species (reviewed in Chesslet et al., 2010). Absence of aggregate formation in our transgenic animals might depend on our mode of generation of these models. Isogenic insertion allows comparable mRNA transcription but results in low expression level as only one copy of transgene is expressed compared to traditional transgenic with multiple insertion sites as discussed previously.

A different argument for the absence of neurotoxicity effect in our transgenic animal models would be the choice of promoter to drive transgene expression. Indeed, we voluntarily decided to drive expression of  $\alpha$ -Synuclein in PCs instead of in the nigro-striatal system which is the main and "classical" target in generation of PD models. Even though PCs are not strongly affected in PD and other synucleopathies, several reasons argue in favor of our choice: (1)  $\alpha$ -Synuclein inclusions have been observed in PC of DLB patients (Mori et al., 2003) and expression of  $\alpha$ -Synuclein is seen in cerebellum and spinal cord e.g. in Thy-1 A30P mice (Kahle et al., 2001), which display a deleterious motor phenotype, (2) neurodegeneration of PCs are supposed to be more facile to be characterized by immunohistochemistry and has been chosen as reference of multiples neurodegeneration models (Reith et al., 2011; Unno et al., 2012; Zu et al., 2004), (3) the driver mouse line Pcp2-tTA is already available for *for-profit* research structures like Boehringer Ingelheim company. We speculate that the absence of neurotoxicity in PCs might be due to certain "properties" of these cells that help to resist better to toxicity mediated by  $\alpha$ -Synuclein overexpression than other neuronal cell populations such as dopaminergic neurons. It has been actually shown that dopaminergic neurons are particularly vulnerable by dopamine-modified  $\alpha$ -Synuclein. This PTM is able to block lysosomal degradation and causes cellular toxicity (Martinez-Vicente et al., 2008).

### 3.3 Outlook

#### 3.3.1 *In vitro* studies

$\alpha$ -Synuclein remains central in PD research and reduction of  $\alpha$ -Synuclein protein levels appears to be a viable therapeutic strategy, although results of our studies cannot confirm a large contribution of the CMA pathway in regulation of  $\alpha$ -Synuclein protein burden under physiological condition since we failed to find a significant difference in half-lives of C-terminal truncated  $\alpha$ -Synuclein *in vitro*. However, we are aware that  $\alpha$ -Synuclein half-lives found in these studies were estimated based on normalization of kinetic curves that might not reflect the effective  $\alpha$ -Synuclein half-life. Alternative methods such as "pulse-chase" with radioactive protein labeling might reveal different values of  $\alpha$ -Synuclein half-life (Vogiatzi et al., 2008). Nevertheless,  $\alpha$ -Synuclein half-lives found in our studies for WT-FL and A53T-FL constructs are close to values found in some other studies using different approaches (Li et al., 2004). The way how  $\alpha$ -Synuclein is degraded in our cellular models remains unexplored since we did not perform pharmacological studies. Inhibition of protein degradation

pathways such as macroautophagy (blocked by 3-MA) or lysosome (blocked by NH<sub>4</sub>Cl) could be interesting to determine the major pathway by which  $\alpha$ -Synuclein is degraded. The role of proteasome (blocked by epoxomicin) could also be interesting to be re-explored since recent data have proposed an explanation for the role proteasome in degradation of mono-ubiquitinated  $\alpha$ -Synuclein (Rott et al., 2012, Abeywarnada et al., 2013). CMA remains an interesting route for reduction of  $\alpha$ -Synuclein protein level. Indeed, several data including our own indicate that overexpression of A53T  $\alpha$ -Synuclein mutant results in increased half-life of  $\alpha$ -Synuclein (Figure 2.4). This result suggests that  $\alpha$ -Synuclein could be targeted to lysosome membrane by the mean of CMA pathway and A53T mutant might act as a blocker at LAMP-2A receptor (Cuervo, 2004). In our studies, we have not however explored the consequence of overexpression of A53T-FL construct in degradation kinetics of other CMA substrates such as GAPDH that could provide substantial proofs for CMA implication in  $\alpha$ -Synuclein pathogenesis. Furthermore, in these studies we have not generated cell lines overexpressing WT-  $\Delta$ CMA-FL or A53T-  $\Delta$ CMA- FL to reproduce experiments of determining kinetics of  $\alpha$ -Synuclein turnover. This experiment would clarify whether  $\alpha$ -Synuclein C-terminus is really involved in CMA targeting mechanisms.

### 3.3.2 *In vivo studies*

Lacks of clear phenotype and neuropathology in our animal models reflect the difficulties in generation of genetic PD models. Indeed, our transgenic animals show lower locomotor activities and motor coordination but with high variation of phenotype between animals. Moreover, we could not identify the link between neuropathology and behavioral changes supporting a link between  $\alpha$ -Synuclein overexpression and behavioral phenotype. The fact that we observed stable locomotor activities over time suggest that overexpressed  $\alpha$ -Synuclein in cerebellum might induce rather functional impairment of PCs than massive neurodegeneration as discussed in 3.2.2. This hypothesis could be verified by a reverse experiment: as expression of  $\alpha$ -Synuclein is induced by Tet-off system, this expression could be turned-off by addition of Dox. If overexpression of  $\alpha$ -Synuclein induces behavioral changes, the locomotor activities of transgenic lines would be "rescued" when expression of  $\alpha$ -Synuclein is suppressed.

To further optimize our animal models using the same  $\alpha$ -Synuclein constructs of this study, one could try to increase protein expression by increasing the copy number of the transgene or resort to other driver lines expressing at potentially higher levels of tTA such as CamKII-tTA (Nuber et al., 2008; Lim et al., 2007) or PITX3-tTA (Lin et al., 2012). The strategy of increasing the copy number by homozygosity is difficult as we did not observe appreciable increase of transgenic protein expression in homozygotes for *tTA* and/or *TetO-SNCA* (Annex 3). Moreover, the risk of higher

expression of *tTA* is not negligible due to its induction of unwanted effects shown in other studies (Morimoto and Kopan, 2009; Sanbe et al., 2003).

Functional deficits in organization or physiology of PCs were not detected by immunohistostaining in our studies despite the large set of markers used. Pathological changes might be more subtle and require additional investigations. Recent report showed that sub-cellular dysfunctions affecting cell compartments such as Golgi apparatus, endoplasmic reticulum, lysosomes or synaptic vesicles would be interesting to be explored (Lin et al., 2012). The physiological change of PCs might not be manifested by only morphology observation but also modifications of electrical activities or dynamic of neurotransmitter release. Additional studies using different technical approaches such as quantification of GABA releasing using *in vivo* microdialysis (Cauli et al., 2011; Manto et al., 2005) or *ex-vivo* whole cell patch-clamp recordings (Unno et al., 2012; Giza et al., 2010) would be interesting to bring complementary information about physiological functions in PC overexpressing  $\alpha$ -Synuclein.

## 4 Materials and Methods

### 4.1 Animal models

#### 4.1.1 Animals

##### 4.1.1.1 *TetO-SNCA animals*

*TetO-SNCA* animals have been produced by Taconic Artemis (Germany). Methods (according to Taconic Artemis): ES cell RMCE (derived from mouse strain C57BL/6NTac-Gt(ROSA)26Sor<sup>tm596Arte</sup>) is grown on a mitotically inactivated feeder layer comprised of mouse embryonic fibroblasts (MEF) in DMEM high glucose medium containing 20% (w/v) FBS and 1200 u/mL Leukemia Inhibitory Factor (Milipore ESG 1107).  $2 \times 10^5$  cells were placed on 3.5 cm dishes in 2 mL medium. For transfection: 3  $\mu$ l of Fugene Reagent (Roche) were mixed with 10  $\mu$ l serum free medium (OptiMEM I with Glutamax I, Invitrogen) and incubated for 5min at room temperature. 100  $\mu$ l of the Fugene/OptiMEM solution was added to the DNA mixture containing 2  $\mu$ g of circular vector and 2  $\mu$ g CAGGS-Flp plasmid. Transfection complex was incubated for 20 min at room temperature and added dropwise to the cells. From 2 days onwards, the medium was replaced daily with medium containing 200  $\mu$ g/mL of G418 (Invitrogen). Single clones were isolated seven days later, expanded and analyzed by Southern blot. For diploid injection: after administration of hormones, super-ovulated BALB/c females were mated with BALB/c males. Blastocysts were isolated from the uterus at 3.5 days *post coitum* (dpc). Blastocysts were placed in a drop of DMEM with 15% FCS under mineral oil. A flat tip, piezo actuated microinjection-pipette with an internal diameter of 12-15  $\mu$ m was used to inject 10-15 targeted C57BL/6NTac ES cells into each blastocyst. After recovery, 8 injected blastocysts were transferred to each uterine horn of 2.5 dpc, pseudopregnant females. Chimerism was measured in chimeras (G0) by coat color contribution of ES cells to the BALB/c host (black/white). Highly chimeric mice were bred to strain C57BL/6 females.

##### 4.1.1.2 *Driver Pcp2-tTA animals*

"Pcp2-tTA" mice (FVB-Tg(Pcp2-tTA)3Horr/J, JR# 005625) were purchased from Jackson laboratories (Germany). The mice are backcrossed to wild-type C57BL/6 mice (Charles River) to obtain C57BL/6 background. The 10<sup>th</sup> backcrossing was considered to be pure for C57BL/6 background.

##### 4.1.1.3 *Animal housing*

Animals were housed in the Green Line IVC Sealsafe PLUS Mouse cages (GM500, Techniplast). Each cage, measured 391 x 199 x 160 mm (wide x deep x height), is covered by a 0.2  $\mu$ m pore size filter and ventilated individually by connection to a closed air flow controlled by an automatic microprocessor. This allows circulating the air inside of the cages constantly and therefore reduces the risk of contamination and possible stress to the animals. The mice were housed in a 12 hours light/dark cycle and with free access to food and water. Cages, food and drink are renewed weekly.

All efforts are made to minimize animal suffering and reduce the number of animals use following the general guidelines approved by the animal healthcare officer of Boehringer Ingelheim.

## 4.1.2 Genotyping

### 4.1.2.1 DNA preparation

Genomic DNA was prepared from tail biopsy (approximately 25 mg of tissue per animal were used) using DNeasy Blood & Tissue kit (Qiagen). Tissues are placed in 1.5 ml Eppendorf cups and digested from 5 hours to overnight at 56°C with Proteinase K in a thermomixer block (Eppendorf), thoroughly vortexed at 1000 rpm, until the samples are completely lysed. All steps of the DNA purification procedure using spin-column are fully automated processed by Qiagen cube (protocol DNA Tissue mini). DNA is eluted in 200 µl of AE buffer and the concentration is measured by UV spectrophotometer (NanoDrop, Thermo Scientific). Genomic DNA is stored at -20°C for further use.

### 4.1.2.2 Tet-O-SNCA transgene PCR

#### 4.1.2.2.1 Standard genotyping

Amplification of *Tet-O SNCA* transgene by PCR is performed using specific primers (ASYN-F, CATGAAAGGACTGAGCAAGGCT; ASYN-R, AAGCCTCATTGTCAGGATCC). PCR reagents are from Qiagen. Each 20µl PCR reaction contains: 1x PCR Buffer (containing 1.5 mM Mg<sup>2+</sup>), 1 mM MgCl<sub>2</sub>, 0.2 mM dNTPs, 0.6 µM ASYN-F, 0.6 µM ASYN-R, 1U Taq Polymerase, 10-20 ng DNA and nuclease-free water. PCR is programmed as following: 95°C 5 min- 95°C 30s, 60°C 30 s, 72°C 1 min (repeating 35 cycles)- 72°C 10 min. PCR products are loaded onto e-Gel (2% (w/v) Agarose, Ethidium Bromide, Invitrogen) and visualized under UV light (ChemiDoc MP, Imaging System, Bio-Rad).

#### 4.1.2.2.2 qPCR

Relative quantification is the chosen method: gene expression levels are calculated by the ratio between the target gene and an endogenous reference gene. Amplification of *SNCA* transgene (target gene) is performed using specific primers (aSyn-F, 5'GGACTGAGCAAGGCTAAGGA; aSyn -R, 5'CTTCAGCCACTCCCTGTTTG) and the Taq Man probe from the Universal Probe Library (UPL#66, Roche). PCR mastermix are from QuantiFast (Qiagen). Amplification of *RNAPol II* internal control gene (reference gene) is performed using specific primers (RNAPol-F, 5' CATCAACCAGGTGGTACAGC; RNAPol -R, 5'GATTCTGGAACACTCAACTCTCC) and the Taq Man probe from the Universal Probe Library (UPL#68, Roche). Triplicate of 12 µl reaction for each sample is done. PCR performed in 7500HT Fast System Thermocycler (ABI Prism) is programmed as following: 95°C 2 min- 95°C 15 s, 60°C 1 min (repeating 40 cycles). Relative quantification is calculated by using the delta delta Ct ( $\Delta\Delta Ct$ ) method.

#### 4.1.2.2.3 *ROSA26* locus amplification method

To distinguish between heterozygote and homozygote *Tet-O ASYN* animals, an alternative method consisting of *ROSA26* locus amplification is used (Soriano, 1999). Expected fragment of *WT ROSA* locus amplicon is 600 pb and of *ROSA* targeted locus amplicon is 331 pb. Amplification of *ROSA26* transgene by PCR is performed using 3 specific primers (*ROSA26-wt-F*, AAAGTCGCTCTGAGTTGTTAT; *ROSA26-wt-R*, GGAGCGGGAGAAATGGATATG; *SA-mut-R*, GCGAAGAGTTTGTCTCAACC). PCR reactions are performed with Accuprime Taq Polymerase (Invitrogen). Each 25 µl PCR reaction contains: 1x PCR Buffer II, 0.2 µM *ROSA26-wt-F*, 0.2 µM *ROSA26-wt-R*, 0.2 µM *SA-mut-R*, 1U Taq Polymerase, 10-20 ng DNA and nuclease-free water. PCR is programmed as following: 94°C 2 min- 94°C 30 s, 55°C 30 s, 68°C 1 min (repeating 35 cycles)- 4°C. PCR products are loaded onto e-Gel (2% (w/v) Agarose, Ethidium Bromide, Invitrogen) and visualized under UV light (ChemiDoc MP, Imaging System, Bio-Rad).

#### 4.1.2.3 *Pcp2-tTA* transgene PCR

##### 4.1.2.3.1 Standard genotyping

Amplification of *Pcp2-tTA* transgene by PCR is performed using specific primers (*PCP-F*, CGCTGTGGGCATTTACTTTAG; *PCP-R*, CATGTCCAGATCGAAATCGTC). PCR reagents are from Qiagen. Each 20µl PCR reaction contains: 1x PCR Buffer (containing 1.5 mM Mg<sup>2+</sup>), 0.2 mM dNTPs, 0.6 µM *PCP-F*, 0.6 µM *PCP-R*, 1U Taq Polymerase, 10-20 ng DNA and nuclease-free water. PCR is programmed as following: 94°C 3 min- 94°C 30 s, 57°C 1 min, 72°C 1 min (repeating 35 cycles)- 72°C 3 min. PCR products are loaded onto e-Gel (2% (w/v) Agarose, Ethidium Bromide, Invitrogen) and visualized under UV light (ChemiDoc MP, Imaging System, Bio-Rad).

##### 4.1.2.3.2 Quantitative PCR

Relative quantification is the chosen method: gene expression levels are calculated by the ratio between the target gene and an endogenous reference gene. Amplification of *Pcp2-tTA* transgene (target gene) is performed using specific primers (*PCP-F*, CGCCATTATTACGACAAGCTATC; *PCP-R*, CAATTCAAGCCGAATAAGAA) and the Taq Man probe from the Universal Probe Library (UPL#55, Roche). PCR mastermix are from QuantiFast (Qiagen). Amplification of *RNAPol II* internal control gene (reference gene) is performed using specific primers (*RNAPol-F*, 5' CATCAACCAGGTGGTACAGC; *RNAPol -R*, 5'GATTCTGGAACTCAACTCTCC) and the Taq Man probe from the Universal Probe Library (UPL#68, Roche). Triplicate of 12 µl reaction for each sample is done. PCR performed in 7500HT Fast System Thermocycler (ABI Prism) is programmed as following: 95°C 2 min- 95°C 15 s, 60°C 1 min (repeating 40 cycles). Relative quantification is calculated by using the delta delta Ct ( $\Delta\Delta Ct$ ) method.

### 4.1.3 Biochemical methods

#### 4.1.3.1 Brain homogenization and protein extraction

Brain tissue are homogenized in 10 volumes of Triton lysis buffer (50 mM Hepes pH7.5, 150 mM NaCl, 1.5 mM MgCl, 1 mM EGTA, 1% (w/v) Triton X-100) supplemented with protease inhibitor cocktail, EDTA free (Roche). Homogenization is performed in Dispomix system (version V1.5, Medic Tools) during 45 s with gradually increasing rotation up to 10000 rpm. The homogenates are incubated at 4°C during 30 min with gentle rocking then clarified by centrifugation at 15000 x g for 15 min at 4°C. The supernatant are quantified for total protein content using BCA kit (Thermo Fisher Scientific). Protein samples are diluted in NuPAGE LDS Sample Buffer supplemented with Reducing agent (Invitrogen) and deionized water then heated up at 70°C for 10 min. Samples are stored at -20°C for further use.

#### 4.1.3.2 Western-blot

Total proteins are separated by 4-12% NuPAGE Bis-Tris PAGE gel (Invitrogen) using MES running buffer (Invitrogen) at constant voltage of 200V for 35 min. Proteins are transferred to nitrocellulose membrane using Semi-dry Transblot (Biorad) at constant current of 65 mA per gel for 2 hours. Immediately after transfer, membrane is placed in boiled PBS for 10 min then blocked with Odyssey blocking buffer (Licor Biosciences) for 1 hour at room temperature. Signals are visualized by infrared light using Odyssey scanning system (Licor Biosciences) at 780nm (green color) and 680nm (red color) wavelengths.

### 4.1.4 Immunohistochemistry

#### 4.1.4.1 Standard immunohistochemistry

##### 4.1.4.1.1 Tissue preparation

Mice are anesthetized and perfused *via* cardiac infusion with formalin solution (4% paraformaldehyde in PBS). Brain tissues are removed and post-fixed in formalin at 4°C. 24 hours after post-fixation, tissues are processed for paraffinization and embedded in paraffin blocks.

Processing for paraffinization (temperature of alcohol solution: 35°C; temperature of paraffin solution: 65°C):

Alcohol 70% (v/v)	1 h
Alcohol 80% (v/v)	1 h
Alcohol 96% (v/v)	1 h
Alcohol 96% (v/v)	1 h
Alcohol 100% (v/v)	1 h
Alcohol 100% (v/v)	1 h
Alcohol 100% (v/v) + Xylol 100% (v/v) 1:1	1 h

Xylol 100%	1 h
Xylol 100%	1 h
Xylol 100%	1 h
Paraffin	1 h

For immunostaining, 5-10 µm thick microtom sections (Leica) are made, tissues sections are loaded onto glass slides (SuperFrost Ultra plus, Thermo Scientific), dried out at 40°C overnight and stored at room temperature for further use.

#### 4.1.4.1.2 Deparaffinization and immunostaining

Tissue sections are progressively deparaffinized in 100% (v/v) xylol – 95% (v/v) ethanol – 70% (v/v) ethanol and washed in Tris buffered saline (TBS, Sigma-Aldrich). Depending on antigen of interest, tissue samples could be subject to a step of pre-treatment. The goal of this pre-treatment is to unmask antigen epitope. For certain antigen categories, this step is essential to break molecular cross-links induced by formalin fixation to increase in efficiency of primary antibody binding and enhance staining intensity. Most common antigen unmasking is done by heating in appropriate buffer (heat induced epitope retrieval). In some circumstances, reduction of protein cross-links could be sufficiently effective by reducing agents such as formic acid. Details of pre-treatment conditions for each antigen are listed below in Table IV.1. Blocking of unspecific binding sites using block buffer (TBS supplemented with 10% (v/v) of goat serum and 0.3% (w/v) of Triton X-100) is performed at room temperature for 1 hour. Incubation with primary antibodies diluted in antibody diluent solution (TBS supplemented with 5% (v/v) of goat serum) is performed overnight at 4°C. Before applying secondary antibodies, sections are washed 3 times in wash buffer (TBS supplemented with 0.1% (w/v) Tween 20) to remove primary antibodies.

Antigen	Antigen retrieval method
α-Synuclein	Citrate+ Formic acid
Calbindin	Citrate
mGluR1	Citrate (short) or EDTA
Syntaxin	Citrate (short) or EDTA
GFAP	Citrate
Iba-1	Citrate
VGAT	Citrate
Ubiquitin	Formic acid
pS129 α-Synuclein	Formic acid

**Table 4.1. Optimal pre-treatment conditions of antigen retrieval after deparaffinization.**

Citrate= Tissues are heated in sub-boiling citrate buffer (10mM citric acid, pH 6.0) (pre-heated at 95-100°C) during 30 min then cooled down to room temperature during 30min

Citrate (short)= Tissues are heated in sub-boiling citrate buffer (10mM citric acid, pH 6.0) (pre-heated at 95-100°C) during 10 min then cooled down to room temperature.

EDTA= Tissues are heated in sub-boiling EDTA buffer (1mM EDTA, 0.05% (w/v) Tween 20, pH 8.0) (pre-heated at 95-100°C) during 30 min then cooled down to room temperature during 30min.

Formic acid= Tissues are submerged in formic acid solution (88% (w/v) formic acid, pH 2.0) during 5 min at room temperature.

#### 4.1.4.1.3 Revelation methods

##### 4.1.4.1.3.1 *Fluorescence staining*

Alexa Fluor conjugated secondary antibodies (Molecular Probes) (Table 4.4) are used to visualize the staining. Incubation with secondary antibodies diluted in wash buffer is also performed overnight at 4°C. Tissues are washed 3 times 10 min in wash buffer and DNA are stained with Hoechst 2 µM (Invitrogen), diluted in ultrapure water. Tissue samples are protected from light to avoid eventual degradation of fluorescence signals.

##### 4.1.4.1.3.2 *Chromogenic staining*

The principle of chromogenic revelation method is based on the use of Avidin-Biotin Complex (ABC) to amplify the signal intensity. Primary antibody is first recognized by a biotinylated secondary antibody. Biotin molecule from secondary antibody binds to avidin which is conjugated itself with biotinylated horseradish peroxidase (HRP). HRP catalyzes oxidization of chromogenic substrates resulting in apparition of colorful signal detectable under light microscopy. Since each avidin molecule contains 4 binding sites for biotin, each avidin molecule could bring up to 3 enzyme molecules and increase the signal 3 times.

The use of chromogenic stain is an alternative to fluorescence stain method. This represents advantages to avoid the auto-fluorescent signals emitted by accumulation of lipofuscin in old animal brain tissues. When using this technique, tissue sections need to be quenched of endogenous peroxidase (sections are incubated in 3% (w/v) H<sub>2</sub>O<sub>2</sub> (Sigma Aldrich) during 10 min right after antigen retrieval steps). After incubation with primary antibodies, tissues are treated with biotinylated secondary antibodies (Vector laboratories) (Table 4.4) diluted in wash buffer during 1h at room temperature. After this incubation, excess of secondary antibodies is removed by 3-4 washes in wash buffer. Parallel to washing steps, biotinylated enzyme (HRP) is pre-incubated with free avidin to form large avidin-biotin-enzyme complexes (ABC) during 30min at room temperature (2 drops of reagent A and two drops of reagent B (from Vectastain kit, Vector laboratories) are mixed in 5 mL of wash buffer). Excess of ABCs are removed from sections by 3 washes of 10 min each. Chromogenic substrate solutions are prepared during the last step of washing according to provider indications

(DAB (Dako) or VIP (Vector laboratories)). Chromogenic substrate is applied to sections until signals are sufficiently developed (5 to 10 min). Stained sections are washed thoroughly in distilled water until they are cleared of excess of chromogenic substrate.

#### 4.1.4.1.4 Dehydration and storage

After revelation, sections are dehydrated by washing progressively in 60% (v/v) ethanol 70% (v/v) ethanol – 80% (v/v) isopropanol – 100% (v/v) xylol and mounted with Etellan mounting media (Merck). Stained tissues are stored at room temperature and fluorescent stained tissues need to be well protected from light.

#### 4.1.4.2 *Proteinase K (PK) digestion*

##### 4.1.4.2.1 PK digestion on PVDF membrane

Pathological deposits of  $\alpha$ -Synuclein could be detected by PK digestion followed by immunostaining (Neumann et al., 2002). PVDF membrane is cut in small pieces (3 cm x 2 cm), one piece of membrane will contain one brain slice. Membranes are activated by a short wash in methanol (Sigma Aldrich) during 30 s followed by two washes in distilled water. Activated membrane could be stored in distilled water during the time of tissue cutting. 5  $\mu$ m-thick brain tissues are cut as described in 4.1.4.1.1. then brain sections are transferred to pre-activated membranes. Tissue sections are dried overnight at 40°C. Deparaffinization is made as for standard immunostaining described in 4.1.4.1.2. However, care should be taken when moving sections in and out of baths since they might go-off from the membranes. After deparaffinization steps, sections are incubated in PK solution (50  $\mu$ g/mL). Stock PK aliquots (20 mg/mL) (Roche) are diluted in PK dilution buffer (10 mM Tris HCl pH 7.8, 100 mM NaCl, 0.1% (w/v) Brij). Beforehand, membranes should be tightly retained between filter papers (pre-equilibrated in PK dilution buffer for 10 min) to ensure homogenous digestion. Digestion is performed at 55°C overnight (14 hours). The next day, membranes are removed from PK solution and transferred into 6-well plate (one membrane per well) to avoid sticking between the membranes during washing and staining steps. PK is removed by 3 times 5 min washes in TBS then incubated in 3% (w/v) H<sub>2</sub>O<sub>2</sub> (Sigma Aldrich) during 10 min for peroxidase quenching. H<sub>2</sub>O<sub>2</sub> is removed by again 3 times 5 min washes in TBS. The proteins on the membranes are denaturated with 3 M Guanidine isothiocyanate (in 10 mM Tris-HCl, pH7.8) during 15 min. This step is followed by 3 times 5 min washes in TBS. Membranes are blocked in Casein I-Block solution (Applied Biosystems) during 1 h at room temperature and processed for standard immunostaining (15G7 antibody, chromogenic revelation method). After dehydration, membranes are dried and stored at room temperature.

##### 4.1.4.2.2 PK digestion on glass slides

Protocol is adapted from Wagner et al., 2013. Thin sections (3 $\mu$ m) are cut and processed as described in 4.1.4.1.1. for deparaffinization. Tissues are pre-treated with 0.2M boric acid, pH 9 at 63°C during

25 min and stored in the same buffer at room temperature during 30 min. PK digestion is performed in 50 µg/mL of PK (Roche) diluted in PK buffer during 10-15 min at 37°C. Tissues are stained using standard immunostaining procedure (15G7 antibody, chromogenic revelation method).

#### 4.1.5 Behavior analysis

##### 4.1.5.1 Animal cohorts

Male and female animals are both used for behavior studies but are separately housed in two different locations. Pcp2-tTA (n=22) from the 8<sup>th</sup> backcrossing and wild-type C57Bl/6 (n=16) are used as control groups.  $\alpha$ -Synuclein transgenic mice are generated by crossing Pcp2-tTA mice from the 7<sup>th</sup> backcrossing to *TetO-SNCA* (A53T- $\Delta$ CT) mice (n=16) and *TetO-SNCA* (A53T-  $\Delta$ CMA) mice (n=18).

##### 4.1.5.2 Rotarod

The mice are trained the day preceding the test. 3 training runs per animal are performed, in a two-hour interval, on a rotarod (RotaRod, TSE Systems) at constant rolling speed of 4 rpm for at least 1 min. On the day of test, mice are habituated in the test room during at least two hours. For the test, mice are placed onto auto-acceleration rod from 0 to 40 rpm. Each line is controlled independently by its own timer and animal falls are detected by light-beam sensors. The length of time the mouse stays on the rod and the speed of fall are recorded by the RotaRod software.

##### 4.1.5.3 Open-field test

Locomotion activity during active phase is measured by recording the running distance and the frequency of rearing using open-field test (ActiMot, TSE Systems). The ActiMot frame is a square-shaped frame (480 mm x 480 mm) which features two pair of light-beam strips, each pair consisting of one transmitter strip and one receiver strip. These light barriers strips are arranged at right angles to each other in the same plane. Each strip is equipped with 32 infra-red sensors. They are used to determine the X and Y coordinates of the animal and thus its location by calculating the center of gravity of the animal. Rearing is detected by additional uni-dimensional barrier strips with adjustable height which are used to determine Z1 coordinates. Experiments are carried on overnight in the dark (active phase) and separately for males or females. Animals are placed in the experiment room at least two hours before the run. The total time of recording is 840min. The total run distance (in m) and number of rearing (n) are calculated by the ActiMot software.

##### 4.1.5.4 Pole climbing test

The mice are placed facing upwards at the top of a wooden pole (50 cm long and 1 cm in diameter) planted in the middle of a square cage box. The mice are trained, three times per day during two consecutive days, to turn to orient downward and traverse the pole onto the floor of the box. On the day of test, mice are habituated in the test room during at least two hours. The mice were tested for the time to turn to orient downward and the total time to descend the pole from the time that the

animal is placed on the pole until it reaches the base of the pole in the cage box. Three trials were performed with each mouse and median data were taken across the trials.

#### 4.1.5.5 *Beam-walk*

Protocol is adapted from (Luong et al., 2011). All experiments are handled in a dark room. The beam apparatus consists of 1 m beams with a flat surface of 3.5 cm width at the starting point and gradually narrowed to 1 cm width at the finish point. The beam is resting 50 cm above the floor. A black box is placed at the end of the beam as the finish point. Nesting material from home cages is placed in the black box to attract the mouse to the finish point. A lamp (with 60 watt light bulb) is used to shine light above the start point and serves as an aversive stimulus. Another lamp (red bulb) is placed on the top of the black box and used to attract the animals stimulated by aversive light. The mice are trained, during two sessions the day before the test, to cross the whole beam. Four trials per session are given to each animal. On the day of test, mice are habituated in the test room during at least two hours. The time required per animal to cross successfully to whole beam is recorded. Falling-out of the beam is not counted as a successful trial. Four trials were performed with each mouse and median data were taken across the trials.

## 4.2 Cell models

### 4.2.1 Generation of stable Tet inducible cell lines

#### 4.2.1.1 *Plasmid preparation*

##### 4.2.1.1.1 pTRE-Tight vectors

$\alpha$ -Synuclein mutant constructs (C-terminus truncated,  $\Delta$ CT 1-130) are generated by directed mutagenesis and subcloned into pTRE-Tight vector by Sloning BioTechnology GmbH (Germany). The subsequent vector is named "pTRE-Tight-ASYN vector". Plasmids are amplified in XL-1 Blue competent cells (Invitrogen) and purified using the NucleoBond Xtra Maxi (Macherey-Nagel). 1 ng of plasmid is used to transform 100  $\mu$ l of bacterial cells. The mixture of vector and competent cells is incubated at 42°C during 45 s, the heat-pulse is stopped by 2 min incubation on ice then the mixture is transferred into 0.9 mL of TB ("Terrific Broth") medium pre-warmed at 42°C. Cells are allowed to grow during 1 h with constant shaking (250 rpm) at 37°C. Cells are spread on TB agar support containing 100  $\mu$ g/mL of ampicillin in 10- cm Petri dish and incubated overnight at 37°C. Well transformed cells should give isolated, round and ampicillin-resistant colonies. Colonies will be picked the next day by a sterilized pipette tips and allowed again to grow in 300 mL of TB medium containing 200  $\mu$ g/mL of ampicillin at 37°C. Low-copy number plasmids (derived of pMB1/ColE1 such as pTRE-Tight, pBR322 etc.) might be difficult to amplified under normal antibiotic pressure since host chromosome continues to be replicated and chromosomal DNA can contaminate the plasmid preparation. Using an additional antibiotic, such as chloramphenicol, can inhibit host protein synthesis and prevents replication of the

host chromosome. Plasmid, however, continues to replicate and accumulates in the cell after several hours (Maniatis et al., 1982). According to this, 170 µg/mL of chloramphenicol is added to TB medium when the cell culture reaches the mid or late of log phase ( $OD_{600} \sim 0.7-0.8$ ) after around 8 h, then cells are allowed to further grow for 12 h. Cells are harvested and proceed to plasmid purification according to the protocol for low-copy plasmid (maxi-preparation) of NucleoBond kit. DNA is resuspended in sterile water and stored at -20°C for further uses.

#### 4.2.1.1.2 pcDNA/FRT/TO vectors

All  $\alpha$ -Synuclein mutant (C-terminus truncated,  $\Delta$ CT 1-130) transgenes are subcloned from pTRE-Tight-ASYN vectors (original vectors) to pcDNA/FRT/TO (host vectors, available in the lab). Original and host vectors are digested with AccGSI and EcoRV enzymes. Restricted host vectors are dephosphorylated by shrimp alkaline phosphatase. Insert and dephosphorylated host vectors are loaded on 2% (w/v) agarose gel and DNA is labeled with 0.001% (w/v) of blue methylene. DNA bands are extracted from the gel using Nucleo Spin Extract kit (Macherey-Nagel). The concentration of DNA is measured by Nanodrop. Inserts are ligated to 100 ng of host vectors at the molar ratio 1/1 (amount of insert is calculated as following: Amount of Insert (ng) = [Amount of vector (ng) x Size of Insert (kB)]/Size of vector (kB)) x molar ratio of (Insert/Vector)]. The ligation reaction is carried out at 16°C overnight. Human wild-type and A53T  $\alpha$ -Synuclein full-length are sub-cloned from pcDNA 3.1-ASYN-Kozak vectors (available in the lab) to pcDNA/FRT/TO. Original and host vectors are digested with BamHI and ApaI enzymes and ligation is repeated as above. Ligation products are used to transform XL-1 Blue competent cells and proceed for plasmid preparation in the same manner as for pTRE-Tight vector using NucleoBond Xtra Maxi kit. However, since pcDNA/FRT/TO is high-copy plasmid, there is no need of adding chloramphenicol during the exponential phase in the growth medium.

#### 4.2.1.2 Cell transfection and selection

##### 4.2.1.2.1 Cell culture

BE (2)-M17 cell clones stably expressing tTA (transfected with pUHD15.1neo, (Gossen and Bujard, 1992)) were previously generated in the lab. HEK 293 Flp-In TRex TO cells were obtained from Invitrogen. The cells are cultured in T75 flasks in presence of maintenance medium and incubated at 37°C, 95% CO<sub>2</sub> (Table 4.2). Passaging is repeated every 3-4 days when cells reach 80-90% of confluency, cells are washed twice with PBS then treated with EDTA solution (Sigma) to be detached from the bottom of the flask. A dilution 1/10 is routinely made for each passage.

##### 4.2.1.2.2 Transfection and stable selection

Prior generating stable lines, titration for optimal concentration of antibiotics was necessary. For that,  $2 \times 10^5$  cells were plated in each well of a 6-well plate. Each well contains 2 mL of medium plus

varying amounts of antibiotic. Cells are incubated during 14-21 days depending on the drug to be tested and medium is refreshed every 2-3 days. The lowest concentration where massive cell death begins is chosen as optimal concentration used for selection culture. For generating stable cell lines, host cells are allowed to grow up to 80-90% of confluency at the day of transfection. Cells are transfected by electroporation using Neon® Transfection System (Invitrogen): cells are split and washed two times in PBS. After the second wash, cell pellets are resuspended in the buffer “R” (Neon Transfection System kit, Invitrogen) and mixed with the appropriate amount of plasmids. The cells are then released in 10 mL pre-warmed medium (RPMI supplemented with 10% FCS) without antibiotics (37°C) contained in 10-cm Petri dish. The medium will be changed the next day and the selection will start at 3 days post-transfection with selection medium. Replacing of fresh selection medium occurs every 2-3 days until resistant colonies distinctly appear after 2-4 weeks. Isolated, large, healthy colonies are picked then aspirated in 200 µl of medium and transferred to a single well in a 96-well plate. The next day cells are split and resuspended in 200 µl of fresh medium. Growing clones are expanded and screened for transgene expression by immunocytochemistry or western-blotting. Clones with comparable mRNA levels of  $\alpha$ -Synuclein transgene (measured by qRT-PCR, see below) are chosen for the studies of kinetic of  $\alpha$ -Synuclein degradation.

#### 4.2.1.2.3 Cell storage

Stock clones then are frozen in FCS supplemented with 10% DMSO at -80°C during 2-3 days then transferred to -150°C for long-term storage. Early passage working clones (passage 1) are expanded from stock clones and cryo-stored at a number of 10 vials/ clone.

#### 4.2.1.2.4 Cell thawing

Early passage working clones are thawed in incubator at 37°C during 5 min. Cells are diluted in pre-warmed medium and cell pellets are collected by centrifugation at 700 g during 5 min. Supernatant containing DMSO is removed in specific waste. Thawed cells are washed twice in PBS (repeating centrifugation at 700 g during 5 min). After the last wash, cells were separated and transferred to appropriate culture medium.

	BE(2)-M17	HEK 293 Flp-In TRex
<b>Maintenance medium</b>	RPMI (Invitrogen) + 10% (v/v) FCS+ 500 µg/mL G418	RPMI (Invitrogen) + 10% (v/v) FCS+ 15 µg/mL Blastidin S+ 200 µg/mL Zeocin
<b>Selection drug</b>	Puromycin (1 µg/mL)	Hygromycin (50 µg/mL)
<b>Culture surface</b>	Collagen I coated flasks	Uncoated flasks
<b>Neon Transfection conditions (Pulse voltage [V]- Pulse width[ms]- Pulse number[n])</b>	1600- 20- 1	1300- 30- 1
<b>Number of cells per pulse/ Total transfected cells per line</b>	1x 10 <sup>6</sup> /10x 10 <sup>6</sup>	1x 10 <sup>6</sup> /5x 10 <sup>6</sup>
<b>Plasmid amounts per pulse</b>	2.5 µg pTRE-Tight-ASYN+ 0.5µg pIRES-Puromycin	4 µg pcDNA/FRT/TO+ 0.5µg pOG44

**Table 4.2: Recapitulation of conditions for generation of stable cell lines.**

#### 4.2.1.3 *Comparison of $\alpha$ -Synuclein mRNA levels by qRT-PCR*

##### 4.2.1.3.1 Total RNA extraction

Cells are allowed to fully express  $\alpha$ -Synuclein (~7 days of induction). 2x 10<sup>5</sup> cells per cell clone are used for RNA extraction using RNeasy Mini kit (Qiagen). All of the steps of RNA purification are handled in RNase-free conditions. Cells are harvested by centrifugation at 700 g during 5 min and washed twice with PBS to completely remove culture medium. Cell pellets can be proceed directly to lysis or store at -70°C for later uses. Cell pellets are disrupted in 350 µl of RTL buffer by thoroughly flicking and pipetting. Cell homogenates are processed for RNA purification according to the protocol from RNeasy Mini kit for animal cells. RNA are eluted in 30 µl RNase-free (Quiagen) water and stored at -20°C.

##### 4.2.1.3.2 Reverse transcription (RT)

To synthesize single-stranded cDNA from total RNA, a step of reverse transcription is necessary. Equal amount of 1 µg of total RNA per cell line taken up in 10 µl of RNase free water is used for a 20 µl-reaction using High-capacity cDNA Reverse Transcription kit (Applied Biosystems). Total RNA is mixed with 10 µl of RT master mix containing 2 µl of 10X RT buffer, 0.8 µl of 25X dNTP mix (100mM), 2 µl of RT Random primers, 1 µl of MultiScribe Reverse transcriptase, 1 µl of RNase inhibitor and completed with 3.2 µl of nuclease-free water. The RT reaction is programmed in the thermal cycler as

following: 25°C 10 min- 37°C 120 min- 85°C 5 s- 4°C ∞. cDNA resulted from RT reaction can be stored at 4°C up to 24 h and then at -20°C for long-term use.

#### 4.2.1.3.3 Quantitative PCR

To determine and compare the expression of  $\alpha$ -Synuclein mRNA between the cell lines, quantitative PCR approach was performed using cDNA template from the RT reaction. Amplification of *ASYN* transgene (target gene) is performed using specific primers (aSyn-F, 5'GGACTGAGCAAGGCTAAGGA; aSyn -R, 5' CTTCAGCCACTCCCTGTTTG) and the Taq Man probe from the Universal Probe Library (UPL#66, Roche). The qPCR master mix is based on the protocol using TaqMan<sup>®</sup>GAPDH control reagents (human) (Applied Biosystems). Cycling program and relative quantification method is set up in the same manner as described in 1.3.2.2.

#### 4.2.2 Cell lysis/ Protein extraction

Medium are removed and cells are washed two times in cold PBS (Sigma-Aldrich) with gentle rocking for 5 min each. Then cells are lysed in Triton lysis buffer (50 mM Hepes pH 7.5, 150 mM NaCl, 1.5 mM MgCl<sub>2</sub>, 1 mM EGTA, 1% Triton X-100) supplemented with protease inhibitors (Roche) or in RIPA lysis buffer (50 mM Tris pH 8.0, 150mM NaCl, 1% (v/v) Nonidet P40, 0.5% (w/v) Sodiumdeoxycholate, 0.1% (w/v) SDS, 100mM NaF) supplemented with protease inhibitors (Roche) and 25 U/ $\mu$ l Benzonase. The cell lysates are incubated on ice during 5 min then clarified by centrifugation at 15000 x g for 15 min at 4°C. The supernatant are quantified for total protein content using BCA kit (Thermo Fisher Scientific). Protein samples are diluted in NuPAGE LDS Sample Buffer (Invitrogen) and deionized water then heated up at 70°C for 10 min. Long-term storage at -20°C requires for further use.

#### 4.2.3 Western-blot

Total proteins are separated and blotted onto nitrocellulose or PVDF membrane following the same procedure as in 4.1.3.2 for protein extracts from brain tissue. Immunoblotting is performed using appropriate primary antibody dilutions in Roti block buffer (Roth) for overnight at 4°C. Revelation is done by Odyssey scanning.

#### 4.2.4 Immunocytochemistry

Cells are transferred from the culture dish to  $\mu$ -slides VI (ibiTreat, ibidi) at 80% of density and incubated in culturing medium at 37°C for at least two hours that allow the cells to adhere onto the bottom of the slide. The cells are washed two times with PBS (100  $\mu$ l per well) to remove medium, each wash step is performed with gentle rocking during 5 min, then fixed in formalin buffered solution (Sigma- Aldrich) (50 $\mu$ l per well) at room temperature for 15 min. Cells are washed two times for 5 min to remove the fixative and permeabilised with 0.1% Triton X diluted in PBS for 10 min at room temperature. After two washes in PBS to remove the Triton solution, cells are blocked with block buffer (5% (v/v) of goat serum, 0.5% (w/v) of BSA in PBG buffer which contains 0,045% (w/v) of

fishgelatine in PBS). The blocking can be done overnight at 4°C or 1 hour at room temperature. After the blocking, cells are washed one time in PBG buffer and immunolabeled with the first antibody diluted in antibody diluent (5% (w/v) goat serum in PBG buffer) at room temperature for 1 hour. The first antibody is removed by three washing steps of 10 min each before applying the secondary antibody Alexa conjugated at room temperature for 45 min. Cells are again washed two times with PBG buffer then stained for DNA with 2µM Hoechst (Invitrogen) diluted in PBS for 10 min at room temperature. Finally, cells are washed two times with PBS and stored at 4°C.

#### 4.2.5 Kinetics of $\alpha$ -Synuclein degradation assay

Assay of kinetic of  $\alpha$ -Synuclein degradation consist of comparing the remaining  $\alpha$ -Synuclein protein levels at different time-point after stopping the expression of  $\alpha$ -Synuclein of inducible cell systems (Vogiatzi et al., 2008). Cells are allowed to fully express  $\alpha$ -Synuclein: Tet- off cells BE(2)-M17 are cultured in absence of Dox, Tet-on cells HEK-293 TRex are cultured in presence of 15 ng/mL of Dox during 7 days with renewing of culture medium every 2-3 days to maintain Dox levels in medium. The day before starting experiment,  $1 \times 10^5$  per well are seeded in 6-well plates in presence of 2 mL of induction medium (the number of wells per cell line depends on the different time points in function of experiment design, a triplicate for each time point is routinely made per experiment).

To stop the expression of  $\alpha$ -Synuclein in Tet-off cells (BE(2)-M17), culture medium are replaced with medium containing Dox (1 µg/mL). Time-point 0h is determined at the moment of adding Dox (1 µg/mL) into Tet-off cells, cells are collected immediately for cell lysis.

To stop the expression of  $\alpha$ -Synuclein in Tet-on cells (HEK-293), cells are collected by centrifugation at 700 g during 5 min following by 2 washes with PBS to completely remove Dox in the medium. Cells are seeded into clean 6-well plates. Time-point 0h is determined as the moment after the second wash with PBS, the cells are collected immediately for cell lysis.

The procedure of cell lysis is performed as described in 4.2 and  $\alpha$ -Synuclein protein levels are determined by western-blotting using 15G7 antibody. The staining of  $\beta$ -Actin is used as loading control. The ratio of  $\alpha$ -Synuclein/  $\beta$ -Actin is calculated for each time-point.

Protein level at each time point is measured by Odyssey software. Raw data are used to calculated relative protein level. All of statistic analysis and graphic design were performed with GraphPad Prism software, version 5.

Primary antibody (antigen)	Host species	Concentration used in the studies			Clone number	Provider
		WB	ICC	IHC		
15G7 ( $\alpha$ -Syn)	Rat	500 ng/ mL	1 $\mu$ g/ mL	1 $\mu$ g/ mL	15G7	Supernatant received from C.Haas's lab
Syn-1 ( $\alpha$ -Syn)	Mouse	500 ng/mL	500 ng/mL	500 ng/mL	42/ $\alpha$ -Synuclein	BD Biosciences
LB509 ( $\alpha$ -Syn )	Mouse	1 $\mu$ g/ mL	n/a	1 $\mu$ g/ mL	LB 509	abcam
GAPDH	Chicken	100 ng/mL	n/a	n/a	Polyclonal	Sigma
$\beta$ -Actin	Mouse	4 $\mu$ g/ mL	n/a	n/a	AC-74	Sigma
Calbindin-D28K	Mouse	200 ng/ mL		200 ng/ mL	CB-955	Sigma
VGAT	Mouse	10 $\mu$ g/ mL	n/a	1 $\mu$ g/ mL	117G4	Synaptic Systems
mGluR1	Rabbit	20 $\mu$ g/ mL	n/a	20 $\mu$ g/ mL	1630	Spring Bioscience
Syntaxin	Mouse	10 $\mu$ g/ mL	n/a	10 $\mu$ g/ mL	HPC-1	Sigma
Synaptophysin	Rabbit	4 $\mu$ g/ mL	n/a	4 $\mu$ g/ mL	YE269	Milipore
SNAP25	Rabbit	2 $\mu$ g/ mL	n/a	2 $\mu$ g/ mL	Polyclonal	Sigma
GFAP	Rabbit	2 $\mu$ g/ mL	n/a	2 $\mu$ g/ mL	Polyclonal	Dako
Iba-1	Rabbit	500 ng/ mL	n/a	1 $\mu$ g/ mL	Polyclonal	Wako
pS129 $\alpha$ -Syn	Rabbit	500 ng/ mL	n/a	1 $\mu$ g/ mL	EP1536Y	Epitomics
Ubiquitin	Mouse	500 ng/ mL	n/a	1 $\mu$ g/ mL	Ubi-1 (aka 042691GS)	Millipore
LC3	Mouse	500 ng/ mL	n/a	n/a	5F10	Nano tools

**Table 4.3: List of primary antibodies used in the studies.** Abbreviations: WB= western-blot, ICC= immunocytochemistry, IHC= immunohistochemistry, n/a= not applied

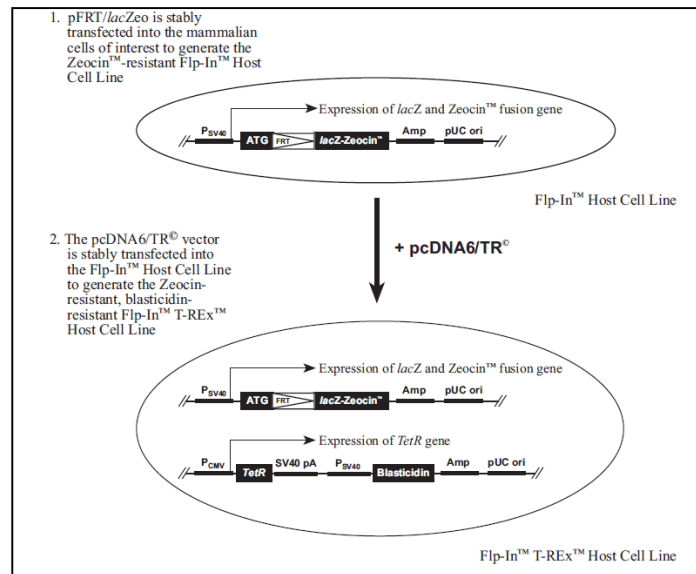
Secondary antibody (antigen)	Host species	Concentration used in the studies			Provider
		WB	ICC	IHC	
Anti-rat IRD800	Goat	1.25 $\mu$ g/ mL	n/a	n/a	Rockland
Anti-rat IRD700	Goat	1.25 $\mu$ g/ mL	n/a	n/a	Rockland
Anti-mouse IRD800	Goat	1.25 $\mu$ g/ mL	n/a	n/a	Rockland
Anti-mouse IRD700	Goat	400 ng/ mL	n/a	n/a	Rockland
Anti-chicken IRD800	Goat	1.25 $\mu$ g/ mL	n/a	n/a	Rockland
Anti-chicken IRD700	Goat	200 ng/ mL	n/a	n/a	Rockland
Anti-mouse Alexa Fluor 488	Goat	n/a	10 $\mu$ g/ mL	10 $\mu$ g/ mL	Molecular probes
Anti-mouse Alexa Fluor 594	Goat	n/a	10 $\mu$ g/ mL	10 $\mu$ g/ mL	Molecular probes

Anti-rabbit Alexa Fluor 488	Goat	n/a	10 µg/ mL	10 µg/ mL	Molecular probes
Anti-rabbit Alexa Fluor 594	Goat	n/a	10 µg/ mL	10 µg/ mL	Molecular probes
Anti-rat 488	Goat	n/a	10 µg/ mL	10 µg/ mL	Molecular probes
Anti-rat 594	Goat	n/a	10 µg/ mL	10 µg/ mL	Molecular probes
Anti-rat (biotinylated)	Goat	n/a	n/a	7.5 µg/ mL	Vector laboratories
Anti-mouse (biotinylated)	Goat	n/a	n/a	7.5 µg/ mL	Vector laboratories
Anti-rabbit (biotinylated)	Goat	n/a	n/a	7.5 µg/ mL	Vector laboratories

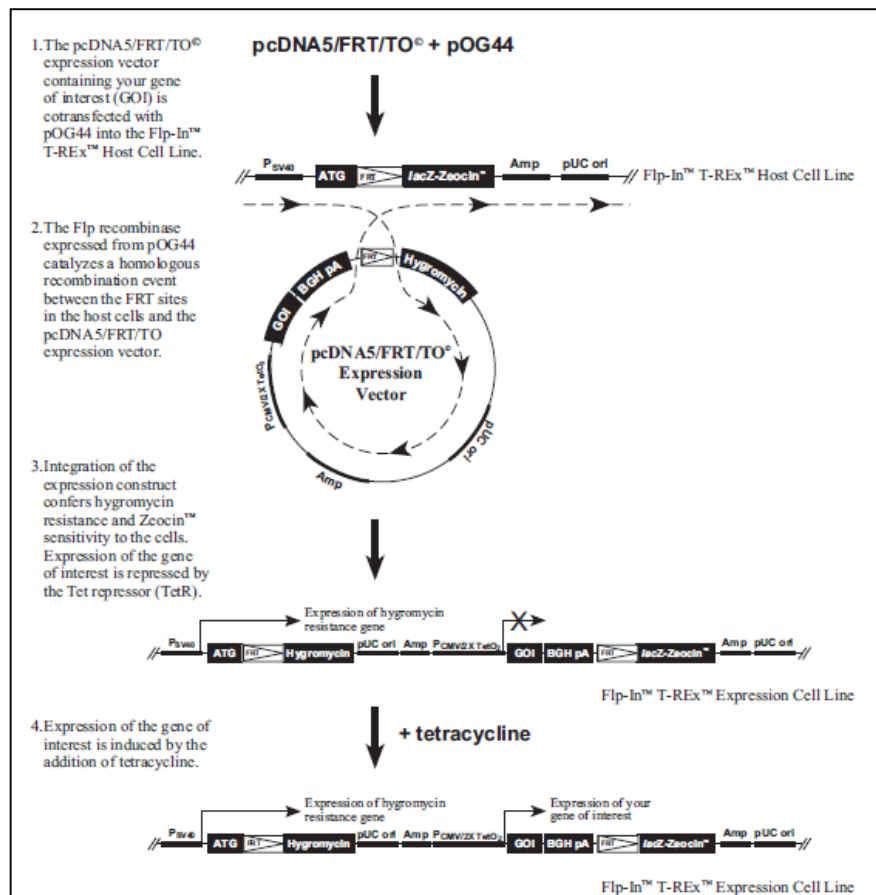
**Table 4.4: List of secondary antibodies used in the studies.** Abbreviations: WB= western-blot, ICC= immunocytochemistry, IHC= immunohistochemistry, n/a= not applied

## 5 Annex figures

A



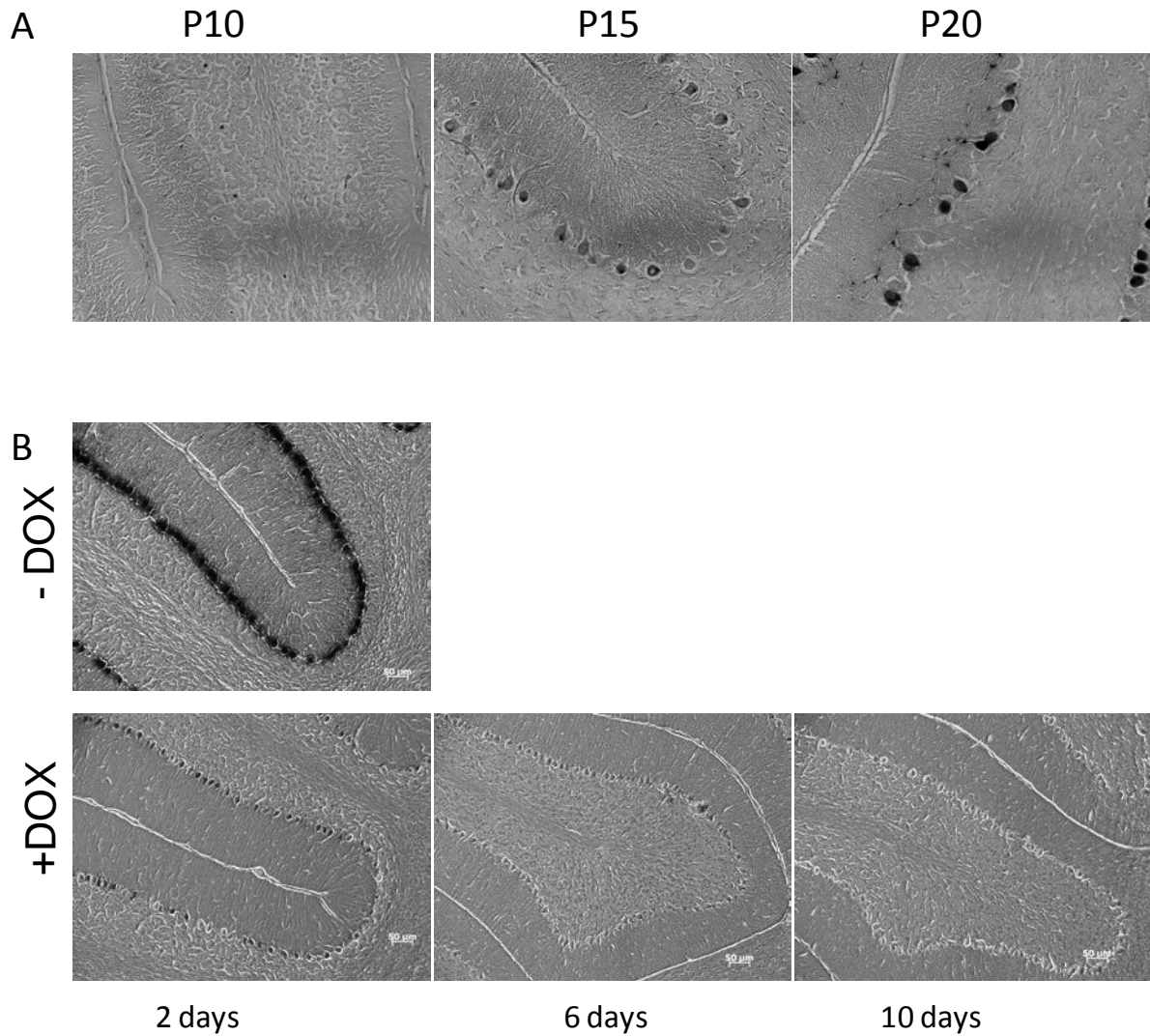
B



### Annex 1: Diagrams showing two steps of generation Tet-on stable cell lines using Flp-In T-REx systems (Life technologies).

A. Step 1: Flp-In T-REx host cell line is generated by stable transfection of pFRT-*LacZ-Zeocin* then pcDNA6/TR vectors. Host cell line contains the FRT sites and is resistant to Zeocin and Blasticidin.

B: Step 2: Flp-In T-REx expression cell line is generated by double stable transfection of pcDNA5/FRT/TO (containing gene sequence of interest) and pOG44 vectors (expressing Flp recombinase which catalyzes recombination between the FRT sites and pcDNA5/FRT/TO vector). Expression cell line loses Zeocin resistance and gains Hygromycin resistance.

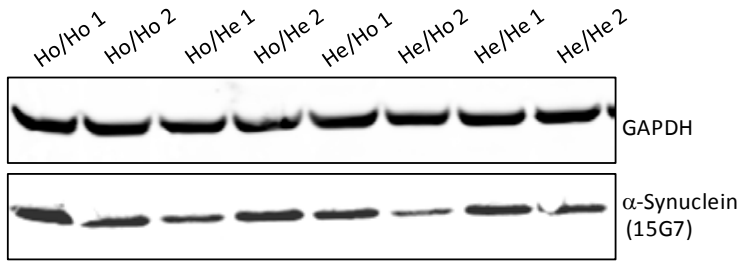


**Annex 2: Inducibility of *LacZ* transgene expression in cerebellum using of *Pcp2*-tTA driver line.**

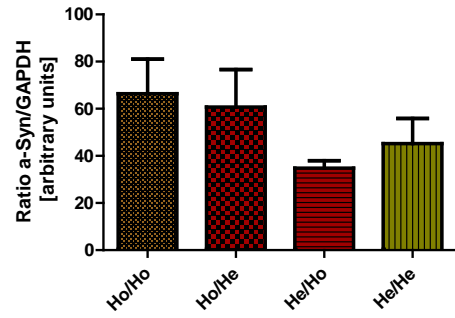
A: X-gal staining showing apparition of  $\beta$ -galactosidase expression level in cerebellum tissue homogenates from *Pcp2*-tTA/TetO-LACZ mice at 10, 15 and 20 days post-natal (P10, P15, P20), pictures of paraffin sections of 7- $\mu$ m thickness.

B: Down-regulation of  $\beta$ -galactosidase expression by adding Dox (Dox chow 200mg/kg, Bioserve) to adult *Pcp2*-tTA/TetO-LACZ mice during 2, 6 or 10 days, pictures of paraffin sections of 7- $\mu$ m thickness. Food pellets were renewed every week.

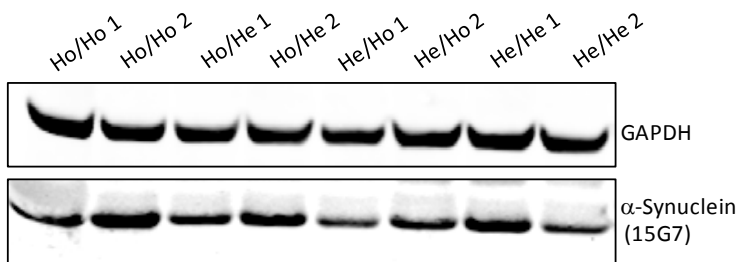
**A. TgA (A53T- $\Delta$ CT), P25**



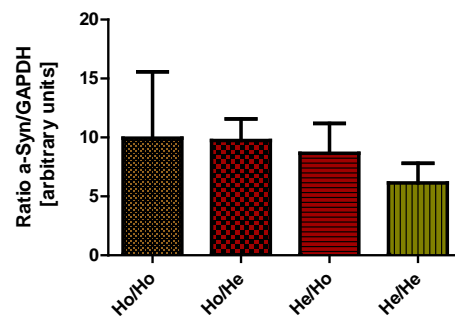
**C. TgA (A53T- $\Delta$ CT), P25**



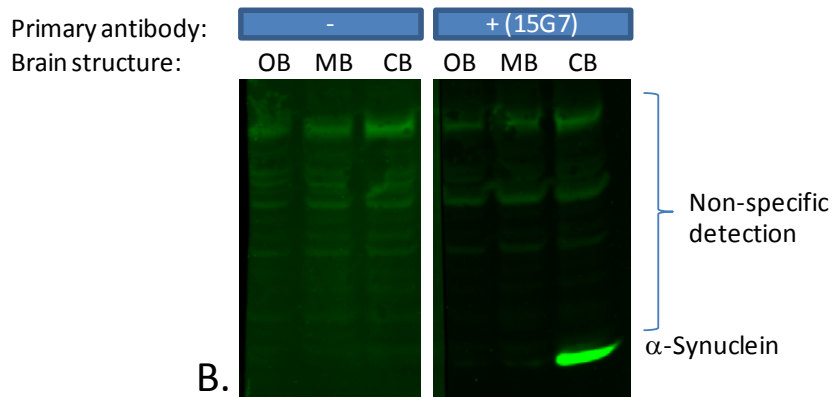
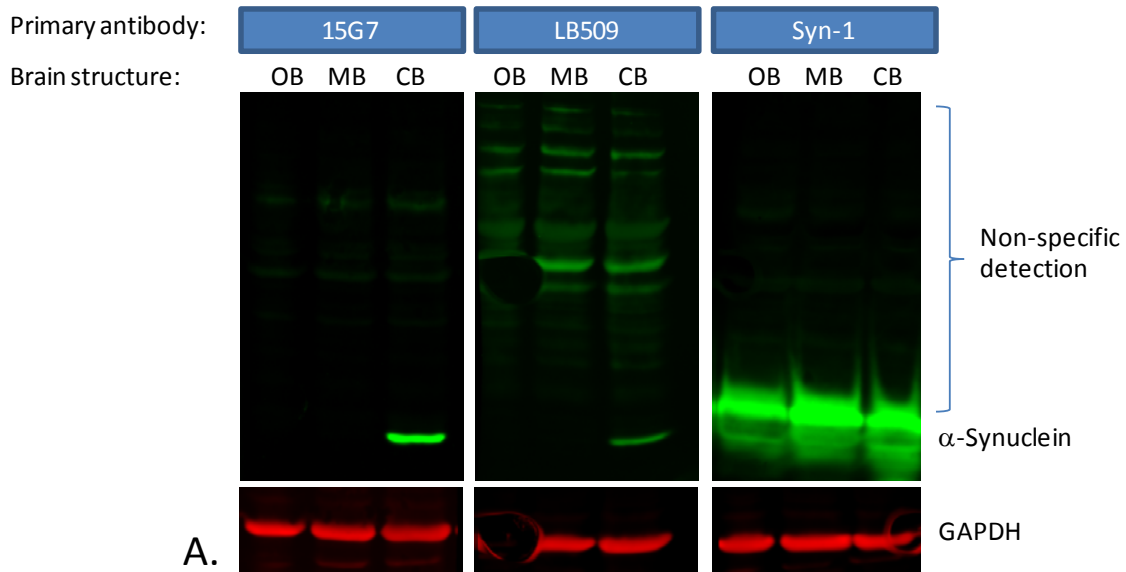
**B. TgB (A53T- $\Delta$ CMA), P25**



**D. TgB (A53T- $\Delta$ CMA), P25**



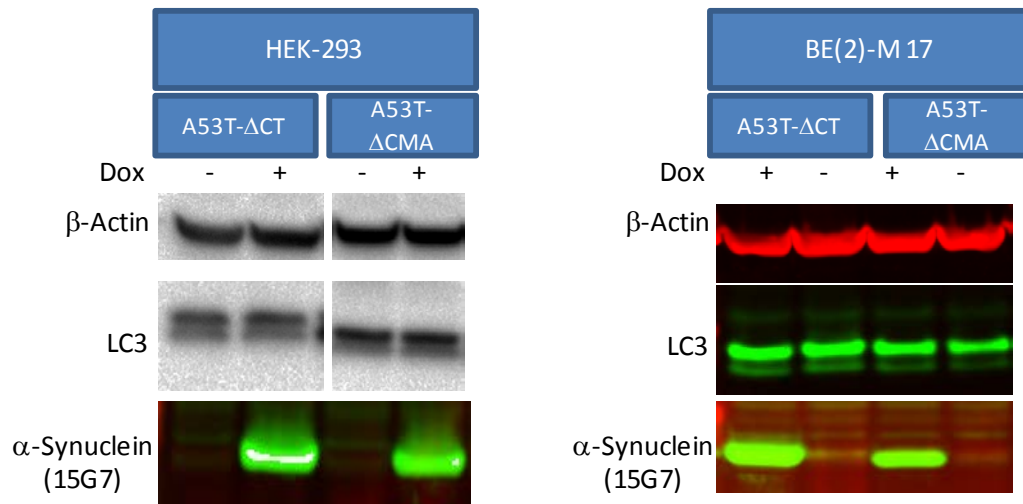
**Annex 3: Homozygotic animals does not show significant difference in  $\alpha$ -Synuclein protein levels.**  
 A, B: Western-blot showing in  $\alpha$ -synuclein level in cerebellum tissue homogenates from TgA mice at 25 day-old post-natal (P25), total protein loaded per lane: 20 $\mu$ g, antibody 15G7 anti- $\alpha$ -Synuclein, GAPDH is used as loading control. C, D: Diagram representing the mean  $\pm$ SEM of signal ratio  $\alpha$ -synuclein/GAPDH of each genotype, n= 3 per genotype (Abbreviations: Ho/Ho: *tTA* homozygote/*SNCA* homozygote; Ho/He: *tTA* homozygote/*SNCA* heterozygote; He/Ho: *tTA* heterozygote/*SNCA* homozygote; He/He: *tTA* heterozygote/*SNCA* heterozygote).



**Annex 4: Optimization of overexpressed  $\alpha$ -Synuclein detection in adult mouse brain (~3mo) homogenates.**

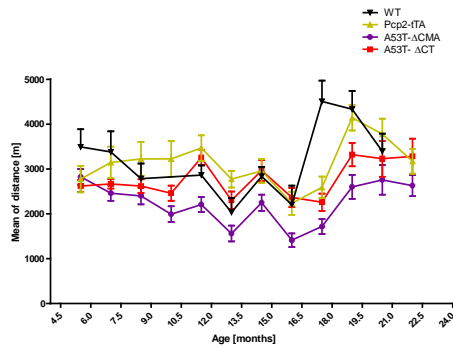
A: Western-blots showing expression of  $\alpha$ -Synuclein in three separate brain structures using different antibodies (15G7 and LB509: human specific, Syn-1: human and mouse specific). Per lane: 20 $\mu$ g of total protein from each brain structure homogenates are loaded (OB= Olfactory bulb, MB= Mid-brain (Cortex+ Basal ganglia), CB= Cerebellum)

B: Western-blots showing signals detection when primary antibody is not applied (left) and when blot was incubated with primary antibody (15G7). Background results from non-specific binding of secondary antibody.

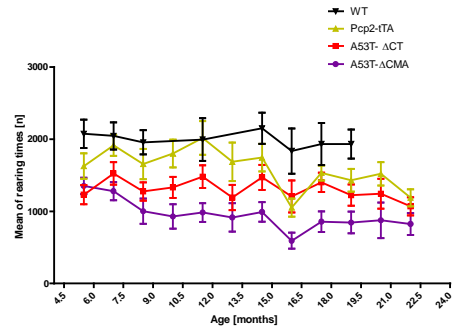


**Annex 5: Overexpression of  $\alpha$ -Synuclein does not lead to change of LC3 protein levels in cell lines.** Western-blot showing LC3 and  $\alpha$ -Synuclein protein levels in induced and non-induced conditions in HEK-293 cells (left) and BE(2)-M17 cells (right),  $\beta$ -Actin is used as loading control.

## A. Traveling distance



## B. Rearing activities



### Annex 6: Locomotor activities of animals recorded by Open-field test during active phase.

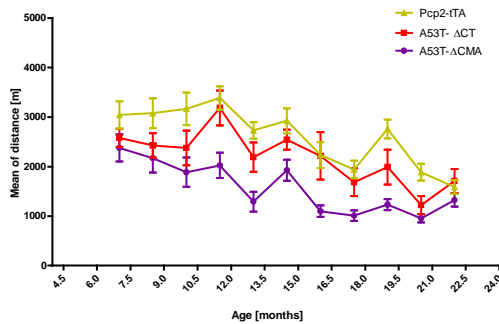
A: Total traveling distance from ages of 6 to 22.5 months. Data represent the mean  $\pm$ SEM of traveling distance.

B: Total rearing activities from ages of 6 to 22.5 months. Data represent the mean  $\pm$ SEM rearing activities.

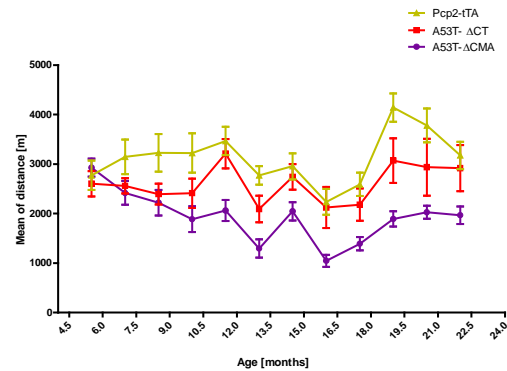
(WT: n= 15, Pcp2-tTA: n=22, A53T-ΔCT: n=16, A53T-ΔCMA: n=18)

## Traveling distance

### “Symptomatic” group

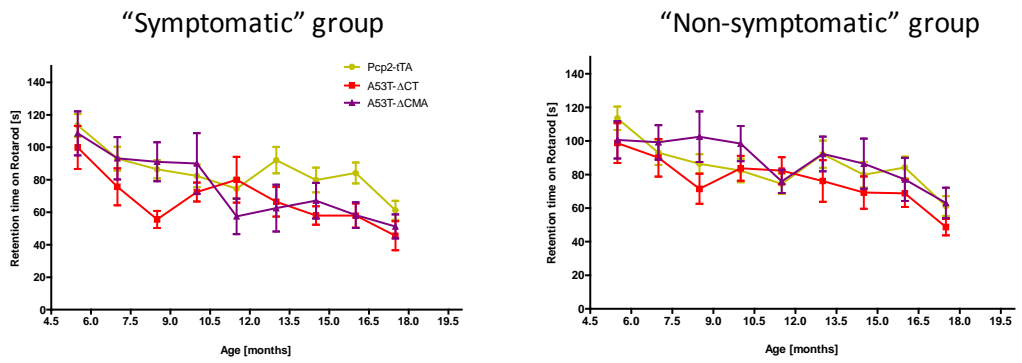
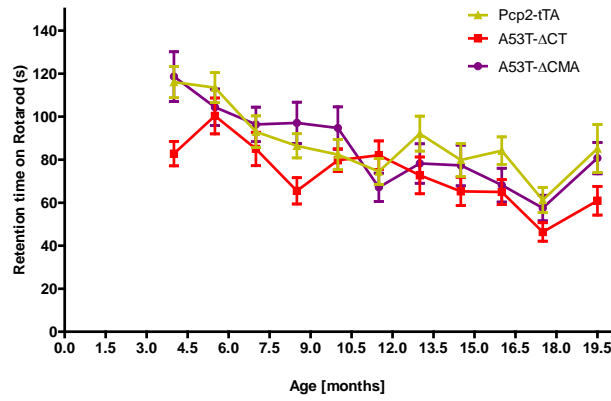


### “Non-symptomatic” group



### Annex 7: Motor coordination and motor balance phenotyping.

Post-analysis of ambulatory movement for “symptomatic” (left) and “non-symptomatic” (right) groups. Data represented the mean  $\pm$ SEM of total traveling distance ages of 6 to 21 months (Pcp2-tTA: n=22, A53T-ΔCT: n=7, A53T-ΔCMA: n=7).



**Annex 8: Motor coordination and motor balance phenotyping.**

A: Latency of animals on rotarod. Data represent the mean of total time to stay on accelerating rod (in s) (Pcp2-tTA: n=22, A53T-ΔCT: n=16, A53T-ΔCMA: n=18).

B: Post-analysis of latency on rotarod for “symptomatic” (left) and “non-symptomatic” (right) groups . Data represented the mean ±SEM of latency ages of 5 to 19.5 months (Pcp2-tTA: n=22, A53T-ΔCT: n=7, A53T-ΔCMA: n=7).

## Reference List

- Abeliovich,A., Schmitz,Y., Farinas,I., Choi-Lundberg,D., Ho,W.H., Castillo,P.E., Shinsky,N., Verdugo,J.M.G., Armanini,M., Ryan,A., Hynes,M., Phillips,H., Sulzer,D., and Rosenthal,A. (2000). Mice Lacking alpha-Synuclein Display Functional Deficits in the Nigrostriatal Dopamine System. *Neuron* 25, 239-252.
- Ahn,M., Kim,S., Kang,M., Ryu,Y., and Doohun Kim,T. (2006). Chaperone-like activities of alpha-synuclein: alpha-Synuclein assists enzyme activities of esterases. *Biochemical and Biophysical Research Communications* 346, 1142-1149.
- Al-Wandi,A., Ninkina,N., Millership,S., Williamson,S.J.M., Jones,P.A., and Buchman,V.L. (2010). Absence of alpha-synuclein affects dopamine metabolism and synaptic markers in the striatum of aging mice. *Neurobiology of Aging* 31, 796-804.
- Alvarez-Erviti,L., Rodriguez-Oroz,M.C., and Cooper,J. (2010). Chaperone-mediated autophagy markers in parkinson disease brains. *Archives of Neurology* 67, 1464-1472.
- Alvarez-Erviti,L., Seow,Y., Schapira,A.H., Rodriguez-Oroz,M.C., Obeso,J.A., and Cooper,J.M. (2013). Influence of microRNA deregulation on chaperone-mediated autophagy and [alpha]-synuclein pathology in Parkinson's disease. *Cell Death Dis* 4, e545.
- Ancolio,K., ves da Costa,C., Ueda,K., and Checler,F. (2000). alpha-Synuclein and the Parkinson's disease-related mutant Ala53Thr-alpha-synuclein do not undergo proteasomal degradation in HEK293 and neuronal cells. *Neuroscience Letters* 285, 79-82.
- Anderson,J.P., Walker,D.E., Goldstein,J.M., de Laat,R., Banducci,K., Caccavello,R.J., Barbour,R., Huang,J., Kling,K., Lee,M., Diep,L., Keim,P.S., Shen,X., Chataway,T., Schlossmacher,M.G., Seubert,P., Schenk,D., Sinha,S., Gai,W.P., and Chilcote,T.J. (2006). Phosphorylation of Ser-129 Is the Dominant Pathological Modification of alpha-Synuclein in Familial and Sporadic Lewy Body Disease. *Journal of Biological Chemistry* 281, 29739-29752.
- Anglade,P., Vyas,S., Javoy-Agid,F., Herrero,M.T., Michel,P.P., Marquez,J., Mouatt-Prigent,A., Ruberg,M., Hirsch,E.C., and Agid,Y. (1997). Apoptosis and autophagy in nigral neurons of patients with Parkinson's disease. *Histol. Histopathol.* 12, 25-31.
- Anwar,S., Peters,O., Millership,S., Ninkina,N., Doig,N., Connor-Robson,N., Threlfell,S., Kooner,G., Deacon,R.M., Bannerman,D.M., Bolam,J.P., Chandra,S.S.,

Cragg,S.J., Wade-Martins,R., and Buchman,V.L. (2011). Functional alterations to the nigrostriatal system in mice lacking all three members of the synuclein family. *J Neurosci* 31, 7264-7274.

Arima,K., Ueda,K., Sunohara,N., Hirai,S., Izumiyama,Y., Tonozuka-Uehara,H., and Kawai,M. (1998). Immunoelectron-microscopic demonstration of NACP/alpha-synuclein-epitopes on the filamentous component of Lewy bodies in Parkinson's disease and in dementia with Lewy bodies. *Brain Res.* 808, 93-100.

Auluck,P.K., Chan,H.Y., Trojanowski,J.Q., Lee,V.M., and Bonini,N.M. (2002). Chaperone suppression of alpha-synuclein toxicity in a Drosophila model for Parkinson's disease. *Science* 295, 865-868.

Azeredo da Silveira,S., Schneider,B.L., Cifuentes-Diaz,C., Sage,D., bbas-Terki,T., Iwatsubo,T., Unser,M.I., and Aebischer,P. (2009). Phosphorylation does not prompt, nor prevent, the formation of alpha-synuclein toxic species in a rat model of Parkinson's disease. *Human Molecular Genetics* 18, 872-887.

Bartels,T., Choi,J.G., and Selkoe,D.J. (2011). a-Synuclein occurs physiologically as a helically folded tetramer that resists aggregation. *Nature* 477, 107-110.

Benabid,A.L., Pollak,P., Louveau,A., Henry,S., and de,R.J. (1987). Combined (thalamotomy and stimulation) stereotactic surgery of the VIM thalamic nucleus for bilateral Parkinson disease. *Appl. Neurophysiol.* 50, 344-346.

Bennett,M.C., Bishop,J.F., Leng,Y., Chock,P.B., Chase,T.N., and Mouradian,M.M. (1999). Degradation of alpha-Synuclein by Proteasome. *Journal of Biological Chemistry* 274, 33855-33858.

Block,M.L., and Hong,J.S. (2007). Chronic microglial activation and progressive dopaminergic neurotoxicity. *Biochem. Soc. Trans.* 35, 1127-1132.

Bové,J., and Perier,C. (2012). Neurotoxin-based models of Parkinson's disease. *Neuroscience* 211, 51-76.

Braak,H. (2003). Staging of brain pathology related to sporadic Parkinson's disease. *Neurobiol Aging* 24, 197-211.

Burré,J., Sharma,M., Tsetsenis,T., Buchman,V., Etherton,M.R., and Sudhof,T.C. (2010). alpha-Synuclein Promotes SNARE-Complex Assembly in Vivo and in Vitro. *Science* 329, 1663-1667.

Bussell,R., and Eliezer,D. (2004). Effects of Parkinson's Disease-Linked Mutations on the Structure of Lipid-Associated alpha-Synuclein. *Biochemistry* 43, 4810-4818.

Cabin,D.E., Shimazu,K., Murphy,D., Cole,N.B., Gottschalk,W., McIlwain,K.L., Orrison,B., Chen,A., Ellis,C.E., Paylor,R., Lu,B., and Nussbaum,R.L. (2002). Synaptic Vesicle Depletion Correlates with Attenuated Synaptic Responses to Prolonged

Repetitive Stimulation in Mice Lacking alpha-Synuclein. *The Journal of Neuroscience* 22, 8797-8807.

Carlson,A. (1959). Detection and assay of dopamine. *Pharmacol. Rev.* 11, 300-304.

Castellani,R.J., Perry,G., Siedlak,S.L., Nunomura,A., Shimohama,S., Zhang,J., Montine,T., Sayre,L.M., and Smith,M.A. (2002). Hydroxynonenal adducts indicate a role for lipid peroxidation in neocortical and brainstem Lewy bodies in humans. *Neurosci. Lett.* 319, 25-28.

Cauli,O., Gonzalez-Usano,A., Agusti,A., and Felipo,V. (2011). Differential modulation of the glutamate-nitric oxide-cyclic GMP pathway by distinct neurosteroids in cerebellum in vivo. *Neuroscience* 190, 27-36.

Cawthorne,C., Swindell,R., Stratford,I.J., Dive,C., and Welman,A. (2007). Comparison of doxycycline delivery methods for Tet-inducible gene expression in a subcutaneous xenograft model. *J. Biomol. Tech.* 18, 120-123.

Chandra,S., Gallardo,G., Fernandez-Chacon,R., Schluter,O.M., and Sudhof,T.C. (2005). alpha-Synuclein Cooperates with CSP $\alpha$  in Preventing Neurodegeneration. *Cell* 123, 383-396.

Chartier-Harlin,M.C., Kachergus,J., Roumier,C., Mouroux,V., Douay,X., Lincoln,S., Levecque,C., Larvor,L., Andrieux,J., Hulihan,M., Waucquier,N., Defebvre,L., Amouyel,P., Farrer,M., and Destee,A. (2004). Alpha-synuclein locus duplication as a cause of familial Parkinson's disease. *Lancet* 364, 1167-1169.

Chen,L., and Feany,M.B. (2005). [alpha]-Synuclein phosphorylation controls neurotoxicity and inclusion formation in a *Drosophila* model of Parkinson disease. *Nat Neurosci* 8, 657-663.

Chen,L., Thiruchelvam,M.J., Madura,K., and Richfield,E.K. (2006). Proteasome dysfunction in aged human alpha-synuclein transgenic mice. *Neurobiology of Disease* 23, 120-126.

Chesselet,M.F., and Richter,F. (2011). Modelling of Parkinson's disease in mice. *Lancet Neurol.* 10, 1108-1118.

Choi,H.s., Liew,H., Jang,A., Kim,Y.M., Lashuel,H., and Suh,Y.H. (2012). Phosphorylation of alpha-synuclein is crucial in compensating for proteasomal dysfunction. *Biochemical and Biophysical Research Communications* 424, 597-603.

Choi,W., Zibae,S., Jakes,R., Serpell,L.C., Davletov,B., Anthony Crowther,R., and Goedert,M. (2004). Mutation E46K increases phospholipid binding and assembly into filaments of human alpha-synuclein. *FEBS Letters* 576, 363-368.

- Ciechanover,A. (2013). Intracellular protein degradation: From a vague idea through the lysosome and the ubiquitin-proteasome system and onto human diseases and drug targeting. *Bioorganic & Medicinal Chemistry* 21, 3400-3410.
- Colton,C.A. (2009). Heterogeneity of microglial activation in the innate immune response in the brain. *J. Neuroimmune. Pharmacol.* 4, 399-418.
- Conway,K.A., Harper,J.D., and Lansbury,P.T. (1998). Accelerated in vitro fibril formation by a mutant alpha-synuclein linked to early-onset Parkinson disease. *Nat Med* 4, 1318-1320.
- Cookson,M.R. (2012). Cellular effects of LRRK2 mutations. *Biochem. Soc. Trans.* 40, 1070-1073.
- Cooper,A.A., Gitler,A.D., Cashikar,A., Haynes,C.M., Hill,K.J., Bhullar,B., Liu,K., Xu,K., Strathearn,K.E., Liu,F., Cao,S., Caldwell,K.A., Caldwell,G.A., Marsischky,G., Kolodner,R.D., LaBaer,J., Rochet,J.C., Bonini,N.M., and Lindquist,S. (2006). alpha-Synuclein Blocks ER-Golgi Traffic and Rab1 Rescues Neuron Loss in Parkinson's Models. *Science* 313, 324-328.
- Corti,O., Lesage,S., and Brice,A. (2011). What Genetics Tells us About the Causes and Mechanisms of Parkinson's Disease. *Physiological Reviews* 91, 1161-1218.
- Crews,L., Spencer,B., Desplats,P., Patrick,C., Paulino,A., Rockenstein,E., Hansen,L., Adame,A., Galasko,D., and Masliah,E. (2010). Selective Molecular Alterations in the Autophagy Pathway in Patients with Lewy Body Disease and in Models of alpha-Synucleinopathy. *PLoS ONE* 5, e9313.
- Cuervo,A.M. (2004). Impaired degradation of mutant alpha-synuclein by chaperone mediated autophagy. *Science* 305, 1292-1295.
- Cullen,V., Sardi,S.P., Ng,J., Xu,Y.H., Sun,Y., Tomlinson,J.J., Kolodziej,P., Kahn,I., Saftig,P., Woulfe,J., Rochet,J.C., Glicksman,M.A., Cheng,S.H., Grabowski,G.A., Shihabuddin,L.S., and Schlossmacher,M.G. (2011). Acid  $\beta$ -glucosidase mutants linked to gaucher disease, parkinson disease, and lewy body dementia alter alpha-synuclein processing. *Ann. Neurol.* 69, 940-953.
- Daher,J., Ying,M., Banerjee,R., McDonald,R., Hahn,M., Yang,L., Flint Beal,M., Thomas,B., Dawson,V., Dawson,T., and Moore,D. (2009). Conditional transgenic mice expressing C-terminally truncated human alpha-synuclein (alphaSyn119) exhibit reduced striatal dopamine without loss of nigrostriatal pathway dopaminergic neurons. *Molecular Neurodegeneration* 4, 34.
- Davidson,W.S., Jonas,A., Clayton,D.F., and George,J.M. (1998). Stabilization of alpha-synuclein secondary structure upon binding to synthetic membranes. *J. Biol. Chem.* 273, 9443-9449.

Davis,G.C., Williams,A.C., Markey,S.P., Ebert,M.H., Caine,E.D., Reichert,C.M., and Kopin,I.J. (1979). Chronic Parkinsonism secondary to intravenous injection of meperidine analogues. *Psychiatry Res* 1, 249-254.

Desplats,P., Lee,H.J., Bae,E.J., Patrick,C., Rockenstein,E., Crews,L., Spencer,B., Masliah,E., and Lee,S.J. (2009). Inclusion formation and neuronal cell death through neuron-to-neuron transmission of alpha-synuclein. *Proc. Natl. Acad. Sci. U. S. A* 106, 13010-13015.

Donald,S., Humby,T., Fyfe,I., Segonds-Pichon,A., Walker,S.A., Andrews,S.R., Coadwell,W.J., Emson,P., Wilkinson,L.S., and Welch,H.C. (2008). P-Rex2 regulates Purkinje cell dendrite morphology and motor coordination. *Proc. Natl. Acad. Sci. U. S. A* 105, 4483-4488.

Dorval,V., and Fraser,P.E. (2006). Small ubiquitin-like modifier (SUMO) modification of natively unfolded proteins tau and alpha-synuclein. *J. Biol. Chem.* 281, 9919-9924.

Ebrahimi-Fakhari,D., Cantuti-Castelvetri,I., Fan,Z., Rockenstein,E., Masliah,E., Hyman,B.T., McLean,P.J., and Unni,V.K. (2011). Distinct roles in vivo for the ubiquitin-proteasome system and the autophagy-lysosomal pathway in the degradation of alpha-synuclein. *J Neurosci* 31, 14508-14520.

Eisbach,S., and Outeiro,T. (2013). alpha-Synuclein and intracellular trafficking: impact on the spreading of Parkinson's disease pathology. *J Mol Med* 1-11.

Emmanouilidou,E., Stefanis,L., and Vekrellis,K. (2010). Cell-produced alpha-synuclein oligomers are targeted to, and impair, the 26S proteasome. *Neurobiology of Aging* 31, 953-968.

Emmer,K.L., Waxman,E.A., Covy,J.P., and Giasson,B.I. (2011). E46K Human alpha-Synuclein Transgenic Mice Develop Lewy-like and Tau Pathology Associated with Age-dependent, Detrimental Motor Impairment. *Journal of Biological Chemistry* 286, 35104-35118.

Fleming,S.M., Salcedo,J., Hutson,C.B., Rockenstein,E., Masliah,E., Levine,M.S., and Chesselet,M.F. (2006). Behavioral effects of dopaminergic agonists in transgenic mice overexpressing human wildtype alpha-synuclein. *Neuroscience* 142, 1245-1253.

Forno,L.S., DeLanney,L.E., Irwin,I., and Langston,J.W. (1996). Electron microscopy of Lewy bodies in the amygdala-parahippocampal region. Comparison with inclusion bodies in the MPTP-treated squirrel monkey. *Adv. Neurol.* 69, 217-228.

Friedman,L.G., Lachenmayer,M.L., Wang,J., He,L., Poulouse,S.M., Komatsu,M., Holstein,G.R., and Yue,Z. (2012). Disrupted autophagy leads to dopaminergic axon and dendrite degeneration and promotes presynaptic accumulation of alpha-synuclein and LRRK2 in the brain. *J Neurosci* 32, 7585-7593.

Fujiwara,H., Hasegawa,M., Dohmae,N., Kawashima,A., Masliah,E., Goldberg,M.S., Shen,J., Takio,K., and Iwatsubo,T. (2002). alpha-Synuclein is phosphorylated in synucleinopathy lesions. *Nat Cell Biol* 4, 160-164.

Gai,W.P. (2000). In situ and in vitro study of colocalization and segregation of alpha synuclein, ubiquitin, and lipids in Lewy bodies. *Exp Neurol* 166, 324-333.

Gallia,G.L., and Khalili,K. (1998). Evaluation of an autoregulatory tetracycline regulated system. *Oncogene* 16, 1879-1884.

Games,D., Seubert,P., Rockenstein,E., Patrick,C., Trejo,M., Ubhi,K., Etle,B., Ghassemiam,M., Barbour,R., Schenk,D., Nuber,S., and Masliah,E. (2013). Axonopathy in an alpha-synuclein transgenic model of Lewy body disease is associated with extensive accumulation of C-terminal-truncated alpha-synuclein. *Am. J. Pathol.* 182, 940-953.

George,J.M. (2002). The synucleins. *Genome Biol.* 3, REVIEWS3002.

Giasson,B.I. (2002). Neuronal alpha-synucleinopathy with severe movement disorder in mice expressing A53T human alpha-synuclein. *Neuron* 34, 521-533.

Giasson,B.I., Uryu,K., Trojanowski,J.Q., and Lee,V.M. (1999). Mutant and wild type human alpha-synucleins assemble into elongated filaments with distinct morphologies in vitro. *J. Biol. Chem.* 274, 7619-7622.

Giasson,B.I., Duda,J.E., Quinn,S.M., Zhang,B., Trojanowski,J.Q., and Lee,V.M.Y. (2002). Neuronal alpha-Synucleinopathy with Severe Movement Disorder in Mice Expressing A53T Human alpha-Synuclein. *Neuron* 34, 521-533.

Giza,J., Urbanski,M.J., Prestori,F., Bandyopadhyay,B., Yam,A., Friedrich,V., Kelley,K., D'Angelo,E., and Goldfarb,M. (2010). Behavioral and cerebellar transmission deficits in mice lacking the autism-linked gene islet brain-2. *J Neurosci* 30, 14805-14816.

Glajch,K.E., Fleming,S.M., Surmeier,D.J., and Osten,P. (2012). Sensorimotor assessment of the unilateral 6-hydroxydopamine mouse model of Parkinson's disease. *Behav. Brain Res.* 230, 309-316.

Glaser,C.B., Yamin,G., Uversky,V.N., and Fink,A.L. (2005). Methionine oxidation, alpha-synuclein and Parkinson's disease. *Biochim. Biophys. Acta* 1703, 157-169.

Gómez-Santos,C., Ferrer,I., Santidrian,A.F., Barrachina,M., Gil,J., and Ambrosio,S. (2003). Dopamine induces autophagic cell death and alpha-synuclein increase in human neuroblastoma SH-SY5Y cells. *J. Neurosci. Res.* 73, 341-350.

Gomez-Tortosa,E., Newell,K., Irizarry,M.C., Sanders,J.L., and Hyman,B.T. (2000). alpha-Synuclein immunoreactivity in dementia with Lewy bodies: morphological staging and comparison with ubiquitin immunostaining. *Acta Neuropathol* 99, 352-357.

Gonzalez-Polo,R.A., Niso-Santano,M., Ortiz-Ortiz,M.A., Gomez-Martin,A., Morin,J.M., Garcia-Rubio,L., Francisco-Morcillo,J., Zaragoza,C.n., Soler,G., and Fuentes,J.M. (2007). Inhibition of Paraquat-Induced Autophagy Accelerates the Apoptotic Cell Death in Neuroblastoma SH-SY5Y Cells. *Toxicological Sciences* 97, 448-458.

Good,P.F., Hsu,A., Werner,P., Perl,D.P., and Olanow,C.W. (1998). Protein nitration in Parkinson's disease. *J. Neuropathol. Exp. Neurol.* 57, 338-342.

Gorbatyuk,O.S., Li,S., Sullivan,L.F., Chen,W., Kondrikova,G., Manfredsson,F.P., Mandel,R.J., and Muzyczka,N. (2008). The phosphorylation state of Ser-129 in human alpha-synuclein determines neurodegeneration in a rat model of Parkinson disease. *Proceedings of the National Academy of Sciences* 105, 763-768.

Gossen,M., and Bujard,H. (1992). Tight control of gene expression in mammalian cells by tetracycline-responsive promoters. *Proc. Natl. Acad. Sci. U. S. A* 89, 5547-5551.

Greenbaum,E.A., Graves,C.L., Mishizen-Eberz,A.J., Lupoli,M.A., Lynch,D.R., Englander,S.W., Axelsen,P.H., and Giasson,B.I. (2005). The E46K Mutation in alpha-Synuclein Increases Amyloid Fibril Formation. *Journal of Biological Chemistry* 280, 7800-7807.

Halliday,G.M., Holton,J.L., Revesz,T., and Dickson,D.W. (2011). Neuropathology underlying clinical variability in patients with synucleinopathies. *Acta Neuropathol.* 122, 187-204.

Halliday,G.M., and Stevens,C.H. (2011). Glia: initiators and progressors of pathology in Parkinson's disease. *Mov Disord.* 26, 6-17.

Hansen,C., Angot,E., Bergstrom,A.L., Steiner,J.A., Pieri,L., Paul,G., Outeiro,T.F., Melki,R., Kallunki,P., Fog,K., Li,J.Y., and Brundin,P. (2011). alpha-Synuclein propagates from mouse brain to grafted dopaminergic neurons and seeds aggregation in cultured human cells. *J. Clin. Invest* 121, 715-725.

Hara,T., Nakamura,K., Matsui,M., Yamamoto,A., Nakahara,Y., Suzuki-Migishima,R., Yokoyama,M., Mishima,K., Saito,I., Okano,H., and Mizushima,N. (2006). Suppression of basal autophagy in neural cells causes neurodegenerative disease in mice. *Nature* 441, 885-889.

Haywood,A.F.M., and Staveley,B.E. (2006). Mutant alpha-synuclein-induced degeneration is reduced by parkin in a fly model of Parkinson's disease. *Genome* 49, 505-510.

Hebron,M.L., Lonskaya,I., and Moussa,C.E.H. (2013). Tyrosine kinase inhibition facilitates autophagic SNCA/alpha-synuclein clearance. *Autophagy* 9, 1249-1250.

Heikkila,R.E., Hess,A., and Duvoisin,R.C. (1985). Dopaminergic neurotoxicity of 1-methyl-4-phenyl-1,2,5,6-tetrahydropyridine (MPTP) in the mouse: relationships between monoamine oxidase, MPTP metabolism and neurotoxicity. *Life Sci.* 36, 231-236.

Hong,D.P., Xiong,W., Chang,J.Y., and Jiang,C. (2011). The role of the C-terminus of human alpha-synuclein: Intra-disulfide bonds between the C-terminus and other regions stabilize non-fibrillar monomeric isomers. *FEBS Letters* 585, 561-566.

Hoyer,W., Cherny,D., Subramaniam,V., and Jovin,T.M. (2004). Impact of the Acidic C-Terminal Region Comprising Amino Acids 109–140 on alpha-Synuclein Aggregation in Vitro. *Biochemistry* 43, 16233-16242.

Ibanez,P., Bonnet,A.M., DeBarges,B., Lohmann,E., Tison,F., Pollak,P., Agid,Y., Durr,A., and Brice,A. (2004). Causal relation between alpha-synuclein gene duplication and familial Parkinson's disease. *Lancet* 364, 1169-1171.

Ihara,Y., Morishima-Kawashima,M., and Nixon,R. (2012). The Ubiquitin–Proteasome System and the Autophagic–Lysosomal System in Alzheimer Disease. *Cold Spring Harbor Perspectives in Medicine* 2.

Iwai,A., Masliah,E., Yoshimoto,M., Ge,N., Flanagan,L., de Silva,H.A., Kittel,A., and Saitoh,T. (1995). The precursor protein of non-A beta component of Alzheimer's disease amyloid is a presynaptic protein of the central nervous system. *Neuron* 14, 467-475.

Kahle,P.J., Neumann,M., Ozmen,L., Muller,V., Odoy,S., Okamoto,N., Jacobsen,H., Iwatsubo,T., Trojanowski,J.Q., Takahashi,H., Wakabayashi,K., Bogdanovic,N., Riederer,P., Kretzschmar,H.A., and Haass,C. (2001). Selective Insolubility of alpha-Synuclein in Human Lewy Body Diseases Is Recapitulated in a Transgenic Mouse Model. *The American Journal of Pathology* 159, 2215-2225.

Kahle,P. (2008). alpha-Synucleinopathy models and human neuropathology: similarities and differences. *Acta Neuropathol* 115, 87-95.

Kalda,A., Yu,L., Oztas,E., and Chen,J.F. Novel neuroprotection by caffeine and adenosine A2A receptor antagonists in animal models of Parkinson's disease. *Journal of the neurological sciences* 248[1], 9-15. 2006.

Ref Type: Abstract

Kaushik,S., and Cuervo,A.M. (2012). Chaperone-mediated autophagy: a unique way to enter the lysosome world. *Trends in Cell Biology* 22, 407-417.

Khurana,R., Ionescu-Zanetti,C., Pope,M., Li,J., Nielson,L., Ramirez-Alvarado,M., Regan,L., Fink,A.L., and Carter,S.A. (2003). A general model for amyloid fibril assembly based on morphological studies using atomic force microscopy. *Biophys. J.* 85, 1135-1144.

Klucken,J., Poehler,A.M., Ebrahimi-Fakhari,D., Schneider,J., Nuber,S., Rockenstein,E., Schlaetzer-Schrehardt,U., Hyman,B.T., McLean,P.J., Masliah,E., and Winkler,J. (2012). Alpha-synuclein aggregation involves a bafilomycin A1-sensitive autophagy pathway. *Autophagy* 8, 754-766.

Komatsu,M., Waguri,S., Chiba,T., Murata,S., Iwata,J.i., Tanida,I., Ueno,T., Koike,M., Uchiyama,Y., Kominami,E., and Tanaka,K. (2006). Loss of autophagy in the central nervous system causes neurodegeneration in mice. *Nature* 441, 880-884.

Komatsu,M., Wang,Q.J., Holstein,G.R., Friedrich,V.L., Iwata,J.i., Kominami,E., Chait,B.T., Tanaka,K., and Yue,Z. (2007). Essential role for autophagy protein Atg7 in the maintenance of axonal homeostasis and the prevention of axonal degeneration. *Proceedings of the National Academy of Sciences* 104, 14489-14494.

Kordower,J.H., Chu,Y., Hauser,R.A., Freeman,T.B., and Olanow,C.W. (2008). Lewy body-like pathology in long-term embryonic nigral transplants in Parkinson's disease. *Nat. Med.* 14, 504-506.

Kuhnel,F., Fritsch,C., Krause,S., Mundt,B., Wirth,T., Paul,Y., Malek,N.P., Zender,L., Manns,M.P., and Kubicka,S. (2004). Doxycycline regulation in a single retroviral vector by an autoregulatory loop facilitates controlled gene expression in liver cells. *Nucleic Acids Res.* 32, e30.

Kurz,A., Double,K.L., Lastres-Becker,I., Tozzi,A., Tantucci,M., Bockhart,V., Bonin,M., Garcia-Arencibia,M., Nuber,S., Schlaudraff,F., Liss,B., Fernandez-Ruiz,J., Gerlach,M., Wullner,U., Luddens,H., Calabresi,P., Auburger,G., and Gispert,S. (2010). A53T-alpha-synuclein overexpression impairs dopamine signaling and striatal synaptic plasticity in old mice. *PLoS. One.* 5, e11464.

Lee,H.J., Choi,C., and Lee,S.J. (2002). Membrane-bound alpha-Synuclein Has a High Aggregation Propensity and the Ability to Seed the Aggregation of the Cytosolic Form. *Journal of Biological Chemistry* 277, 671-678.

Lee,H.J., Khoshaghideh,F., Patel,S., and Lee,S.J. (2004). Clearance of alpha-Synuclein Oligomeric Intermediates via the Lysosomal Degradation Pathway. *The Journal of Neuroscience* 24, 1888-1896.

Lee,J.T., Wheeler,T.C., Li,L., and Chin,L.S. (2008). Ubiquitination of alpha-synuclein by Siah-1 promotes alpha-synuclein aggregation and apoptotic cell death. *Human Molecular Genetics* 17, 906-917.

Lennox,G., Lowe,J., Landon,M., Byrne,E.J., Mayer,R.J., and Godwin-Austen,R.B. (1989). Diffuse Lewy body disease: correlative neuropathology using anti-ubiquitin immunocytochemistry. *J. Neurol. Neurosurg. Psychiatry* 52, 1236-1247.

- Leverenz, J.B., Umar, I., Wang, Q., Montine, T.J., McMillan, P.J., Tsuang, D.W., Jin, J., Pan, C., Shin, J., Zhu, D., and Zhang, J. (2007). Proteomic identification of novel proteins in cortical lewy bodies. *Brain Pathol.* *17*, 139-145.
- Levitan, K., Chereau, D., Cohen, S.I.A., Knowles, T.P.J., Dobson, C.M., Fink, A.L., Anderson, J.P., Goldstein, J.M., and Millhauser, G.L. (2011). Conserved C-Terminal Charge Exerts a Profound Influence on the Aggregation Rate of alpha-Synuclein. *Journal of Molecular Biology* *411*, 329-333.
- Lewis, K., Yaeger, A., DeMartino, G., and Thomas, P. (2010). Accelerated formation of alpha-synuclein oligomers by concerted action of the 20S proteasome and familial Parkinson mutations. *J Bioenerg Biomembr* *42*, 85-95.
- Li, J.Y., Englund, E., Holton, J.L., Soulet, D., Hagell, P., Lees, A.J., Lashley, T., Quinn, N.P., Rehncrona, S., Bjorklund, A., Widner, H., Revesz, T., Lindvall, O., and Brundin, P. (2008). Lewy bodies in grafted neurons in subjects with Parkinson's disease suggest host-to-graft disease propagation. *Nat. Med.* *14*, 501-503.
- Li, J., Uversky, V.N., and Fink, A.L. (2001). Effect of Familial Parkinson's Disease Point Mutations A30P and A53T on the Structural Properties, Aggregation, and Fibrillation of Human alpha-Synuclein. *Biochemistry* *40*, 11604-11613.
- Li, W., Lesuisse, C., Xu, Y., Troncoso, J., Price, D. and Lee, M. (2004). Stabilization of alpha-Synuclein Protein with Aging and Familial Parkinson's Disease-Linked A53T Mutation. *The Journal of Neuroscience*, *24*(33):7400 –7409
- Liani, E., Eyal, A., Avraham, E., Shemer, R., Szargel, R., Berg, D., Bornemann, A., Riess, O., Ross, C.A., Rott, R., and Engelender, S. (2004). Ubiquitylation of synphilin-1 and alpha-synuclein by SIAH and its presence in cellular inclusions and Lewy bodies imply a role in Parkinson's disease. *Proceedings of the National Academy of Sciences of the United States of America* *101*, 5500-5505.
- Lim, Y., Kehm, V.M., Lee, E.B., Soper, J.H., Li, C., Trojanowski, J.Q., and Lee, V.M. (2011). alpha-Syn suppression reverses synaptic and memory defects in a mouse model of dementia with Lewy bodies. *J. Neurosci.* *31*, 10076-10087.
- Lin, X., Parisiadou, L., Sgobio, C., Liu, G., Yu, J., Sun, L., Shim, H., Gu, X.L., Luo, J., Long, C.X., Ding, J., Mateo, Y., Sullivan, P.H., Wu, L.G., Goldstein, D.S., Lovinger, D., and Cai, H. (2012). Conditional Expression of Parkinson's Disease-Related Mutant alpha-Synuclein in the Midbrain Dopaminergic Neurons Causes Progressive Neurodegeneration and Degradation of Transcription Factor Nuclear Receptor Related 1. *J. Neurosci.* *32*, 9248-9264.
- Liu, C.W., Giasson, B.I., Lewis, K.A., Lee, V.M., Demartino, G.N., and Thomas, P.J. (2005a). A precipitating role for truncated alpha-synuclein and the proteasome in alpha-synuclein aggregation: implications for pathogenesis of Parkinson disease. *J Biol Chem* *280*, 22670-22678.

Liu,C.W., Giasson,B.I., Lewis,K.A., Lee,V.M., DeMartino,G.N., and Thomas,P.J. (2005b). A Precipitating Role for Truncated alpha-Synuclein and the Proteasome in alpha-Synuclein Aggregation: IMPLICATIONS FOR PATHOGENESIS OF PARKINSON DISEASE. *Journal of Biological Chemistry* 280, 22670-22678.

Lu,X.H. (2009). BAC to degeneration bacterial artificial chromosome (BAC)-mediated transgenesis for modeling basal ganglia neurodegenerative disorders. *Int. Rev. Neurobiol.* 89, 37-56.

Luchtman,D.W., Meng,Q., and Song,C. (2012). Ethyl-eicosapentaenoate (E-EPA) attenuates motor impairments and inflammation in the MPTP-probenecid mouse model of Parkinson's disease. *Behav. Brain Res.* 226, 386-396.

Luk,K.C., Song,C., O'Brien,P., Stieber,A., Branch,J.R., Brunden,K.R., Trojanowski,J.Q., and Lee,V.M. (2009). Exogenous alpha-synuclein fibrils seed the formation of Lewy body-like intracellular inclusions in cultured cells. *Proc. Natl. Acad. Sci. U. S. A* 106, 20051-20056.

Luong,T.N., Carlisle,H.J., Southwell,A., and Patterson,P.H. (2011). Assessment of motor balance and coordination in mice using the balance beam. *J. Vis. Exp.*

Magen,I., and Chesselet,M.F. (2010). Chapter 4 - Genetic mouse models of Parkinson's disease: The state of the art. In *Progress in Brain Research Recent Advances in Parkinson's Disease Translational and Clinical Research*, M.A.C. nders Bjorklund and, ed. Elsevier), pp. 53-87.

Mak,S.K., McCormack,A.L., Manning-Bo-f,A.B., Cuervo,A.M., and Di Monte,D.A. (2010). Lysosomal Degradation of alpha-Synuclein in Vivo. *Journal of Biological Chemistry* 285, 13621-13629.

Malkus,K.A., and Ischiropoulos,H. (2012). Regional deficiencies in chaperone-mediated autophagy underlie alpha-synuclein aggregation and neurodegeneration. *Neurobiology of Disease* 46, 732-744.

Mandolesi,G., Grasselli,G., Musella,A., Gentile,A., Musumeci,G., Sepman,H., Haji,N., Fresegna,D., Bernardi,G., and Centonze,D. (2012). GABAergic signaling and connectivity on Purkinje cells are impaired in experimental autoimmune encephalomyelitis. *Neurobiol. Dis.* 46, 414-424.

Manto,M., Laute,M.A., and Pandolfo,M. (2005). Depression of extra-cellular GABA and increase of NMDA-induced nitric oxide following acute intra-nuclear administration of alcohol in the cerebellar nuclei of the rat. *Cerebellum.* 4, 230-238.

Manzoni,C. (2012). LRRK2 and autophagy: a common pathway for disease. *Biochem. Soc. Trans.* 40, 1147-1151.

- Marin-Teva, J.L., Dusart, I., Colin, C., Gervais, A., van, R.N., and Mallat, M. (2004). Microglia promote the death of developing Purkinje cells. *Neuron* 41, 535-547.
- Maroteaux, L., Campanelli, J.T., and Scheller, R.H. (1988). Synuclein: a neuron-specific protein localized to the nucleus and presynaptic nerve terminal. *The Journal of Neuroscience* 8, 2804-2815.
- Marques, O., and Outeiro, T.F. (2012). Alpha-synuclein: from secretion to dysfunction and death. *Cell Death Dis* 3, e350.
- Martinez-Vicente, M., Tallochy, Z., Kaushik, S., Massey, A.C., Mazzulli, J., Mosharov, E.V., Hodara, R., Fredenburg, R., Wu, D.C., Follenzi, A., Dauer, W., Przedborski, S., Ischiropoulos, H., Lansbury, P.T., Sulzer, D., and Cuervo, A.M. (2008). Dopamine-modified alpha-synuclein blocks chaperone-mediated autophagy. *J Clin Invest* 118, 777-788.
- Marxreiter, F., Nuber, S., Kandasamy, M., Klucken, J., Aigner, R., Burgmayer, R., Couillard-Despres, S., Riess, O., Winkler, J., and Winner, B. (2009). Changes in adult olfactory bulb neurogenesis in mice expressing the A30P mutant form of alpha-synuclein. *Eur. J. Neurosci.* 29, 879-890.
- Maslah, E., Rockenstein, E., Veinbergs, I., Mallory, M., Hashimoto, M., Takeda, A., Sagara, Y., Sisk, A., and Mucke, L. (2000). Dopaminergic Loss and Inclusion Body Formation in alpha-Synuclein Mice: Implications for Neurodegenerative Disorders. *Science* 287, 1265-1269.
- McFarland, N.R., Fan, Z., Xu, K., Schwarzschild, M.A., Feany, M.B., Hyman, B.T., and McLean, P.J. (2009). Alpha-synuclein S129 phosphorylation mutants do not alter nigrostriatal toxicity in a rat model of Parkinson disease. *J Neuropathol Exp Neurol* 68, 515-524.
- McGeer, P.L., Itagaki, S., Boyes, B.E., and McGeer, E.G. (1988). Reactive microglia are positive for HLA-DR in the substantia nigra of Parkinson's and Alzheimer's disease brains. *Neurology* 38, 1285-1291.
- McNaught, K.S., and Jenner, P. (2001). Proteasomal function is impaired in substantia nigra in Parkinson's disease. *Neuroscience Letters* 297, 191-194.
- McNaught, K.S., Mytilineou, C., JnoBaptiste, R., Yabut, J., Shashidharan, P., Jenner, P., and Olanow, C.W. (2002). Impairment of the ubiquitin-proteasome system causes dopaminergic cell death and inclusion body formation in ventral mesencephalic cultures. *Journal of Neurochemistry* 81, 301-306.
- Meier, F., Abeywardana, T., Dhall, A., Marotta, N.P., Varkey, J., Langen, R., Chatterjee, C., and Pratt, M.R. (2012). Semisynthetic, Site-Specific Ubiquitin Modification of alpha-Synuclein Reveals Differential Effects on Aggregation. *J. Am. Chem. Soc.* 134, 5468-5471.

- Mhyre,T., Boyd,J., Hamill,R., and Maguire-Zeiss,K.A. (2012). Parkinson's Disease. In Protein Aggregation and Fibrillogenesis in Cerebral and Systemic Amyloid Disease, J.R. Harris, ed. Springer Netherlands), pp. 389-455.
- Miller,C.J., Kassem,H.S., Pepper,S.D., Hey,Y., Ward,T.H., and Margison,G.P. (2003). Mycoplasma infection significantly alters microarray gene expression profiles. *Biotechniques* 35, 812-814.
- Mori,F., Piao,Y.S., Hayashi,S., Fujiwara,H., Hasegawa,M., Yoshimoto,M., Iwatsubo,T., Takahashi,H., and Wakabayashi,K. (2003). Alpha-synuclein accumulates in Purkinje cells in Lewy body disease but not in multiple system atrophy. *J Neuropathol Exp Neurol* 62, 812-819.
- Morimoto,M., and Kopan,R. (2009). rtTA toxicity limits the usefulness of the SP-C-rtTA transgenic mouse. *Dev. Biol.* 325, 171-178.
- Mullett,S., Maio,R., Greenamyre,J.T., and Hinkle,D. (2013). DJ-1 Expression Modulates Astrocyte-Mediated Protection Against Neuronal Oxidative Stress. *J Mol Neurosci* 49, 507-511.
- Muntané,G., Ferrer,I., and Martinez-Vicente,M. (2012). alpha-synuclein phosphorylation and truncation are normal events in the adult human brain. *Neuroscience* 200, 106-119.
- Murphy,D.D., Rueter,S.M., Trojanowski,J.Q., and Lee,V.M.Y. (2000). Synucleins Are Developmentally Expressed, and alpha-Synuclein Regulates the Size of the Presynaptic Vesicular Pool in Primary Hippocampal Neurons. *The Journal of Neuroscience* 20, 3214-3220.
- Murray,I.V.J., Giasson,B.I., Quinn,S.M., Koppaka,V., Axelsen,P.H., Ischiropoulos,H., Trojanowski,J.Q., and Lee,V.M.Y. (2003). Role of alpha-Synuclein Carboxy-Terminus on Fibril Formation in Vitro. *Biochemistry* 42, 8530-8540.
- Naiki,H., Higuchi,K., Hosokawa,M., and Takeda,T. (1989). Fluorometric determination of amyloid fibrils in vitro using the fluorescent dye, thioflavin T1. *Anal. Biochem.* 177, 244-249.
- Neumann,M., Kahle,P.J., Giasson,B.I., Ozmen,L., Borroni,E., Spooen,W., Muller,V., Odoy,S., Fujiwara,H., Hasegawa,M., Iwatsubo,T., Trojanowski,J.Q., Kretschmar,H.A., and Haass,C. (2002). Misfolded proteinase K-resistant hyperphosphorylated alpha-synuclein in aged transgenic mice with locomotor deterioration and in human alpha-synucleinopathies. *J Clin Invest* 110, 1429-1439.
- Nonaka,T., Watanabe,S.T., Iwatsubo,T., and Hasegawa,M. (2010). Seeded aggregation and toxicity of {alpha}-synuclein and tau: cellular models of neurodegenerative diseases. *J. Biol. Chem.* 285, 34885-34898.

Nonaka,T., Iwatsubo,T., and Hasegawa,M. (2004). Ubiquitination of alpha-Synuclein. *Biochemistry* 44, 361-368.

Nuber,S., Petrasch-Parwez,E., Winner,B., Winkler,J., von Horsten,S., Schmidt,T., Boy,J., Kuhn,M., Nguyen,H.P., Teismann,P., Schulz,J.B., Neumann,M., Pichler,B.J., Reischl,G., Holzmann,C., Schmitt,I., Bornemann,A., Kuhn,W., Zimmermann,F., Servadio,A., and Riess,O. (2008). Neurodegeneration and Motor Dysfunction in a Conditional Model of Parkinson's Disease. *The Journal of Neuroscience* 28, 2471-2484.

Okochi,M., Walter,J., Koyama,A., Nakajo,S., Baba,M., Iwatsubo,T., Meijer,L., Kahle,P.J., and Haass,C. (2000). Constitutive Phosphorylation of the Parkinson's Disease Associated alpha-Synuclein. *Journal of Biological Chemistry* 275, 390-397.

Olanow,C.W., Stern,M.B., and Sethi,K. (2009). The scientific and clinical basis for the treatment of Parkinson disease (2009). *Neurology* 72, S1-S136.

Oluwatosin-Chigbu,Y., Robbins,A., Scott,C.W., Arriza,J.L., Reid,J.D., and Zysk,J.R. (2003). Parkin suppresses wild-type alpha-synuclein-induced toxicity in SHSY-5Y cells. *Biochemical and Biophysical Research Communications* 309, 679-684.

Ono,K., Hirohata,M., and Yamada,M. (2007). Anti-fibrillogenic and fibril-destabilizing activity of nicotine in vitro: Implications for the prevention and therapeutics of Lewy body diseases. *Experimental. Neurology* 205, 414-424.

Ono,S., Hirai,K., and Tokuda,E. (2009). Effects of pergolide mesilate on metallothionein mRNAs expression in a mouse model for Parkinson disease. *Biol. Pharm. Bull.* 32, 1813-1817.

Oueslati,A., Fournier,M., and Lashuel,H.A. (2010). Role of post-translational modifications in modulating the structure, function and toxicity of alpha-synuclein: implications for Parkinson's disease pathogenesis and therapies. *Prog. Brain Res.* 183, 115-145.

Oueslati,A., Paleologou,K.E., Schneider,B.L., Aebischer,P., and Lashuel,H.A. (2012). Mimicking Phosphorylation at Serine 87 Inhibits the Aggregation of Human alpha-Synuclein and Protects against Its Toxicity in a Rat Model of Parkinson's Disease. *The Journal of Neuroscience* 32, 1536-1544.

Paleologou,K.E., Oueslati,A., Shakked,G., Rospigliosi,C.C., Kim,H.Y., Lamberto,G.R., Fernandez,C.O., Schmid,A., Chegini,F., Gai,W.P., Chiappe,D., Moniatte,M., Schneider,B.L., Aebischer,P., Eliezer,D., Zweckstetter,M., Masliah,E., and Lashuel,H.A. (2010). Phosphorylation at S87 is enhanced in synucleinopathies, inhibits alpha-synuclein oligomerization, and influences synuclein-membrane interactions. *J Neurosci* 30, 3184-3198.

Paleologou,K.E., Schmid,A.W., Rospigliosi,C.C., Kim,H.Y., Lamberto,G.R., Fredenburg,R.A., Lansbury,P.T., Fernandez,C.O., Eliezer,D., Zweckstetter,M., and

Lashuel,H.A. (2008). Phosphorylation at Ser-129 but Not the Phosphomimics S129E/D Inhibits the Fibrillation of alpha-Synuclein. *Journal of Biological Chemistry* 283, 16895-16905.

Park,H., Shim,J.S., Kim,H.G., Lee,H., and Oh,M.S. (2013). *Ampelopsis Radix* Protects Dopaminergic Neurons against 1-Methyl-4-phenylpyridinium/1-methyl-4-phenyl-1,2,3,6-tetrahydropyridine-Induced Toxicity in Parkinson's Disease Models In Vitro and In Vivo. *Evid. Based. Complement Alternat. Med.* 2013, 346438.

Peng,X.M., Tehranian,R., Dietrich,P., Stefanis,L., and Perez,R.G. (2005). alpha-Synuclein activation of protein phosphatase 2A reduces tyrosine hydroxylase phosphorylation in dopaminergic cells. *Journal of Cell Science* 118, 3523-3530.

Perez,R.G., Waymire,J.C., Lin,E., Liu,J.J., Guo,F., and Zigmond,M.J. (2002). A Role for alpha-Synuclein in the Regulation of Dopamine Biosynthesis. *The Journal of Neuroscience* 22, 3090-3099.

Periquet,M., Fulga,T., Myllykangas,L., Schlossmacher,M.G., and Feany,M.B. (2007). Aggregated + $\beta$ -Synuclein Mediates Dopaminergic Neurotoxicity In Vivo. *The Journal of Neuroscience* 27, 3338-3346.

Porras,G., Li,Q., and Bezdard,E. (2012). Modeling Parkinson's Disease in Primates: The MPTP Model. *Cold Spring Harbor Perspectives in Medicine* 2.

Price,D.L., Rockenstein,E., Ubhi,K., Phung,V., MacLean-Lewis,N., Askay,D., Cartier,A., Spencer,B., Patrick,C., Desplats,P., Ellisman,M.H., and Masliah,E. (2010). Alterations in mGluR5 expression and signaling in Lewy body disease and in transgenic models of alpha-synucleinopathy--implications for excitotoxicity. *PLoS. One.* 5, e14020.

Przedborski,S., Tieu,K., Perier,C., and Vila,M. (2004). MPTP as a mitochondrial neurotoxic model of Parkinson's disease. *J Bioenerg Biomembr* 36, 375-379.

Quik,M., Perez,X.A., and Bordia,T. (2012). Nicotine as a potential neuroprotective agent for Parkinson's disease. *Mov. Disord.* 27, 947-957.

Rakovic,A., Grunewald,A., Kottwitz,J., Bruggemann,N., Pramstaller,P.P., Lohmann,K., and Klein,C. (2011). Mutations in PINK1 and Parkin Impair Ubiquitination of Mitofusins in Human Fibroblasts. *PLoS ONE* 6, e16746.

Ramsey,C.P., Tsika,E., Ischiropoulos,H., and Giasson,B.I. (2010). DJ-1 deficient mice demonstrate similar vulnerability to pathogenic Ala53Thr human alpha-syn toxicity. *Human Molecular Genetics* 19, 1425-1437.

Reith,R.M., Way,S., McKenna,J., III, Haines,K., and Gambello,M.J. (2011). Loss of the tuberous sclerosis complex protein tuberin causes Purkinje cell degeneration. *Neurobiol. Dis.* 43, 113-122.

- Rekas,A, Ahn,K.J., Kim,J., and Carver,J.A. (2012). The chaperone activity of alpha-synuclein: Utilizing deletion mutants to map its interaction with target proteins. *Proteins* 80, 1316-1325.
- Rideout,H.J., Larsen,K.E., Sulzer,D., and Stefanis,L. (2001). Proteasomal inhibition leads to formation of ubiquitin/alpha-synuclein-immunoreactive inclusions in PC12 cells. *Journal of Neurochemistry* 78, 899-908.
- Rieker,C., Dev,K.K., Lehnhoff,K., Barbieri,S., Ksiazek,I., Kauffmann,S., Danner,S., Schell,H., Boden,C., Ruegg,M.A., Kahle,P.J., van der,P.H., and Shimshek,D.R. (2011). Neuropathology in mice expressing mouse alpha-synuclein. *PLoS. One.* 6, e24834.
- Rott,R., Szargel,R., Haskin,J., Bandopadhyay,R., Lees,A.J., Shani,V., and Engelender,S. (2011). alpha-Synuclein fate is determined by USP9X-regulated monoubiquitination. *Proceedings of the National Academy of Sciences* 108, 18666-18671.
- Rott,R., Szargel,R., Haskin,J., Shani,V., Shainskaya,A., Manov,I., Liani,E., Avraham,E., and Engelender,S. (2008). Monoubiquitylation of alpha-Synuclein by Seven in Absentia Homolog (SIAH) Promotes Its Aggregation in Dopaminergic Cells. *Journal of Biological Chemistry* 283, 3316-3328.
- Sampathu,D.M., Giasson,B.I., Pawlyk,A.C., Trojanowski,J.Q., and Lee,V.M.Y. (2003). Ubiquitination of alpha-Synuclein Is Not Required for Formation of Pathological Inclusions in alpha-Synucleinopathies. *The American Journal of Pathology* 163, 91-100.
- Sanbe,A., Gulick,J., Hanks,M.C., Liang,Q., Osinska,H., and Robbins,J. (2003). Reengineering inducible cardiac-specific transgenesis with an attenuated myosin heavy chain promoter. *Circ. Res.* 92, 609-616.
- Sawada,H., Kohno,R., Kihara,T., Izumi,Y., Sakka,N., Ibi,M., Nakanishi,M., Nakamizo,T., Yamakawa,K., Shibasaki,H., Yamamoto,N., Akaike,A., Inden,M., Kitamura,Y., Taniguchi,T., and Shimohama,S. (2004). Proteasome Mediates Dopaminergic Neuronal Degeneration, and Its Inhibition Causes alpha-Synuclein Inclusions. *Journal of Biological Chemistry* 279, 10710-10719.
- Schmidt,M.L., Murray,J., Lee,V.M., Hill,W.D., Wertkin,A., and Trojanowski,J.Q. (1991). Epitope map of neurofilament protein domains in cortical and peripheral nervous system Lewy bodies. *Am. J. Pathol.* 139, 53-65.
- Schwab,R.S., England,A.C., Jr., Poskanzer,D.C., and Young,R.R. (1969). Amantadine in the treatment of Parkinson's disease. *JAMA* 208, 1168-1170.
- Shannon,K.M., Goetz,C.G., Carroll,V.S., Tanner,C.M., and Klawans,H.L. (1987). Amantadine and motor fluctuations in chronic Parkinson's disease. *Clin. Neuropharmacol.* 10, 522-526.

Shiba-Fukushima,K., Imai,Y., Yoshida,S., Ishihama,Y., Kanao,T., Sato,S., and Hattori,N. (2012). PINK1-mediated phosphorylation of the Parkin ubiquitin-like domain primes mitochondrial translocation of Parkin and regulates mitophagy. *Sci. Rep.* 2, 1002.

Singleton,A.B. (2003). alpha-Synuclein locus triplication causes Parkinson's disease. *Science* 302, 841.

Smith,W.W., Margolis,R.L., Li,X., Troncoso,J.C., Lee,M.K., Dawson,V.L., Dawson,T.M., Iwatsubo,T., and Ross,C.A. (2005). Alpha-synuclein phosphorylation enhances eosinophilic cytoplasmic inclusion formation in SH-SY5Y cells. *J Neurosci* 25, 5544-5552.

Snyder,H., Mensah,K., Theisler,C., Lee,J., Matouschek,A., and Wolozin,B. (2003). Aggregated and Monomeric alpha-Synuclein Bind to the S6' Proteasomal Protein and Inhibit Proteasomal Function. *Journal of Biological Chemistry* 278, 11753-11759.

Snyder,S.H., and D'Amato,R.J. (1986). MPTP: a neurotoxin relevant to the pathophysiology of Parkinson's disease. The 1985 George C. Cotzias lecture. *Neurology* 36, 250-258.

Soriano,P. (1999). Generalized lacZ expression with the ROSA26 Cre reporter strain. *Nat. Genet.* 21, 70-71.

Souza,J.M., Giasson,B.I., Chen,Q., Lee,V.M., and Ischiropoulos,H. (2000a). Dityrosine cross-linking promotes formation of stable alpha -synuclein polymers. Implication of nitrative and oxidative stress in the pathogenesis of neurodegenerative synucleinopathies. *J. Biol. Chem.* 275, 18344-18349.

Souza,J.M., Giasson,B.I., Lee,V.M., and Ischiropoulos,H. (2000b). Chaperone-like activity of synucleins. *FEBS Lett.* 474, 116-119.

Spillantini,M.G., Crowther,R.A., Jakes,R., Hasegawa,M., and Goedert,M. (1998). alpha-Synuclein in filamentous inclusions of Lewy bodies from Parkinson's disease and dementia with lewy bodies. *Proc Natl Acad Sci USA* 95, 6469-6473.

Spillantini,M.G., Schmidt,M.L., Lee,V.M., Trojanowski,J.Q., Jakes,R., and Goedert,M. (1997). Alpha-synuclein in Lewy bodies. *Nature* 388, 839-840.

Steele,J.W., Ju,S., Lachenmayer,M.L., Liken,J., Stock,A., Kim,S.H., Delgado,L.M., Alfaro,I.E., Bernales,S., Verdile,G., Bharadwaj,P., Gupta,V., Barr,R., Friss,A., Dolios,G., Wang,R., Ringe,D., Protter,A.A., Martins,R.N., Ehrlich,M.E., Yue,Z., Petsko,G.A., and Gandy,S. (2012). Latrepirdine stimulates autophagy and reduces accumulation of [alpha]-synuclein in cells and in mouse brain. *Mol Psychiatry*.

Stefanis,L. (2001). Expression of A53T mutant but not wild-type alpha-synuclein in PC12 cells induces alterations of the ubiquitin-dependent degradation system, loss of dopamine release, and autophagic cell death. *J Neurosci* 21, 9549-9560.

Surguchov,A. (2008). Chapter 6 Molecular and Cellular Biology of Synucleins. In *International Review of Cell and Molecular Biology*, W.J. Kwang, ed. Academic Press), pp. 225-317.

Tanaka,Y., Engelender,S., Igarashi,S., Rao,R.K., Wanner,T., Tanzi,R.E., Sawa,A., Dawson,L., Dawson,T.M., and Ross,C.A. (2001). Inducible expression of mutant alpha-synuclein decreases proteasome activity and increases sensitivity to mitochondria-dependent apoptosis. *Human Molecular Genetics* 10, 919-926.

Tanik,S.A., Schultheiss,C.E., Volpicelli-Daley,L.A., Brunden,K.R., and Lee,V.M.Y. (2013). Lewy Body-like alpha-Synuclein Aggregates Resist Degradation and Impair Macroautophagy. *Journal of Biological Chemistry* 288, 15194-15210.

Tieu,K. (2011). *A Guide to Neurotoxic Animal Models of Parkinson's Disease*. Cold Spring Harbor Perspectives in Medicine 1.

Tofaris,G.K., Garcia,R.P., Humby,T., Lambourne,S.L., O'Connell,M., Ghetti,B., Gossage,H., Emson,P.C., Wilkinson,L.S., Goedert,M., and Spillantini,M.G. (2006). Pathological changes in dopaminergic nerve cells of the substantia nigra and olfactory bulb in mice transgenic for truncated human alpha-synuclein(1-120): implications for Lewy body disorders. *J Neurosci* 26, 3942-3950.

Tofaris,G.K. (2012). Lysosome-dependent pathways as a unifying theme in Parkinson's disease. *Mov. Disord.* 27, 1364-1369.

Tofaris,G.K., Layfield,R., and Spillantini,M.G. (2001). alpha-Synuclein metabolism and aggregation is linked to ubiquitin-independent degradation by the proteasome. *FEBS Letters* 509, 22-26.

Tofaris,G.K., Razzaq,A., Ghetti,B., Lilley,K.S., and Spillantini,M.G. (2003). Ubiquitination of alpha-Synuclein in Lewy Bodies Is a Pathological Event Not Associated with Impairment of Proteasome Function. *Journal of Biological Chemistry* 278, 44405-44411.

Unno,T., Wakamori,M., Koike,M., Uchiyama,Y., Ishikawa,K., Kubota,H., Yoshida,T., Sasakawa,H., Peters,C., Mizusawa,H., and Watase,K. (2012). Development of Purkinje cell degeneration in a knockin mouse model reveals lysosomal involvement in the pathogenesis of SCA6. *Proceedings of the National Academy of Sciences* 109, 17693-17698.

Usenovic,M., Knight,A.L., Ray,A., Wong,V., Brown,K.R., Caldwell,G.A., Caldwell,K.A., Stagljar,I., and Krainc,D. (2012a). Identification of novel ATP13A2 interactors and their role in alpha-synuclein misfolding and toxicity. *Hum. Mol. Genet.* 21, 3785-3794.

Usenovic,M., Tresse,E., Mazzulli,J.R., Taylor,J.P., and Krainc,D. (2012b). Deficiency of ATP13A2 leads to lysosomal dysfunction, alpha-synuclein accumulation, and neurotoxicity. *J Neurosci* 32, 4240-4246.

Uversky,V.N., Lee,H.J., Li,J., Fink,A.L., and Lee,S.J. (2001a). Stabilization of Partially Folded Conformation during alpha-Synuclein Oligomerization in Both Purified and Cytosolic Preparations. *Journal of Biological Chemistry* 276, 43495-43498.

Uversky,V.N., Li,J., and Fink,A.L. (2001b). Evidence for a Partially Folded Intermediate in alpha-Synuclein Fibril Formation. *Journal of Biological Chemistry* 276, 10737-10744.

van der Putten,H., Wiederhold,K.H., Probst,A., Barbieri,S., Mistl,C., Danner,S., Kauffmann,S., Hofele,K., Spooren,W.P.J.M., Ruegg,M.A., Lin,S., Caroni,P., Sommer,B., Tolnay,M., and Bilbe,G. (2000). Neuropathology in Mice Expressing Human alpha-Synuclein. *The Journal of Neuroscience* 20, 6021-6029.

Vogiatzi,T., Xilouri,M., Vekrellis,K., and Stefanis,L. (2008). Wild Type alpha-Synuclein Is Degraded by Chaperone-mediated Autophagy and Macroautophagy in Neuronal Cells. *Journal of Biological Chemistry* 283, 23542-23556.

Volpicelli-Daley,L.A., Luk,K.C., Patel,T.P., Tanik,S.A., Riddle,D.M., Stieber,A., Meaney,D.F., Trojanowski,J.Q., and Lee,V.M. (2011). Exogenous alpha-synuclein fibrils induce Lewy body pathology leading to synaptic dysfunction and neuron death. *Neuron* 72, 57-71.

Wagner,J., Ryazanov,S., Leonov,A., Levin,J., Shi,S., Schmidt,F., Prix,C., Pan-Montojo,F., Bertsch,U., Mitteregger-Kretschmar,G., Geissen,M., Eiden,M., Leidel,F., Hirschberger,T., Deeg,A., Krauth,J., Zinth,W., Tavan,P., Pilger,J., Zweckstetter,M., Frank,T., Bähr,M., Weishaupt,J., Uhr,M., Urlaub,H., Teichmann,U., Samwer,M., Botzel,K., Groschup,M., Kretschmar,H., Griesinger,C., and Giese,A. (2013). Anle138b: a novel oligomer modulator for disease-modifying therapy of neurodegenerative diseases such as prion and Parkinson's disease. *Acta Neuropathol* 1-19.

Wakamatsu,M., Ishii,A., Iwata,S., Sakagami,J., Ukai,Y., Ono,M., Kanbe,D., Muramatsu,S.i., Kobayashi,K., Iwatsubo,T., and Yoshimoto,M. (2008). Selective loss of nigral dopamine neurons induced by overexpression of truncated human alpha-synuclein in mice. *Neurobiology of Aging* 29, 574-585.

Wang,P., Li,B., Zhou,L., Fei,E., and Wang,G. (2011a). The KDEL receptor induces autophagy to promote the clearance of neurodegenerative disease-related proteins. *Neuroscience* 190, 43-55.

Wang,W., Perovic,I., Chittuluru,J., Kaganovich,A., Nguyen,L.T.T., Liao,J., Auclair,J.R., Johnson,D., Landeru,A., Simorellis,A.K., Ju,S., Cookson,M.R., Asturias,F.J., Agar,J.N., Webb,B.N., Kang,C., Ringe,D., Petsko,G.A., Pochapsky,T.C., and Hoang,Q.Q. (2011b).

A soluble alpha-synuclein construct forms a dynamic tetramer. *Proceedings of the National Academy of Sciences* 108, 17797-17802.

Watanabe,Y., Tatebe,H., Taguchi,K., Endo,Y., Tokuda,T., Mizuno,T., Nakagawa,M., and Tanaka,M. (2012). p62/SQSTM1-Dependent Autophagy of Lewy Body-Like alpha-Synuclein Inclusions. *PLoS ONE* 7, e52868.

Webb,J.L. (2003). Alpha-Synuclein is degraded by both autophagy and the proteasome. *J Biol Chem* 278, 25009-25013.

Weinreb,P.H., Zhen,W., Poon,A.W., Conway,K.A., and Lansbury,P.T. (1996). NACP, A Protein Implicated in Alzheimer's Disease and Learning, Is Natively Unfolded. *Biochemistry* 35, 13709-13715.

Winslow,A.R. (2010). alpha-Synuclein impairs macroautophagy: implications for Parkinson's disease. *J Cell Biol* 190, 1023-1037.

Wirdefeldt,K., Adami,H.O., Cole,P., Trichopoulos,D., and Mandel,J. (2011). Epidemiology and etiology of Parkinson's disease: a review of the evidence. *Eur J Epidemiol* 26, 1-58.

Wong,E., and Cuervo,A.M. (2010). Autophagy gone awry in neurodegenerative diseases. *Nat Neurosci* 13, 805-811.

Xilouri M,V.T.V.K.P.D.S.L. (2009). Abberant alpha-synuclein confers toxicity to neurons in part through inhibition of chaperone-mediated autophagy. *PLoS ONE* 4, e5515.

Xilouri,M., Vogiatzi,T., Vekrellis,K., Park,D., and Stefanis,L. (2009). Abberant alpha-synuclein confers toxicity to neurons in part through inhibition of chaperone-mediated autophagy. *PLoS ONE* 4, e5515.

Xilouri,M., Brekk,O.R., Landeck,N., Pitychoutis,P.M., Papasilekas,T., Papadopoulou-Daifoti,Z., Kirik,D., and Stefanis,L. (2013a). Boosting chaperone-mediated autophagy in vivo mitigates alpha-synuclein-induced neurodegeneration. *Brain* 136, 2130-2146.

Xilouri,M., Brekk,O., and Stefanis,L. (2013b). Alpha-synuclein and Protein Degradation Systems: a Reciprocal Relationship. *Mol Neurobiol* 47, 537-551.

Zarranz,J.J. (2004). The new mutation, E46K, of alpha-synuclein causes Parkinson and Lewy body dementia. *Ann Neurol* 55, 164-173.

Zhang,D., Hu,X., Qian,L., O'Callaghan,J.P., and Hong,J.S. (2010). Astroglial pathology in CNS pathologies: is there a role for microglia? *Mol. Neurobiol.* 41, 232-241.

Zhang,N.Y., Tang,Z., and Liu,C.W. (2008). alpha-Synuclein Protofibrils Inhibit 26 S Proteasome-mediated Protein Degradation: UNDERSTANDING THE

CYTOTOXICITY OF PROTEIN PROTOFIBRILS IN NEURODEGENERATIVE DISEASE PATHOGENESIS. *Journal of Biological Chemistry* 283, 20288-20298.

Zhao,Z., Wang,J., Zhao,C., Bi,W., Yue,Z., and Ma,Z.A. (2011). Genetic ablation of PLA2G6 in mice leads to cerebellar atrophy characterized by Purkinje cell loss and glial cell activation. *PLoS. One.* 6, e26991.

Zu,T., Duvick,L.A., Kaytor,M.D., Berlinger,M.S., Zoghbi,H.Y., Clark,H.B., and Orr,H.T. (2004). Recovery from Polyglutamine-Induced Neurodegeneration in Conditional SCA1 Transgenic Mice. *The Journal of Neuroscience* 24, 8853-8861.